DEVELOPMENT OF ANALYTICAL SENSORS FOR THE IDENTIFICATION AND QUANTIFICATION OF METALS IN ENVIRONMENTAL SAMPLES

Report to the
Water Research Commission

by

V Somerset, C van der Horst, B Silwana and C Walters
CSIR, Natural Resources and the Environment, Stellenbosch

In collaboration with

E Iwuoha
Department of Chemistry, University of the Western Cape, Bellville

S le Roux
Department of Applied Sciences, Cape Peninsula University of Technology, Bellville

WRC Report No. 2013/1/12
ISBN 978-1-4312-0279-9

August 2012

OBTAINABLE FROM

Water Research Commission
Private Bag X03
Gezina, 0031
REPUBLIC OF SOUTH AFRICA

www.orders.co.za or download from www.wrc.org.za

EXECUTIVE SUMMARY

South Africa has a wealth of mineral resources consisting of coal, gold, platinum uranium, and other minerals. However the mining activities for these resources have in some cases brought about some serious environmental problems in a country with limited water resources. These environmental problems are both historic and current. The reliance on coal-fired power stations for energy production has contributed to the environmental impact. Many of the big rivers in the country descend from the Great Escarpment of the interior to the coastal lowlands, contributing to an unusual high rate of runoff and associated soil erosion.

There is also a need to determine whether the current tools and techniques used to detect and quantify the impact on metals on the aquatic environment are adequate. The use of fast, reliable and continuous monitoring techniques for routine analysis of water quality and to quantify pollution events has become essential in order to manage the discharge of potentially harmful wastes to the environment.

In this project the emphasis was on: (i) assessing the aquatic environment around platinum group metals mining activities to determine which national water resources are in close proximity to these mines, and determining to what extent the aquatic environment has been polluted by these mining activities; and (ii) to determine whether the current analytical tools and techniques used to analyse heavy and precious metal containing effluent is adequate for the task at hand. The project was therefore designed with a main objective and several objectives were identified.

Environmental samples were collected and the results revealed the following: The metal concentrations were low in the surface water samples analysed. For some sampling sites elevated nutrient concentrations were obtained during both the August and November 2010 sampling trips. Seasonal influences affected the diversity of taxa for the biota samples collected and the metal concentrations within these samples. Higher Ni, Pb and Zn concentrations were recorded compared to the other metals investigated and it is therefore possible that these metals are released from the sediment-water interface into solution in the overlying waters. Once in solution these metals may then be absorbed in the overlying algae that were collected, since the algae also contained elevated Ni, Pb and Zn concentrations. The concentrations measured in the biota and algae were low, indicating that mining activities had a low impact on the aquatic environment at the sampling sites. Nevertheless, in the case of the metal concentrations in biota samples, results for the August 2010 samples showed higher concentrations of Al, Fe, Ni, Zn and Pt for all biota sampled compared to that in samples from November 2010. This may be due to higher water flow during November 2010, since sampling was done during the rainy season.

This study also investigated the applicability of ion exchange resins in the removal or adsorption of Pt(II), Pd(II) and Rh(III) from acidic ($pH \leq 2$) and alkaline ($pH \geq 8$) aqueous solutions. For this purpose, two synthetic sidestream solutions (designated A and B) were prepared and used in the adsorption experiments. The results obtained have shown that at $pH \leq 2$, the highest removal efficiency of 64% was obtained when Chitosan was used on solution A. In the case of Amberlite® IRP-69, the highest removal efficiency was 57% when solution B was subjected to the adsorption studies. For both solutions A and B, Amberlite® IRA-400 was able to absorb Pt more effectively, followed closely by Pd and least effective results were obtained for Rh. The highest removal efficiency was 99% for Pt from solution A. Dowex® 50WX8-100 resin showed limited removal of Pt, Pd and Rh from the synthetic sidestream solutions, especially when the results are compared to the three other resins efficiencies. The removal efficiencies of the PGMs ranged between 40-99% and the sorbents interacted well with solution A, removing Pd from both solutions at acidic pH. Under alkaline conditions the highest removal efficiency of 99% was obtained with Amberlite® IRA-400 and Dowex® 50WX8-100 and Rh. The highest removal efficiency of Pd was 65% using Amberlite® IRA-400, while the weakest results (0.6%) were obtained using Dowex® 50WX8-100. Amberlite® IRA-400 removed 90% Pt – the highest Pt removal at pH 8 – and Amberlite® IRP-69 the lowest (5%).

The main focus of this project was on the development and construction of an electrochemical sensor for the identification and quantification of metals in environmental samples. The results obtained have shown that modifying the surface of a glassy carbon electrode with a bismuth film (BiF) assists in the stripping analysis of the M$(HDMG)_2$ complexes, with M as the PGM (Pd, Pt and Rh) and dimethylglyoxime (DMG) as the chelating agent. The results obtained for the evaluation of the GCE/BiF/M$(HDMG)_2$ sensor in 0.1 M HCl buffer (pH ≈ 2), 0.2 M NaOAc buffer (pH = 4.5) and 0.1 M ammonia (pH = 9) buffer solutions have showed varying results. For analytical purposes and the successful application of the electrochemical sensor, several parameters were optimised that included the pH, DMG concentration, deposition potential, deposition time and PGM concentration. The effect of interfering ions was also investigated and the results obtained showed that Ni(II) and Co(II) are the main metal ion interferences that affect the stripping analysis of Pt, Pd and Rh when the GC/BiFE/$(HDMG)_2$ sensor are applied to the stripping analysis of PGMs. The limit of detection (LOD) was also determined for the developed sensor and the LOD values for individual metal ion determination were found to be 0.12 ± 0.06 µg/ℓ for Pd, 0.04 ± 0.007 µg/ℓ for Pt and 0.23 ± 0.04 µg/ℓ for Rh respectively. The linear ranges to which the sensor can be applied were determined as 0.1-3.5 µg/ℓ for Pd, 0.5-4.0 µg/ℓ for Pt and 0.1-4.0 µg/ℓ for Rh. The GC/BiFE/$(HDMG)_2$ sensor was successfully applied in the determination of Pd, Pt and Rh in freshwater samples and sediment sample fractions. The results obtained for the analysis of the freshwater samples for its Pd, Pt and Rh concentrations, involved spiking the freshwater samples with a known amount of PGM concentration (4 µg/ℓ), and followed by voltammetric analysis of these samples to determine the accuracy and sensitivity of the constructed sensor. Analysis of the results obtained indicated that the technique is very sensitive towards the determination of Pd in freshwater samples, while further optimisation of deposition time and / or deposition potential may still be required for the determination of Pt and Rh in these samples. Applying the same sensor to the analysis of the sediment sample fractions showed that good recoveries were obtained for Pd in the carbonate-bound fraction, with weaker recoveries for Pt in the Fe-Mn bound fractions, while poor results for Rh in the organic-bound fraction of the sample matrix were obtained.

Overall, the results presented in this study have demonstrated that modifying the surface of a glassy carbon electrode with a bismuth film (BiF) aids in the stripping analysis of Pt, Pd and Rh with the use of dimethylglyoxime (DMG) as chelating agent, utilising adsorptive stripping voltammetry as technique. The results further encourages the advances and efforts towards on-site environmental and industrial monitoring, enabling decentralised testing and complete replacement of common toxic mercury electrodes for stripping analysis of metal ions.

ACKNOWLEDGMENTS

Water Research Commission Project Reference Group
The financing of the project by the Water Research Commission and the contributions of the members of the Reference Group are gratefully acknowledged. The following people per-reviewed this report prior to publication.

- Dr J Burgess (Water Research Commission), Chairperson
- Prof B Pletschke (Rhodes University)
- Prof C Ngila (University of Johannesburg)
- Ms K Slatter (Anglo American Platinum)
- Dr R Moutlouali (Mintek)
- Dr MW Gitari (University of Venda)

Research Team

Project Leader
Dr VS Somerset (NRE, CSIR)

Project Team
Prof EI Iwuoha (University of the Western Cape)
Mrs S Le Roux (Cape Peninsula University of Technology)
Mrs C Walters (NRE, CSIR)
Mr C Van der Horst (University of the Western Cape)
Ms B Silwana (University of the Western Cape)
Ms Uthi Skepe (Cape Peninsula University of Technology)

CAPACITY BUILDING

Students

Mr Charlton van der Horst (M, C)

Stripping voltammetric characterisation of palladium, platinum and rhodium in environmental samples using dimethylglyoxime $(HDMG)_2$ complexes at modified carbon electrode surfaces. Master of Science (Chemistry), Faculty of Science, University of the Western Cape.

Ms Bongiwe Silwana (F, B)

Heavy and precious metal toxicity evaluation using a horseradish peroxidise immobilised biosensor. Master of Science (Chemistry), Faculty of Science, University of the Western Cape.

Ms Uthi Skepe (F, B)
Determination of the bioaccumulation of selected heavy and precious metal concentrations in earthworms and their soil substrates. B Tech (Chemistry), Faculty of Applied Sciences, Cape Peninsula University of Technology.

PUBLICATIONS

VAN DER HORST C, SOMERSET V and IWUOHA E. Adsorptive stripping voltammetric determination of Pd using dimethylglyoxime (DMG) as complexing agent. Poster presentation at ANALITIKA 2010 International Conference, University of Stellenbosch, 5-9 December 2010, Stellenbosch, South Africa.

SOMERSET V, VAN DER HORST C, SILWANA B, WILLIAMS C and IWUOHA E. Assessment of bioaccumulation of platinum group metals in a river system in close proximity to mining activities in South Africa. Poster presentation at the 21st SETAC Europe Annual Meeting and Conference, 15-19 May 2011, Italy, Milan.

VAN DER HORST C, SILWANA B, IWUOHA E and SOMERSET V. 2012. Stripping voltammetric determination of palladium, platinum and rhodium in South African water resources. Journal of Environmental Science and Health, Part A. Submitted.

Table of Contents

List of Tables

List of Figures

List of Abbreviations

AAS	Atomic absorption spectrometry
AdSV	Adsorptive stripping voltammetry
AE	Auxiliary electrode
AES	Atomic emission spectroscopy
AFS	Atomic fluorescence spectrometry
ASV	Anodic stripping voltammetry
BAR	Bioaccumulation ratio
BiF	Bismuth film
CPE	Carbon paste electrode
CMCPE	Chemically modified carbon paste electrode
cm^3/a	Cubic centimetres per annum
CV	Cyclic voltammetry
DME	Dropping mercury electrode
DMG	Dimethylglyoxime
DPASV	Differential pulse anodic stripping voltammetry
DPASVs	Differential pulse anodic stripping voltammograms
DPAdSV	Differential pulse adsorptive stripping voltammetry
DPAdSVs	Differential pulse adsorptive stripping voltammograms
DPV	Differential pulse voltammetry
DWA	Department of Water Affairs (formerly DWAF)
DWAF	Department of Water Affairs and Forestry (now DWA)
d.wt	Dry weight
DO	Dissolved oxygen
EC	Electrical conductivity
Ed	Deposition potential
FTIR	Fourier transformed infrared spectroscopy
GCE	Glassy carbon electrode
GFAAS	Graphite furnace atomic absorption spectrometry
HMDE	Hanging mercury drop electrode
HMTA	Hexamethylene tetramine
ICP-AES	Inductively coupled absorption emission spectrometry
ICP-OES	Inductively coupled optical emission spectrometry
ICP-MS	Inductively coupled plasma-mass spectrometry
INAA	Instrumental neutron activation analysis
ISE	International Society of Electrochemistry
MAP	Mean annual precipitation
MAR	Mean annual runoff
MBT	Mercaptobenzothiazole
mm/a	Millimetres per annum
m^3/a	Cubic metres per annum
NAEBP	South African National Aquatic Ecosystem Biomonitoring Programme
ORP	Oxidation-reduction potential
PANI	Polyaniline
PDTDA	Poly(2,2´-dithiodianline)
PEL	Probable-effects level
PGM	Platinum group metal
PGMs	Platinum group metals
PP	Polypropylene
PT	Periodic table
QA	Quality assurance
QC	Quality control
q_e	Quantity of the precious metal ion adsorbed

RHP	River Health Programme
SASS	South African scoring system
SMA	Sub-management area
SPCE	Screen-printed carbon electrode
TDS	Total dissolved solids
t_d	Deposition time
TEL	Threshold-effects level
TotHg	Total mercury
TXRF	Total reflectance X-ray fluorescence spectrometry
UG2	Upper group 2
USEPA	United States Environmental Protection Agency
WE	Working electrode
WMA	Water management area
WMAs	Water management areas
WQGVs	Water quality guideline values
w.wt	Wet weight
XRF	X-ray fluorescence spectrometry

CHAPTER 1: INTRODUCTION

1.1 Introduction and rationale

One of the most crucial environmental problems in the last decade has been the pollution of surface waters with chemical contaminants. Waterborne chemical pollution entering rivers and streams causes tremendous amounts of destruction. Despite the fact that some water pollution can occur through natural processes, most of the pollution is anthropogenic (Sonune and Ghate, 2004). Wastewaters arising from human activities are generally treated and discharged to South Africa's water resources. Such wastewaters arise from domestic residences, institutions, and commercial and industrial establishments, and often mingle with surface and stormwater, runoff and groundwater. Wastewater can contain a high load of oxygen demanding wastes, pathogenic or disease-causing agents, organic materials, nutrients that stimulate plant growth, inorganic chemicals and minerals, including sediments and toxic compounds. The characteristics of industrial wastewaters however can differ considerably both within and among industries and their impacts on the receiving environment differ accordingly. Three options are generally available for managing industrial wastewater: i) controlling the wastewater at the point of generation in the plant; ii) pre-treatment of the wastewater for discharge into municipal treatment sources; iii) complete treatment of the wastewater at the plant for re-use or direct discharge into receiving waters (Sonune and Ghate, 2004).

All mine sites in South Africa adhere to the zero discharge law which states that no solutions may be returned into the environment without the permission of the Department of Water Affairs (DWA). In the case where spills do occur, these need to be reported immediately to the DWA and volumes of the spills and analysis of the spills need to be given to the DWA.

The work in this study is focussed on determining whether there is any platinum group metal (PGM) contamination occurring within the vicinity of platinum mines and, if present, the concentrations of the PGMs in the environment. Platinum group metals (PGMs) is the collective name used when referring to platinum (Pt), palladium (Pd), rhodium (Rh), iridium (Ir), ruthenium (Ru) and osmium (Os). In the Earth's crust, the average concentration of these metals is estimated to range from 0.0001 g/t for rhodium to 0.015 g/t for palladium, with platinum, ruthenium, osmium and iridium present in equally small concentrations (Ravindra *et al*., 2004). The PGMs have unique properties: they are corrosion resistant, heat resistant; have high melting points; high mechanical strengths; they are ductile and have catalytic capabilities (Ravindra *et al*., 2004). These properties have led to extensive use in jewellery manufacture, automotive catalyst manufacture, and in the electronics, glass, electrical, petroleum and medical industries (Johnson-Matthey, 2002; Ravindra *et al*., 2004).

All the PGMs are generally associated with one another in the Earth's crust, occurring naturally in nickel, copper and iron sulphide seams (Ravindra *et al*., 2004).. The relative proportions of the individual PGMs are not constant in all PGM deposits. The world's largest source of PGMs is the South African Bushveld Igneous Complex (BIC), formed around 2 000 million years ago. The BIC consists of a series of distinct layers, three of which are of economic importance as sources of PGMs – the Merensky Reef, the Upper Group 2 (UG2) Reef, and the Platreef. The Merensky Reef has been the principal source of PGMs since it was first worked in 1925 and now produces 50% of all the platinum-bearing ore processed in South Africa. In 1999, the UG2 Reef increased production to yield 42% of the country's platinum, and the Platreef only began to be exploited on a large scale in 1993 (Johnson-Matthey, 2003). Mill head grades of ore (a measure of the PGM content of the ore on entering the first processing stage) are typically between 4 and 7 g/ton. This translates to between 7 and 12 tons of ore being processed to produce a single ounce of platinum (Johnson-Matthey, 2003).

Once the ore has been mined it is transported to a concentrator where it is crushed and milled to expose the minerals containing the PGMs. In the concentrator process the rock is mixed with water and other reagents, through which air is pumped to create bubbles to which the PGM-containing particles adhere – the flotation process. These bubbles float to the surface and are removed as a froth, called concentrate, which generally has a PGM concentration of 100-1000 g/ton (Johnson-Matthey, 2003). The concentrate is dried and then smelted in furnaces to produce a matte product containing the PGMs and a slag waste that contains the unwanted minerals. The matte is transferred to converters, where iron and sulphur are removed. The PGM content of converter matte is > 1400 g/ton (Johnson-Matthey, 2003).

Following smelting the base metals are separated from the PGMs at the base metal refinery, where sulphate and metals such as cobalt, nickel and copper are refined for the marketplace. Following base metal removal the PGM matte is then sent to a precious metal refinery where the six PGMs, along with gold and silver, are separated using methods such as solvent extraction and ion exchange.

An overview of the entire process involved in producing PGM products is shown in Figure 1, and Figure 2 illustrates the order in which the precious metals are extracted from the matte. The soluble metals are removed first followed by the insoluble metals with rhodium usually last to be extracted from the concentrate (Robinson, 2002, pers. comm.).

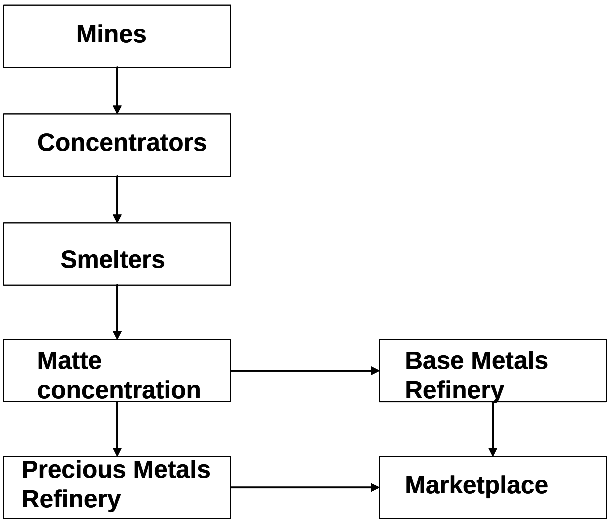

Figure 1. **Simple overview of the PGM production process (Robinson, 2002, pers. comm).**

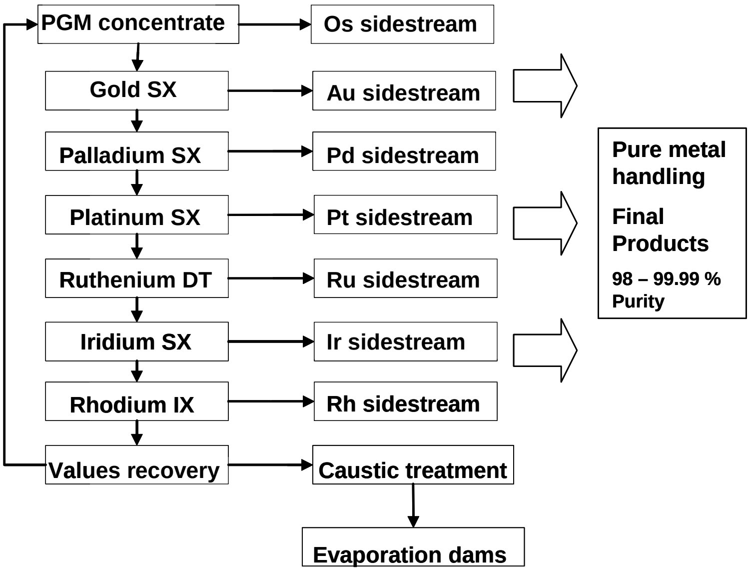

Figure 2. **Overview of Anglo Platinum Precious Metal Refinery (PMR) flow sheet. SX: Solvent extraction, DT: Distillation, IX: Liquid ion exchange (Robinson, 2002, pers. comm.).**

Each PGM extraction process produces a metal and a liquid by-product, called a sidestream. The sidestreams contain residual amounts of PGMs which are then further returned to the process until only small volumes, with extremely low concentrations of PGM, are returned to a lined evaporation pond for later recovery of the “waste” PGMs. These low volume final PGM sidestreams are characterised by extremes of pH – both high and low, high inorganic ion content (such as chloride), significant residual metal loads and small amounts of entrained organic compounds such as those mentioned previously . The composition of these sidestreams precludes any direct discharge to surrounding surface waters, thus, they must be managed within the refinery. Hence no solutions are released into the environment from the precious metal refineries and it is unlikely that any seepage will occur due to the dams being lined. However, the increasing uses of PGMs in vehicle exhaust catalysts (VECs) have seen these metals being present in fine particulate matter emitted through exhaust fumes. This fine particulate matter originates from the abrasion and deterioration of the surface of the catalyst and may be deposited along roadways, on adjacent vegetation and soil, and in water bodies, either directly or through runoff (Moldovan *et al.*, 2001).

Sources of PGMs finding their way into the environment are dominated by emissions from automotive catalytic converters but may also include fugitive emissions during production. Monitoring of air, soil and water quality in locations affected by human activities is extremely important and should include base, precious and other metals owing to their potential effects on environmental and human health (see section 2.3).

Thus there is a need to develop fast, reliable techniques for monitoring water quality to detect the presence of metals in the environment. Since water monitoring is limited to chemical and biological testing, different types of electrochemical sensors and principles can be used in water quality monitoring (Tønning *et al*., 2005).

1.2 Aims

The main aim of this project was to design, synthesise and characterise an electrochemical sensor with controlled surface structure and chemical activity towards metal ions such as lead, zinc, cadmium, nickel, arsenic, platinum, palladium and rhodium.

In order to address and meet the above aim, the following objectives were identified:

1. To design, develop and synthesise new electrochemical sensor materials and chemical compounds with nanoscopic and controlled surface structure and chemical activity towards metal ions such as lead, zinc, cadmium, nickel, arsenic, aluminium, platinum and palladium.
2. To characterise and identify the metals typically found in areas which contain mining activity.
3. To integrate synthesised nanoscopic chemical compounds into electrochemical sensor and screen-printed electrode format, and optimise screen-printing parameters.
4. To develop, integrate and apply ion-exchange materials in electrochemical sensor construction for identification of metal ions.
5. To develop, integrate, test and optimise (screen-printed) chemical sensor formats into a portable potentiostat tool-kit for laboratory testing of samples.
6. To test and optimise the (screen-printed) chemical sensor formats and portable tool-kit for on-site analysis of identified heavy and precious metals.
7. To develop identification and application of chemical precipitation techniques for specific metal ions, focussing on solution equilibria, speciation, pH-dependence and related chemical parameters.

Throughout the project, different aspects of the electrochemical sensor development were addressed and reported, with the purpose of meeting all of the above objectives or meeting most of the aspects identified.

CHAPTER 2: LITERATURE REVIEW

2.1 Platinum group metals

Platinum group metals are occasionally divided into two sub-classes – light (Ru, Rh, Pd) and heavy platinum metals (Os, Ir, Pt). Their defining characteristics include high chemical stability in the elemental state, distinct catalytic properties, and capabilities to form stable complex structures (Earnshaw and Greenwood, 1997). Apart from ICP-MS, determination of PGMs can be accomplished using carbon paste electrodes (CPEs) and their chemically modified variants (CMCPEs), offering an alternative to controversial mercury-based electrodes (Economou, 2005; Wang, 2005; Kalcher *et al*., 1995; Svancara *et al*., 2001).

Owing to its corrosion resistance nature and alloying ability, palladium is an important element in metallurgy. Its alloys are used in dental and medicinal devices and in jewellery manufacturing. Moreover, palladium is used in automobile catalysts and as a catalyst in the organic synthesis industry (Wise, 1968; Gaita and Al-Bazi, 1995). Other applications of these elements comprise dental alloys (Au, Pd and Pt), electronics (Ir, Pd and Pt), glass-making equipment (Pt and Rh), electrode coatings (Ir and Ru), temperature sensors (Pt and Rh), medical implants (Pt), jewellery (Au, Pt) and medicines (Pt compounds are used as anti-cancer drugs while Au compounds serve as anti-rheumatic products) (Resano *et al*., 2007).

In the study of PGMs, the optimisation of the critical parameters, i.e. ionic strength, electrode area, pre-concentration time, transport rate to the electrode and potential scan rate are very important. In this study optimisation of deposition time and deposition potential of the PGMs will be performed followed with the optimisation of chelating agent concentrations with PGMs. The detection of PGMs in atomic absorption spectroscopy (AAS) standards and real samples are done by using adsorptive stripping voltammetry and inductive coupled plasma optical emission spectrometry (ICP-OES).

Platinum group metals are naturally found only at very low concentration in the Earth's crust. However, the increasing uses of PGMs in vehicle exhaust catalysts (VECs), in addition to some other applications (e.g. jewellery, anticancer drugs) cause their anthropogenic emission and spread in the environment. Platinum group elements contamination initially occurs in airborne particulate matter, roadside dust, soil, sludge and water, etc.; which finally results in bioaccumulation of these elements in living organisms through diverse pathways. The metallic form of these elements is generally considered to be biologically inert but some salts, such as hexachloroplatinate and tetrachloroplatinite, are among the most potent allergens and sensitizers. These PGMs have also been associated with asthma, nausea, increased hair loss, increased spontaneous abortion, dermatitis and other serious health problems in humans (Rao and Reddi, 2000).

Platinum best illustrates the significance of speciation in metal toxicity. The allergenic effects of Pt is confined to a small group of charged compounds that contain reactive ligands, the most effective of which comprises chlorides (Cleare *et al.,* 1976; WHO, 1991; Merget, 2000). Metallic Pt is considered to be biologically inert and non-allergenic. Its sensitising potential is probably very low because Pt emitted from VECs is in metallic or oxide forms. Platinum in road dust, however, can be solubilised, and enters the waters, sediments, soils and the food chain. Certain Pt compounds are also known to be cytotoxic and have mutagenic and carcinogenic effects, and have some effects on microorganisms at very low concentrations (WHO, 1991; Bünger *et al.,* 1996; Gebel *et al*., 1997; Lantzsch and Gebel, 1997). In addition, some Pt complexes can bind to N and S in proteins producing a reduction in enzymatic activity (Melius and Friedman, 1977; Helmers *et al*., 1994).

The first Pt was discovered in chromitite mineral ore in 1906 by Bettel and this ore is today called the Upper Group 2 (UG2) chromitite reef. Another reef is the Platreef that is situated near Mokopane (Potgietersrust; Figure 4). Both the Merensky and UG2 reefs are narrow, while the Platreef is slightly thicker, and the PGM ores are mined through conventional underground or open pit techniques (Glaister and Mudd, 2010).

South Africa currently dominates the global annual production of PGMs with a total of 165.8 tonnes of Pt and 86.5 tonnes of Pd mined in 2007. The rest of the global players and the total amount of Pt and Pd mined in 2007 are represented in Figure 3 (Glaister and Mudd, 2010).

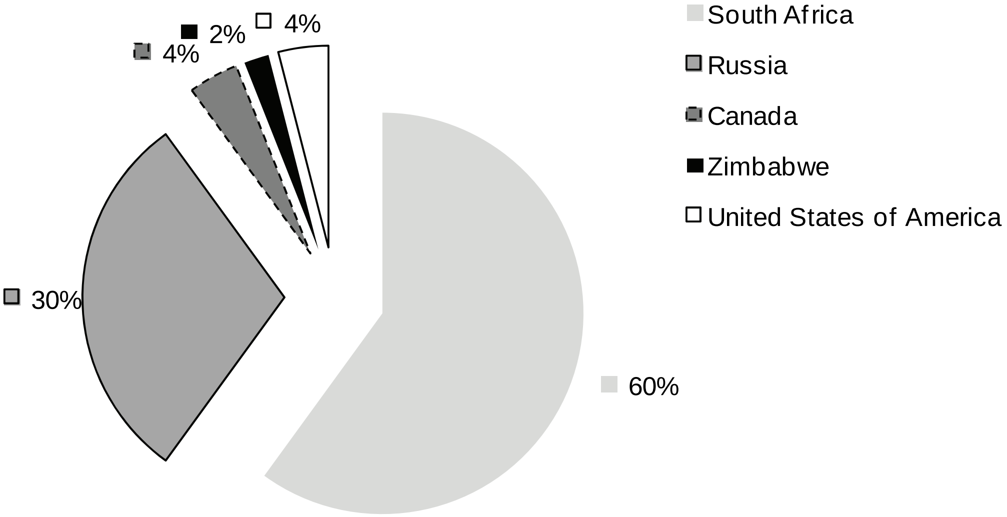

Figure 3. **Global production of Pt and Pd in 2007. Adapted from Glaister and Mudd (2010).**

Mining is not a delicate activity and generally involves the blasting, moving and processing of massive amounts of rock, in which > 50% of the original material becomes waste in which > 50% of the original material becomes waste. Dust from solid wastes, as well as fugitive liquids can contribute to the environmental presence of metals over and above the amount accounted for by the geology of an area.

South Africa’s reserves of coal, gold, PGMs, uranium, and other minerals have provided economic development but have also caused some serious environmental problems in a country with limited water resources. These problems are both historic and current. The reliance on coal-fired power stations for energy production has contributed to the environmental impact. Many of the big rivers in the country descend from the Great Escarpment of the interior to the coastal lowlands, contributing to an unusually high rate of runoff and associated soil erosion. Water is required for agricultural activities and has led to the building of approximately 519 dams with a total capacity of 50 billion cubic metres (Davies, 2010; Naicker *et al*., 2003). With the Vaal River providing most of the water for the industrial zone around the Witwatersrand region, the river has reached its maximum capacity for water utilisation and hence has suffered extensive industrial pollution. The location of coal, gold and uranium mines along the Vaal River and its tributaries are extensive and the environmental impacts have been devastating to some areas of the Witwatersrand with the acid mine drainage (AMD) problem becoming almost unstoppable in 2010 (Davies, 2010; Naicker *et al*., 2003).

This study will focus on the detection and quantification of PGMs in environmental samples collected from four South African Water Management Areas (WMAs) (Figure 5) using electrochemical sensors.

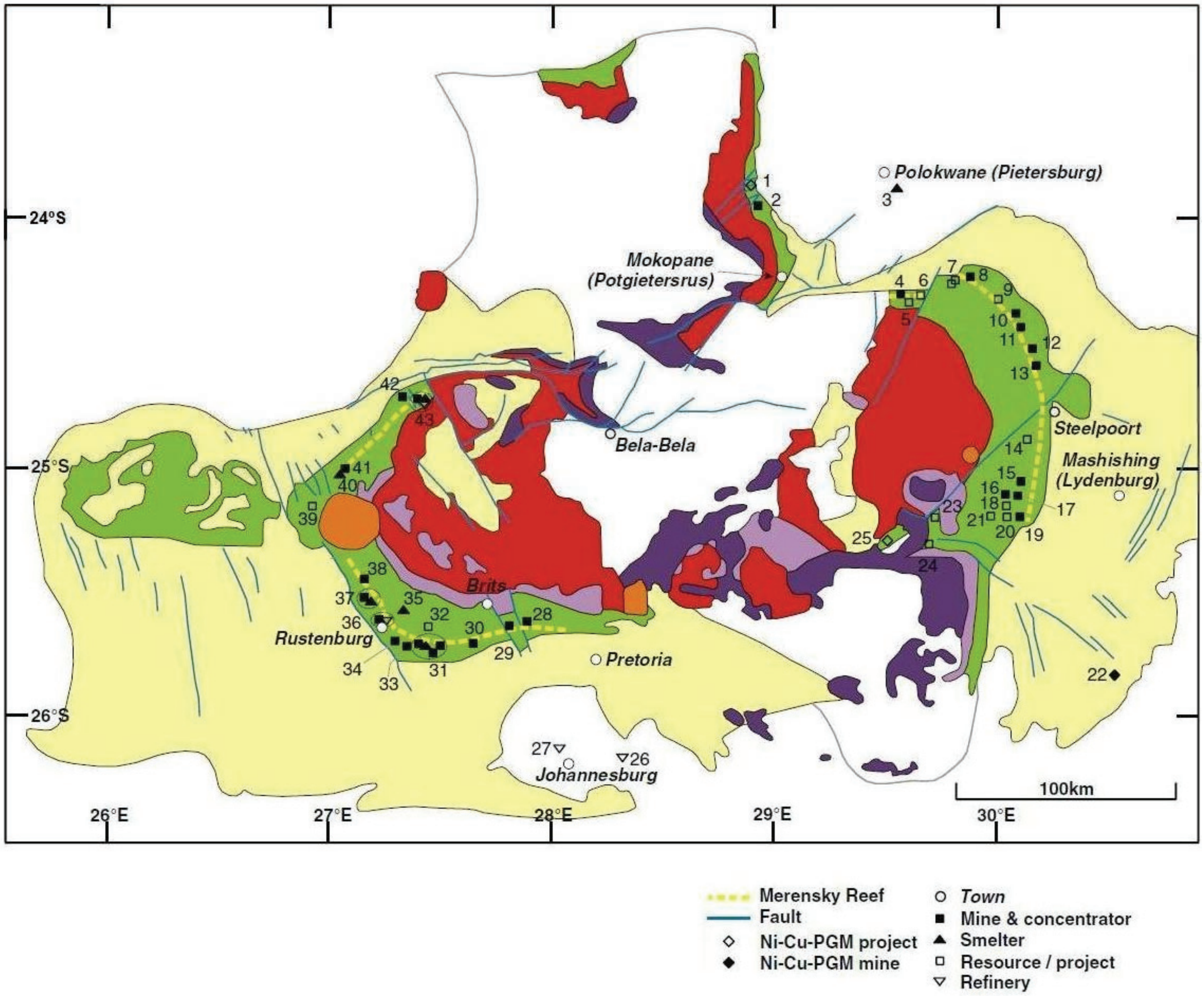

Figure 4. **Map showing the location of the Merensky Reef. Adapted from Glaister and Mudd (2010).**

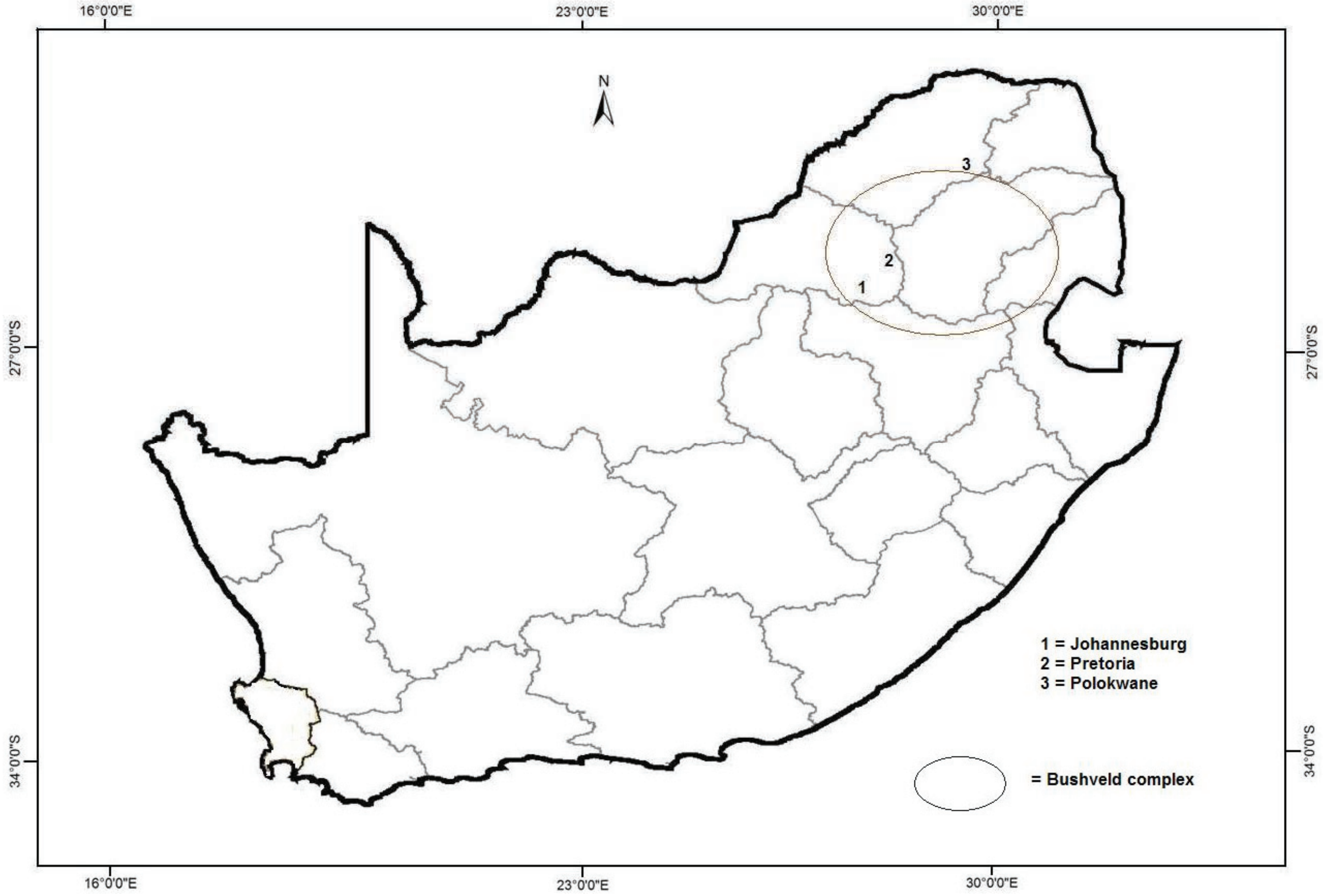

Figure 5. Map of South Africa’s Water Management Areas.

2.2 Mining and the natural environment

It is known that heavy metals occur naturally in the environment as trace constituents in soil, rocks, water, plants and animals. The areas in which higher than normal concentrations of heavy metals occur are, of course, the areas in which activity to extract those minerals is greatest. Through anthropogenic activities, metal concentrations may increase in terrestrial and aquatic environments with diffuse pollution playing a big contributing role. If these heavy metals undergo redox and dissolution processes in the receiving environment, via various mechanisms, it may result in serious contamination and ultimate destruction of the aquatic environment may occur. It has therefore become essential to monitor the effect of mining activities on the surrounding environment, in order to quantify long-term dispersal and bioaccumulation of heavy metals and to assess ecosystem health (Elberling *et al*., 2003; Peramaki and Decker, 2000).

The soils and surface waters of historical mining areas are commonly affected by metal pollution. Although metals can be retained by soils, they can also be mobilised in soil solutions via different biological and chemical mechanisms. This results in the potential contamination of drinking water supplies or uptake by vegetation with potential food chain impacts. Metals that are introduced into the environment through human activities are usually present in various forms such as: dissolved in the aqueous phase of soil (pore waters); occupying exchange site on inorganic soil constituents; specifically adsorbed on inorganic soil constituents; associated with insoluble soil organic matter; and precipitated as pure or mixed solids. The measurement of the total concentration of metals in soils is useful as a means to detect any net change and to quantify any related pollution (Pagnanelli *et al*., 2004).

Many metals are highly soluble in water and are absorbed by aquatic organisms. Once these metals enter the food chain, large concentrations of heavy metals may accumulate in the human body. If ingested beyond the permitted concentration levels, these metals can cause mild to serious health disorders such as depression, lethargy, seizures and ataxia, liver damage, Wilson's disease, renal disorder, dermatitis, asthma and human carcinogen disorders (Kurniawan *et al*., 2006; Fatin-Rouge *et al*., 2006; Chatain *et al*., 2004; Fu *et al*., 2008; Lim *et al*., 2008; Li *et al*., 2007; Zheng *et al*., 2007; Reis *et al*., 2007).

In the case of the platinum mining activities occurring in the North-West Province of South Africa, it is the extraction value metals from the coarse grained feldspar pyroxenite ($K\text{-}NaAlSi_3O_8$) that may cause some environmental pollution, if these metals and inorganic ions enter the aquatic or atmospheric environment. The concentrations of these contaminants and their effects on human health need to be fully assessed; cognisance should also be taken of any adverse health effects on those working within the industry. In general, environmental exposure from mining activities occurs through the dust generated from the tailings storage disposal facilities. It is therefore important to determine the effects of these activities on the environment, especially in South Africa where there is a general paucity of data in the scientific literature pertaining to diffuse pollution from PGM mining (Maboeta *et al*., 2006; Gomez *et al*., 2002).

The interest in determining the concentrations and presence of palladium (Pd), platinum (Pt) and rhodium (Rh) in environmental materials has increased since the introduction of combustion engine catalytic converters. It is now commonly regarded that these pollutants are present in our environment, and result from the emission from vehicle exhausts in the form of catalyst dust (Moldovan *et al*., 2001; Gomez *et al*., 2002). Dust is deposited along roadways, on adjacent vegetation and soil, and in water bodies either directly or through runoff from mining activities and/or wastewater. Before any conclusions may be made regards the negative effects of this dust to the environment, the concentrations of heavy metals imparted to the environment need to be determined, along with their oxidation states as metallic Pt, Pd and Rh are assumed to be biologically inert. Thus it is also essential to determine the bioavailability of these metals as its presence provides a pathway for Pt, Pd and Rh to enter and accumulate in aquatic ecosystems, especially in the sediment and their effect on aquatic life normally depends on the bio-availability of the PGMs (Moldovan *et al*., 2001; Gomez *et al*., 2002).

Depending on their oxidation states and associated forms, PGMs may be toxic or harmless. The halogenated Pt compounds (e.g. $PtCl_2$, cisplatin) and Pt salts (PtO, PtO_2) are highly potent sensitizing substances that can cause asthma, rhinoconjunctivitis and contact urticaria, particularly in occupationally exposed workers working in PGM refineries and catalyst production facilities. When reviewing the health concerns of Pt, a clear distinction needs to be made between elemental (metallic) Pt and halogenated Pt compounds. The Pt metal is considered to be virtually biologically inert. However, in the case of finely dispersed Pt particles, no data are available for the South African environment. The medical use of the anticancer drug cisplatin provides a route for this compound to enter our aquatic ecosystem through domestic wastewater; therefore the endocrine disrupting effect of this compound needs investigation (Merget and Rosner, 2001).

Palladium (Pd), rhodium (Rh) and iridium (Ir) are used in smaller quantities than Pt, but the increasing presence of these compounds in the environment still warrants investigation. The use of Pd as catalyst to substitute the use of Pt is common, while Ir has also been used. Halogenated forms of these other PGMs, e.g. palladium chloride ($PdCl_2$) and rhodium chloride ($RhCl_3$), are known to be carcinogenic (Merget and Rosner, 2001; Gomez *et al*., 2002).

2.3 Metals in the environment

The determination of PGM traces in environmental matrices requires highly sensitive analytical methodology. The element that has received the most attention among the PGMs is Pt, while Pd and Rh have been monitored in more recent research projects (Zischka *et al*., 2002). The number of studies dealing with PGM in airborne particles is restricted by the limited analytical methods. Low levels of PGMs in environmental samples combined with numerous interferences in the most sensitive analytical techniques are the major difficulties in sample analysis (Rauch *et al.,* 2000).

Johnson *et al*. (1975) reported that the Pt concentration in air near a freeway in California was < 0.05 pg/m^3. In Europe, prior to the use of VECs, Pt was not found in the ambient air above the detection limit (0.05-1 pg/m^3) of the existing analytical methodology (König *et al.,* 1992). The total Pt concentration of air studied in Germany was 0.02-5.1 pg/m^3 in urban areas, whilst along a highway it reached 30 pg/m^3 with the Pt mainly present in the small (0.5-0.8 mm) particle size fraction (Alt *et al*., 1993).

Soils, dust and plants close to heavily travelled highways show high concentrations of PGMs which exceed the natural background levels. Hence, most studies have been involved in the sampling of soil and vegetation adjacent to busy highways, and dust swept from the surface of roads. These environmental samples have been analysed and the results showed an upward trend of PGM concentrations over time and a strong impact of the traffic conditions. However, in several reports regarding roadside vegetation, the data do not necessarily represent the real PGM uptake, rather the dust deposition, collection and adsorption on the external surface of the plants (Rosner *et al.,* 1991; Wäber *et al.,* 1996). High concentrations of Pt and Pd, 0.7 and 0.3 ppm respectively, were observed by Hodge and Stallard (1986) in dust collected from the surface of the leaves of roadside plants. The Pt:Pd ratio was found to be 2:5, which agreed well with the ratio in catalysts of the type utilised before the sampling period. Dust deposited on plants at the edges of streets and highways with heavy traffic shown the highest levels of both metals. The lowest concentrations were found in grass growing at the streets with light traffic.

The increasing concentration of PGMs in various parts of the water ecosystem, i.e. ground- and seawater; rain-, drinking-, sewage sludge, river and oceanic sediments are reported in several studies (Ravindra *et al.*, 2004). The PGMs enrichment in these matrices can mostly be linked to the release from VECs and it also provides evidence for post-depositional mobility of Pt and Pd in contaminated sediments. Lee (1983) and Goldberg *et al*. (1986) reported in earlier studies dating back to the 1980s levels of 40 and 150 pg/L for Pd and Pt respectively. Freshly deposited coastal sediments in the moat that surrounded the Emperor’s Palace in Tokyo were analysed and enhanced Pd levels were observed. This local Pd gradient was attributed to the run-off from adjacent roads of frequent automobile traffic (Lee, 1983).

The above literature indicates clearly that the concentration of PGMs in the environment has significantly increased. Despite some works asserting the low transportability of these pollutants, Barbante *et al*. (1999; 2001) showed that the spread of PGMs in the environment is rather a global process. Therefore, it is important to study how these metals may become chemically/bio-chemically active and mobile in interactions with various environmental matrices under the changing weather conditions. This will also enable the prediction on the possible hazards of PGMs for human health.

To study the mobility of PGMs via species transformations, a catalytic converter (monolith) was crushed and milled to a particle size of < 6.3 mm. The solubility of Pt and Rh were determined by keeping the model material in contact with soil under varying conditions, such as pH, Cl^- and sulphate concentrations. The results were compared with those performed with the use of various environmental materials (soil, run-off sediment, surface water and tunnel dust) in order to understand the mobility of PGMs in the environment (Zereini *et al.,* 1997).

2.4 Analytical techniques used for the detection of metals in environmental samples

Accurate determination of low levels of metals in environmental samples has been possible using instrumental methods which possess good sensitivities. The most appropriate methods and techniques for the determination of PGMs in the environment include inductively coupled plasma mass spectrometry (ICP-MS), instrumental neutron activation analysis (INAA), total reflection X-ray fluorescence (TXRF), inductively coupled plasma atomic emission spectroscopy (ICP-AES), and graphite furnace atomic absorption spectrometry (GFAAS) can be applied. These are well established methods and are characterised by low detection limits. However, these classical techniques require expensive instrumentation and cannot be used for field and on-site measurements (Bontidean *et al*., 2004; Peng *et al*., 2005; Emteborg *et al*., 1996; Liu *et al*., 1998).

Other instrumental techniques possess sufficient sensitivities so that a pre-concentration step is not required. One of these, adsorptive stripping voltammetry (ASV), has been used for the determination of both Pt and Rh in environmental materials (Helmers *et al*., 1998).

Electrochemical methods are routinely used in analytical chemistry. Also known as electroanalytical techniques, they have been developed for measurements in the laboratory, mostly for fundamental research. In aquatic systems oxidation-reduction potentials (ORP) and pH are measured by potentiometry (measurement of a potential), whilst trace metals and speciation are measured by voltammetry (measurement of currents over a range of potentials). Electrochemical sensors are increasingly being investigated to perform measurements *in situ* for single or multiple analytes (Taillefert *et al.*, 2000).

Electrochemical sensors have been used for years in the environmental health fields, and they have proven to be valuable tools for screening and or definitive analysis of workplace toxins. Over the last twenty five years voltammetry has been successfully used with microelectrodes to determine the concentration and speciation of some redox species in situ (Luther *et al*., 1999).

2.4.1 Different types of sensors

Some of the different approaches and techniques that have been reported in the development of different electrochemical sensors are discussed and listed below.

Švancara *et al*. (2007) developed a carbon paste electrode modified *in situ* with cationic surfactants of the quaternary ammonium salt type for the determination of platinum metals. A pre-concentration step is based on a specific accumulation mechanism involving ion-pair formation; the detection step uses cathodic scanning in the differential pulse voltammetric mode. Regarding the individual forms of platinum metals, the method has been found effective for the determination of three platinum group metals: Pt(IV), Ir(III) and Os(IV).

Somerset *et al*. (2010) reported the construction of screen-printed carbon electrode (SPCEs) and carbon paste electrode (CPEs) as “mercury free” electrochemical sensors for the determination of trace metal ions in aqueous solutions. The screen-printed carbon electrode was coated with conducting polymer films for stripping voltammetric detection. Carbon paste electrodes were modified with the conducting polymers of polyaniline (PANI) as well as with mercaptobenzothiazole (MBT). Somerset *et al*. (2010) modified the SPCE surface with poly(2,2´-dithiodianiline) (PDTDA) for the determination of inorganic mercury. The Hg^{2+} ions were determined first by pre-concentration and reduction on the modified electrode surface and secondly by subsequent stripping from the electrode surface during positive potential sweep. The experimental conditions optimised for Hg^{2+} determination included the supporting electrolyte concentration and accumulation time.

Tesarova *et al*. (2009) reported the construction of an antimony film CPE (SbF-CPE) for the determination of some selected trace heavy metals in non-deaerated model solutions of 0.01 M HCl with (pH = 2.0). Square-wave anodic stripping voltammetry were used and some important operational parameters, such as deposition potential, deposition time, and concentration of antimony ions were optimised. The newly developed sensor revealed highly linear behaviour in the examined concentration range from 5 to 50 µg/ℓ.

2.4.1.1 Amperometric Sensors

An amperometric sensor is a detection and quantitative measurement device in which redox events associated with the selective recognition of an analyte of interest are processed by an electrochemical transducer to produce signal in the form of current, the magnitude of which is proportional to the quantity of analyte present. The recognition component of an amperometric sensor usually consists of an electroactive redox substance or composite of chemical or biological origin intimately connected to the transducer's electronics. This entry deals with a special type of amperometric sensors referred to as biosensors. This class of sensors incorporates at least one biochemical step in the analyte recognition process which is coupled to the interfacial electron transfer reaction at the electrode, either directly or through an electron transfer mediator. Biomolecules (particularly redox enzymes), their immobilisation or electron relay platforms, and transducer (electrode) formats used in the development of amperometric sensors are described (Britten and Pal, 2000).

2.4.1.2 Potentiometric Sensors

Potentiometry is an analytical technique widely used for monitoring because it presents a number of advantages, such as simplicity, low cost, short measurement time, selectivity, adequate precision and accuracy, as well as ability to determine the analytes in coloured and turbid samples (Koryta *et al.,* 1983). In the functioning of a potentiometric sensor, a general operating condition of near-zero current flow is maintained and it measures the difference in potential between the working electrode and the reference electrode. The transducer may be an ion selective electrode (ISE), which is an electrochemical sensor, based on thin films or selective membranes as recognition materials. The output of a potentiometric sensor is a potential difference as a function of time. It should be noted that potentiometry is less sensitive than amperometry with a detection limit usually in the order of millimoles. Also, it is possible to determine and differentiate between chemical species of one metal depending on the compound utilised as the sensing component of the sensor. The potentiometric sensors must be robust to avoid the loss of their analytical characteristics when they are for *in situ* measurements of complicated samples or in flow analysis. Potentiometric sensors based on carbon paste matrices are economic and easy to construct. They present stable electrochemical responses and have lower ohmic resistance and longer functional lifetime than potentiometric sensor based on polymeric membranes (Abbas *et al.,* 2003; Gismera *et al.,* 2003; Khaled *et al.,* 2008).

Composite electrodes consist of at least one conductor phase (e.g. silver, gold or graphite) and one insulator phase (e.g. methacrylate or epoxy resin) (Navratil *et al.,* 2009). These electrodes offer attractive electrochemical, physical, mechanical, and economical properties. They are relatively stable in organic solvents, have long working life, present high mechanical resistance, exhibit very good sensitivity responses and signal to noise ratios. They are easily modifiable and relatively simple in preparation and surface renewal. They also have low fabrication cost and permit the incorporation of different filler components such as ligands, enzymes, cofactors, mediators, catalysts (Navratil *et al.,* 2009; Barsan *et al.,* 2009). Several new approaches and different techniques have been reported in the development of potentiometric sensors.

Sánchez-Moreno *et al*. (2010) constructed, characterized and developed a robust potentiometric sensor for determination of chromium (VI). For this purpose carbon paste and composite platforms are used to obtain potentiometric sensors based on solid-state membranes. An epoxy resin is tested for the composite electrode preparation. The carbon paste and the composite matrix are modified with diphenylcarbazide (DPC), a selective reagent for chromium (VI) widely used for its spectrophotometric determination. In both cases, this modifier is distributed and blended throughout the electrode material. The composition of sensor matrices is optimised for the carbon paste and composite electrodes. The principal analytical parameters of the sensors such as linear response range, detection limit, pH effect, response time and selectivity to other species were evaluated.

2.4.1.3 Voltammetric techniques for electrochemical detection

Voltammetry is an electrochemical method that is based upon the measurement of current as a function of applied potential. Voltammetric measurements are carried out with working or indicator electrodes. The voltage is controlled and the current at the electrode is measured. Linear sweep (scan) voltammetry involves the varying of voltage linearly with time. Cyclic voltammetry is linear sweep voltammetry cycling between limits. Experimental techniques in voltammetry involve the use of three electrodes e.g. working electrode (WE), auxiliary electrode (AE) and reference electrode (RE). A potentiostat controls the potential between WE and RE, while current flows between WE and AE. Examples of working electrodes are platinum (Pt), gold (Au), glassy carbon, pyrolytic graphite and dropping mercury electrode (DME). Working electrode design may be in disk, foil or wire form. Reference electrode includes Ag/AgCl and SCE. Auxiliary electrode is usually of the form of large surface area platinum (Somerset, 2010).

2.4.1.4 Cyclic voltammetry

Cyclic voltammetry (CV) is popular for its relative simplicity and gives much analytical information. Cyclic voltammetry is often used as a diagnostic tool for elucidating electrode mechanisms. In the past it was first practised at a hanging mercury drop electrode (HMDE), and now it has gained widespread use when solid electrodes like Pt, Au and carbonaceous electrodes were used to study anodic oxidations. A major advance was made when mechanistic diagnostics and accompanying quantifications became known through computer simulations (Kemula and Kumblik, 1958; Adams, 1968).

A cyclic voltammogram is obtained when a voltage is applied to a working electrodes, this voltage varies linearly with time. Cyclic voltammetry is performed at a specific scan rate (v, mV/s), which is also the slope (V/s). Voltammetry is performed at a specific potential (E_p) window which starts from an initial potential (E_i), proceeds to a switching potential (E_λ) and continuous on a reverse scan (Somerset, 2010).

2.4.1.5 Stripping voltammetry

According to Willemse (2009), stripping voltammetry is a very sensitive electrochemical technique for the determination of trace metal analysis. This technique consists of three steps. In the first step the metal ions are deposited onto the electrode surface, which is held at a suitable potential and the solution is stirred to minimize the amount of metal deposited. The second step is where stirring is stopped so that the solution becomes quiescent. In the third and final step, the metals which were deposited are to be stripped from the electrode by scanning the potential. The voltammogram recorded during the step provides the analytical information of interest. The observed stripping current is related to the amount of metal in the solution.

2.4.1.6 Chronoamperometry

Stationary electrodes are used in chronoamperometry, the solution is kept unstirred to facilitate mass transport by diffusion. A constant potential is applied between electrodes and the measurement is current *vs.* time.

Assume $\text{Oxidation} + ne^- \leftrightarrow \text{Reduction}$ **Eqn. 1**

The oxidation and reduction reactions are both soluble, chronoamperometry is a reversible reaction (electrochemically), and the potential is set so reduction goes to completion at the electrode surface. Chronoamperometry can measure concentration by measuring current *vs.* concentration at any fixed time. It can also analyze the shape of the current-time curve in order to study coupled chemical reactions. In chronoamperometry there are better ways to do both of these with more modern techniques. Chronoamperometry is important because it is a fundamental method on which other techniques are based (Bard and Faulkner, 2001).

2.4.1.7 Use of complexing agents

Platinum and rhodium complexes can be studied with hexamethylene tetramine (HMTA) as complexing agent. Hexamethylene tetramine contains ‘N’ donor atoms and has excellent adsorbing properties at a chemical sensor surface. There are reports dealing with the adsorptive stripping voltammetric determination of platinum group metals. Using HMTA as the complexing agent is superior in terms of sensitivity and stability (Dalvi *et al*., 2008). Dimethylglyoxime (DMG) is a chelating agent, which can form complexes with metal ions. Tschugaeff (1905) first used DMG as an analytical reagent for the gravimetric determination of Ni. According to Zhang *et al*. (1996) DMG is an excellent spectrophotometric reagent, and can also be used in electroanalytical methods. Dimethylglyoxime (DMG) can be also used to determined Ni(II), Pd(II), and Co(II) by adsorptive voltammetry. Trojanowicz and Matuszewski (1989) proposed a pentiometric stripping procedure for the determination of nickel with DMG-CPEs. A differential pulse polarographic method was described by Baldwin *et al*. (1986) for the quantification of Ni(II).

A number of ligands, such as dimethylglyoxime, the derivatives of phenolthiozine have been studied for the determination of palladium by ASV. In the DMG-base and phenolthiozine-base methods, the detection limit was 1 ng/mℓ, in the presence of interfering ions, such as Ag(II) and Zn(II) (Wang and Varughese, 1987; Sanke Gowda *et al*., 1975; Sanke Gowda *et al*., 1976).

CHAPTER 3: SOUTH AFRICAN WATER MANAGEMENT AREAS (WMAs)

The River Health Programme (RHP) was initiated in 1994 by the Department of Water Affairs and Forestry (DWAF), now called the Department of Water Affairs (DWA). With DWA as the leading agent, the initial programme was formally started as the South African National Aquatic Ecosystem Biomonitoring Programme (NAEBP). With the programme focussing on riverine ecosystems, the name was changed and it was called the River Health Programme (RHP).

As the custodian of water resources in South Africa, the DWA is responsible for the protection of the health of aquatic ecosystems, thereby ensuring the ability of these systems to support utilisation for the benefit of current and future generations. The RHP was further designed to develop the capacity and information base to enable researchers in the fields of limnology, aquatic ecosystems, water quality and toxicology, etc. to report on the ecological state of the river systems, in an objective and scientifically sound manner. At the same time, it was envisaged that the programme audits management strategies and actions related to water resources. The information generated through various RHP State-of-the-River Reports assists in identifying areas of sustainable utilisation and unacceptable ecological deterioration (RHP, 2006).The following paragraphs contain a map of South Africa that is divided into 19 Water Management Areas (Figure 6, p. 16), of which WMAs 1 to 4 are pertinent to this study. The four WMAs are described below (see sections 3.1 to 3.4).The following paragraphs contain a descriptive summary of the WMAs of interest.

3.1 Limpopo (WMA 1)

The Limpopo WMA is situated in the Northern Province and borders Mozambique to the east, Botswana to the west and Zimbabwe to the north. Major tributary rivers in this WMA include the Lephalala, Mokolo and Mogalakwena rivers which, together with other minor perennial and seasonal rivers, flow into the Limpopo River. The mean annual rainfall for this WMA is 300-700 mm per annum (mm/a), with the climate strongly seasonal with characteristic wet summers and dry winters. The main topographic features comprise the Soutpansberg mountain range in the north-east and the Waterberg mountain range in the south. Vegetation is characterised by grasslands and bushveld, while the geology is characterised by igneous and metamorphic rocks in the north and east, with sedimentary rocks dominating in the south and west. This WMA comprises five sub-catchments due to variations in climatic conditions and water availability and utilisation. It is characterised by very low surface runoff of approximately 986 million cubic metres per annum (m^3/a), mainly due to the relatively low rainfall and high to very high rates of evaporation. Groundwater is the major water source in this WMA particularly for rural settlements. Major industries in this WMA include agriculture, coal, PGM and base metal mining, and cement milling/blending. Approximately 74% of the region’s water is required for irrigation with the rest of the resource utilised for urban, industrial and mining operations (DWAF, 2003a).

This WMA has very limited water resources (which are on the verge of stress due to pollution) but they are in balance with the water requirements of the WMA. The possibility of further development of the groundwater supply for basic human needs and for community gardens exists, but careful planning and investigation is required to ensure sustainable management of the resource. The existence of the rich, but largely unexploited mineral deposits of the Bushveld Igneous Complex holds the greatest potential for economic growth in this WMA. It is not certain yet when the development and mining of this mineral deposit will commence, but it is prudent that water be reserved for this purpose (DWAF, 2004).

The sub-areas in this WMA are the Matlabas/Mokolo, Lephalala, Mogalakwena, Sand and Nzhele/Nwaned area. Several PGM mining activities can be found in this WMA that overlaps in the Matlabas/Mokolo, Lephala and Mogalakwena sub-areas.

In Table 1 a description of the eco-region(s) and/or sub-management areas close to PGM mining activities are given.

Table 1. **Information on the sub-management areas in the Limpopo WMA is provided with the main rivers and tributaries listed, while the state of the water quality is indicated.**

Sub-Management Areas (SMAs)	Main Rivers and Tributaries	Water Quality
Matlabas/Mokolo	Matlabas; Mokolo; Sterkstroom; Nyl; Sand; Klein-Sand	1. FAIR to GOOD 2. Intermediate levels of nutrients are emerging and can be attributed to various sources.
Lephalala	Lephalala; Goud; Bloklandspruit; Melk	1. FAIR to GOOD 2. Intermediate levels of nutrients are emerging and can be attributed to various sources.
Mogalakwena	Mogalakwena; Seepabana; Matlalane; Dorps; Mokamole; Doorndraai; Nyl; Sterk	1. FAIR to POOR 2. Intermediate levels of nutrients and emerging signs of water quality problems attributable to organic pollution. 3. Impacts on water quality originate primarily from human activities; mines acting as a salt sink; increasing salinity levels in both surface and groundwater resources.

Table 1 evinces that the water quality in the Mogalakwena sub-management area (SMA) is fair to poor, with PGM mining occurring in this SMA. This WMA did not form part of the RHP programme and the only assessment on the state of the rivers is available from the Department of Water Affairs (DWA). A lack of information is making it difficult to properly assess the current state of the WMA. No pollution information is available on the heavy and PGMs associated with mining activities.

3.2 Luvuvhu-Letaba (WMA 2)

This WMA lies within the Limpopo Province and borders Zimbabwe to the north and Mozambique to the east. It also borders the Olifants and Limpopo WMA to the south and west, respectively. Its major rivers include the Letaba, Shingwedzi and Luvuvhu. On the western periphery, the Letaba River rises in the Drakensberg Mountains, flows eastwards through the Kruger National Park and joins the Olifants River close to the Mozambiquan border. Other rivers on the eastern side of this WMA include the Olifants River that enters Mozambique and joins the Limpopo River, before discharging into the Indian Ocean. Similarly, the Shingwedzi River joins the Limpopo River near the Mozambique border. The Luvuvhu River rises in the Soutpansberg Mountains and flows through the Kruger National Park to join the Limpopo River at the South African border. This WMA generally experiences a sub-tropical climate, with a summer rainfall regime that is influenced by the topography of the Drakensberg and Soutpansberg Mountains. The natural mean annual runoff is approximately 1185 million m^3/a (RHP, 2006; DWAF, 2003b).

The Tzaneen and Letsitele regions of the Letaba Catchment support the farming of citrus, mango, and banana crops. The Klein Letaba, Molototsi and Nsama river catchments are also dominated by rural populations involved in subsistence farming activities with cattle, goats and vegetables. In the Levubu agricultural area in the Luvuvhu Catchment the production of citrus, mangos, bananas and macadamias can be found. Further downstream in the Luvuvhu Catchment, the Mutshindudi and the Mutale River catchments are dominated by the presence of rural community gardens, cattle and goats for subsistence farming. Siltation originating from forestry roads in this WMA is a serious problem. It is recommended that improved management practices be incorporated in timer felling practices during the rainy season, as this will reduce wash-off of soil into the associated rivers (RHP, 2001).

Luvuvhu-Letaba was chosen as a reference site and was sampled close to Haenertsburg, north of Polokwane and east of Tzaneen, in the absence of PGM mining activities in this area.

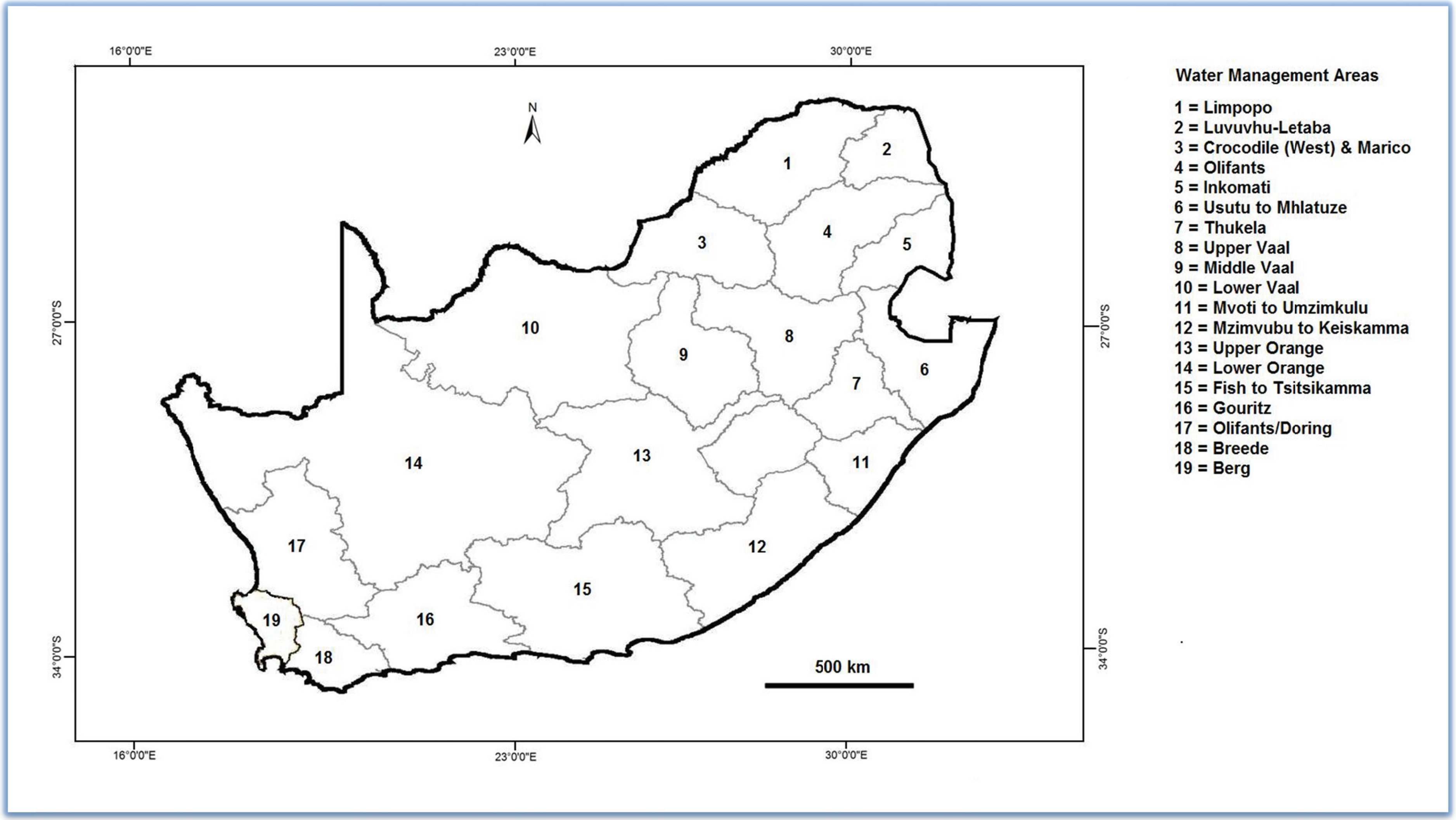

Figure 6. **Map identifying the location of the 19 Water Management Areas of South Africa. Adapted from Somerset *et al*., 2010.**

Table 2 describes the eco-region(s) and/or sub-management areas close to PGM mining activities for Luvuvhu-Letaba and shows that this WMA has a fair to good assessment of its water quality. Similarly, the information further indicates that a lack of information is making it difficult to fairly assess the current state of the WMA. No pollution information is available on the heavy metals and PGMs associated with the metals industrial sector.

Table 2. Information on the sub-management area in the Luvuvhu-Letaba WMA is provided with the main rivers and tributaries listed, while the state of the water quality is indicated.

Sub-Management Area	Main Rivers and Tributaries	Water Quality
Central Highlands (Ecoregion 2.15)	Broederstroom; Politsi; Debengeni; Great Letaba	1. FAIR to GOOD 2. Sandmining for building purposes has disrupted the river channel and riparian zone of the Broederstroom as well as several tributaries.

3.3 Crocodile (West) and Marico (WMA 3)

The Crocodile (West) and Marico WMA is mainly situated in the North West Province, bordering Gauteng and Limpopo Provinces in the north and southwest, respectively. The Crocodile and Marico are the two main rivers. The topography is fairly homogeneous and includes the Magaliesberg, Waterberg, Pilanesberg and Witwatersrand. This WMA receives a mean annual rainfall of 400-800 mm/a, and has a mean annual runoff of approximately 855 million m^3/a. The geology of the catchment consists largely of rocks forming the Bushveld Igneous Complex, which contain extensive mineral deposits. This has resulted in extensive mining operations impacting the WMA, particularly the platinum and chrome mines near Rustenburg. Water from the Crocodile River is also extensively used for irrigation of agricultural produce. The main dam in this WMA is the Hartbeespoort Dam, and is severely impacted by effluents from municipal wastewater treatment works and industry in Gauteng, as well as diffuse pollution from the adjacent agricultural areas. This has resulted in hyper-eutrophication and the presence of dense cyanobacterial blooms (often toxic) in many of the area’s water resources (RHP, 2005).

The overall ecological status of the Crocodile (West) Marico WMA is poor, with 13 of the 23 units within the WMA surveyed classified as poor. This data reflects the status of the WMA at the time of the compilation of the RHP report, March 2005. The industrial, mining and agricultural sectors within this WMA play a vital role in contributing to the economic achievements of this area and are highly dependent on water resources within the WMA to succeed. It should be noted that some parts of the WMA are still in good to natural condition, primarily in the headwaters of catchments with very little development and human impact (RHP, 2005).

Table 3 describes the eco-region(s) and/or sub-management areas close to PGM mining activities. The information indicates that the water quality in this WMA and the indicated sub-management areas (SMAs) ranges from fair to poor. This WMA is the heart of the platinum mining activities in the country but no data on the extent to which the mining activities influence ecosystem health are available, except for the RHP assessment.

Table 3. Information on the sub-management areas in the Crocodile (West) and Marico WMA is provided with the main rivers and tributaries listed, while the state of the water quality is indicated.

Sub-Management Areas	Main Rivers and Tributaries	Water Quality
Elands	Elands; Koster; Selons; Hex; Klein Hex	1. FAIR 2. Large settlements and mines present in the area. 3. Flows have intermediate levels of nutrients and there is emerging evidence of organic pollution – this might be nutrients from the surrounding platinum mines.
Upper Crocodile	Sterkstroom; Magalies; Skeerpoort; Rosespruit; Kareespruit; Crocodile; Hennops; Jukskei; Klein Jukskei	1. FAIR 2. Intermediate levels of nutrients and emerging signs of water quality problems attributable to organic pollution – signs of eutrophication visible. 3. Impacts on water quality originate primarily from human activities; mines acting as a salt sink; increasing salinity levels in both surface and groundwater resources.
Lower Crocodile	Sundays; Crocodile downstream of Roodekopjes	1. POOR 2. River flows have between low and intermediate levels of nutrients and are heavily contaminated with organic pollution.

3.4 Olifants (WMA 4)

The Olifants WMA is situated in three of South Africa’s provinces, including the Gauteng, Mpumalanga and the Limpopo Province. The Olifants River is the major water resource in this WMA. The geology of the WMA is largely represented by hard rock formations and is dominated by granite and dolerite. The highly seasonal rainfall mostly occurs during summer, when high temperatures produce low pressure and high moisture contents. The mean annual precipitation is higher in the south-west regions of the WMA and declines towards the east, with the annual value for the entire WMA estimated at 630 mm/a. Commercial afforestation (e.g. pines, eucalyptus and acacias) accounts for the main industry found in the WMA and stretches over a total area of approximately 1988 km². Rich coal deposits are located close to the Upper Olifants River catchment in this WMA and it contains the largest area of coal mining activity in South Africa. The success of South Africa’s electricity sector can be attributed to the coal reserves in the Highveld region of this WMA, where most of the country’s coal-fired power stations are located. Other mineral deposits of gold, platinum, phosphate, copper and diamond are also found in this WMA, with the associated mining activities also occurring (DWAF, 2003c).

This is a large catchment and the existence of extensive alien vegetation invasion and regulation of river flows by about 30 storage dams has caused environmental degradation downstream, particularly in the middle and lower parts of the catchment. The Olifants River catchment is dominated by mining activities, with some industries and large areas of agriculture contributing to the current poor state of the catchment (DWAF, 2003c).

Of particular interest is the Steelpoort River sub-basin, which is one of the eight sub-basins of the Olifants River basin. The Steelpoort River sub-basin is further divided into three sub-basins called the: Upper Steelpoort, Central Steelpoort and Lower Steelpoort sub-basins (Stimie *et al*., 2001).

Table 4 describes the eco-region(s) and/or sub-management areas close to platinum mining activities for this WMA indicating that the water quality in this WMA and sub-basins ranges from fair to poor, highlighting the current poor state of the ecosystem health in this WMA. The Steelpoort sub-basins support the second most intensive PGM mining activities in the country and these activities have already impacted the WMA to a large extent. No pollution information is available on the heavy and PGMs associated with mining.

Table 4. **Information on the sub-management areas in the Olifants WMA and Steelpoort sub-basins are provided with the main rivers and tributaries listed, while the state of the water quality is indicated.**

Sub-Management Areas	Main Rivers and Tributaries	Water Quality
Steelpoort sub-basins		
Upper Steelpoort	Witpoort; Waterval	1. FAIR to POOR 2. Increasing levels of contaminants from industrial, agricultural, mining and residential sources.
Middel Steelpoort	Groot Dwars; Spekboom	1. FAIR to POOR 2. Increasing levels of contaminants from industrial, agricultural, mining and residential sources.
Lowe Steelpoort	Klip; Klein Dwars; Tonteldoosloop	1. FAIR to POOR 2. Increasing levels of contaminants from industrial, agricultural, mining and residential sources.

3.5 Conclusions

The current state of the WMAs in which platinum mining activities are currently taking place were identified and assessed with the limited data on water quality available. A scope of the current PGM mining activities in the country was presented as well as a focus on how it impacts on the water resources. The health risks associated with the metal pollutants were highlighted. Little or no information is available in the scientific literature on any pollution that could be associated with mining in the four selected WMAs. This is not a good state of the environment report and highlights that a lot of work of still needs to be done.

CHAPTER 4: ANALYSIS OF SELECTED METAL CONCENTRATIONS IN RIVER CATCHMENTS OF THE NORTH WEST AND LIMPOPO PROVINCES

The presence and determination of the levels of platinum (Pt), palladium (Pd) and rhodium (Rd) (precious group metals – PGMs) in the environment has received increased attention due to increased mining of these minerals and their applications in automobile catalytic converters. River sediments act as sinks for metals and can provide important information for aquatic pollution research (Kishe and Machiwa, 2003). If a sediment column remains relatively undisturbed, it can provide a historical record of the geochemical characteristics in the aquatic ecosystem. It also allows geochemical evaluations over time and allows researchers to establish baseline levels that can be used in the comparison of pollution levels. This is helpful in the determination of pollution levels of heavy metals, since cadmium (Cd), mercury (Hg), lead (Pb), copper (Cu) and zinc (Zn) are regarded as serious pollutants of aquatic ecosystems due to their environmental persistence, toxicity and ability to be incorporated into food chains (Kishe and Machiwa, 2003; Phillips, 1995; Alcorlo *et al*., 2006). Contamination by PGMs mainly occurs from airborne particles such as roadside dust, although contamination from sludge and wastewater has also been reported. Once in the aquatic ecosystem metals may bioaccumulate in living organisms through diverse pathways (Ravindra *et al*., 2004).

In this chapter the concentrations of heavy metals and PGMs from sampling sites adjacent to platinum mining activities are assessed, to evaluate the heavy metal burden in the aquatic environment that might have resulted from anthropogenic origin. The study area included the four WMAs described in Chapter 3. The geographical location of the sampling sites is shown in Figure 7, with a brief description of the location of the sampling sites given in Table 5.

The purpose of this chapter was to provide a basic understanding of the regional impacts of potential PGM mining activities on aquatic ecosystems, by assessing selected metal ion concentrations in water, sediment and biota samples collected from the Limpopo, Luvuvhu-Letaba, Crocodile (West) and Marico and Olifants WMAs. With this information in hand, it is hoped that a better understanding will be obtained on the current status of the regional aquatic ecosystems around PGM mining activities. This report aims to provide information that will enable mining companies to improve current and future environmental management practices, thereby ensuring a sustainable environment for all stakeholders.

This section has been structured so that there is clear focus on what was found in each of the environmental compartments of the aquatic ecosystem, pertaining to the metal ion concentrations.

4.1 Surface water quality

4.1.1 Methods

4.1.1.1 Field measurements and sample collection

Surface water field measurements were performed *in situ* upon arrival at each site with portable field meters. Samples were collected during low (August 2010) and high flow (November 2010) seasons to represent seasonal variability. The following physico-chemical parameters of the water were measured at each sampling site: pH, temperature, electrical conductivity (EC), total dissolved solids (TDS) and dissolved oxygen (DO). Electrical conductivity and TDS were measured using a Hanna Instrument Model 9033 conductivity meter, for which the TDS is defined as a factor of 5.5 multiplied with the EC measurement as described in the operational manual. Measurement of pH was conducted using a Hanna Instrument Model 9025 pH Meter; while temperature and DO were measured using the YSI Model 51B Oxygen Meter.

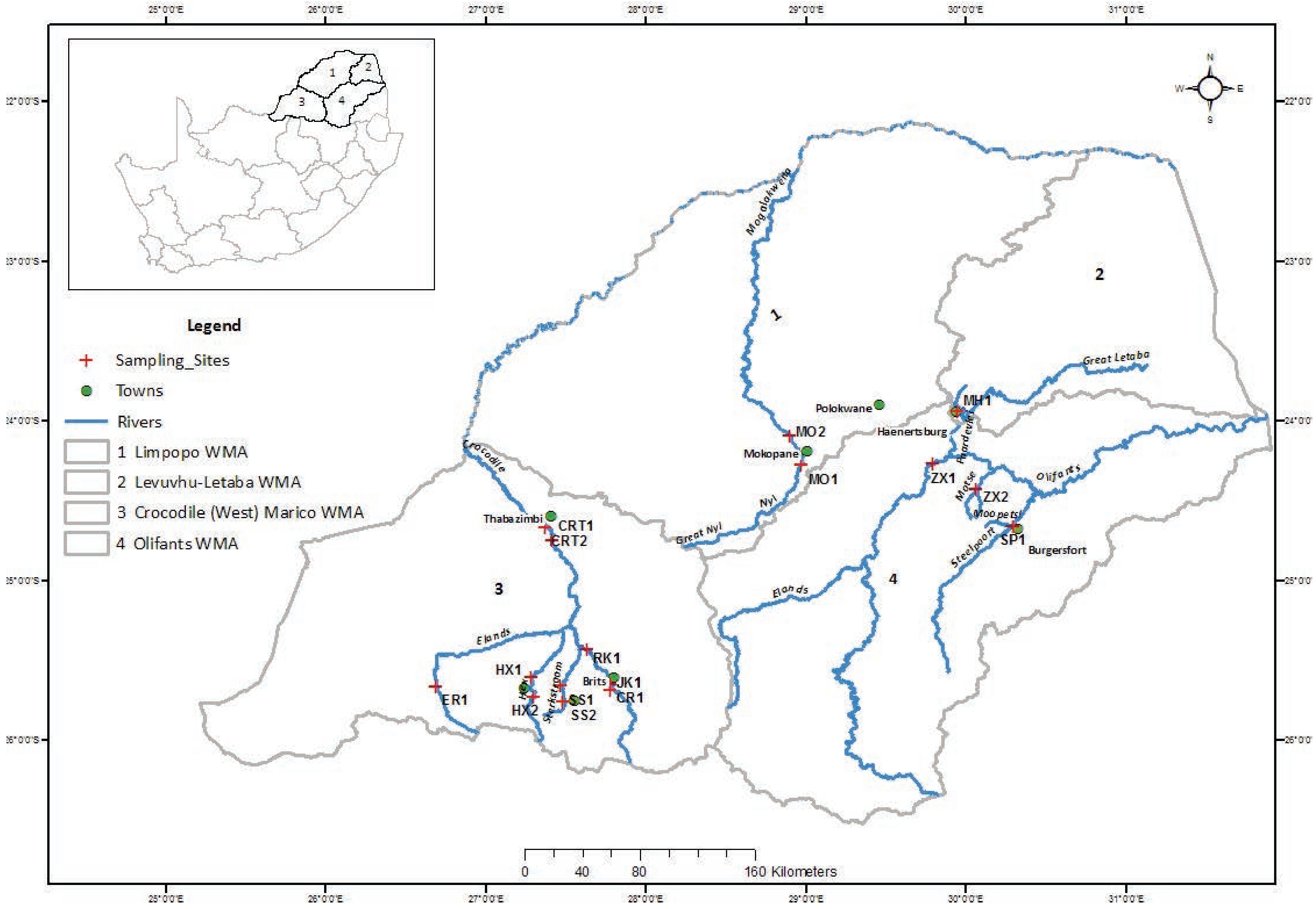

Figure 7. Map of the geographical location of the sampling sites in four different WMAs in South Africa.

Table 5. **Location and brief description of sampling sites selected in close proximity to PGM mining activities in four WMAs.**

Site Code	River	Site Description	WMA	Geographical Coordinates	
				Latitude	Longitude
JK1	Maretlwane River	Close to the mining facility and Wonderkop Township	Crocodile (West) & Marico	S 25º 39.452'	E 27º 28.159'
HX1	Hex River	Downstream of Pt mines, close to Boitekong Township off R510	Crocodile (West) & Marico	S 25º 43.620'	E 27º 18.272'
HX2	Hex River	Upstream of Pt mines, at bridge over N4	Crocodile (West) & Marico	S 25º 36.498'	E 27º 17.338'
CR1	Crocodile River	South of Brits CBD on R512 to Rustenburg	Crocodile (West) & Marico	S 25º 38.844'	E 27º 46.767'
RK1	Rooikoppies Dam	Downstream of Pt mines on Crocodile River, off R511 close to gate entrance to camping site on dam	Crocodile (West) & Marico	S 25º 25.885'	E 27º 38.015'
CRT1	Crocodile River	Close to the Amandelbult mine, upstream of the mines near R511	Crocodile (West) & Marico	S 24º 44.655'	E 27º 24.957'
CRT2	Crocodile River	Next to R510 road into Thabazimbi, downstream of the mines	Crocodile (West) & Marico	S 24º 39.842'	E 27º 22.511
MO1	Mogalakwena River	Upstream of Pt mine near Mokopane (wetland conditions)	Limpopo	S 24º 16.580'	E 28º 58.512'
MO2	Mogalakwena River	Downstream of Pt mine at bridge on R511	Limpopo	S 24º 05.637'	E 28º 54.122'
ZX1	Olifants River	Outside Zeekoeigat close to Bokoni Pt Mine	Olifants	S 24º 16.052'	E 29º 47.964'
ZX2	Motse River	At bridge over dried-up Motse river close to Twickenham Pt mine after turn-off on R37	Olifants	S 24º 25.814'	E 30º 04.173'
SP1	Steelpoort River	Downstream of Pt mine under bridge on R37 towards Burgersfort	Olifants	S 24º 39.513'	E 30º 18.189'
MH1	Mohlapitsi River	Just outside Haenertsburg, close to the Tzaneen turn-off on R71	Luvuvhu-Letaba	S 23º 56.320'	E 29º 56.842'
ER1	Elands River	Elands River at Swartruggens Dam – Reference site	Crocodile (West) & Marico	S 25º 39.806'	E 26º 41.490'
SS1	Sterkstroom River	Downstream of Pt Mines near Marikana	Crocodile (West) & Marico	S 25º 39.452'	E 27º 28.159'
SS2	Sterkstroom River	Upstream of Pt Mines near Marikana	Crocodile (West) & Marico	S 25º 45.357'	E 27º 29.040'

Clean handling techniques were followed during all phases of sample collection, storage and analyses. Surface water samples for standard chemical analysis were collected in duplicate (*n = 2*) in pre-rinsed, 500 mL polyethylene bottles that were firmly sealed following acidification with a 0.5% v/v HCl solution. The samples were then labelled, double-bagged and transported on ice to the analytical laboratory for analysis within 72 hours of collection in the field (Somerset *et al*., 2010; Williams *et al*., 2010).

4.1.1.2 Laboratory analyses

Water samples were processed as follows, with the duplicate samples collected. On arrival at the laboratory, all samples were stored at 4ºC in a cold room for up to a maximum of 72 hours prior to analysis. The standard chemical analysis procedures for all the water samples followed the analytical methods detailed in "*Standard Methods for the Analysis of Water and Wastewater*" (APHA *et al*., 1992). The following water quality variables were analysed in all water samples: aluminium (Al), cadmium (Cd), iron (Fe), nickel (Ni), lead (Pb), zinc (Zn), palladium (Pd), platinum (Pt), rhodium (Rh), sulphate (SO_4^{2-}), nitrate-nitrogen plus nitrite-nitrogen and total phosphate. All results were expressed in milligrammes per litre (mg/ℓ) (Oberholster *et al*., 2009).

Spectrophotometric analysis was performed on the water samples. Atomic emission spectrometry (AES) analyses were used to quantify the metals of interest (*i.e.,* Pb, Cd, Fe, Al, Ni, Pt, Pd and Rh). The modified XP1500 Method and inductively coupled atomic emission spectrometry (ICP-AES) were used to analyse metal concentrations of Pb, Cd, Fe, Al, Ni, Pt, Pd and Rh in all water (Madejon *et al*., 2004; Ip *et al*., 2007).

Total mercury (TotHg) determination in water samples followed the US EPA Method 1631 (USEPA, 2002).

4.1.1.3 Quality control

Adherence to Quality Assurance (QA) and Quality Control (QC) procedures was of high standard throughout the collection and analysis of samples in this study. Therefore, it is believed that the QA / QC program followed in this study allowed for the creation of a reasonably reliable dataset of measurements of heavy metal concentrations.

Details of the QA / QC process involved the following steps: (i) weekly validation of the analytical methods employed; (ii) continuous monitoring of the measurement performance of the analytical instruments; (iii) estimation of associated measurement uncertainties and establishing metrological traceability with the use of certified reference materials (CRMs); (iv) use of ultrapure standards and CRMs for calibration performances; (v) use of a logbook for record keeping of a summary of the precision (measurement reproducibility expressed as relative standard deviation) and accuracy (bias expressed as relative difference to the certified value) established from QC measurements; (vi) standardised communication of results; (vii) controlled sample submission and processing procedures; (viii) routine laboratory environment checks; (ix) adherence to general laboratory practice (GLP) guidelines.

4.1.2 Results

4.1.2.1 Field measurements

The results for the field measurements in August 2010 (Table 6) show that the pH of most of the rivers were slightly alkaline with values >8 for a total of eight sites, while for three sites circumneutral values were measured. Similarly, the water temperature measurements reflect the cooler winter conditions during August 2010 as the readings were 10.4-23.3ºC. Electrical conductivity and TDS values were low and varied between the sites. The DO concentrations were 0.58-10.70 mg/ℓ between sampling sites reflecting very low to moderate concentrations. In the case of Maretlwane River, Crocodile River and Olifants River the DO readings indicated poor water quality (shown in grey shade). The results for the redox potential measurements were all positive values between 66.9 and 207.5 mV, indicating that there was sufficient DO present in the surface water to allow any dissolved metals to be oxidised.

The results obtained in November 2010 (Table 7) indicate that the pH of rivers was 6.98-8.87. The water temperature ranged between 16.5ºC and 28.6ºC reflecting the summer conditions. As with the August results, EC and TDS values were low and varied between the sites. Similar results for the DO and Eh readings were obtained in November as in August. For sites Mogalakwena River 1, Olifants River and Sterkstroom River 2 the DO readings reflected poor water quality (shown in grey shade). The results for the Eh measurements were 67.8-139.5 mV.

4.1.2.2 Results of laboratory chemical analyses

Sulphate concentrations were within the guideline values (DWAF) during both sampling periods.. The results obtained showed nitrate-nitrogen plus nitrite-nitrogen levels were also low except for sites Maretlwane River and Hex River 1 (August 2010), and Hex River 2 (November 2010) which exceeded the DWAF guideline value. This is shown in grey shade in Tables 6 and 7. High phosphate concentrations were observed during both sampling trips, with six sites (August 2010) and eight sites (November 2010) showing concentrations exceeding the guideline value. This is shown in grey shade in Tables 6 and 7.

The results for the concentrations of almost all the metals were below the detection limits of the laboratory analyses in both August and November. No DWA water quality guideline values currently exist for PGMs. For some PGMs elevated concentrations were obtained in both August and November 2010.

Table 6. **Comparison of water quality data collected at sampling sites in August 2010. Data are compared to DWAF 1996 water quality guidelines (Target Water Quality Range) for aquatic ecosystems, domestic and irrigation. Results shaded in grey indicate that the limit is exceeded. NS = No sample collected; ND = parameter not determined.**

		Guideline Values (DWAF)			Sampling Site															
Field Data		Ecosystems	Domestic use	Irrigation	Maretlwane River	Hex River 1	Hex River 2	Crocodile River 1	Rooikoppies Dam	Crocodile River (Thabazimbi) 1	Crocodile River (Thabazimbi) 2	Mogalakwena River 1	Mogalakwena River 2	Olifants River	Motse River	Steelpoort River	Mohlapitsi River	Elands River	Sterkstroom River 1	Sterkstroom River 2
pH		-	-	-	8.27	8.22	7.64	8.76	9.22	8.54	8.78	6.66	NS	8.18	NS	8.55	7.05	NS	NS	NS
Temp.	ºC	-	-	-	13.3	17.4	13.9	13.3	20.7	17.0	23.3	13.9	NS	20.6	NS	20.6	10.4	NS	NS	NS
EC	mS/m	-	-	-	82.5	92.0	30.0	58.5	63.5	84.0	105.0	17.0	NS	62.0	NS	51.5	2.0	NS	NS	NS
TDS	mg/ℓ	-	-	-	453.8	506.0	165.0	321.8	349.3	462.0	577.5	93.5	NS	341.0	NS	283.3	11.0	NS	NS	NS
DO	mg/ℓ	-	-	-	**0.58**	9.35	10.05	**2.38**	4.50	5.62	6.97	6.76	NS	**2.96**	NS	5.22	10.70	NS	NS	NS
Eh	mg/ℓ	-	-	-	194.8	155.3	207.5	130.2	155.9	78.4	66.9	85.4	NS	199.9	NS	91.9	115.9	NS	NS	NS
Major Anions																				
SO_4	S mg/ℓ	-	<200	-	33.0	22.4	7.1	14.6	23	26.7	29.3	0.5	NS	36.6	NS	11.6	<0.3	NS	NS	NS
Nutrients																				
NO_3 + NO_2	N mg/ℓ	-	<6	-	**10.3**	**11.3**	0.9	2.9	1.3	1.5	1.4	<0.1	NS	0.1	NS	1.9	0.3	NS	NS	NS
Total PO_4	P mg/ℓ	<0.005	<0.1	-	<0.05	**0.29**	<0.05	**0.21**	**0.17**	**0.23**	**0.13**	**0.05**	NS	<0.05	NS	<0.05	<0.05	NS	NS	NS
Trace metals																				
All	mg/ℓ	<0.005	<0.015	<5	<0.02	<0.02	<0.02	<0.02	<0.02	<0.02	<0.02	<0.02	NS	<0.02	NS	<0.02	<0.02	NS	NS	NS
Cd	mg/ℓ	<0.25	-	<0.01	<0.005	<0.005	<0.005	<0.005	<0.005	<0.005	<0.005	<0.005	NS	<0.005	NS	<0.005	<0.005	NS	NS	NS
Fe	mg/ℓ	-	<0.05	<0.02	<0.01	<0.01	<0.01	<0.01	<0.01	<0.01	0.01	1.8	NS	0.04	NS	<0.01	0.57	NS	NS	NS
Ni	mg/ℓ	-	-	<0.2	<0.01	0.01	<0.01	<0.01	<0.01	<0.01	0.01	<0.01	NS	<0.01	NS	<0.01	<0.01	NS	NS	NS
Pb	mg/ℓ	<0.0002	<0.01	<0.2	<0.02	<0.02	<0.02	<0.02	<0.02	<0.02	<0.02	<0.02	NS	<0.02	NS	<0.02	<0.02	NS	NS	NS
Zn	mg/ℓ	<0.2	<3	<1.0	<0.01	<0.01	<0.01	<0.01	<0.01	<0.01	<0.01	<0.01	NS	<0.01	NS	<0.01	<0.01	NS	NS	NS
PGMs																				
Pd	mg/ℓ	-	-	-	<0.01	<0.01	<0.01	0.011	<0.01	<0.01	<0.01	<0.01	NS	<0.01	NS	<0.01	<0.01	NS	NS	NS
Pt	mg/ℓ	-	-	-	<0.01	<0.01	0.02	0.01	0.01	0.01	<0.01	0.02	NS	0.03	NS	0.02	<0.01	NS	NS	NS
Rh	mg/ℓ	-	-	-	<0.01	<0.01	<0.01	<0.01	<0.01	<0.01	<0.01	<0.01	NS	<0.01	NS	<0.01	<0.01	NS	NS	NS

Table 7. **Comparison of water quality data collected at sampling sites in November 2010. Data are compared to DWAF 1996 water quality guidelines (Target Water Quality Range) for aquatic ecosystems, domestic and irrigation. Results shaded in shaded grey indicate that the limit is exceeded. NS = No sample collected; ND = parameter not determined.**

		Guideline Values (DWAF)			**Sampling Site**															
Field Data		Ecosystems	Domestic use	Irrigation	Maretlwane River	Hex River 1	Hex River 2	Crocodile River 1	Rooikoppies Dam	Crocodile River (Thabazimbi) 1	Crocodile River (Thabazimbi) 2	Mogalakwena River 1	Mogalakwena River 2	Olifants River	Motse River	Steelpoort River	Mohlapitsi River	Elands River	Sterkstroom River 1	Sterkstroom River 2
pH		-	-	-	NS	7.86	7.86	8.23	7.62	8.31	8.87	7.01	NS	8.64	NS	8.41	6.98	7.24	NS	8.32
Temp.	ºC	-	-	-	NS	22.1	23.0	21.7	23.9	24.8	28.6	22.4	NS	26.1	NS	23.0	16.5	24.4	NS	24.9
EC	mS/m	-	-	-	NS	45.5	136.0	69.5	82.5	111.5	131.5	37.0	NS	88.0	NS	88.0	4.5	15.5	NS	27.5
TDS	mg/ℓ	-	-	-	NS	250.3	748.0	382.3	453.8	613.3	723.3	203.5	NS	484.0	NS	484.0	24.8	85.3	NS	151.3
DO	mg/ℓ	-	-	-	NS	6.13	4.75	9.50	7.90	7.57	6.04	**1.37**	NS	**2.82**	NS	4.49	3.95	7.83	NS	**2.79**
Eh	mg/ℓ	-	-	-	NS	115.0	97.4	139.5	126.6	106.5	100.9	122.2	NS	105.9	NS	67.8	122.2	112.5	NS	101.6
Major Anions																				
SO_4	S mg/ℓ	-	<200	-	NS	9.3	36	18.7	25.7	31	28.9	0.5	NS	34.6	NS	15.7	0.4	0.7	NS	1.9
Nutrients																				
NO_3 + NO_2	N mg/ℓ	-	<6	-	NS	0.4	**12.2**	2.3	0.4	1.2	0.5	<0.1	NS	<0.1	NS	1.7	0.2	<0.1	NS	0.3
Total PO_4	P mg/ℓ	<0.005	<0.1	-	NS	<0.05	**1.37**	**0.22**	**0.19**	**0.26**	**0.3**	**0.14**	NS	<0.05	NS	**0.08**	<0.05	<0.05	NS	**0.05**
Trace metals																				
Al	mg/ℓ	<0.005	<0.015	<5	ND	0.06	<0.02	<0.02	0.02	<0.02	<0.02	<0.02	ND	0.02	ND	0.32	0.04	0.03	ND	<0.02
Cd	mg/ℓ	<0.25	-	<0.01	ND	<0.01	<0.01	<0.01	<0.01	<0.01	<0.01	<0.01	ND	<0.01	ND	<0.01	<0.01	<0.01	ND	<0.01
Fe	mg/ℓ	-	<0.05	<0.02	ND	0.34	0.09	<0.01	0.3	0.03	0.02	2.9	ND	0.01	ND	0.06	1.47	0.2	ND	1.28
Ni	mg/ℓ	-	-	<0.2	ND	<0.01	0.03	0.01	0.01	0.01	0.01	<0.01	ND	<0.01	ND	0.01	0.01	0.01	ND	0.01
Pb	mg/ℓ	<0.0002	<0.01	<0.2	ND	<0.02	<0.02	<0.02	<0.02	<0.02	<0.02	<0.02	ND	<0.02	ND	<0.02	<0.02	<0.02	ND	<0.02
Zn	mg/ℓ	<0.2	<3	<1.0	ND	<0.01	0.01	<0.01	<0.01	<0.01	<0.01	<0.01	ND	<0.01	ND	<0.01	<0.01	<0.01	ND	<0.01
PGMs																				
Pd	mg/ℓ	-	-	-	ND	<0.01	<0.01	<0.01	<0.01	0.01	0.02	<0.01	ND	<0.01	ND	<0.01	<0.01	<0.01	ND	<0.01
Pt	mg/ℓ	-	-	-	ND	0.01	0.01	<0.01	<0.01	<0.01	<0.01	<0.01	ND	<0.01	ND	0.01	0.01	0.01	ND	0.01
Rh	mg/ℓ	-	-	-	ND	<0.01	<0.01	<0.01	<0.01	<0.01	<0.01	<0.01	ND	<0.01	ND	0.01	<0.01	<0.01	ND	<0.01

Table 8 shows the results for the average total mercury (TotHg) concentrations in water samples from three sampling sites. Both the results obtained during August and November 2010 were below the Target Water Quality Range (TWQR) of < 40 ng/ℓ for aquatic ecosystems (DWAF, 1996a) and the US EPA guideline of 12 ng/ℓ (USEPA, 1992). In the study conducted by Walters *et al.* (2011) that presented a review on the status of mercury (Hg) as a pollutant in South African aquatic ecosystems, it was found that the Hg concentrations in surface water varies in all of the 19 WMAs. For the Olifants WMA, it was found that the TotHg concentrations in surface water varied between 10-20 ng/ℓ, the highest for all of the 19 WMAs investigated, due to the location and influence of the coal-fired power stations in the Mpumalanga Province. For the Crocodile (West) and Marico WMA, the same study reported the TotHg concentrations to vary between 1.5-2.0 ng/ℓ. Therefore, the levels recorded in this study are considered to be relatively low and may be attributed to atmospheric deposition or effluent discharge from some industrial activities and pose no risk at this stage.

Table 8. The results for the average TotHg concentrations in ng/ℓ in surface water samples collected during August and November 2010.

Site	WMA	Aug. 2010	Nov. 2010
		Ave TotHg	**Ave TotHg**
Rooikoppies Dam	Crocodile (West) & Marico	*1.67*	*1.68*
Olifants River	Olifants	*0.62*	*0.94*
Steelpoort River	Olifants	*2.51*	*1.27*

4.2. Surface sediment evaluation

4.2.1 Methods

Duplicate surface sediment samples (up to 6 cm in depth) were extruded using a 5 cm diameter polypropylene sediment corer and sectioned at 2 cm intervals. Each section was collected in a 50 mℓ centrifuge tube, labelled and double-bagged then transported on ice to the laboratory, where they were stored at -20ºC until analysis (Balcom *et al.*, 2004; Somerset *et al.*, 2010).

Sediment samples were analysed in duplicate for total mercury (TotHg) concentrations by thermal decomposition, gold amalgamation, and atomic absorption detection (USEPA Method 7473). Total Hg concentrations in surface sediment were determined using a DMA-80 Direct Mercury Analyzer (Milestone Inc., Monroe, USA) where approximately 0.5-1.0 g of homogenized wet sample was weighed into individual quarts boats and loaded into the combustion chamber of the DMA-80, pre-programmed for automatic Hg detection (Williams *et al*., 2010).

An acid digestion procedure and atomic emission spectrometry (AES) were used to quantify the metals of interest. The modified XP1500 Method and inductively coupled atomic emission spectrometry (ICP-AES) were used to analyse concentrations of Pb, Cd, Fe, Al, Ni, Pt, Pd and Rh in sediment samples. Prior to acid digestion, sediment samples were freeze-dried for 48 hours then ground in a ceramic ball mill for five minutes. For recovery of the metals, the samples were prepared using a modified acid digestion procedure which accomplished a total digestion of the entire sample matrix and therefore allowed the crustal elements to be quantified. Duplicate 0.5 g portions of the dried sample were digested with a mixture of 69% nitric acid, 70% hypochlorate acid, and 30% hydrogen peroxide. The mixture was diluted to 50 mℓ using deionised water. A 0.45 µm polyvinyl difluoride (PVDF) syringe filter was used to filter the dilute acid mixture into ICP vials. From the digested samples the crustal elements could be quantified (Madejon *et al.*, 2004; Ip *et al.*, 2007).

4.2.2 Results

4.2.2.1 Heavy metal concentrations in surface sediment samples

The results (Tables 9 and 10) obtained for aluminium (Al), iron (Fe), cadmium (Cd), nickel (Ni), lead (Pb), zinc (Zn), palladium (Pd), platinum (Pt), rhodium (Rh) and mercury (Hg) concentrations in sediment samples were compared to the Canadian sediment quality guidelines for the protection of aquatic life (CCME, 2001); since no sediment guideline values for South Africa exist. The Canadian Council of Ministers of the Environment (CCME) has published Canadian sediment-quality guidelines for the protection of aquatic life as it pertains to metals in freshwater sediment. These sediment-quality guidelines are further divided into two types a threshold-effects level (TEL) and a probable-effects level (PEL). The TEL represents the concentration below which adverse biological effects are expected to occur rarely, and the PEL defines the level above which adverse effects are expected to occur frequently(CCME, 2001; Lalonde *et al.*, 2011).In the case of the Ni, Pd, Pt and Rh concentrations no guideline values exist in the CCME guidelines.

Table 9. Mean trace metal concentrations (mg/kg d.wt) in surface sediment layers (0-6 cm) for each sampling sites sampled in August 2010. (NS = No sample collected).

Site	Al	Fe	Cd	Ni	Pb	Zn	Pd	Pt	Rh
Maretlwane River	*32042*	*12114*	*<0.5*	*76*	*<2.5*	*13.4*	*2.3*	*0.9*	*<0.3*
Hex River 1	*31563*	*17604*	*<0.5*	*64.1*	*4.3*	*27.9*	*<0.5*	*0.3*	*<0.3*
Hex River 2	*35695*	*10597*	*<0.5*	*44.7*	*<2.5*	*15.7*	*<0.5*	*0.8*	*<0.3*
Crocodile River 1	*21214*	*16215*	*<0.5*	*33.1*	*12.9*	*64.9*	*<0.5*	*1.1*	*<0.3*
Rooikoppies Dam	*9783*	*15218*	*<0.5*	*6.0*	*5.6*	*34.5*	*<0.5*	*0.3*	*<0.3*
Crocodile River (Thabazimbi) 1	*12778*	*13534*	*<0.5*	*16.8*	*4.7*	*17.5*	*<0.5*	*0.5*	*<0.3*
Crocodile River (Thabazimbi) 1	*44258*	*54206*	*<0.5*	*62.1*	*12.0*	*44.3*	*<0.5*	*0.5*	*<0.3*
Mogalakwena River 1	*37273*	*23755*	*<0.5*	*30.8*	*25.0*	*67.7*	*<0.5*	*0.5*	*0.3*
Mogalakwena River 2	*17460*	*14964*	*<0.5*	*29.3*	*8.2*	*18.9*	*<0.5*	*0.8*	*<0.3*
Olifants River	*53334*	*38173*	*<0.5*	*55.1*	*5.6*	*37.3*	*<0.5*	*0.4*	*0.6*
Steelpoort River 1	*27760*	*39500*	*<0.5*	*27.9*	*4.5*	*38.5*	*<0.5*	*<0.2*	*0.4*
Mohlapitsi River	*16890*	*36004*	*<0.5*	*23.8*	*8.1*	*71.6*	*<0.5*	*0.9*	*<0.3*
Steelpoort River 2	33927	42019	<0.5	42.9	2.6	33.9	<0.5	<0.2	0.3
Sterkstroom River 1	NS	NS	NS	NS	NS	NS	NS	NS	NS
Sterkstroom River 2	NS	NS	NS	NS	NS	NS	NS	NS	NS
Motse River	NS	NS	NS	NS	NS	NS	NS	NS	NS
Elands River	NS	NS	NS	NS	NS	NS	NS	NS	NS
Threshold-effects level (TEL)	-	-	*0.60*	-	*35.0*	*123.0*	-	-	-
Probable-effects level (PEL)	-	-	*3.50*	-	*91.3*	*315.0*	-	-	-

The Al and Fe concentrations were variable and the highest concentrations were obtained at Crocodile River (Thabazimbi) 2, Olifants River and Steelpoort River. All Cd concentrations were < 0.5 mg/kg d.wt and within the TEL guideline. Similar observations were made for Pb, while the Ni results were generally higher than the Pb. The Zn concentrations were 13.4-71.6 mg/kg d.wt, also below the TEL guideline. Most sites had Pb values < 0.5 mg/kg d.wt, and low Pt concentrations. Most sites' Rh concentrations were < 0.3 mg/kg d.wt.

Table 10. Mean trace metal concentrations (mg/kg d.wt) in surface sediment layers (0-6 cm) for all sampling sites sampled in November 2010. (NS = No sample collected).

Site	Al	Fe	Cd	Ni	Pb	Zn	Pd	Pt	Rh
Crocodile River 1	*19510*	*16987*	*<0.5*	*29.1*	*15.6*	*118.9*	*<0.5*	*<0.2*	*<0.3*
Rooikoppies Dam	*9193*	*14746*	*<0.5*	*1.1*	*6.6*	*29.0*	*<0.5*	*<0.2*	*0.4*
Crocodile River (Thabazimbi) 1	*24518*	*23619*	*<0.5*	*30.2*	*6.6*	*28.8*	*<0.5*	*<0.2*	*<0.3*
Crocodile River (Thabazimbi) 2	*35638*	*54969*	*<0.5*	*38.1*	*18.3*	*32.1*	*<0.5*	*1.0*	*0.7*
Elands River	*53458*	*69694*	*<0.5*	*59.7*	*25.4*	*46.0*	*<0.5*	*<0.2*	*0.5*
Hex River 1	*40086*	*23442*	*<0.5*	*85.1*	*3.2*	*24.5*	*0.7*	*<0.2*	*<0.3*
Hex River 2	*76661*	*23978*	*<0.5*	*71.3*	*2.3*	*26.5*	*1.2*	*0.7*	*<0.3*
Maretlwane River A	*44371*	*20018*	*<0.5*	*115.2*	*2.5*	*24.4*	*<0.5*	*0.3*	*<0.3*
Maretlwane River B	*44698*	*22556*	*<0.5*	*109.6*	*2.5*	*19.2*	*1.6*	*<0.2*	*0.8*
Sterkstroom River 1	*53906*	*25497*	*<0.5*	*70.5*	*3.5*	*22.3*	*<0.5*	*<0.2*	*1.1*
Sterkstroom River 2	*11002*	*9181*	*<0.5*	*31.6*	*5.4*	*9.0*	*0.7*	*0.2*	*1.1*
Mogalakwena River 1	*45767*	*26097*	*<0.5*	*43.2*	*36.9*	*113.7*	*<0.5*	*2.2*	*0.7*
Olifants River	*14357*	*16750*	*<0.5*	*12.4*	*3.9*	*16.0*	*2.6*	*0.2*	*1.0*
Steelpoort River	*28572*	*89660*	*<0.5*	*72.6*	*5.5*	*81.5*	*1.8*	*<0.2*	*<0.3*
Motse River	*59456*	*7199*	*<0.5*	*30.1*	*2.5*	*8.8*	*2.0*	*2.8*	*<0.3*
Mohlapitsi River	*25127*	*15483*	*<0.5*	*24.2*	*11.7*	*24.8*	*<0.5*	*2.5*	*3.0*
TEL	-	-	*0.60*	-	*35.0*	*123.0*	-	-	-
PEL	-	-	*3.50*	-	*91.3*	*315.0*	-	-	-

Variable results were obtained for Al and Fe, with the highest concentrations observed at Crocodile River (Thabazimbi) 2, Elands River, Hex River 2, Sterkstroom River 1 and Steelpoort River. The Cd concentrations were < 0.5 mg/kg d.wt and within the TEL guideline, similar to the observations made in August 2010. Higher Ni concentrations than in August were observed for Maretlwane River, Hex River 1, Hex River 2 and Steelpoort River. The Pb concentration at Mogalakwena River 1 exceeded the TEL value. The Zn concentrations were 8.8-118.9 mg/kg d.wt, and were within the TEL value. The Pd concentrations for sites Hex River 1, Hex River 2, Maretlwane River B, Sterkstroom River 2, Olifants River, Motse River and Steelpoort River were 0.7-2.6 mg/kg d.wt, while the results were < 0.5 mg/kg d.wt for the rest of the sites. Crocodile River (Thabazimbi) 2, Hex River 2, Maretlwane River A, Sterkstroom River 2, Mogalakwena River 1, Olifants River, Motse River and Mohlapitsi River had Pt results varying between 0.2 and 2.8 mg/kg d.wt and the remaining sites had concentrations < 0.2 mg/kg d.wt. The Rh concentrations in November 2010 were higher than the August 2010 results. The results showed that the concentrations of Al, Fe, Ni, Pb, Pd and Pt higher than in August 2010.

The results for the average TotHg concentrations in surface sediment samples from three sampling sites are shown in Table 11, which shows that the concentrations varied between sites and the values obtained in August 2010 ranged between 4.32 and 6.13 ng/g. All of the measured concentrations were much lower than the USEPA guideline value of 200 ng/g (US EPA, 2000), probably because sampling area does not fall within the gold mining area of the Witwatersrand.

Table 11. The results for the average TotHg concentrations in ng/g (w.wt) in sediment samples collected during August and November 2010.

	Aug. 2010	Nov. 2010
Site	**Ave TotHg**	**Ave TotHg**
Rooikoppies Dam	*4.32*	*3.07*
Olifants River	*5.07*	*0.45*
Steelpoort River	*6.13*	*11.00*

The lower concentrations in November 2010 at sites Rooikoppies Dam and Olifants River may be attributed to the dilution effect of the increased flow in the rivers. The Hg is bound to the sediment of these sites and could have been re-suspended into the water column with the increased river flow. For Steelpoort River, the increased concentration can be attributed to the Hg bound to other matter in the sediment at the site, which did not allow for the Hg to be re-suspended into the water column (Bank *et al*., 2007; Zhang *et al*., 2009).

4.3 Biota evaluation

In an aquatic ecosystem, the term “bioaccumulation” refers to the active metabolic process that causes an increase in chemical concentration in an organism compared to that in its environment, water and / or sediment. Bioaccumulation occurs if a chemical is bioavailable and, once it has bioaccumulated, transfer to the food chain may occur. This process is dependent on the chemical’s physico-chemical properties and is subjected to biomagnifications, whereby the chemical’s concentration in an organism exceeds that present in its diet. “Biomagnification” refers to the process where an increase in trace metal concentration occurs through aquatic organisms at least by two trophic levels in the food chain (Ruus *et al*., 2005; Barwick and Maher, 2003; Gray, 2002). Different views are expressed on how this process actually occurs and the manner in which it can be quantified, with terms such as bioconcentration also to be considered (Ruus *et al*., 2005; Barwick and Maher, 2003; Gray, 2002). The view is further expressed that the determination of bioaccumulation in a biological system cannot merely be determined by chemical analysis of contaminants in sediments and biota. Various other aspects such as the physico-chemical properties of the contaminants (e.g. lipophilicity and defiance against biological degradation) and sediment characteristics (e.g. particle size and organic content) should be considered as they affect the bioavailability of the contaminant and the fraction of the total contaminant that is available for uptake by organisms (Ruus *et al*., 2005).

In this study a simple approach, using a simplified equation(s) (Ruus *et al*., 2005), was adopted to evaluate the magnitude of bioaccumulation of specific contaminants. The following equation enables the calculation of the Bioaccumulation Ratio (BAR) of a contaminant (z) that is defined as (Ruus *et al*., 2005; Ferguson and Chandle, 1998; Mackay and Fraser, 2000):

$$\mathrm{BARz} = \frac{\left[C_{\mathrm{organism,\,pollut.}}\right]}{\left[C_{\mathrm{organism,\,controlled}}\right]} \qquad \textbf{Eqn. 2}$$

With Z being defined as a specific contaminant (pollutant), where:

$[C_{\mathrm{organism,\ pollut.}}]$ = the mean concentration of the pollutant (z) in the organism exposed to the contaminated sediment (pollutant);

$[C_{\mathrm{organism,\ controlled}}]$ = the mean concentration of the pollutant (z) in the organism exposed to control-sediment, or sediment collected at a controlled site.

No data on the bioaccumulation of PGMs in the South African environment are available and no discussion on trends could be included.

4.3.1 Biota evaluation methods

Biota (invertebrate and fish) samples were collected at each sampling site with a South African Scoring System (SASS) net, which was lowered into the water followed by kick-sampling and sweeping of the river sediment and the area around vegetation in the riverbed. The contents of the net were then transferred to a polyvinylchloride tray containing river water for identification, grouping and sorting of the biota samples. Thereafter, samples were double-bagged, labelled, and stored on ice during transportation to the laboratory, where they were frozen at -20 °C, for later analysis (Johnson *et al*., 2009; Haase *et al*., 2004). Laboratory analyses proceeded as described previously.

4.3.2 Results

4.3.2.1 Biota recorded

Studying macro-invertebrates is a well-established method to determine pollution effects and accumulation of metals in river sediments. Invertebrates are permanent members of the ecosystem and cannot escape pollution events, and are therefore good bio-indicators. Furthermore, invertebrates inhabit many feeding niches and include individuals classed as grazers, scrapers, filter feeders and predators; a change in the abundance of these groups signals disturbances within the ecosystem (Van Damme *et al*., 2008; Zalack *et al*., 2010).

Table 12 lists the biota collected during August 2010. The data in the table shows how the existence of two to five taxa in the rivers sampled. The list of invertebrates is dominated by insect larvae, such as mayflies (*Ephemeoptera*); larvae of dragonflies and damselflies (*Odonata*); water bugs (*Hemiptera*) and water beetles (*Coleoptera*) and, in lesser numbers, freshwater shrimps and crabs (*Crustacea*). Species known to be sensitive to mining pollution are mayflies, caddis flies and dragonflies (Tarras-Wahlberg *et al*., 2001). Mining activities reduce the biodiversity and alter species in affected streams, resulting in the absence of macroinvertebrates (Soucek *et al*., 2000; Malmqvist and Hoffsten, 1999; Beltman *et al*., 1999). Therefore, from the results listed in Table 12, it can be assumed that the pollution levels due to mining appear to be minimum to moderate when evaluating the invertebrate diversity of the various sampling sites.

The same species of mosquitofish (*Gambusia affinis)* was present at Maretlwane River, Hex River 1, Hex River 2 and Crocodile River (Thabazimbi) 1, indicating minimal pollution effects. Furthermore, since fish are at the top of the aquatic food chain they are indicative of long-term effects within a river system, in this case indicating minimum habitat disturbance due to pollution (Malmqvist and Hoffsten, 1999; Wang *et al*., 2008).

Table 13, biota found in November 2010, is also dominated by larvae of dragonflies and damselflies (*Odonata*); water bugs (*Hemiptera*) and water beetles (*Coleoptera*) and in lesser numbers insect larvae of mayflies (*Ephemeoptera*); snails (*Mollusca*); freshwater shrimps and crabs (*Crustacea*). Sampling took place at the start of the rainy season around the WMAs and may have resulted in a decrease in taxa diversity in invertebrates due to an increase in flow and volume in the rivers sampled (Wang *et al*., 2008; Davis *et al*., 2006). Samples taken in November 2010 delivered Mosquitofish (*Gambusia affinis)* at site Crocodile River 1, while banded tilapia (*Tilapia sparmanii)* were sampled at sites Crocodile River (Thabazimbi) 1, Mogalakwena River 1 and Olifants River. As indicated for the fish sampling results of August 2010, the diversity of biota sampled is an indication of minimal pollution effects due to mining (Malmqvist and Hoffsten, 1999).

Table 12. List of biota (invertebrate and fish) species collected during August 2010.

Site	Invertebrate Species		Fish species	
	Family name	**Common name**	**Species name**	**Common name**
Maretlwane River	Naucoridae	Creeping waterbugs	*Gambusia affinis*	Mosquitofish
	Baetidae	Small minnow mayflies		
	Coenagrionidae	Damselflies		
	Gerridae	Pond skaters		
Hex River 1	Naucoridae	Creeping waterbugs	*Gambusia affinis*	Mosquitofish
	Coenagrionidae	Damselflies		
	Gerridae	Pond skaters		
Hex River 2	Coenagrionidae	Damselflies	*Gambusia affinis*	Mosquitofish
	Atyidae	Freshwater shrimp		
Crocodile River 1	Coenagrionidae	Damselflies	No fish collected	
Rooikoppies Dam	No biota collected			
Crocodile River (Thabazimbi) 1	Coenagrionidae	Damselflies	*Gambusia affinis*	Mosquitofish
	Naucoridae	Creeping waterbugs		
	Atyidae	Freshwater shrimp		
Crocodile River (Thabazimbi) 2	No biota collected			
Mogalakwena River 1	Aeshnidae	Dragonflies	No fish collected	
	Coenagrionidae	Damselflies		
	Gerridae	Pond skaters		
	Belostomatidae	Giant water bugs		
	Lymnaeidae	Pond snails		
	Hydrophilidae	Water scavenger beetles		
Mogalakwena River 2	No biota collected			
Olifants River	Gomphidae	Dragonflies	*Gambusia affinis*	Mosquitofish
	Libellulidae	Dragonflies		
	Coenagrionidae	Damselflies		
	Baetidae	Small minnow mayflies		
	Belostomatidae	Giant water bugs		
Motse River	No biota collected			
Steelpoort River	Libellulidae	Dragonflies	No fish collected	
	Baetidae	Small minnow mayflies		
	Naucoridae	Creeping waterbugs		
Mohlapitsi River	Coenagrionidae	Damselflies	No fish collected	
	Belostomatidae	Giant water bugs		
	Libellulidae	Dragonflies		
	Aeshnidae	Dragonflies		
	Tabanidae	Horse flies		
	Baetidae	Small minnow mayflies		
	Potamonautidae	Freshwater crab		
Elands River	No biota collected			
Sterkstroom River 1	No biota collected			
Sterkstroom River 2	No biota collected			

Table 13. Biota (invertebrate and fish) species collected during November 2010.

Site	Invertebrate Species		Fish Species	
	Family name	Common name	Species name	Common name
Maretlwane River	No biota collected			
Hex River 1	Coenagrionidae Belostomatidae Gyrinidae Atyidae Potamonautidae	Damselflies Giant water bugs Whirligig beetles Freshwater shrimp Freshwater crab	No fish collected	
Hex River 2	Gerridae Aeshnidae Belostomatidae Coenagrionidae Libellulidae	Pond skaters Dragonflies Giant water bugs Damselflies Dragonflies	No fish collected	
Crocodile River 1	Gerridae Gomphidae Coenagrionidae	Pond skaters Dragonflies Damselflies	*Gambusia*	Mosquitofish
Rooikoppies Dam	No biota collected			
Crocodile River (Thabazimbi) 1	Coenagrionidae Belostomatidae Corbiculidae	Damselflies Giant water bugs Freshwater clams	*Tilapia sparmanii*	Banded tilapia
Crocodile River (Thabazimbi) 2	No biota collected			
Mogalakwena River 1	Belostomatidae Gomphidae Physidae Dytiscidae	Giant water bugs Dragonflies Snails Predacious diving beetles	*Tilapia sparmanii*	Banded tilapia
Mogalakwena River 2	No biota collected			
Olifants River	Gyrinidae Belostomatidae Gomphidae Coenagrionidae Nepidae	Whirligig beetles Giant bugs Dragonflies Damselflies Water scorpion	*Tilapia sparmanii*	Banded tilapia
Motse River	No biota collected			
Steelpoort River	No biota collected			
Mohlapitsi River	Coenagrionidae Aeshnidae Naucoridae Potamonautidae	Damselflies Dragonflies Creeping waterbugs Freshwater crab	No fish collected	
Elands River	No biota collected			
Sterkstroom River 1	No biota collected			
Sterkstroom River 2	Gyrinidae Belostomatidae Coenagrionidae Notonectidae	Whirligig beetles Giant bugs Damselflies Backswimmers	No fish collected	

4.3.2.2 Heavy metal concentrations in biota samples

The results obtained for various metal concentrations in biota samples from the different sampling sites (Table 14) link with the description of the biota that were sampled at each site as listed in Tables 12 and 13. Higher Al and Fe concentrations were obtained in the biota samples at all sites. In the case of Cd, concentrations were relatively low for most sites, except for site Crocodile River 1 where higher concentrations were obtained in the biota and sites Hex River 2 and Olifants River that had Cd concentrations in the fish. Cadmium is considered as one of the most toxic heavy metals in the freshwater environment and enters the aquatic environment through industrial waste discharge, surface runoff and deposition (Girgin *et al*., 2010). Therefore the elevated concentration observed in the fish should be reason for concern.

Table 14. Trace metal concentrations (mg/kg w.wt) in biota (invertebrates and fish) samples for all sampling sites sampled in August 2010.

Site	Al	Fe	Cd	Ni	Pb	Zn	Pd	Pt	Rh
Invertebrates									
Maretlwane River	*141*	*146*	*1.0*	*12.8*	*<1.5*	*23.9*	*<1.0*	*5.0*	*1.0*
Hex River 1	*238*	*264*	*1.0*	*4.7*	*<1.5*	*33.7*	*<1.0*	*<1.0*	*<1.0*
Hex River 2	*200*	*314*	*2.5*	*2.4*	*<1.5*	*19.0*	*<1.0*	*5.0*	*5.0*
Crocodile River 1 (Thabazimbi)	*209*	*262*	*1.0*	*1.6*	*1.5*	*14.4*	*<1.0*	*1.5*	*<1.0*
Mogalakwena River 1	*85*	*394*	*<0.5*	*<0.5*	*<1.5*	*19.0*	*<1.0*	*<1.0*	*<1.0*
Olifants River	*281*	*393*	*1.0*	*1.0*	*<1.5*	*26.0*	*<1.0*	*2.0*	*1.0*
Steelpoort River	*57*	*75*	*5.0*	*5.0*	*<1.5*	*31.5*	*1.5*	*10.0*	*2.6*
Mohlapitsi River	*219*	*862*	*<0.5*	*<0.5*	*<1.5*	*18.1*	*<1.0*	*<1.0*	*<1.0*
Crocodile River 1	*275*	*410*	*30*	*20.0*	*20.0*	*49.4*	*10.0*	*40.0*	*14.7*
Fish									
Maretlwane River	*42*	*50*	*1.0*	*0.8*	*<1.5*	*74.2*	*<1.0*	*1.5*	*<1.0*
Hex River 2	*82*	*143*	*10.0*	*10.0*	*10.0*	*125.5*	*3.0*	*15.0*	*2.0*
Olifants River	*110*	*201*	*10.0*	*10.0*	*10.0*	*183.8*	*5.0*	*20.0*	*3.7*

High Ni was also observed at several sites. Nickel is commonly used as a catalyst and in batteries and metal plating (Lawrence *et al*., 2004). It is possible that anthropogenic activities have led to the accumulation of Ni in the sediment, or the geology of the environment causes high Ni concentrations in the ore. As a result, it is possible that Ni is released from the sediment-water interface into the overlying waters and has bioaccumulated in the residing biota. The highest Ni concentrations were observed at Maretlwane River and Crocodile River 1 for invertebrates and Hex River 2 and Olifants River for fish.

In the case of Pb, higher concentrations were obtained at site Crocodile River 1 for invertebrates and sites Hex River 2 and Olifants River for fish.

In the case of the PGM concentrations, most sites samples showed Pd, Pt and Rh concentrations of ≤ 1.0 mg/kg w.wt. Crocodile River 1 had higher Pd, Pt and Rh concentrations for the invertebrates sampled compared with the other sites, while the fish sampled at sites Hex River 2 and Olifants River showed elevated Pd, Pt and Rh concentrations.

Zinc concentrations were higher than other metals in the biota samples for from both August and November. Zinc is released into the aquatic environment through brass plating and metal processing. Zinc is also an essential element and abundant in the Earth's crust, which results in its ubiquitous occurrence at natural background concentrations in the environment (Martins *et al*., 2004; Naito *et al*., 2010; Andres *et al*., 2000).

Table 15 shows that fewer biota were collected in November than in August, probably due to the increase in flow. This can be attributed to the start of the summer rainy season that was already underway at the time of the fieldtrip.

Table 15. **Trace metal concentrations (mg/kg w.wt) in biota (invertebrates and fish) samples for all sampling sites sampled in November 2010.**

Site	Al	Fe	Cd	Ni	Pb	Zn	Pd	Pt	Rh
Invertebrates									
Hex River 1	*299*	*345*	*<0.5*	*2.4*	*<1.0*	*19.9*	*<1.0*	*<1.0*	*<1.0*
Hex River 2	*340*	*363*	*<0.5*	*2.0*	*<1.0*	*32.6*	*<1.0*	*<1.0*	*<1.0*
Crocodile River 1	*137*	*161*	*<0.5*	*0.5*	*1.1*	*27.9*	*<1.0*	*<1.0*	*<1.0*
Mogalakwena River 1	*723*	*740*	*<0.5*	*1.4*	*1.1*	*21.4*	*<1.0*	*<1.0*	*<1.0*
Olifants River 1	*334*	*364*	*<0.5*	*0.6*	*1.1*	*34.9*	*<1.0*	*<1.0*	*<1.0*
Mohlapitsi River	*177*	*350*	*<0.5*	*<0.5*	*<1.0*	*17.8*	*<1.0*	*<1.0*	*<1.0*
Sterkstroom River 2	*38*	*179*	*<0.5*	*<0.5*	*<1.0*	*29.5*	*3.7*	*<1.0*	*<1.0*
Invertebrates (Crabs)									
Mohlapitsi River	*123*	*232*	*<0.5*	*0.5*	*<1.0*	*16.8*	*<1.0*	*<1.0*	*<1.0*
Fish									
Mohlapitsi River	*285*	*503*	*<0.5*	*0.5*	*<1.0*	*20.1*	*<1.0*	*<1.0*	*<1.0*

The Al and Fe concentrations were still relatively high in the biota samples analysed, while a sharp increase in concentrations of the invertebrates from site Mogalakwena River 1 for November 2010 was observed. The Cd concentrations were stable with all sites having values < 0.5 mg/kg w.wt and lower values compared to August 2010. Similarly, the Ni and Pb concentrations in all biota were lower than the August results. The Zn concentrations were relatively similar in August and November 2010. The PGM concentrations were < 1.0 mg/kg w.wt at all sites except for Sterkstroom River 2 where the Pd concentration in invertebrates was 3.7 mg/kg w.wt. Higher concentrations of Al, Fe, Ni, Zn and Pt than the other metals were observed for all biota sampled in August and November, but the November concentrations were lower than in August.

4.4 Algae

4.4.1 Methods

Algae samples were collected at each of the sampling sites where sediment and biota were collected. The samples were scooped with polypropylene sample holders and completely filled with water at the site, labelled and double-bagged, placed in a cooler, and transported to the laboratory on ice. Samples were frozen at -20 °C, for later analysis (Desy *et al*., 2002).). Spectrophotometric analysis was performed of the algae samples in a similar fashion as described for the sediment and biota samples. An acid digestion procedure and atomic emission spectrometry (AES) analyses were used to quantitatively analyse the metals of interest (*i.e.,* Pb, Cd, Fe, Al, Ni, Pt, Pd and Rh).

4.4.2 Results

It is known that microalgae play an important role in aquatic ecosystems since they occupy an important position in the trophic chain as primary producers, making the aquatic biota of higher trophic levels dependent upon their photosynthetic activity. Furthermore, phytoplankton, benthic and epiphytic attached microalgae, macroalgae and macrophytes are primary energy sources for most aquatic ecosystems (Pereira *et al*., 2005; Sterner *et al*., 2004; Lewis, 1995).

Studies have shown that heavy metal polluted waters lead to a decrease in algal productivity and diversity, with worst case scenarios altering the algal species composition. Algae occurring in polluted rivers can also be used as ecological indicators, especially since the presence of some metals (e.g. Pb, Zn) corresponds to the elevated concentration of a polluting metal, or is specific to a polluting metal species (Takamura *et al*., 1989; Woodfine *et al*., 2002).

It is also known that many heavy metals are necessary micronutrients of algae and fungi, but high concentrations can be fatal. Once metal toxicity has occurred, the metabolic protein denaturation occurs due to the blockage of functional groups, displacement of an essential metal, modification of the active conformation of the molecule or rupture of cellular and organellar membrane integrity (Das *et al*., 2009; Greig *et al*., 2010).

Tables 16 and 17 list the trace metal concentrations in algae samples collected in August and November 2010. The Al, Fe, Ni and Zn concentrations were higher than the other metals (Table 16), while the Cd concentrations were < 1.0 mg/kg w.wt and the Pb concentrations were 1.0-9.8 mg/kg w.wt. The Pd concentrations were consistently < 0.2 mg/kg w.wt, Pt concentrations were < 1.0 mg/kg w.wt and Rh concentrations < 0.3 mg/kg w.wt.

Table 16. Trace metal concentrations (mg/kg w.wt) in algae samples for sampling sites sampled in August 2010.

Site	Al	Fe	Cd	Ni	Pb	Zn	Pd	Pt	Rh
Maretlwane River	*17039*	*7808*	*<1.0*	*208.9*	*<1.5*	*19.6*	*<0.2*	*<1.0*	*<0.3*
Hex River	*31978*	*25183*	*<1.0*	*132.0*	*9.4*	*104.6*	*<0.2*	*<1.0*	*<0.3*
Crocodile River 1	*11361*	*10305*	*<1.0*	*26.6*	*8.3*	*44.7*	*<0.2*	*<1.0*	*<0.3*
Rooikoppies Dam	*9789*	*11528*	*<1.0*	*20.4*	*5.1*	*29.4*	*<0.2*	*<1.0*	*<0.3*
Mogalakwena River 1	*7373*	*9545*	*<1.0*	*14.4*	*9.8*	*38.3*	*<0.2*	*<1.0*	*<0.3*
Steelpoort River	*18877*	*19933*	*<1.0*	*33.0*	*1.0*	*20.0*	*<0.2*	*<1.0*	*<0.3*

The November 2010 results in Table 17 show the Al and Fe concentrations for sites Crocodile River 1, Rooikoppies Dam are much lower for November compared to August 2010. The Ni was lower in November than in August 2010. This may be attributed to the higher water flow in the rainy season of November as observed in the field. In the case of the Cd, Ni, Pb and Zn concentrations, much lower values were also observed for November 2010 compared to August 2010. The PGM concentrations for November 2010 were also lower.

Table 17. Trace metal concentrations (mg/kg w.wt) in algae samples for sampling sites sampled in November 2010.

Site	Al	Fe	Cd	Ni	Pb	Zn	Pd	Pt	Rh
Crocodile River 1	*759*	*776*	*0.1*	*2.4*	*0.4*	*6.0*	*<0.1*	*<0.1*	*<0.1*
Rooikoppies Dam	*1997*	*3596*	*0.7*	*2.7*	*1.1*	*8.4*	*<0.1*	*<0.1*	*<0.1*
Crocodile River (Thabazimbi) 1	*1182*	*1520*	*0.3*	*3.5*	*0.4*	*3.2*	*<0.1*	*<0.1*	*<0.1*
Crocodile River (Thabazimbi) 2	*1396*	*1590*	*0.3*	*3.7*	*0.3*	*3.1*	*<0.1*	*<0.1*	*<0.1*
Mogalakwena River 1	*665*	*1263*	*0.2*	*2.9*	*0.3*	*5.0*	*<0.1*	*<0.1*	*<0.1*
Sterkstroom River 2	*173*	*475*	*0.1*	*0.9*	*0.1*	*1.6*	*<0.1*	*0.1*	*<0.1*

The Ni and Zn concentrations were higher those of Cd and Pb in the algae. The concentrations did vary across all sites for all four metals. The Ni, Pb and Zn concentrations were higher in August compared to November. One reason for this may be the reduced flow in the river during August 2010, while in November 2010 the rainy season increased the volume and flow of water at most sampling sites.

The surface sediment (Tables 9 and 10) also contained higher Ni, Pb and Zn concentrations than the other metals. It is therefore possible that these four metals are released from the sediment-water interface into solution in the overlying waters. Once in solution these metals are possibly absorbed in the overlying algae that were collected (Lewis, 1995; Greig *et al*., 2010). The same conclusion could not be made for the PGM concentrations.

In general it was observed that the Al and Fe concentrations were higher than the other metals, but lower in November than in August 2010. The algae also contained higher Ni, Zn and Pb in August 2010 than in

November. Low PGM concentrations were observed during both August and November, although the concentrations were slightly higher in August 2010.

4.5 Conclusions

The metal concentrations were low in the surface water. For some sampling sites elevated nutrient concentrations were obtained during both the August and November 2010 sampling trips. Seasonal influences affected the diversity of taxa and the metal concentrations.

Higher Ni, Pb and Zn concentrations were recorded than the other metals and it is therefore possible that these metals are released from the sediment-water interface into solution in the overlying waters. Once in solution these metals may then be absorbed in the overlying algae that were collected, since the algae also contained elevated Ni, Pb and Zn concentrations. The concentrations measured in the biota and algae were low, indicating that mining activities had a low impact on the aquatic environment at the sampling sites. Nevertheless, in the case of the metal concentrations in biota, during August 2010 higher concentrations of Al, Fe, Ni, Zn and Pt were observed for all biota sampled than in November 2010. This may be due to higher water flow during November 2010, since sampling was done during the rainy season.

CHAPTER 5: ION-EXCHANGE MATERIAL AND IDENTIFICATION OF CHEMICAL PARAMETERS FOR SENSOR DEVELOPMENT

5.1 Introduction

Several studies have investigated processes for the recovery of Pt, Pd and Rh metals from aqueous solutions (Chassary *et al*., 2005; Das, 2010; Kramer *et al*., 2004). Techniques such as pyrometallurgical and hydrometallurgical processes have been utilised for the recovery of PGMs from sidestreams, all with limited success. In other cases the focus has been on the use of solvent extraction and conventional or improved ion exchange and chelating resins. This was followed by the continuous development of alternative processes that are more selective for Pt, Pd and Rh extractions from authentic precious metal refinery (PMR) waste streams (Chassary *et al*., 2005; Das, 2010; Kramer *et al*., 2004).

However, despite the search for alternative techniques in the recovery of PGMs, some of the existing techniques are still employed for the removal of metals from solution , including precipitation, ion exchange, reductive exchange, electrolytic recovery, solvent extraction, membrane separation and adsorption (Das, 2010; Els *et al*., 2000; Hubicki and Wołowicz, 2009; Dobson and Burgess, 2007).

This chapter considers the use of ion exchange materials to determine their selectivity for Pt, Pd and Rh and the subsequent removal of these metals from solution. The application of ion exchange resins has been widespread, using a variety of commercially available products. These resins (cationic, anionic or selective and chelating resins) are insoluble polymeric or macromolecular materials with fixed ions or reactive ionic groups. The reactive groups can be incorporated during resin manufacturing, but for applications standard materials can be functionalised for specific needs (Wołowicz and Hubicki, 2010; Rovira *et al*., 1998; Kramer *et al*., 2004).

The specific focus of this chapter is the determination of the applicability of ion exchange resins in the removal or adsorption of Pt(II), Pd(II) and Rh(II) from acidic ($pH \leq 2$) and alkaline ($pH \geq 8$) aqueous solutions. Two synthetic sidestream solutions (designated A and B) were prepared and used in the adsorption experiments. Four resins were investigated: (i) strongly acidic cation exchange resin (Amberlite IRP-69); (ii) cation exchange resin (Dowex 50WX8-100); (iii) strongly basic anion exchange resin (Amberlite IRA-400); and (iv) universal pH ranged (Chitosan).

The removal of Pt(II), Pd(II) and Rh(II) in the presence of interfering ions such as Ni^{2+}, Co^{2+}, Fe^{3+}, Na^{+}, SO_4^{2-} and PO_4^{2-} were also investigated, although the resulting concentrations of the interfering ions were not evaluated. The study further investigated the quantity of the precious metal ions adsorbed (q_e) for each resin and the results were plotted against the mass of resin (or adsorbent) used, to investigate the removal of the metal ions under the experimental conditions identified. Lastly, the removal efficiency (%) for each PGM was calculated to determine which resins were able to adsorb the metals from the solutions most efficiently.

5.2 Methods

5.2.1 Reagents and materials

The metal standards (AAS grade) for platinum (Pt), palladium (Pd), rhodium (Rh), nickel (Ni), lead (Pb), and cobalt (Co) were purchased from Fluka (Germany). The iron (III) chloride (97%), chitosan, Amberlite® IRA-400, and Amberlite® IRP-69 were obtained from Aldrich, Germany. The resin of Dowex® 50WX8-100 was supplied by Sigma-Aldrich, Germany. The potassium dihydrogen orthophosphate (KH_2PO_4) and hydrochloric acid (HCl) solution were supplied by Merck, South Africa. Sodium sulphate (Na_2SO_4) anhydrous (AR) was purchased from Kimix, South Africa. All solutions were prepared using Milli-Q (Millipore) water.

5.2.2 Quality control

Adherence to Quality Assurance (QA) and Quality Control (QC) procedures was of high standard throughout the collection and analysis of samples in this study. All glassware, polypropylene (PP) and other experimental containers were subjected to an adapted USEPA (2000) cleaning procedure, which entails an 8 hour cleaning in a 25% nitric acid solution, followed by rinsing in deionised water and cleaning in a 10% hydrochloric acid solution for another 8 hours. This was followed by rinsing with deionised water and drying in a laminar flowhood before containers were used in laboratory experiments.

Details of the QA / QC process involved the following steps: (i) validation of the analytical methods employed on a continuous weekly basis; (ii) the continuous monitoring of the measurement performance of the analytical instruments; (iii) estimation of associated measurement uncertainties and establishing metrological traceability with the use of certified reference materials (CRMs); (iv) use of ultrapure standards and certified reference materials (CRMs) for calibration performances; (v) use of a logbook for record keeping of a summary of the precision (measurement reproducibility expressed as relative standard deviation) and accuracy (bias expressed as relative difference to the certified value) established from QC measurements; (vi) standardised communication of results; (vii) controlled sample submission and processing procedures; (viii) routine laboratory environment checks; (ix) adherence to general laboratory practice (GLP) guidelines.

5.2.3 Synthetic precious metal wastewater preparation

Synthetic PGM sidestream solutions were prepared with the following compositions, based on analytical data provided by Anglo American Platinum (Hageman, 2010, pers. comm.): Solution A = Pt(II) (5 µg/ℓ), Pd(II) (5 µg/ℓ), Rh(II) (5 µg/ℓ), Ni(II) (2.5 µg/ℓ), Co(II) (2.5 µg/ℓ), Pb(II) (2.5 µg/ℓ), Cu(II) (2.5 µg/ℓ), $FeCl_3$ (2.5 µg/ℓ), Na_2SO_4 (2.5 µg/ℓ) and KH_2PO_4 (2.5 µg/ℓ); and Solution B = Pt(II) (5 µg/ℓ), Pd(II) (5 µg/ℓ), Rh(II) (5 µg/ℓ), Ni(II) (5 µg/ℓ), Co(II) (5 µg/ℓ), Pb(II) (5 µg/ℓ), Cu(II) (5 µg/ℓ), $FeCl_3$ (5 µg/ℓ), Na_2SO_4 (5 µg/ℓ) and KH_2PO_4 (5 µg/ℓ). All solutions contained 5% (w/w) HCl solution and were prepared using Milli-Q (Millipore) water.

5.2.4 Ion exchange procedure

Batch experiments were performed in which the synthetic PGM sidestream were reacted with the ion exchange resins of Chitosan, Amberlite IRP-69, Amberlite IRA-400 and Dowex 50WX8-100. The batch experiments were conducted at room temperature and different amounts of resin, 1.0, 1.5, 2.0 and 3.0 g were weighed and added to 100 mg/ℓ of synthetic sidestream in polypropylene bottles, providing sorbent concentrations of 100, 150, 200 and 300 g/ℓ. The pH was kept ≤ 2. The bottles were sealed and then shaken on laboratory orbital shaker (Lasec) for 2 hours at 250 rpm, at room temperature (20 ± 1ºC) (Lai *et al.*, 2010; Wołowicz and Hubicki, 2011).

At the end of the two hours, the bottles were removed from the shaker and the resin was then filtered using filter paper (Whatman® no. 41). The filtered solutions were analysed by ICP-AES and ICP-MS for its metal concentrations and were determined quantitatively to allow calculation of the amount of metal ions adsorbed on the resin, by difference with respect to the starting concentrations. The results reported are the average values obtained for duplicate measurements (Al-Anber and Al-Anber, 2008; Walcarius and Delacote, 2008).

5.2.5 Voltammetric analysis

Electrochemical protocols were performed with a PalmSens handheld potentiostat / galvanostat, with the PSTrace program and accessories (Palm Instruments BV, 3992 BZ Houten, The Netherlands), using cyclic voltammetry (CV), or differential pulse voltammetry (DPV) amperometric modes. A conventional three electrode system was employed, consisting of a BASi 1.6 mm diameter gold (Au) disc working electrode, a BASi 3M NaCl-type Ag/AgCl reference electrode, and a platinum wire auxiliary electrode (Somerset *et al.*, 2010; Labuda *et al.*, 1995; Labuda and Buckova, 2000).

5.2.6 Analytical procedure for metal ion determination

The different solutions collected after the batch experiments were left to stand for 30-60 minutes to allow the ion exchange resins to settle. The solutions were then filtered with Whatman® (no. 41) filters and separated from the ion exchange resins and kept at 4 C in PP containers until analysis was performed. Samples were submitted and analysed within 24-48 hours of collection on an Inductively Coupled Plasma Mass Spectrometer (ICP-MS) supplied by Agilent Technologies (Agilent, South Africa) or an Inductively Coupled Plasma Atomic Emission Spectrometer (ICP-AES) supplied by Thermo® (South Africa). The following metal ion concentrations were analysed in all aqueous samples: palladium (Pd), platinum (Pt), rhodium (Rh), nickel (Ni), cobalt (Co), iron (Fe), sodium (Na), including the sulphate (SO_4^{2-}) and phosphate (SO_4^{2-}) concentrations. All results for solutions were expressed in microgrammes per litre (µg/ℓ) or milligrammes per gram (mg/g) where appropriate (Somerset *et al*., 2011).

5.3 Results

5.3.1 Physical characterisation of adsorbents

Table 18 indicates that the ion exchange resins used in this study have differing characteristics in terms of physical forms, functionalities, pH ranges and moisture retention. For some of these characteristics, similar properties are evident but it is seen that interactions with the synthetic PGM sidestream deliver varying results.

Table 18. Physical-chemical characteristics of ion exchange resins investigated.

Characteristics	Chitosan	Amberlite IRA-400	Amberlite IRP-69$^{\$}$	Dowex 50WX8-100
Physical form	Cream-coloured coarse ground flakes and powder	Dark yellow fine spheres	Dark cream-coloured fine powder	Light brown fine spheres
Delivery (ionic) form	ND	Cl^-	Na^+	H^+
Functionality	ND	Quaternary ammonium	Sulphonic acid	Sulphonic acid
pH range	0-4	0-14	0-14	0-14
Total exchange capacity/TCEC$^{\pi}$/IEC$^{£}$	~ 0.342 meq/g	≥ 1.4 meq/ml	4.3 meq/g$^{\pi}$	1.7 meq/ml
Moisture retention	ND	40-47%	ND	50-58%
Particle size (mm)	NS	~ 0.3-0.9	NS	~ 0.15-0.3
Additional information	ND	Strongly basic anion exchange resin	Strongly acidic cation exchange resin	Cation exchange resin

ND = Not determined; NS = No specification

π = Total cation exchange capacity

£ = Ion exchange capacity; Choudhari and Kariduraganavar, 2009

$ = Chabani *et al*., 2009

Limited information is available on the physico-chemical properties of chitosan, particularly on the general properties of the materials discussed in this section. Chitosan, also known as poly(-glucosamine), is obtained through the decatylation of chitin which is the second most abundant polysaccharide on earth, after cellulose. It is non-toxic, hydrophilic, biodegradable, biocompatible and anti-bacterial and has therefore been widely applied. Particular to this study is the fact that chitosan is an excellent adsorbent for the removal of metal ions. Its chemical structure contains hydroxyl and amino groups that form stable chelate compounds with many transition metal ions. These groups are also advantageous for modifying the resin, while the amine groups are easily protonated in acidic solutions; chitosan is therefore mainly applied in acidic environments (Fujiwara *et al*., 2007; Ramesh *et al*., 2008).

5.3.2 Voltammetric characterisation of adsorbents at acidic pH

Figure 8 shows the results for the cathodic adsorptive differential pulse stripping voltammogram (AdDPSV) of Chitosan and Dowex 50WX8-100. The AdDPVs were collected for each mass of ion exchange resin that was exposed to the synthetic PGM sidestream.

Wołowicz and Hubicki (2010) demonstrated that Fourier Transformed Infrared Spectrosocopy (FTIR) analysis can be employed to show structural changes in the ion exchange resins Amberlyst® and Dowex®, after the sorption of Pd(II) from chloride-nitrate solutions. In this section it will be shown that voltammetry can also be used to study differences in the chemical composition of ion exchange resins after sorption of PGM ions from solution. Figure 8(a) illustrates that Chitosan had characteristic peaks for each of the different masses of resin employed. These peaks can be attributed to the metal ions incorporated into the structure of chitosan and for which the characteristic peaks were obtained. In the case of the Chitosan blank, a limited current response was observed and the peaks were attenuated for the Chitosan subjected to adsorption experiments. The first peak was obtained at 1.35 V (vs. Ag/AgCl), followed by the second at 1.0 V (vs. Ag/AgCl). The second peak had a maximum current response when 1.0 g Chitosan was used. In the case of the Chitosan blank, the second peak was observed at a potential of 0.75 V (vs. Ag/AgCl), indicating that after adsorption a change in the Chitosan resin had occurred. A strong third peak was then observed at -0.5 V (vs. Ag/AgCl), with a small shoulder peak at -1.0 V (vs. Ag/AgCl). The third peak had a maximum current response when 2.0 g of Chitosan was used. When 1.5 g Chitosan was used, a broad peak from -0.11 to -0.65 V (vs. Ag/AgCl) was observed rather than the sharp peaks obtained for the other masses.

Figure 8(b) shows that Dowex® 50WX8-100 had its own characteristic peaks and also shows maximum current peaks around -0.55 V (vs. Ag/AgCl). The first peak was obtained at 1.4 V (vs. Ag/AgCl) and the second at 1.1 V (vs. Ag/AgCl). When 2.0 g of resin was used a broader peak was obtained at 1.3 V (vs. Ag/AgCl). It can also be seen that the blank resin had the maximum current responses around 1.3 V (vs. Ag/AgCl) and -0.5 V (vs. Ag/AgCl), with the peak current reducing when different amounts of this resin was used in the adsorption studies. Other differences in the peak current data were also observed.

Figure 9 displays the results for the ion exchange resin of: (a) Amberlite® IRP-69 and (b) Amberlite® IRA-400. Similar to the observations made for the Dowex® 50WX8-100 resin in Figure 8(b), Figure 9(a) also displays that the highest current responses were observed for the blank resin. This resin had characteristic peaks with the first, minor peak observed at 1.35 V (vs. Ag/AgCl), adjacent to the major peak at 1.1 V (vs. Ag/AgCl). A shift in this peak potential was observed for Amberlite® IRP-69 after adsorption, with the resulting peaks obtained at 0.95 V and 0.65 V (vs. Ag/AgCl). A total shift in the peak potentials and a limited current response for the resin was obtained when 1.5 g resin was used. The third peak was obtained at -0.55 V (vs. Ag/AgCl) and had the highest current response for the blank, with the current decreasing once the resin was used in adsorption. For 1.0 g of resin, a shoulder peak at -0.65 V (vs. Ag/AgCl) was obtained, while in the case of 3.0 g used two distinct peaks were obtained at -0.65 V and -0.9 V (vs. Ag/AgCl). These results indicate that the resin showed chemical compositional changes after adsorption.

Figure 9(b) indicates an increase in the current responses for Amberlite® IRA-400 used in adsorption, compared to the Amberlite® IRA-400 blank, except when 1.5 g resin was used. The first peak obtained was a shoulder peak at 1.35 V (vs. Ag/AgCl) with the main peak at 1.0 V (vs. Ag/AgCl). This peak had the highest current response when 1.0 g of resin was used. The third peak was obtained from -0.45 V to -0.55 V (vs. Ag/AgCl) and the fourth at potentials between -0.75 V and -0.85 V (vs. Ag/AgCl).

The results showed chemical compositional changes of the four resins used in the adsorption experiments. This may be attributed to the incorporation of metal ions from the synthetic sidestreams. Each resin had characteristic voltammetric results, although for some comparative results were obtained. These results obtained will be further elucidated with the adsorption results discussed in the section that follows.

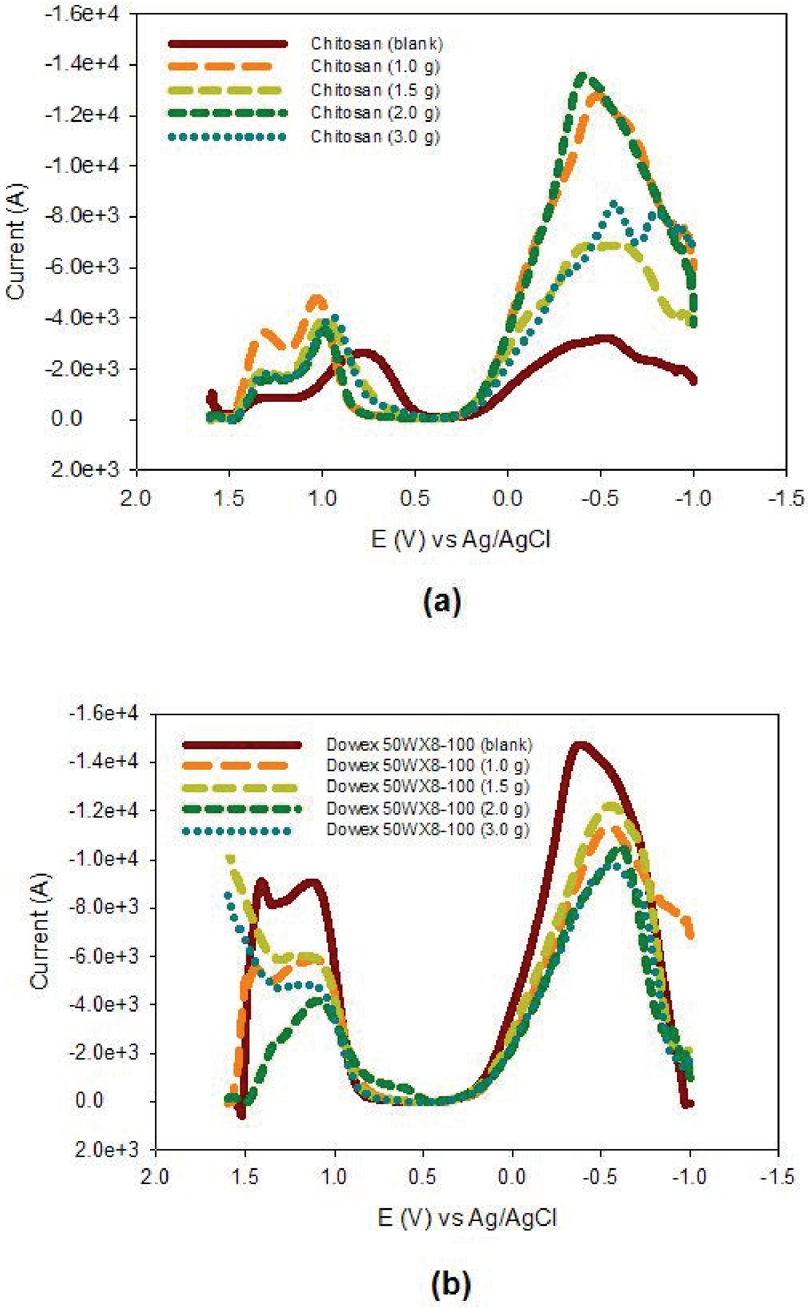

Figure 8. **The AdDPSV of the (a) chitosan and (b) DOWEX® 50WX8-100 ion exchange resins, collected after reacting with synthetic PGM sidestream for 2 hours. The potential was scanned between +2.0 to -1.5 V (vs. Ag/AgCl), at a scan rate of 40 mV/s; deposition potential (Ed) = -0.7 V; deposition time (td) = 120 s.**

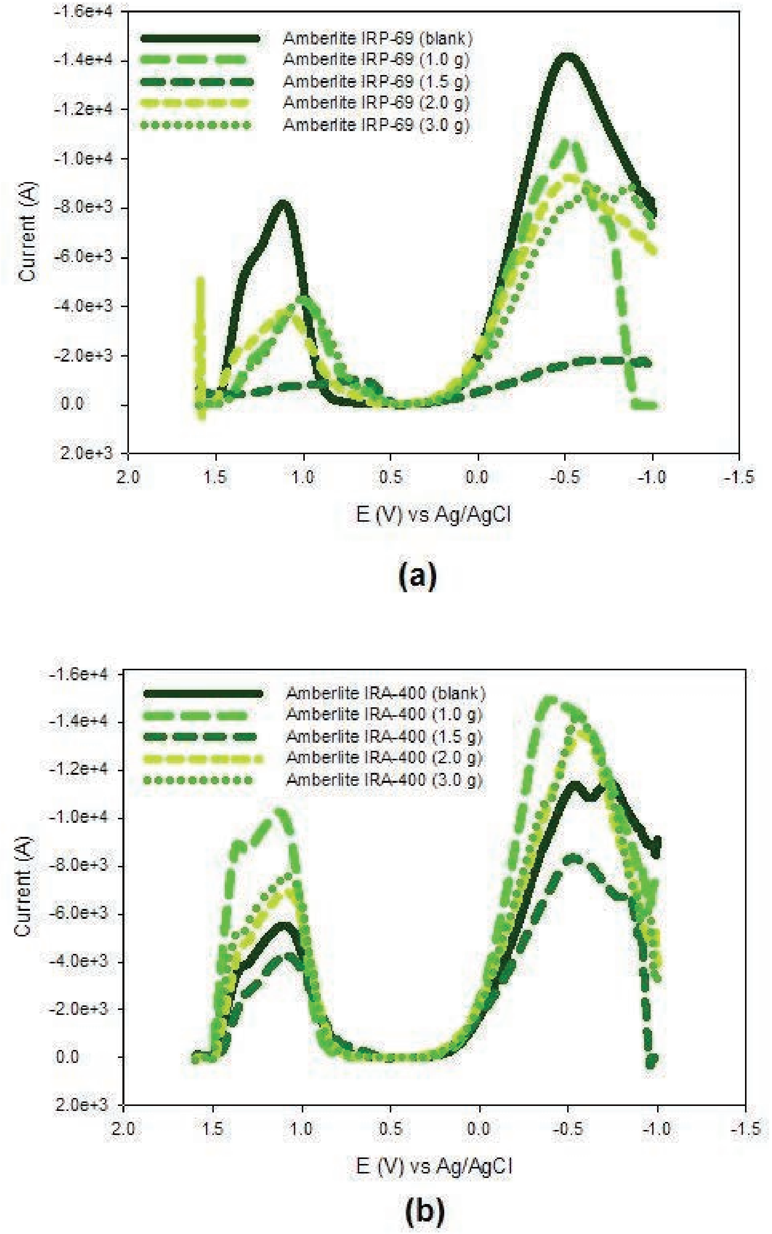

Figure 9. **The AdDPSV of the (a) Amberlite® IRP-69 and (b) Amberlite® IRA-400 ion exchange resins, collected after reacting with synthetic PGM sidetream for 2 hours. The potential was scanned between +2.0 to -1.5 V (vs. Ag/AgCl), at a scan rate of 40 mV/s; deposition potential (Ed) = -0.7 V; deposition time (td) = 120 s.**

5.3.3 Metal adsorption studies at acidic pH

Adsorption experiments were performed at 20 ± 1ºC in polypropylene (PP) bottles using an orbital shaker operating at 250 rpm. In the typical adsorption experiments, varying amounts (1.0, 1.5, 2.0 and 3.0 ± 0.05 g) of Chitosan, Amberlite® IRP-69, Amberlite® IRA-400 and Dowex® 50WX8-100 resins were added to 100 mℓ of a synthetic precious metal sidestream solution. The synthetic PGM sidestream solutions were as described in section 5.2.3. The amount of metal ion adsorbed on the ion exchange resin was estimated using the following equation (Ramadan *et al*., 2010; El-Said *et al*., 2010; Chabani *et al*., 2009):

]

$$q_e = \frac{C_i - C_e}{m} V \qquad \textbf{Eqn. 3}$$

Where:
q_e = quantity of metal ion adsorbed (mg/g),
C_i = initial equilibrium liquid-phase concentrations of metal ion (mg/ℓ),
C_e = equilibrium liquid-phase concentrations of metal ion (mg/ℓ),
V = volume of the solution (ℓ), and
m = mass of adsorbent used (g).

The pH was kept at ≤ 2 and the contact time between the different masses of each of the ion exchange resin was 2 hours for the duplicate experiments performed.

In adsorption studies it is known that the process involves separation of a substance (e.g. metal ion) from one phase, which is followed by the accumulation of that substance onto the surface of the adsorbent. The adsorption process can be very competitive and depends on the adsorbent's available surface area, polarity, contact time, pH and the degree of hydrophobic nature of the adsorbent (Abdullah *et al.*, 2009).

The work done by Fujiwara *et al.* (2007) and Zhou *et al.* (2010) reported that the speciation of Pt and Pd depends on both the pH and chloride concentrations. At low pH they have found that Pt and Pd are usually present in its most stable forms, *i.e.* Pt(IV) and Pd(II). In these oxidation states these metal ions can form stable complexes with amino group chelation sites of selected resins, to form complexes such as K_2PtCl_2 and $PdCl_2$. The presence of these complexes as precipitates in the adsorption studies were not isolated and quantified. It should therefore be noted that a very limited investigation into the adsorption of PGMs on 4 different ion-exchange resins have been performed in this investigation. Not all of the aforementioned variables have been investigated thoroughly and the results obtained in this study should provide background information for more detailed future investigations.

5.3.4 Effect of adsorbent dose (acidic pH)

Four different masses of each of the ion exchange resin were investigated in the duplicate adsorption experiments and 1.0, 1.5, 2.0 and 3.0 (± 0.05) g of each resin was shaken with 100 mℓ of a synthetic PGM sidestream. The compositions of Solutions A and B used in the following adsorption experiments are described in Section 5.2.4.

5.3.4.1 Chitosan

The quantities of the PGM ions adsorbed (q_e) are plotted against the mass of chitosan used, to investigate the removal of the ions under the experimental conditions, are shown in Figure 10. The q_e values for Pt and Rh decreased indicating that increasing the sorbent present increased the total amount of PGM removed from solution. This indicates that the sorption sites on the chitosan were saturated at the lower doses. The maximum quantity of chitosan used was insufficient to remove the entire Pt or Rh, showing that the sorbent's specific uptake capacity could not be determined under these experimental conditions. The chitosan was able to adsorb 46% of the Pt and 33% of the Rh from the synthetic sidestream (Figure 10(a)). The results have not shown a steady decrease in the q_e values of Pd for the increased amount of adsorbent, which is attributed to the lowest value of q_e obtained for 1.0 g of adsorbent used. However, comparing the removal efficiency results for the three PGMs in Table 19 shows that Pd had the highest removal efficiency of all three PGMs evaluated.

Consistent decreases were observed for Pt, Pd and Rh when subjected to the increased amounts of resin (Figure 10(b)). For this reason the graphs of $\frac{1}{q_e}$ *vs.* the mass of adsorbent are more linear than in Figure 10(a).

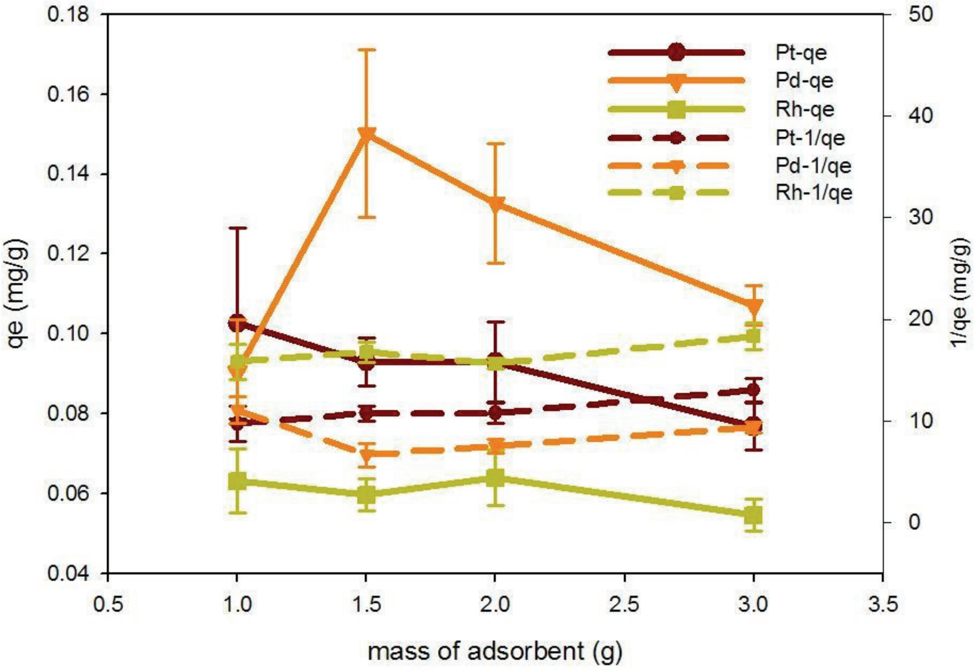

(a)

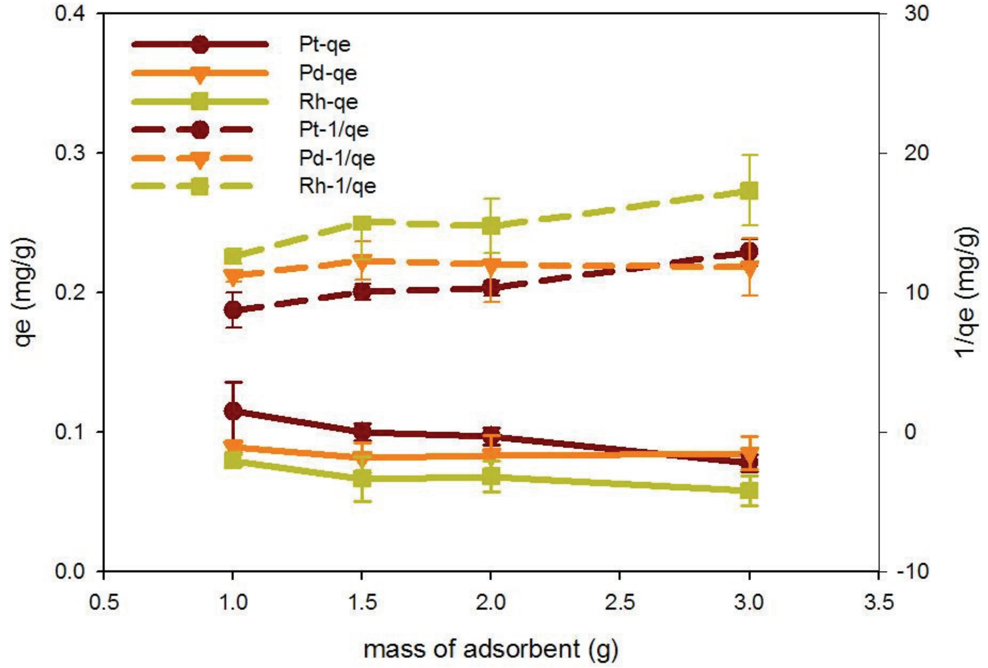

(b)

Figure 10. **Influence of Chitosan adsorbent dose on PGM ion concentrations after 2 hours of contact time. Solution volume = 100 mℓ; pH ≤ 2; Temp. = 21ºC. In (a) Solution A and in (b) Solution B results with the $[Pt]_0 = [Pd]_0 = [Rh]_0 = 5$ µg/ℓ; Anion concentrations = 2.5 µg/ℓ in (a) and 5.0 µg/ℓ in (b) (*n* = *2*).**

Chitosan was able to remove the highest amount of Pd (*vs.* Pt and Rh) from the synthetic sidestream solution A when 3.0 g of the resin was used.

The results obtained for the adsorption of PGMs from solution B using Chitosan are shown in Table 19 and indicate that the removal efficiency results for Pt and Rh in solution B were similar to solution A, however in the case of Pd the best results were obtained for solution A.

Table 19. **Removal efficiencies and q_e values after mixing synthetic PGM sidestreams (solutions A and B) with Chitosan for 2 hours at pH ≤ 2.**

	Result	**Concentration of Chitosan (g/ℓ)**			
Solution A		**100**	**150**	**200**	**300**
Pt	q_e (mg/g)	0.10	0.09	0.09	0.08
	Removal efficiency (%)	20.5	27.9	37.1	46.1
Pd	q_e (mg/g)	0.09	0.15	0.13	0.11
	Removal efficiency (%)	18.1	45.0	53.1	64.3
Rh	q_e (mg/g)	0.06	0.06	0.06	0.05
	Removal efficiency (%)	12.6	17.9	25.5	32.7
Solution B					
Pt	q_e (mg/g)	0.12	0.10	0.10	0.08
	Removal efficiency (%)	23.0	30.0	38.8	46.6
Pd	q_e (mg/g)	0.18	0.24	0.33	0.51
	Removal efficiency (%)	17.9	24.4	33.4	50.9
Rh	q_e (mg/g)	0.16	0.20	0.27	0.35
	Removal efficiency (%)	15.9	19.9	27.1	34.7

5.3.4.2 Amberlite IRP-69

Figure 11(a) illustrates the results for solution A and Amberlite® IRP-69. The q_e values for Pt and Rh decreased as the amount of adsorbent increased, but the same was not true for Pd. The graphs of $\frac{1}{q_e}$ *vs.* the mass of adsorbent show that Pt and Rh were more linear than Pd, although the two previous graphs also exhibit quasi-linearity.

The results obtained when solution B was subjected to increasing amounts of ion exchange resin are shown in Figure 11(b). The q_e values for Pt and Rh decreased whereas those for Pd did not. The trends for Pt and Rh are linear and Rh are linear and better removal results were obtained in solution B than solution A.

The q_e values for each of the PGMs are shown in Table 20. The removal efficiencies are also listed: it can be seen that the removal efficiency increased with increasing amounts of resin and the highest removal efficiency was obtained when 3 g of resin was used. An increase in the amount of resin resulted in an increase in the removal efficiency for all three PGMs, illustrating that the sorbents were saturated. Comparing removal efficiencies of Chitosan to Amberlite® IRP-69 shows that the highest efficiency of 64% was obtained for Pd, solution A and Chitosan. In the case of Amberlite IRP-69, the highest efficiency was 57% Pd removal from solution B.

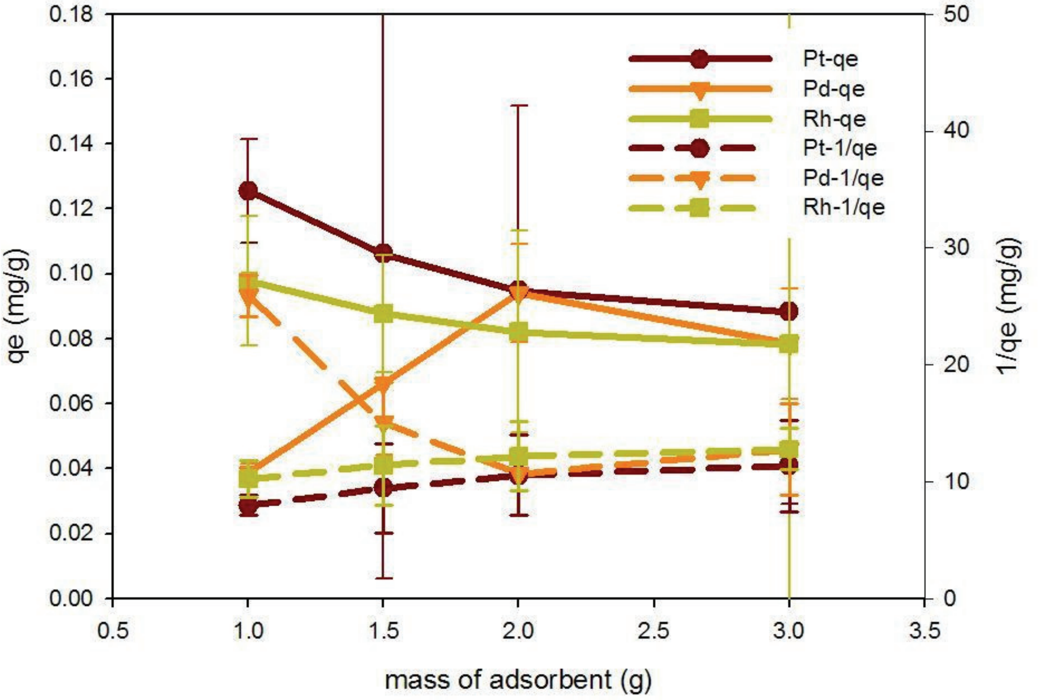

(a)

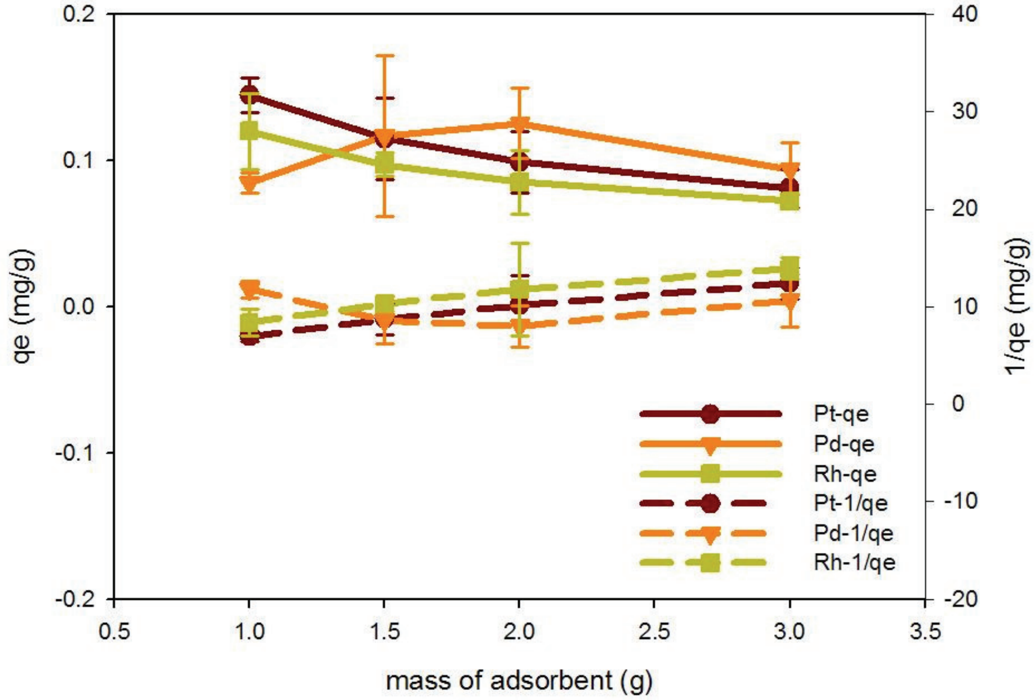

(b)

Figure 11. **Influence of Amberlite® IRP-69 adsorbent dose on precious metal ion concentrations after 2 hours of contact time. Solution volume = 100 mℓ; pH ≤ 2; Temp. = 21ºC. In (a) Solution A and in (b) Solution B results with the $[Pt]_0 = [Pd]_0 = [Rh]_0 = 5$ µg/ℓ; Anion concentrations = 2.5 µg/ℓ in (a) and 5.0 µg/ℓ in (b) (*n = 2*).**

Table 20. Removal efficiencies and q_e values after mixing synthetic PGM sidestreams (solutions A and B) with Amberlite® IRP-69 for 2 hours at pH ≤ 2.

	Result	Concentration of Amberlite® IRP-69 (g/ℓ)			
Solution A		**100**	**150**	**200**	**300**
Pt	q_e (mg/g)	0.13	0.11	0.09	0.09
	Removal efficiency (%)	25.1	31.8	38.0	52.9
Pd	q_e (mg/g)	0.04	0.07	0.09	0.08
	Removal efficiency (%)	7.7	19.9	37.6	47.1
Rh	q_e (mg/g)	0.10	0.09	0.08	0.08
	Removal efficiency (%)	19.6	26.3	32.9	47.0
Solution B					
Pt	q_e (mg/g)	0.14	0.11	0.10	0.08
	Removal efficiency (%)	28.9	34.5	39.6	48.5
Pd	q_e (mg/g)	0.08	0.12	0.13	0.09
	Removal efficiency (%)	17.0	35.0	50.0	56.5
Rh	q_e (mg/g)	0.12	0.10	0.08	0.07
	Removal efficiency (%)	24.0	29.1	34.0	43.2

5.3.4.3 Amberlite IRA-400

Similar to the previous sections, increased amounts of Amberlite® IRA-400 decreased the Pt, Pd and Rh q_e values. However, the decrease in the Rh q_e values was different from those of Pt and Rh (Table 21).

Evaluation of the graphs of $\frac{1}{q_e}$ *vs.* the mass of adsorbent in Figure 12(a) for Pt and Pd indicate that they are linear and that good removal from the synthetic sidestream solution A was obtained. This was not the case for Rh. The results obtained when solution B was subjected to the adsorption experiments are shown in Figure 12(b). These results indicate that for all three of Pt, Pd and Rh the q_e values decreased indicating that an increased amount of adsorbent was able to reduce the final concentration of these metals in the synthetic sidestream. However, in the case of Rh, the decrease in the q_e values was different compared to that of Pt and Rh (Table 21).

Table 21. Removal efficiencies and q_e values after mixing synthetic PGM sidestreams (solutions A and B) with Amberlite® IRA-400 for 2 hours at pH ≤ 2.

	Result	Concentration of Amberlite® IRA-400 (g/ℓ)			
Solution A		**100**	**150**	**200**	**300**
Pt	q_e (mg/g)	0.48	0.33	0.25	0.16
	Removal efficiency (%)	96.7	97.7	98.0	98.5
Pd	q_e (mg/g)	0.44	0.30	0.23	0.16
	Removal efficiency (%)	87.1	91.2	91.7	93.7
Rh	q_e (mg/g)	0.11	0.10	0.09	0.05
	Removal efficiency (%)	21.3	29.2	37.0	28.8
Solution B					
Pt	q_e (mg/g)	0.49	0.33	0.25	0.16
	Removal efficiency (%)	97.2	97.9	98.0	98.4
Pd	q_e (mg/g)	0.40	0.29	0.22	0.15
	Removal efficiency (%)	79.3	87.8	88.5	91.2
Rh	q_e (mg/g)	0.06	0.06	0.06	0.05
	Removal efficiency (%)	11.6	18.9	23.4	28.1

Similar to the results for solution A, evaluation of the graphs of $\frac{1}{q_e}$ *vs.* the mass of adsorbent for Pt and Pd indicate that they are linear and that good results for the removal from the synthetic sidestream solution B was obtained. The behaviour of Rh in these experiments was different as shown in the results and graph in Figure 12(b).

The results in Table 21 show very high removal efficiency for Pt and Pd from Solution A. The Rh removal from Solution A very low, indicating that some competition may be possible between the PGMs during adsorption and should be verified in future experiments.

Further evaluation of the Solution B results in Table 21 gives more details on the respective q_e values for the PGMs and for Rh the decrease observed was very minimal. The removal efficiencies show that Pt had the highest removal efficiency (98%) of these metal ions by Amberlite® IRA-400, followed by Pd with 91%. The removal efficiencies were similar for solutions A and B. For both solutions, Amberlite® IRA-400 was able to absorb Pt most effectively, followed by Pd and the least effective results were obtained for Rh.

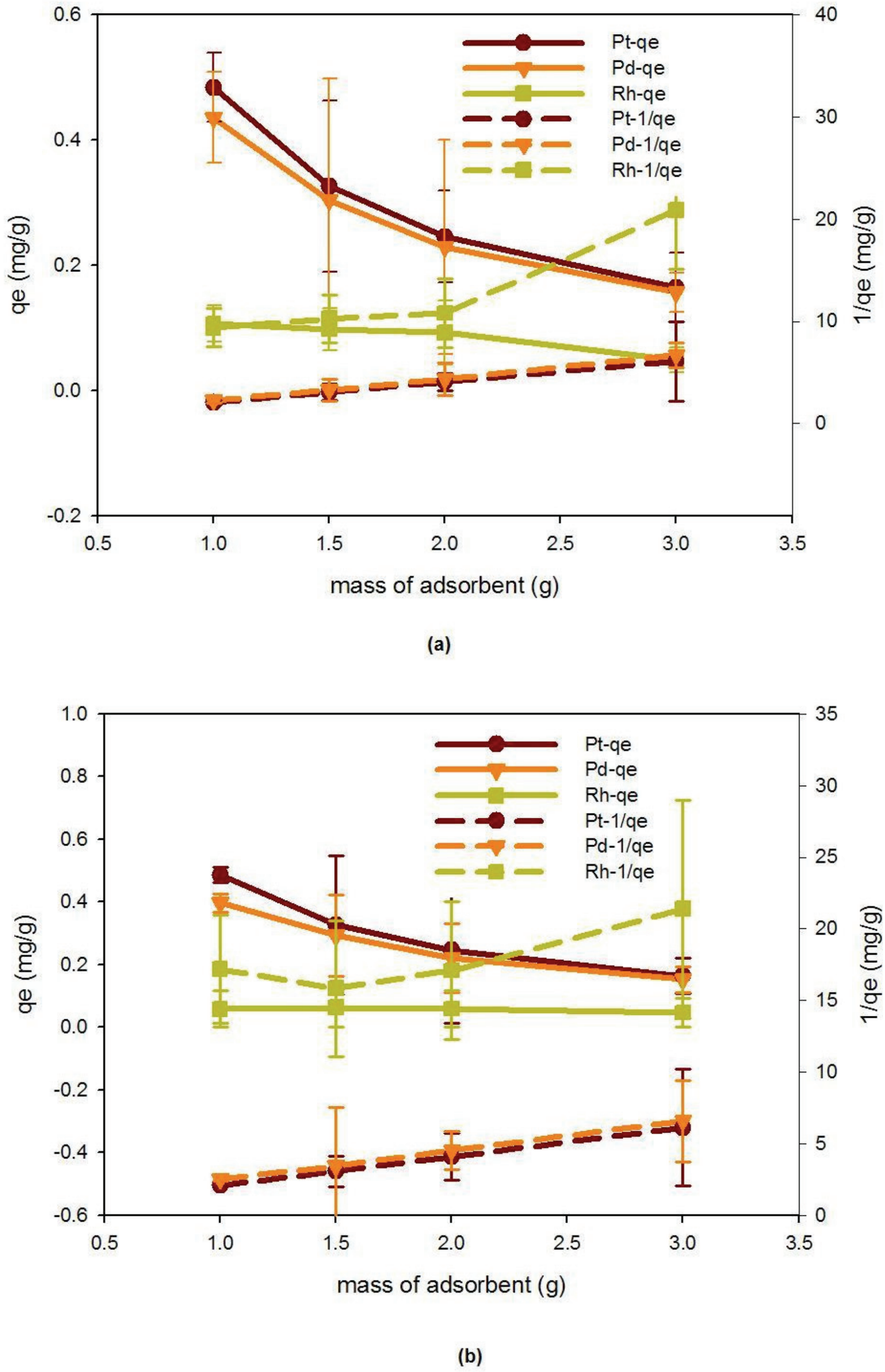

(a)

(b)

Figure 12. **Influence of Amberlite® IRA-400 adsorbent dose on precious metal ion concentrations after 2 hours of contact time. Solution volume = 100 mℓ; pH ≤ 2; Temp. = 21ºC. In (a) Solution A and in (b) Solution B results with the $[Pt]_0 = [Pd]_0 = [Rh]_0$ = 5 µg/ℓ; Anion concentrations = 2.5 µg/ℓ in (a) and 5.0 µg/ℓ in (b) (*n = 2*).**

5.3.4.4 Dowex 50WX8-100

Figure 13(a) shows that the results for the q_e values of Pt and Pd with Dowex® 50WX8-100 indicate that no clear increasing or decreasing trend was obtained in solution A. A decreasing trend in the q_e values for Rh is observed. This also resulted in no linear (or quasi-linear) response for the graphs of $\frac{1}{q_e}$ *vs.* the mass of adsorbent for Pt and Pd, while similar results were obtained for the Rh graph. In Table 22 the results for the removal efficiency of the PGMs are shown and although the results were relatively low, in comparison with the results discussed in the previous sections, it shows that Pd had the highest removal efficiency of 40%. It can also be observed that Rh had the lowest results in the presence of Pt and Pd in solution A.

Figure 13(b) shows the results for Solution B and it was observed that for Pt a clear decrease in the q_e values are observed indicating that an increased amount of adsorbent was able to reduce the final concentration of this metal in the synthetic sidestream. In the case of Rh, the q_e values remained relatively constant during the decrease in mass of adsorbent and for Pd no trend was observed. These results influenced the response for the graphs of $\frac{1}{q_e}$ *vs.* the mass of adsorbent, giving no clear indication on the effectiveness of adsorption during the use of the adsorbent.

Evaluation of the solution B results in Table 22 shows that the results were rather low and even less than obtained for solution A (Table 22). It can therefore be concluded that for both solutions A and B, the Dowex® 50WX8-100 resin showed very limited removal of Pt, Pd and Rh from the synthetic sidestream solutions, compared to the three other sorbents.

Table 22. Removal efficiencies and q_e values after mixing synthetic PGM sidestreams (solutions A and B) with Dowex® 50WX8-100 for 2 hours at pH ≤ 2.

	Result	**Concentration of Dowex® 50WX8-100 (g/ℓ)**			
Solution A		**100**	**150**	**200**	**300**
Pt	q_e (mg/g)	0.05	0.10	0.08	0.05
	Removal efficiency (%)	10.6	29.8	30.3	31.4
Pd	q_e (mg/g)	0.06	0.05	0.07	0.07
	Removal efficiency (%)	11.5	14.1	29.9	39.7
Rh	q_e (mg/g)	0.05	0.04	0.04	0.03
	Removal efficiency (%)	9.3	10.8	14.7	16.1
Solution B					
Pt	q_e (mg/g)	0.05	0.05	0.04	0.03
	Removal efficiency (%)	10.8	14.4	14.9	15.6
Pd	q_e (mg/g)	0.02	0.03	0.03	0.03
	Removal efficiency (%)	3.0	9.1	11.3	16.6
Rh	q_e (mg/g)	0.01	0.01	0.01	0.01
	Removal efficiency (%)	2.6	4.0	5.9	7.7

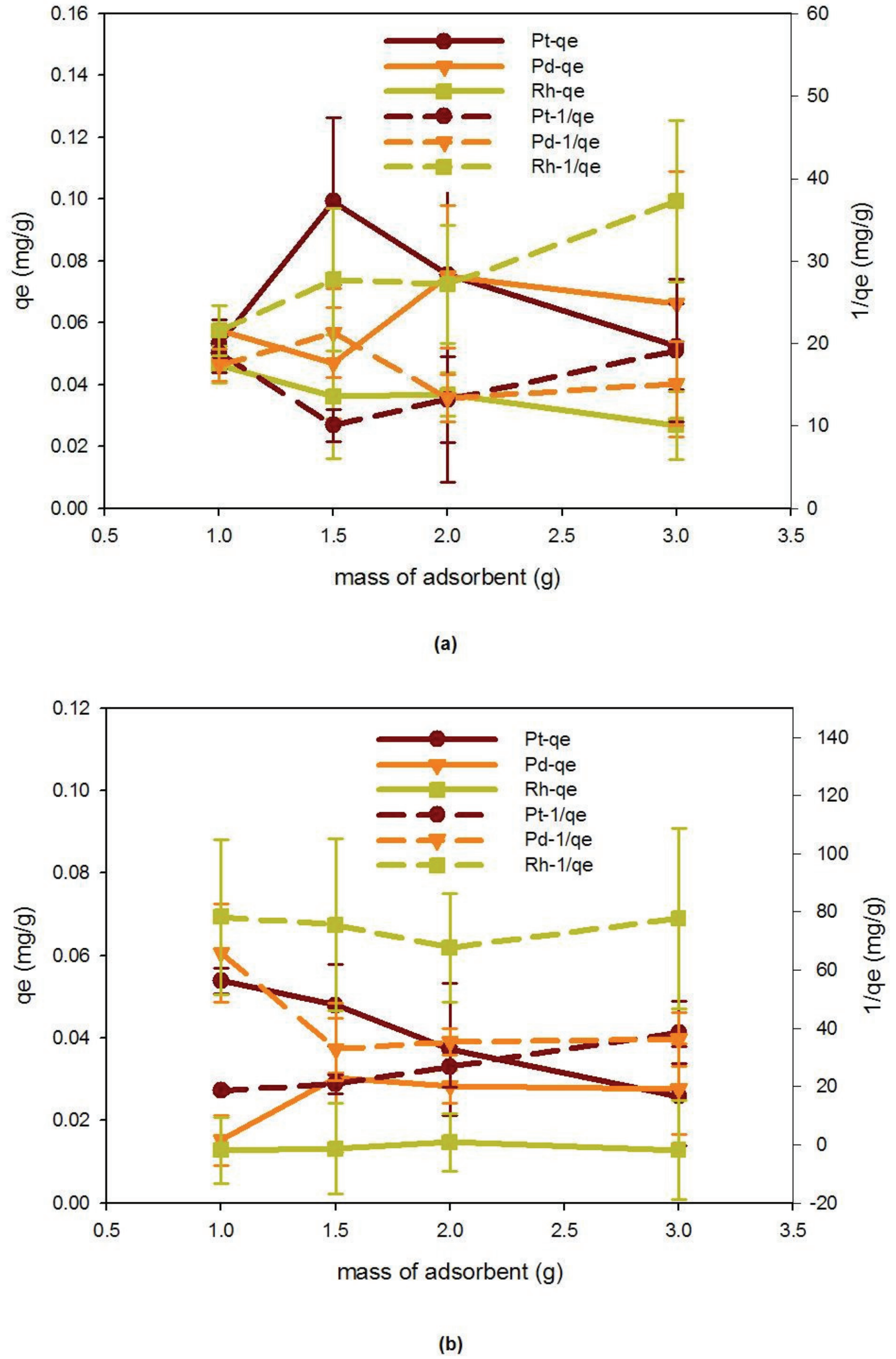

Figure 13. **Influence of Dowex® 50WX8-100 adsorbent dose on precious metal ion concentrations after 2 hours of contact time. Solution volume = 100 mℓ; pH ≤ 2; Temp. = 21ºC. In (a) Solution A and in (b) Solution B results with the $[Pt]_0 = [Pd]_0 = [Rh]_0 = 5$ µg/ℓ; Anion concentrations = 2.5 µg/ℓ in (a) and 5.0 µg/ℓ in (b) (*n* = *2*).**

5.3.4.5 Comparison of results for different ion exchange resins at acidic pH

Table 23 summarises the results obtained for the metal adsorption studies and lists the highest removal efficiency obtained for each ion exchange material. The highest removal efficiency of 99% was obtained when Amberlite® IRA-400 as resin was used to remove Pd from solution A. The removal efficiency of the PGMs was 40-99% and the resins interacted well with solution A.

Table 23. Results for each of the ion exchange resin evaluated and the highest removal efficiency obtained for the PGM ion listed.

Resin	Solution	Removal efficiency (%)	PGM
Chitosan	A	64	Pd
Amberlite® IRP-69	B	57	Pd
Amberlite® IRA-400	A	99	Pt
Dowex® 50WX8-100	A	40	Pd

All these results were collected with both solutions A and B at acidic pH and in section 5.3.6 the same results will be collected at alkaline pH to further understand the behaviour of the sorbents at different pH values.

5.3.5 Voltammetric characterisation of adsorbents at alkaline pH

In this section the results collected for the cathodic adsorptive differential pulse stripping voltammetric characterisation of the ion exchange resins are displayed. A synthetic PGM sidestream containing Pt, Pd, Rh, Ni, Co. Pb, Cu, Fe, Na, sulphate and phosphate ions was prepared and subjected to different masses of sorbents. This study was done at pH ≥ 8 in a 0.1 M NaOH solution.

In Figure 14 the results for the AdDPSV of Chitosan and Dowex® 50WX8-100 collected at alkaline pH are shown. The AdDPVs were collected for each mass of ion exchange resin that was subjected to the adsorption experiments with the synthetic precious metal sidestream solution.

Figure 14(a) shows that Chitosan had two characteristic peaks for each different mass of resin, which can be attributed to the metal ions incorporated into the structure of chitosan and for which the characteristic peaks were obtained. A limited to no current response was observed in the Chitosan blank and the peaks were attenuated for the Chitosan subjected to adsorption. The first peak was obtained at 0.95 V (vs. Ag/AgCl), followed by the second at -0.67 V (vs. Ag/AgCl). The second peak had a maximum current response when 2.0 g Chitosan was used. In the case of the first peak obtained, it was observed that no significant change in the peak current was observed as all masses had a similar voltammetric response. A complete drop in current was observed after the first peak and was followed by a broad second peak obtained at -0.67 V (vs. Ag/AgCl). A shoulder peak is present at -0.35 V (vs. Ag/AgCl), indicating that more than one of the metals in the sidestream is locked into the Chitosan.

Figure 14(b) displays the results for the Dowex® 50WX8-100, which showed current peak responses at similar peak potentials to the Chitosan. The first current peak responses were obtained at approximately 0.82 V (vs. Ag/AgCl). The second responses were obtained at -0.71 V (vs. Ag/AgCl) and the voltammograms obtained were incomplete in the potential window used. With the use 3.0 g of the resin a maximum peak current was obtained at -0.69 V (vs. Ag/AgCl). The Dowex® resin had higher current responses around -0.71 V (vs. Ag/AgCl) than the Chitosan.

Figure 15 displays the results for the ion exchange resin of: (a) Amberlite® IRP-69, and (b) Amberlite® IRA-400 used in the adsorption experiments at alkaline pH. Figure 15(a) also displays that the highest peak current responses were observed at approximately -0.62 V (vs. Ag/AgCl), similar to the results in Figure 14.

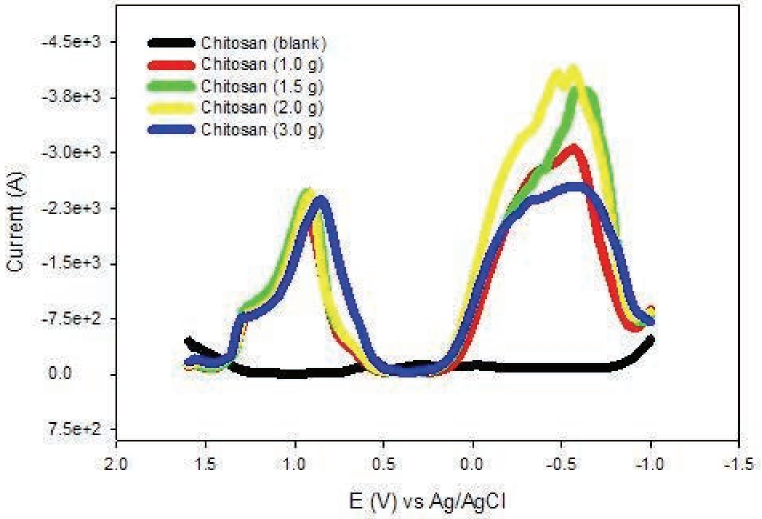

(a)

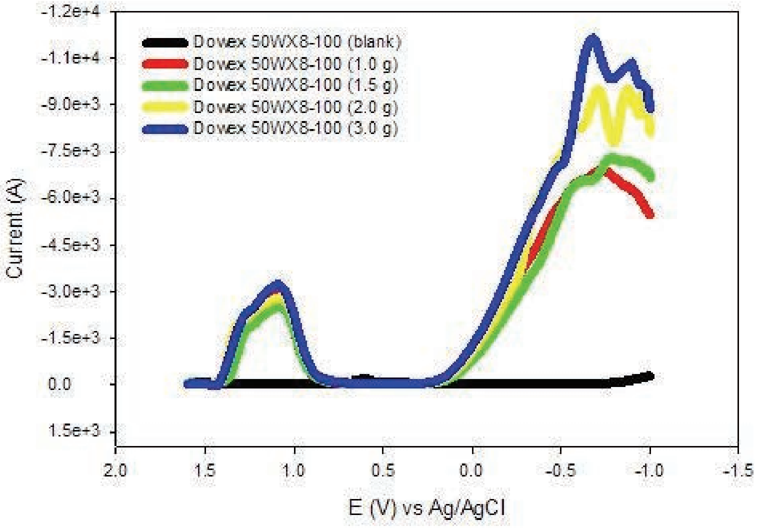

(b)

Figure 14. **The results for the AdDPSV of the (a) chitosan and (b) Dowex® 50WX8-100 ion exchange resins, collected after reacting with synthetic precious metal wastewater for 2 hours (pH ≥ 8). The potential was scanned between +2.0 to -1.5 V (vs. Ag/AgCl), at a scan rate of 40 mV/s; deposition potential (Ed) = -0.7 V; deposition time (td) = 120 s.**

A maximum current response was obtained when 3.0 g of Amberlite® IRP-69 resin was used. No clear single sharp voltammetric peak was obtained, indicating that two or three metals have been incorporated into the resin. However, the extent of this investigation does not allow for a detailed interrogation of the voltammetric peak data to elucidate the peak data for each metal ion. It was observed that the peak currents obtained at approximately -0.62 V (vs. Ag/AgCl), is the highest for Amberlite® IRP-69. The results also show that current peak maxima were obtained at 0.96 V (vs. Ag/AgCl) for all masses of Amberlite® IRP-69 investigated, but the maximum peak current responses were relatively close. The voltammograms also have a small shoulder peak, indicating the presence of more than one metal ion in the Amberlite® IRP-69.

Figure 15(b) shows that the highest peak current responses for Amberlite® IRA-400 were observed at approximately -0.60 to -1.1 V (vs. Ag/AgCl), similar to Figure 15(a). The highest peak current was obtained when 2.0 g of Amberlite® IRA-400 was used. The voltammograms for 1.0 g and 1.5 g also have a shoulder peak at approximately -0.51 V (vs. Ag/AgCl) that indicates the presence of other metal ions in the resin. Further studies and comparative analysis will be needed to fingerprint the shoulder peak obtained and attribute the peak potential to a specific metal ion.

Current peak maxima were also obtained at 0.96 V (vs. Ag/AgCl) for all masses of Amberlite® IRA-400, but the maximum peak current responses have increasing peak current values for increasing amounts of resin used. Again, a shoulder peak was obtained for each mass investigated at approximately 1.26 V (vs. Ag/AgCl) that current peak maxima were also obtained at 0.96 V (vs. Ag/AgCl) for all masses of the resin investigated, but the maximum peak current responses have increasing peak current values for increasing amounts of resin used. Again, a shoulder peak was obtained for each mass investigated at approximately 1.26 V (vs. Ag/AgCl).

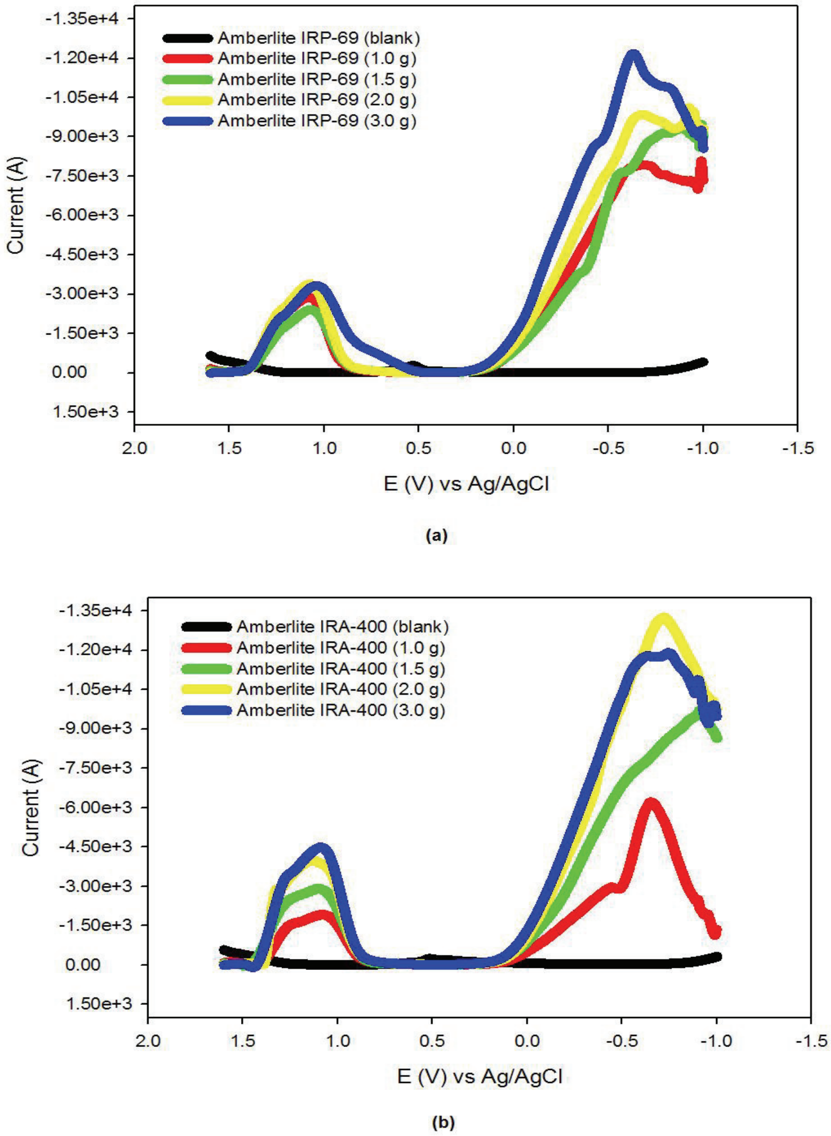

Figure 15. The results for the AdDPSV of the (a) Amberlite® IRP-69 and (b) Amberlite® IRA-400 ion exchange resins, collected after reacting with synthetic precious metal wastewater for 2 hours (pH ≥ 8). The potential was scanned between +2.0 to -1.5 V (vs. Ag/AgCl), at a scan rate of 40 mV/s; deposition potential (Ed) = -0.7 V; deposition time (td) = 120 s.

5.3.6 Metal adsorption studies at alkaline pH

Varying amounts of Chitosan, Amberlite® IRP-69, Amberlite® IRA-400 and Dowex® 50WX8-100 (1.0, 1.5, 2.0 and 3.0 g) were added to 100 mℓ of a synthetic precious metal sidestream solution ($pH \geq 8$). The sidestream solutions were as described in section 5.2.3. The amount of metal ion adsorbed on the ion exchange resin was estimated as described in section 5.3.3. The pH was kept at equal or higher to 8, the bottles were shaken at 150 rpm at room temperature and the contact time between the sorbents and solution was 2 hours. The use of 0.1 M NaOH solution was employed to adjust the pH to ≥ 8.

No speciation studies were performed in this work, therefore limited data is available on the characterisation of the ion-exchange resins collected at the end of the adsorption studies. It is further known that the PGMs investigated in this study can be present in different oxidation states, depending on whether it is introduced as salts into solution. Other researchers (Rao and Trivedi, 2005; Zhou *et al.*, 2010) have shown that at alkaline pH, precious metals such as Pt, Pd and Rh form various complexes. In the case of Pt, some of the complexes and compounds are $Pt(NH_3)_4^{2+}$, $Na_2Pt(OH)_6$ and $[Pt(NO_2)_2(SO_4)]^{2-}$. Pd complexes and compounds include $Pd(NH_3)4(NO_3)_2$, $Pd(NH_3)_4Cl_2$ and $PdCl_2$. Lastly, in the case of Rh it is known that this metal can be precipitated as rhodium hydroxide in the presence of ammonium hydroxide. Future studies are suggested to investigate the precipitation properties of Pt, Pd and Rh at alkaline pH that will assist the extension of the work conducted in this study.

5.3.7 Effect of adsorbent dose (alkaline pH)

5.3.7.1 Chitosan

Figure 16 shows that the quantity of the metal ions adsorbed (q_e) plotted against the mass of sorbent. In the case of Solution A, the Pd, Pt and Rh qe values decreased. The decreasing order of qe values obtained at 3.0 g of resin used are Pd > Pt > Rh (Table 24). Further evaluation of the results in Figure 16(a) and Table 24 show that, a relatively small increase in the Pt removal efficiency for increased amount of adsorbent used was obtained with Solution A. Similar results were obtained for Rh, while higher adsorption results were obtained for Pd. The graphs of $\frac{1}{q_e}$ vs. the mass of adsorbent (Figure 16(a)) are not linear, indicating that no consistent decrease was observed for Pt, Pd and Rh.

The results for Solution B shown in Figure 16(b) indicate that better adsorption was obtained for Pt and Rh, compared to Figure 16(a). The decreasing order of q_e values obtained at 3.0 g of resin used are Rh > Pt > Pd (Table 24). A Rh removal efficiency of greater than 80% was obtained for all masses of resin, with weak to moderate removal efficiencies for Pt and Pd. Evaluation of the graphs of $\frac{1}{q_e}$ vs. the mass of adsorbent in Figure 16(b) indicate that more linear graphs were obtained for Pd and Rh, but not for Pt. Consistent decreases were observed for Pd and Rh when subjected to the increased amounts of resin, while the results were better than the values for Figure 16(a). Chitosan was able to remove the highest amount of Pd (vs. Pt and Rh) from the synthetic sidestream solution A when 3.0 g of the resin was used.

Table 24 indicates that the removal efficiency results for Rh in solution B were the highest, while that for Pd was similar for increased mass of resin. In the case of Pt a steady increase was observed.

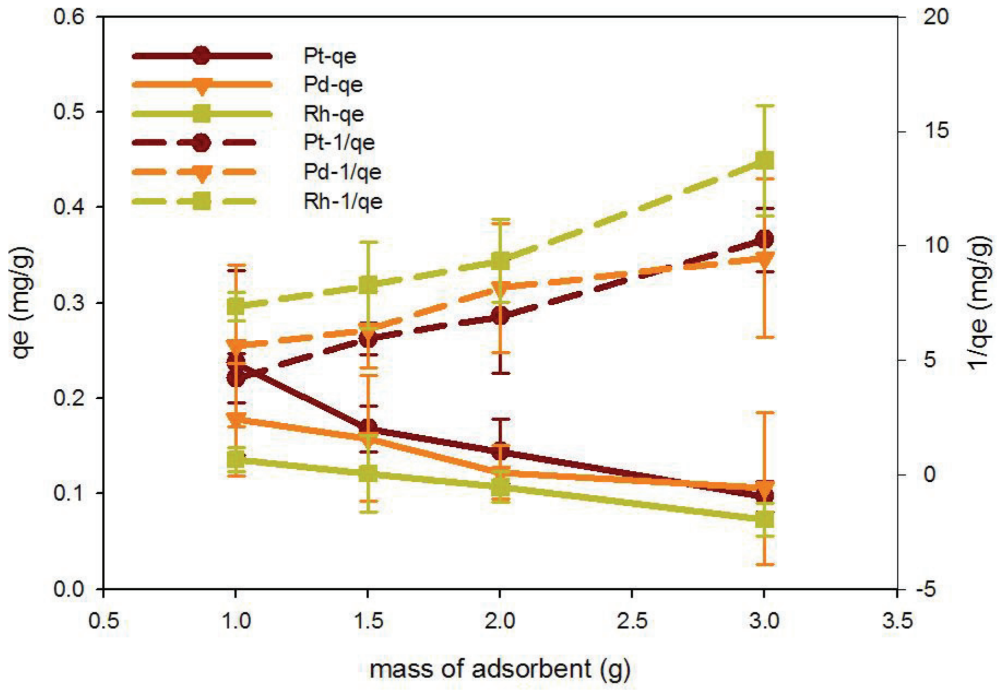

(a)

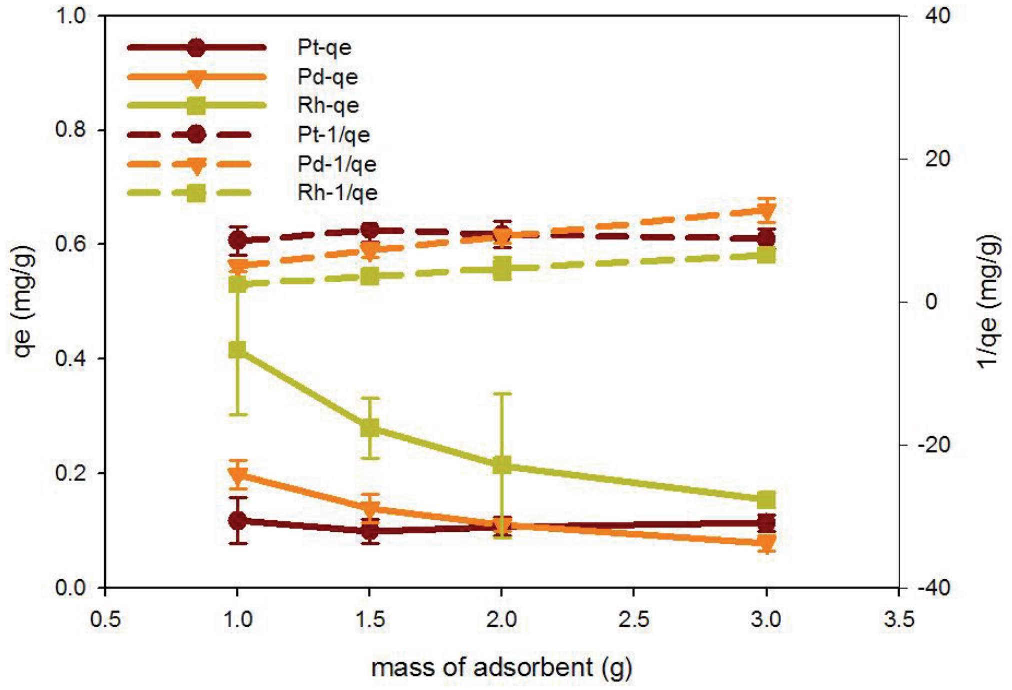

(b)

Figure 16. **Influence of Chitosan adsorbent dose on precious metal ion concentrations after 2 hours of contact time. Solution volume = 100 mℓ; pH ≥ 8; Temp. = 21°C. In (a) Solution A and in (b) Solution B results with the $[Pt]_0$ = $[Pd]_0$ = $[Rh]_0$ = 5 μg/ℓ; Anion concentrations = 2.5 μg/ℓ in (a) and 5.0 μg/ℓ in (b) (*n = 2*).**

Table 24. **Removal efficiencies and q_e values after mixing synthetic PGM sidestreams (solutions A and B) with Chitosan for 2 hours at pH ≥ 8.**

	Result	**Concentration of Chitosan (g/ℓ)**			
Solution A		**100**	**150**	**200**	**300**
Pt	q_e (mg/g)	0.24	0.17	0.14	0.10
	Removal efficiency	47.4	50.4	57.9	58.5
Pd	q_e (mg/g)	0.18	0.16	0.13	0.11
	Removal efficiency	35.6	47.4	49.0	63.4
Rh	q_e (mg/g)	0.14	0.12	0.11	0.07
	Removal efficiency	27.2	36.3	42.8	43.8
Solution B					
Pt	q_e (mg/g)	0.12	0.10	0.10	0.11
	Removal efficiency	23.5	29.8	42.7	68.1
Pd	q_e (mg/g)	0.20	0.14	0.11	0.08
	Removal efficiency	39.6	41.6	43.8	46.8
Rh	q_e (mg/g)	0.42	0.28	0.21	0.15
	Removal efficiency	83.1	83.8	85.5	92.0

5.3.7.2 Amberlite IRP-69

Solutions A and B were contacted with increased amounts of Amberlite® IRP-69. The results Figure 17(a) and Table 25 show that for Rh in Solution A the qe values decreased but the Pd and Pt showed no steady decrease in q_e. The plot of $\frac{1}{q_e}$ vs. mass of adsorbent indicates that a quasi-linear response was obtained for Rh and not for Pt and Pd as can be seen in Figure 17(a). Figure 17(b) provides the results of exposing Solution B to increasing amounts of Amberlite® IRP-69. The q_e values for Pt and Rh decreased indicating that an increased amount of adsorbent decreased the final concentration of these metals in the synthetic sidestream. Mixed results were obtained for Pd. Evaluation of the graphs of $\frac{1}{q_e}$ vs. the mass of adsorbent for Pt and Rh showed quasi-linear responses and that better results for the removal of the metal ions from solution B were obtained than from solution A.

Table 25 indicates the highest removal efficiency result of 78% was obtained for Rh in Solution A, with lower removal efficiencies obtained for Pt and Pd. Good Rh results were obtained when 1.5 g and 2.0 g of resin was used. The highest solution B removal efficiency results were obtained for Rh at all masses of resin, with the highest result of 92.9% for 1.5 g of resin used. Conversely, low removal efficiency results were obtained for Pt and Pd. The resin was successful in removing higher amounts of Rh than the other PGMs from Solution B.

Table 25. **Removal efficiencies and q_e values after mixing synthetic PGM sidestreams (solutions A and B) with Amberlite IRP-69 for 2 hours at pH ≥ 8.**

	Result	**Concentration of Amberlite® IRP-69 (g/ℓ)**			
Solution A		**100**	**150**	**200**	**300**
Pt	q_e (mg/g)	0.02	0.05	0.06	0.05
	Removal efficiency	4.9	14.3	22.4	29.8
Pd	q_e (mg/g)	0.06	0.07	0.08	0.05
	Removal efficiency	12.7	20.3	30.7	30.4
Rh	q_e (mg/g)	0.28	0.25	0.20	0.09
	Removal efficiency	55.6	74.6	78.0	52.5
Solution B					
Pt	q_e (mg/g)	0.09	0.10	0.09	0.08
	Removal efficiency	18.1	28.7	35.8	46.8
Pd	q_e (mg/g)	0.09	0.06	0.10	0.08
	Removal efficiency	17.9	18.5	40.0	50.0
Rh	q_e (mg/g)	0.38	0.31	0.21	0.15
	Removal efficiency	75.7	92.9	83.6	88.7

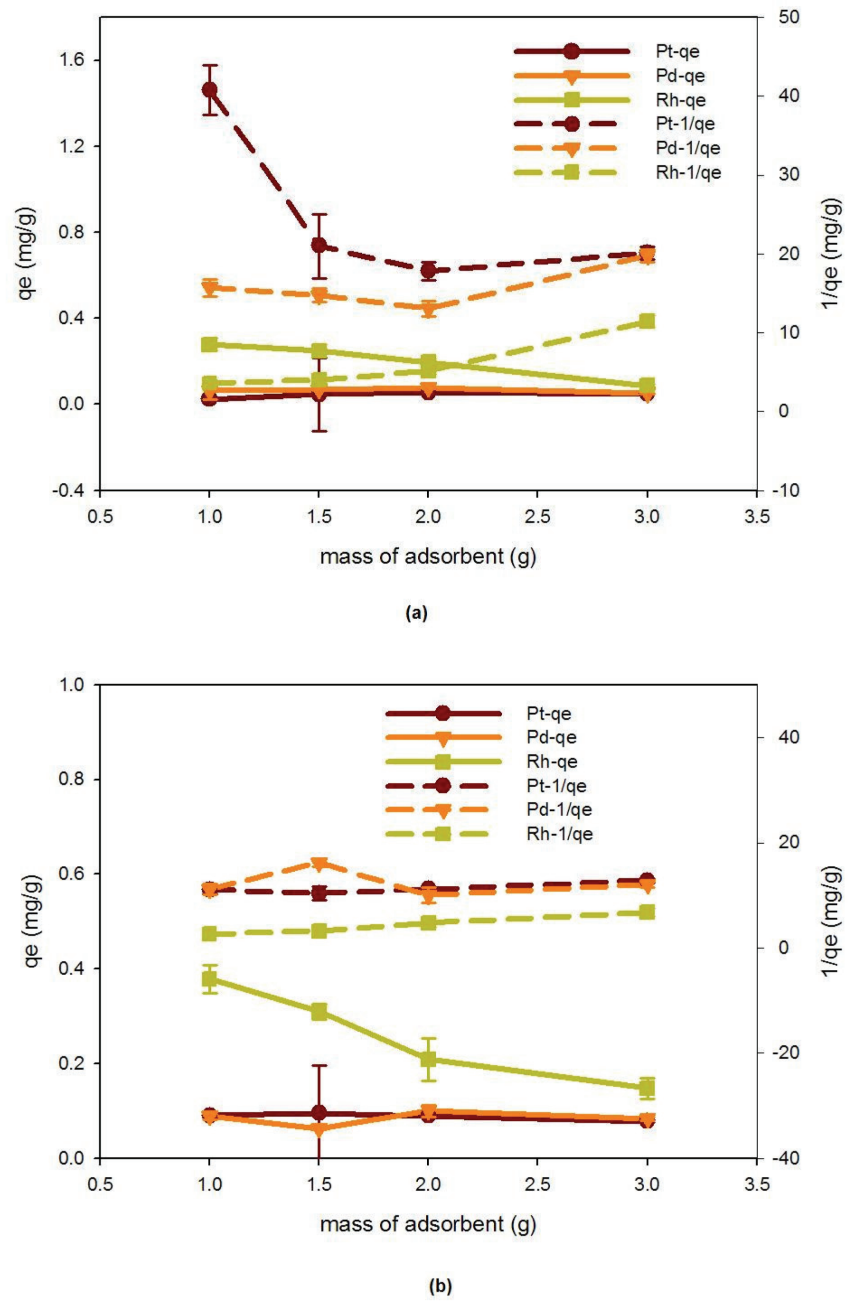

Figure 17. **Influence of Amberlite® IRP-69 adsorbent dose on precious metal ion concentrations after 2 hours of contact time. Solution volume = 100 mℓ; pH ≥ 8; Temp. = 21ºC. In (a) Solution A and in (b) Solution B results with the [Pt]0 = [Pd]0 = [Rh]0 = 5 µg/ℓ; Anion concentrations = 2.5 µg/ℓ in (a) and 5.0 µg/ℓ in (b) (*n* = *2*).**

5.3.7.3 Amberlite IRA-400

Increasing the amounts of Amberlite® IRA-400, a strongly basic anion exchange resin, decreased the Pt and Rh q_e values but provided mixed results for Pd Figure 18(a). The $\frac{1}{q_e}$ *vs.* mass of adsorbent graphs for Pt and Rh are linear (Figure 18(a)) and that good results for the removal from Solution A were obtained. This was not the case for Pd. Table 26 displays the results for the % removal of the PGMs from Solution A using Amberlite® IRA-400 that were shown in Figure 18(a). Very high removal efficiencies for Pt and Rh were obtained, with all the results for Rh > 90% and > 80% for Pt. The results for Pd were mixed and had the lowest removal efficiency of 65%.

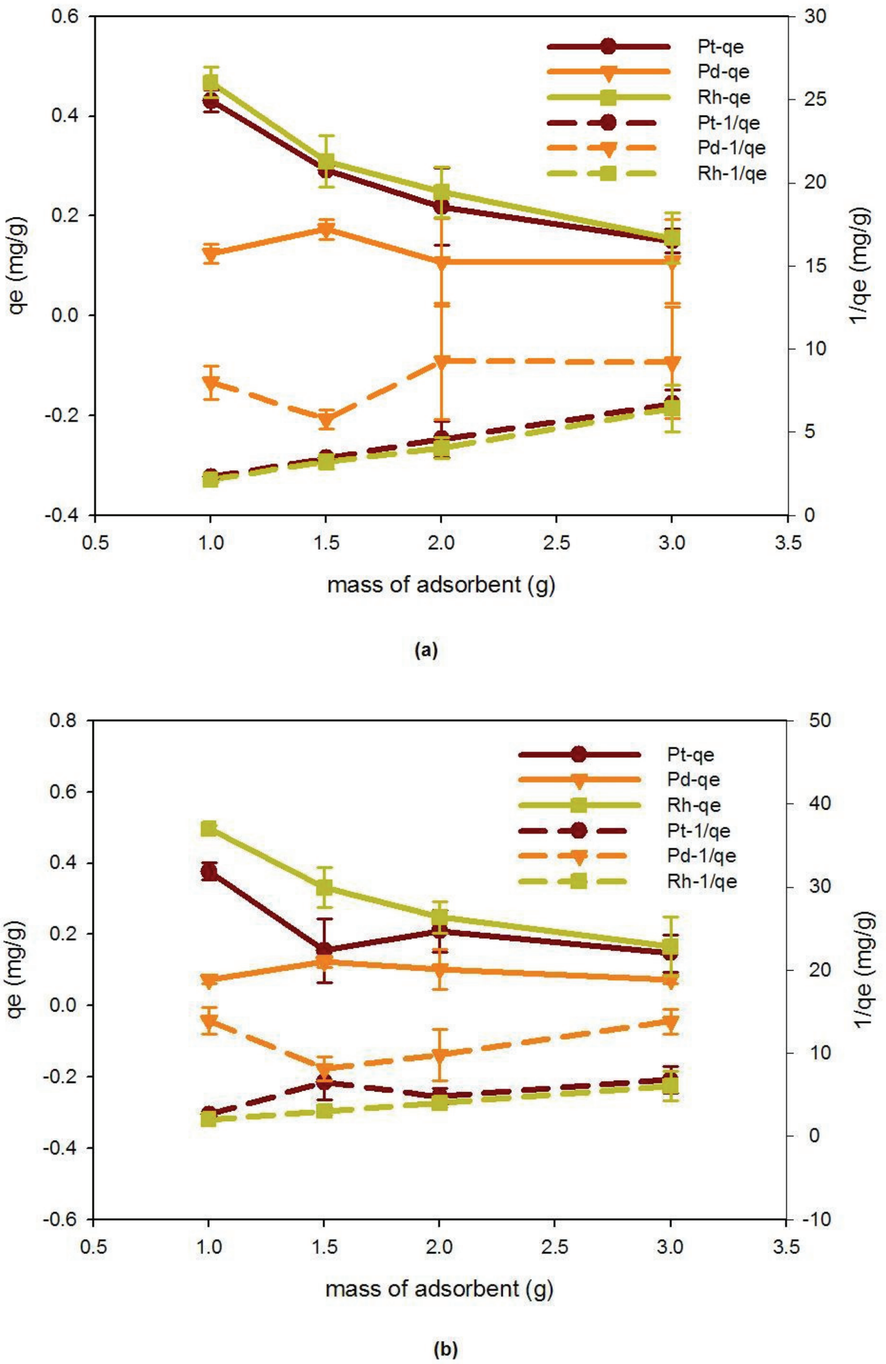

Figure 18. **Influence of Amberlite® IRA-400 adsorbent dose on precious metal ion concentrations after 2 hours of contact time. Solution volume = 100 mℓ; pH ≥ 8; Temp. = 21ºC. In (a) Solution A and in (b) Solution B results with the $[Pt]_0 = [Pd]_0 = [Rh]_0 = 5$ µg/ℓ; Anion concentrations = 2.5 µg/ℓ in (a) and 5.0 µg/ℓ in (b) (*n = 2*).**

The results obtained when solution B was subjected to the adsorption experiments are shown in Figure 18(b). Only the q_e for Rh decreased constantly. Mixed results were obtained for Pt and Pd (Table 26). The graphs of $\frac{1}{q_e}$ *vs.* the mass of adsorbent were only linear for Rh indicating that Amberlite® IRA-400 was effective for the removal of Rh from Solution B. The best results obtained for Solution B were 99% removal of Rh. For both solutions A and B, Amberlite® IRA-400 was able to remove Rh the most effectively from the synthetic solutions, followed closely by Pt and least effective results were obtained for Pd.

Table 26. **Removal efficiencies and q_e values after mixing synthetic PGM sidestreams (solutions A and B) with Amberlite® IRA-400 for 2 hours at pH ≥ 8.**

	Result	Concentration of Amberlite® IRA-400 (g/ℓ)			
Solution A		**100**	**150**	**200**	**300**
Pt	q_e (mg/g)	0.43	0.29	0.22	0.15
	Removal efficiency	86.2	87.7	87.4	89.7
Pd	q_e (mg/g)	0.13	0.17	0.11	0.11
	Removal efficiency	25.0	52.1	43.1	65.4
Rh	q_e (mg/g)	0.47	0.31	0.25	0.16
	Removal efficiency	93.6	92.7	99.2	93.5
Solution B					
Pt	q_e (mg/g)	0.38	0.15	0.21	0.15
	Removal efficiency	75.3	46.4	83.7	88.4
Pd	q_e (mg/g)	0.07	0.12	0.10	0.07
	Removal efficiency	14.4	37.0	40.7	43.5
Rh	q_e (mg/g)	0.50	0.33	0.25	0.17
	Removal efficiency	99.2	99.3	99.3	99.4

5.3.7.4 Dowex 50WX8-100

Dowex® 50WX8-100 produced results in which the q_e values of Pt and Rh indicate a clear decreasing trend in Solution A (Figure 19(a)) but no clear trend in Pd adsorption. Therefore, the graphs of $\frac{1}{q_e}$ *vs.*the mass of adsorbent for Pt and Rh showed linear responses, while in the case of the Pd results no linear trend was obtained.

The removal efficiency was also low (Figure 19(a), with the best results obtained for the removal of Rh, followed by Pt and then Pd. Using Solution B composition (Figure 19(b), only 1 g of resin was needed to yield the best adsorption results for Rh and Pt. A clear decrease in the q_e values was observed for both Rh and Pt in Solution B. Mixed results in the q_e values for Pd was obtained indicating that Dowex® 50WX8-100 was unable to adsorb Pd effectively.

Table 27. **Removal efficiencies and q_e values after mixing synthetic PGM sidestreams (solutions A and B) with Dowex® 50WX8-100 for 2 hours at pH ≥ 8.**

	Result	Concentration of Dowex® 50WX8-100 (g/ℓ)			
Solution A		**100**	**150**	**200**	**300**
Pt	q_e (mg/g)	0.28	0.17	0.12	0.07
	Removal efficiency	56.5	52.3	48.1	41.8
Pd	q_e (mg/g)	0.03	0.05	0.03	0.02
	Removal efficiency	6.5	16.2	10.4	11.2
Rh	q_e (mg/g)	0.49	0.33	0.22	0.13
	Removal efficiency	98.9	98.1	87.7	79.5
Solution B					
Pt	q_e (mg/g)	0.08	0.14	0.09	0.08
	Removal efficiency	16.2	41.0	36.1	45.9
Pd	q_e (mg/g)	0.01	0.01	0.01	0.04
	Removal efficiency	1.6	0.6	2.6	24.9
Rh	q_e (mg/g)	0.49	0.33	0.24	0.16
	Removal efficiency	97.6	99.2	96.9	98.1

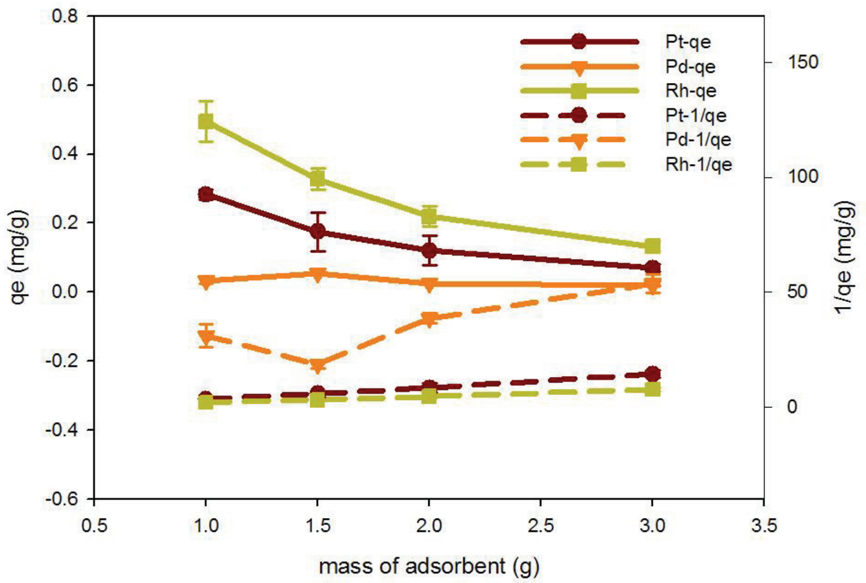

(a)

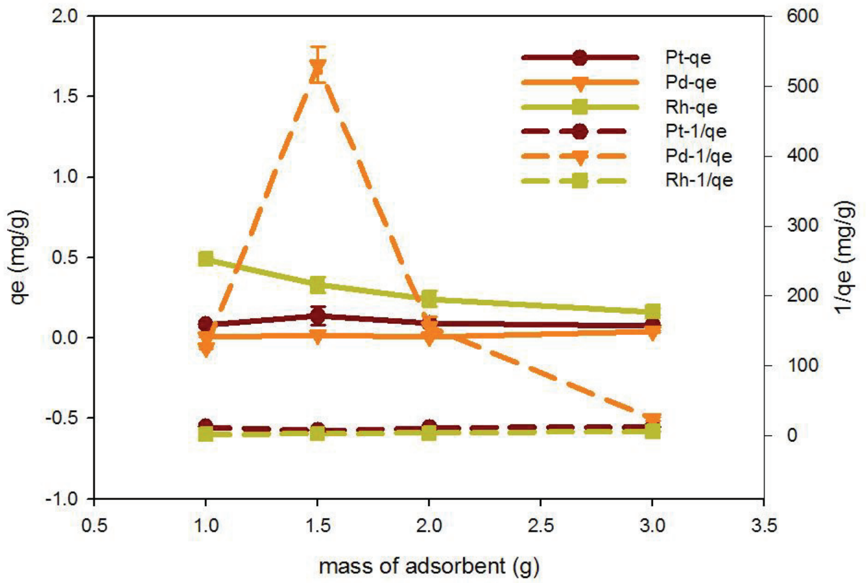

(b)

Figure 19. **Influence of Dowex® 50WX8-100 adsorbent dose on precious metal ion concentrations after 2 hours of contact time. Solution volume = 100 mℓ; pH ≥ 8; Temp. = 21ºC. In (a) Solution A and in (b) Solution B results with the $[Pt]_0 = [Pd]_0 = [Rh]_0 = 5$ µg/ℓ; Anion concentrations = 2.5 µg/ℓ in (a) and 5.0 µg/ℓ in (b) (*n = 2*).**

5.3.7.5 Comparison of results for different ion exchange resins at alkaline pH

A summary of the results obtained for the metal adsorption studies using four different ion exchanges resins is shown in Table 28.

Table 28. Results for each of the ion exchange resin evaluated at alkaline pH and the highest removal efficiency obtained for the PGM ion listed.

Resin	Solution	Removal efficiency (%)	PGM
Chitosan	B	92	Rh
Amberlite® IRP-69	B	93	Rh
Amberlite® IRA-400	A; B	99	Rh
Dowex® 50WX8-100	A	99	Rh

The highest removal efficiency of 99% was obtained with Amberlite® IRA-400 and Dowex® 50WX8-100 adsorbing Rh from Solution B. Medium results were obtained for adsorption of Pd (maximum 65% with Amberlite IRA-400), while the lowest efficiency (0.6%) was obtained with Dowex® 50WX8-100. In the case of Pt medium to high removal efficiency results were obtained, with 90% removal using Amberlite® IRA-400 and only 5% with Amberlite® IRP-69.

5.4 Conclusions

The voltammetric evaluation at both acidic and alkaline pH revealed chemical compositional changes of the resins, which may be attributed to the incorporation of metal ions from the sidestream solutions. Each resin had characteristic voltammogram, although similar results were obtained for some.

This was followed by the preparation and evaluation of two synthetic precious metal sidestream solutions A and B, in which the precious metal ion concentrations in the presence of interfering cations and anions were evaluated. Interesting results were obtained for the metal ion adsorption experiments performed in which increasing amounts (1.0, 1.5, 2.0 and 3.0 g) of the respective resins (adsorbents) were evaluated.

At pH 2, the highest removal efficiency of 64% was obtained when Chitosan was used on solution A. In the case of Amberlite® IRP-69, the highest removal efficiency was 57% when solution B was subjected to the adsorption studies. For both solutions A and B, Amberlite® IRA-400 was able to absorb Pt more effectively, followed closely by Pd and least effective results were obtained for Rh. The highest removal efficiency was 99% for Pt from solution A. Dowex® 50WX8-100 resin showed limited removal of Pt, Pd and Rh from the synthetic sidestream solutions, especially when the results are compared to the three other resins efficiencies. The removal efficiencies of the PGMs ranged between 40-99% and the sorbents interacted well with solution A, removing Pd from both solutions at acidic pH.

Under alkaline conditions the highest removal efficiency of 99% was obtained with Amberlite® IRA-400 and Dowex® 50WX8-100 and Rh. The highest removal efficiency of Pd was 65% using Amberlite® IRA-400, while the weakest results (0.6%) were obtained using Dowex® 50WX8-100. Amberlite® IRA-400 removed 90% Pt – the highest Pt removal at pH 8 – and Amberlite® IRP-69 the lowest (5%).

CHAPTER 6: SENSOR MATERIAL SYNTHESIS AND SENSOR CONSTRUCTION AND ANALYSIS OF PRECIOUS GROUP METALS

6.1 Introduction

Several methods have been established for the simultaneous analysis and determination of metal ions. These methods include inductively coupled plasma-mass spectrometry (ICP-MS), X-ray fluorescence spectrometry (XRF), atomic absorption spectrometry (AAS), and atomic fluorescence spectrometry (AFS). Although these methods are highly efficient, they require tedious sample pre-treatments, highly qualified technicians and sophisticated instruments. Furthermore, these methods are also known to be time consuming and not suitable for field analysis of multiple samples (Somerset *et al*., 2011).

In the last few decades, electrochemistry has played an increasing role in the determination of heavy metals, especially since the invention of polarography as a technique. The use of stripping voltammetry as an electro-analytical technique for trace metal analysis has grown over the last decades. The remarkable sensitivity of stripping analysis has been attributed to its pre-concentration step, which allows for trace metals to accumulate onto the working electrode. This step is followed by the stripping (measurement) step, in which the metals are “stripped” away from the electrode during an appropriate potential scan. Using an adsorptive stripping protocol, the procedure allows for the interfacial accumulation of the complex, ligand or target metal on the electrode surface that is quantified during the stripping step of the analysis procedure (Wang and Lu, 2000; Zhu *et al*., 2006; Mandil *et al*., 2010).

The use of various mercury-free electrodes including bismuth film electrodes, gold-coated electrodes, silver electrodes, glassy carbon electrodes, carbon paste electrodes, carbon nanotube electrodes or screen-printed carbon electrodes has been applied for sensitive metal determinations using the technique of stripping voltammetry (Somerset *et al*., 2011).

In this section, the experimental conditions and parameters for the stripping analysis of Pd(II) in the presence of dimethylglyoxime (DMG) as chelating agent was investigated. The surface of a glassy carbon electrode was modified with a bismuth film (BiF) and then applied in the stripping analysis of the $Pd(HDMG)_2$ complex, while results were obtained for evaluation of the GCE/BiF/$Pd(HDMG)_2$ sensor in 0.1 M HCl buffer (pH ≈ 2), 0.2 M NaOAc buffer (pH = 4.5) and 0.1 M ammonia (pH = 9) buffer solutions.

6.2 Methods

6.2.1 Reagents and materials

The potassium dihydrogen phosphate (99%) and disodium hydrogen phosphate (98%) were obtained from Aldrich (Germany), while Fluka (Germany) supplied the mercaptobenzothiazole (MBT). Merck’s (RSA) sulfuric acid (95%), hydrochloric acid (32%), sodium chloride and ethanol (absolute 99.9%) were used as received. All electrochemical measurements were carried out in phosphate buffered saline (PBS) solution (0.1M phosphate, 0.1M KCl, pH 7.2).

Precious metal standards (AAS grade) for platinum, palladium and rhodium were purchased from Fluka (Germany). Sodium acetate, ammonium hydroxide solution, glacial acetic acid, and dimethylglyoxime (DMG) were purchased from Sigma, Germany. All solutions were prepared using ultra pure water obtained from a Milli-RO Milli-Q Plus (MilliporeWater) system.

6.2.2 Apparatus

Electrochemical protocols were performed with an Epsilon electrochemical analyzer (BASi Instruments, 2701 Kent Ave., West Lafayette, IN 47906, USA), using cyclic voltammetry (CV), or differential pulse voltammetry (DPV) amperometric modes. A conventional three electrode system (Figure 18) was employed, consisting of a BASi 3.0 mm diameter glassy carbon disc working electrode (GCE), a BASi 3M NaCl-type Ag/AgCl reference electrode, and a platinum wire auxiliary electrode (Somerset *et al*., 2006; Somerset *et al*., 2010).

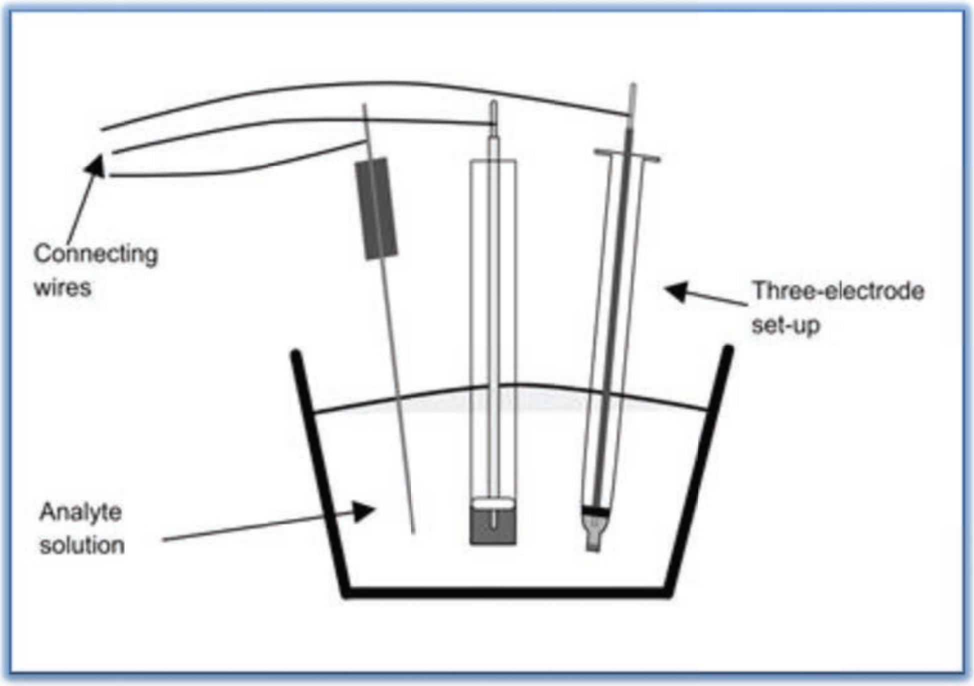

Figure 20. **Batch cell conventional three electrode set-up for the electrochemical determination of metal ions in aqueous solution.**

6.2.3 Quality control

Adherence to Quality Assurance (QA) and Quality Control (QC) procedures was of high standard throughout the collection and analysis of samples in this study. All glassware, polypropylene (PP) and other experimental containers were subjected to an adapted USEPA (2000) cleaning procedure, which entails an 8 hour cleaning in a 25% nitric acid solution, followed by rinsing in deionised water and cleaning in a 10% hydrochloric acid solution for another 8 hours. This was followed by rinsing with deionised water and drying in a laminar flowhood before containers were used in laboratory experiments.

6.2.4 Analytical procedure

The GCE was coated with a bismuth film (BiF) at the surface of the disc electrode using an electrochemical deposition step. The deposition step was performed at -1.0 V (*vs.* Ag/AgCl) using a 0.2 M sodium acetate (NaOAc) solution (pH = 4.8), containing 500 µg/ℓ Bi(III) for a duration of 240 s (Tesarova *et al*., 2009).

This was followed by differential pulse anodic stripping voltammetry (DPASV) characterisation, with following parameters: (i) differential pulse amplitude (peak to peak), 50 mV; step amplitude, 5 mV; pulse width, 50 ms; pulse period, 200 ms; scan rate, 25 mV/s (Somerset *et al*., 2010; Somerset *et al*., 2011).

Cyclic voltammetric characterisation of the metal-dimethylglyoxime (M(HDMG)$_2$) complexes was performed by scanning the potential from -1.4 to +0.8 V (*vs.* Ag/AgCl) at an initial scan rate of 40 mV/s.

6.3. Results and discussion

6.3.1 Characterisation of a bare and modified glassy carbon electrode

A GCE was used in the electrochemical characterisation and construction of the sensor electrode towards the detection of PGM. Figure 21 shows the results for the bare GCE, compared to the GCE coated with a bismuth film (BiF) that was characterised in 0.1 M HCl, 0.1 M ammonia and 0.2 M NaOAc buffer solutions. For the results in Figure 21 it was observed that the bare GCE showed minimal voltammetric response in the 0.2 M NaOAc buffer solution (pH = 4.8), with a reduction peak observed (E_p = 0.72 *vs.* Ag/AgCl) in the cathodic scan direction from +0.8 to -1.5 V (*vs.* Ag/AgCl).

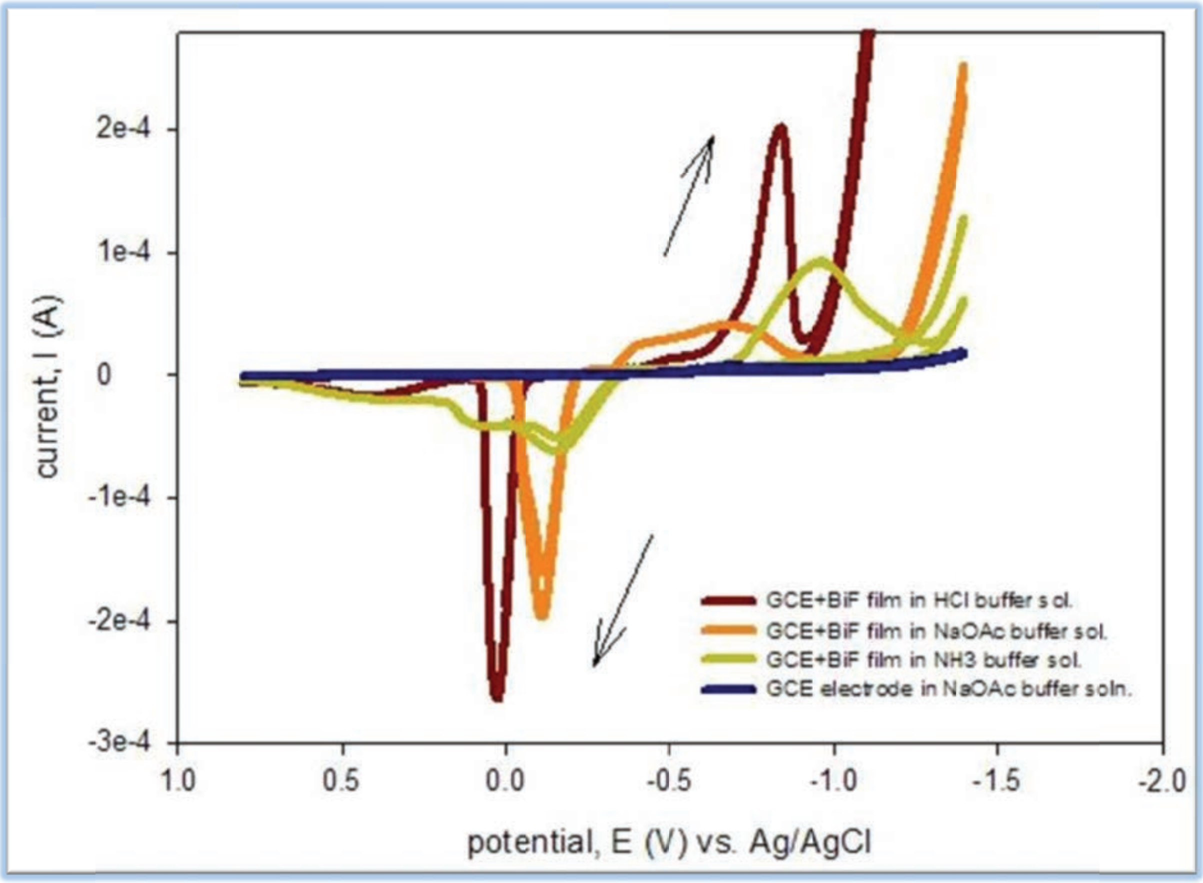

Figure 21. **Cyclic voltammetric (CV) results for the combined evaluation of the clean GCE versus the GCE+BiF sensor electrode in various buffer solutions of (a) 0.1 M HCl, (b) 0.1 M ammonia (pH = 9) and (c) 0.2 M NaOAc (pH = 4.8). The potential was scanned between -1.5 and 0.8 V (vs. Ag/AgCl) at a scan rate of 40 mV/s.**

Further analysis of the results in Figure 21 indicate that oxidation peaks in the region -0.2 to 0.1 V (*vs.* Ag/AgCl) were obtained in each of the buffer solutions investigated. The peak potentials were observed in the same potential region as in the study conducted by Tesarova *et al.* (2009). The decreasing magnitude of anodic peak current ($I_{p,a}$) was $I_{HCl} > I_{NaOAc} > I_{NH3}$ in the respective solutions. In the case of the reduction peaks that were observed from -0.7 to -1.1 V (*vs.* Ag/AgCl), the decreasing order of cathodic peak current ($I_{p,c}$) was $I_{HCl} > I_{NH3} > I_{NaOAc}$ in the respective solutions.

6.3.2 Optimisation of dimethylglyoxime (DMG) concentration

Dimethylglyoxime (DMG) is a chelating agent that forms complexes with metal ions. In electro-analytical methods it has been used with Pd(II), Ni(II) and Co(II) for the adsorptive voltammetric determination of these metal ions, since it forms 1:2 complexes with DMG to yield $Pd(HDMG)_2$, $Ni(HDMG)_2$ and $Co(HDMG)_2$ as compounds (Zhang *et al*., 2006; Ramirez *et al*., 2009; Georgieva and Pihlur, 1996).

Typically, the DMG is mixed with the target metal solution to form a complex that is subsequently accumulated on the electrode surface. The accumulation step is then followed by a stripping step in which the metal complex is stripped off the electrode surface using either voltammetric or chronopotentiometric techniques. It was further established that these complexes have different adsorption behaviour that depends on the surface concentration and sensor surface used in adsorptive voltammetric studies (Ramirez *et al*., 2009; Hutton *et al*., 2003).

During adsorptive voltammetry, the electroreduction process of Pd reacting with DMG can be represented by the following equation (Eqn. 4):

$$Pd(HDMG)_2(ads)\ (ads) + 2H^+ + 2e^- \leftrightarrows Pd + 2H_2DMG\ (aq) \qquad \textbf{Eqn. 4}$$

where the rate determining step involves one proton (H^+) and the transfer of the first electron (e^-) (Ramirez *et al*., 2009).

Figure 22 presents the results obtained for the optimisation of the $Pd(HDMG)_2$ complexes with varying DMG concentrations. A Pd(II) concentration of 10 mg/ℓ was used in 0.2 M sodium acetate buffer (pH = 4.5) solutions, with the deposition time varying from 30 to 240 seconds. The highest peak current was obtained when deposition times (t_d) from 30 to 150 s was used, with [DMG] = 5×10^{-5} M evaluated. In the case of the [DMG] = 2×10^{-4} M, a steady increase in peak current was absorbed as the deposition time increased from 30 to 150 s. During the next three deposition times, the peak current remained the same for the above two concentrations of DMG, while at a deposition time of 240 s, the highest peak current was obtained for the [DMG] = 2×10^{-4} M. In the case of the [DMG] = 1×10^{-4} M, the peak current was only comparable to the other two concentrations at a deposition time of 240 s. After further evaluation of these results it was decided to conduct all future experiments with a [DMG] = 5×10^{-5} M and a deposition time of 240 s.

After further investigation and evaluation of literature, it was established that DMG also forms complexes with Pd(II), Ni(II) and Co(II) in the alkaline pH range when ammonia buffer solution is used. Similarly, DMG also forms complexes with Pt(II) and Rh(III). This section of the sensor development procedure is currently being evaluated.

In recent studies the use of ammonia buffer solution with pH = 9 have been reported (Cordon *et al*., 2002; Hutton *et al*., 2003). When ammonia buffer solution is used, a catalytic hydrogen wave is also absorbed, which can be explained by the following reactions taking place:

$$Pd(HDMG)_2 + NH_4^+ \leftrightarrows Pd(HDMG)_2H^+ + NH_3(g) \qquad \textbf{Eqn. 5}$$

$$Pd(HDMG)_2H^+ + e^- \leftrightarrows Pd(HDMG)_2H \qquad \textbf{Eqn. 6}$$

$$2Pd(HDMG)_2H \longrightarrow 2Pd(HDMG)_2 + H_2(g) \qquad \textbf{Eqn. 7}$$

The equations shows that both ammonia (Eqn. 5) and hydrogen (Eqn. 7) as gases may evolve at the electrode surface with the formation of bubbles as indicator which has been reported in some studies (Cordon *et al*., 2002).

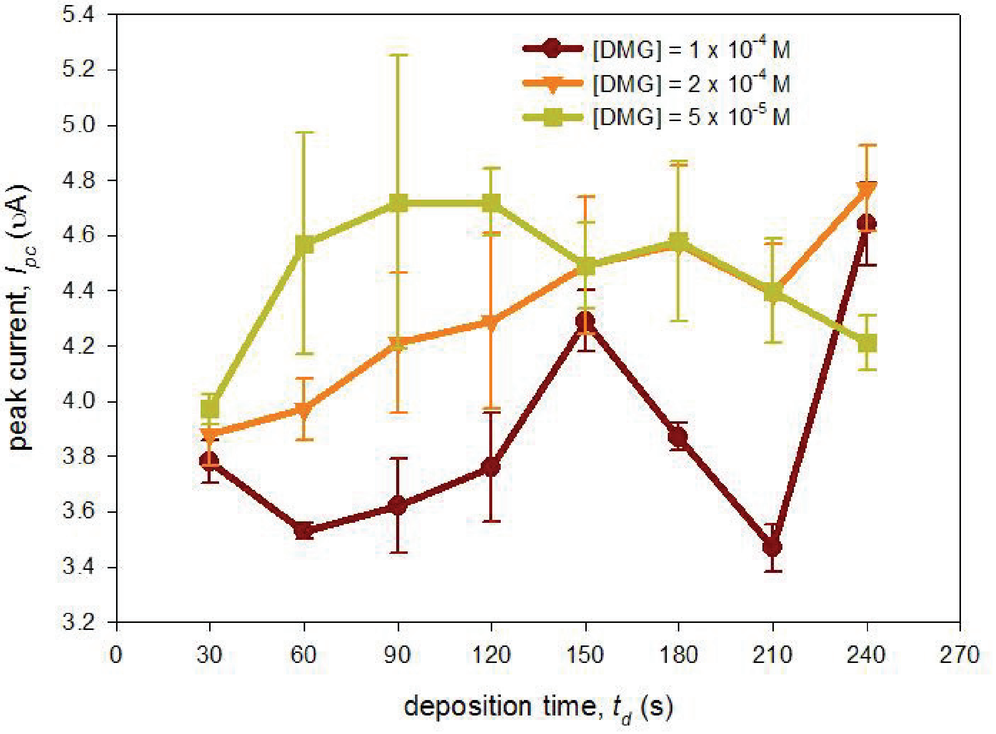

Figure 22. **Peak current results for the optimisation of varying dimethylglyoxime (DMG) concentrations and different deposition of Pd(HDMG)$_2$ complexes evaluated. Stripping differential pulse analysis was performed with a GCE+BiF sensor electrode in a 0.2 M sodium acetate buffer (pH = 4.5) solution and parameters; pulse amplitude of 50 mV; step amplitude of 5 mV; pulse width of 50 ms; pulse period of 200 ms; and a scan rate of 25 mV/s (*n = 2*).**

6.3.3 Optimisation of deposition potential

The next parameter optimised in the stripping voltammetric determination of Pd(II) as one of the PGMs was the deposition potential. Stripping analysis is a two-step technique with step 1 dealing with the deposition of the metal ions of interest onto the electrode surface, with the use of a complex ion as in our case. In step 2, which is called the stripping (measurement) step, the metal in the adsorbed complex is reduced and the signal recorded. The current response of the surface-confined species is directly related to its concentration (Wang, 2006).The deposition potential deals with the appropriate potential at which the reduced metal ion of interest needs to be determined and has to be optimised for analytical procedure (Wang, 2006). The effect of the deposition time on the peak current obtained for the Pd(HDMG)$_2$ complex evaluated in a 0.2 M sodium acetate buffer (pH = 4.5) solutions, with Pd(II) concentration of 10 mg/ℓ is shown in Figure 23. For potentials more negative than -500 mV, a gradual increase in the peak current was observed, with a sudden drop at -400 mV and the highest peak current obtained at a potential of -300 mV. Considering these observations made, the value of -300 mV was selected as the optimum deposition potential in a 0.2 M NaOAc buffer (pH = 4.5) solution (Tesarova *et al*., 2009; Somerset s*et al*., 2010; Kokkinos *et al*., 2009).

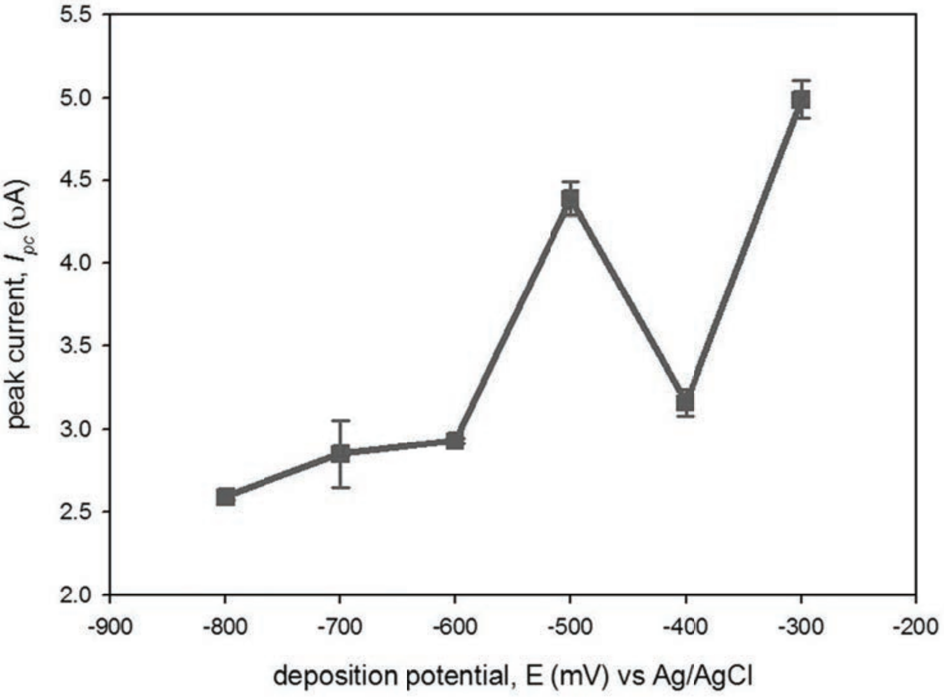

Figure 23. **Results obtained for the optimisation of the stripping (deposition) potential at various potential values for the Pd(HDMG)$_2$ complex evaluated. Stripping differential pulse analysis was performed with a GCE+BiF sensor electrode in a 0.2 M sodium acetate buffer (pH = 4.5) solution and parameters; pulse amplitude of 50 mV; step amplitude of 5 mV; pulse width of 50 ms; pulse period of 200 ms; and a scan rate of 25 mV/s (*n = 2*).**

6.3.4 Cyclic voltammetric (CV) evaluation of Pd(HDMG)$_2$ complex in various buffer solutions

6.3.4.1 Evaluation of Pd(HDMG)$_2$ complex in 0.1 M HCl (pH $\approx$ 2) buffer solution

The results obtained for the evaluation of the Pd(HDMG)$_2$ complex on a GCE/BiF sensor platform in a 0.1 M HCl buffer solution at various scan rates (Figure 24) showed that the peak height and current (I_p) increased as the scan rate (ν) increased from 40 to 120 mV/s. The intensity of the peaks was well-resolved and clearly defined, with the peak-to-peak separation (ΔE_p) ranging between 400 to 800 V (*vs.* Ag/AgCl). This is a clear indication that the adsorbed electroactive material undergoes quasi-reversible electrochemistry.

6.3.4.2 Evaluation of Pd(HDMG)$_2$ complex in 0.2 M NaOAc (pH = 4.8) buffer solution

Figure 25 shows the results obtained for the evaluation of the Pd(HDMG)$_2$ complex on a GCE/BiF sensor platform in a 0.2 M NaOAc buffer solution, and it can be seen that mixed peak current responses were obtained with not all peaks well defined or a definite increasing peak current observed, for the scan rates (ν) from 40 to 120 mV/s evaluated. The results obtained for the peak-to-peak separation (ΔE_p) were also not promising, indicating that optimisation of the cyclic voltammetric conditions are required. It was thus resolved to further investigate the voltammetric evaluation of the Pd(HDMG)$_2$ in the 0.2 M NaOAc buffer solution.

6.3.4.3 Evaluation of Pd(HDMG)$_2$ complex in 0.1 M ammonia (pH = 9) buffer solution

Figure 26 illustrates the results of the evaluation of the Pd(HDMG)$_2$ complex on a GCE/BiF sensor platform in a 0.1 M ammonia buffer solution,, where it was again observed that the peak height and current (I_p) increased as the scan rate (ν)increased from 40 to 120 mV/s.

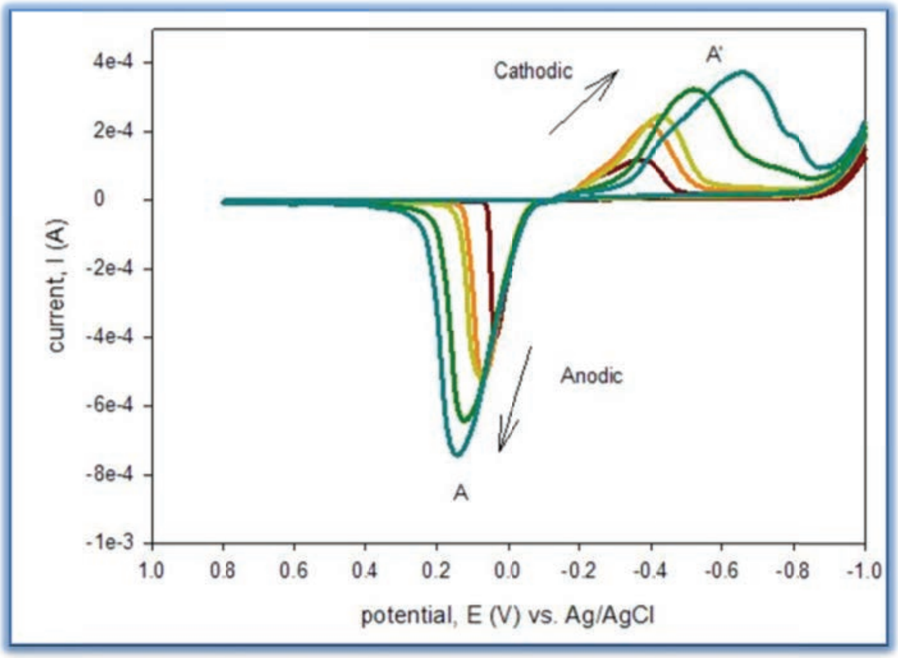

Figure 24. Cyclic voltammetric (CV) results for the evaluation of the Pd(HDMG)$_2$ complex on a GCE/BiF sensor platform in a 0.1 M HCl buffer solution at various scan rates. The Pd concentration used was 10 mg/ℓ, while the potential was scanned from -1.4 to +0.8 V (vs. Ag/AgCl) at an initial scan rate of 40 mV/s.

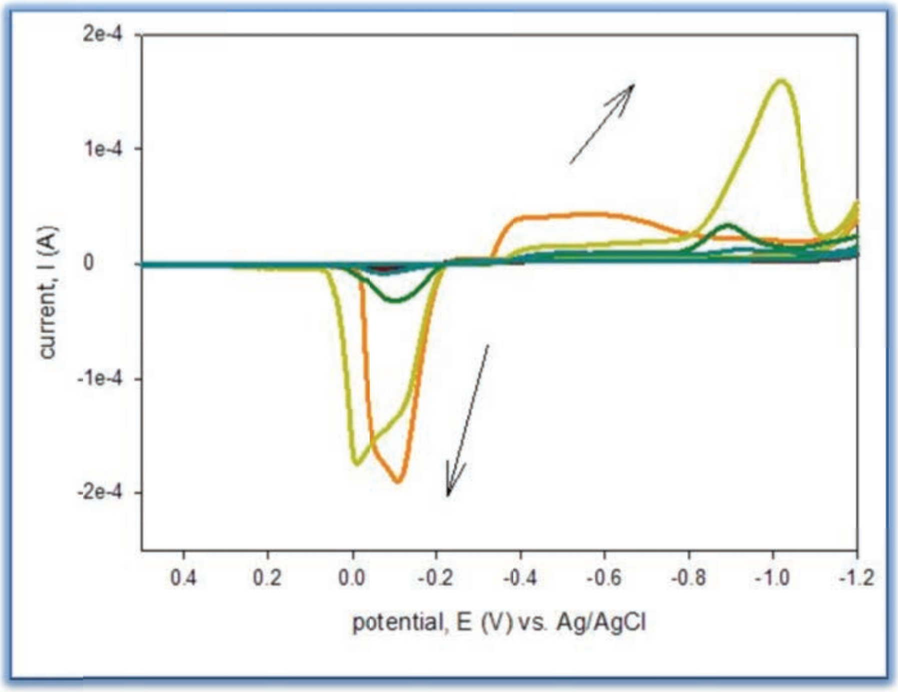

Figure 25. Cyclic voltammetric (CV) results for the evaluation of the Pd(HDMG)$_2$ complex on a GCE/BiF sensor platform in a 0.2 M sodium acetate (NaOAc) buffer solution at various scan rates. The Pd concentration used was 10 mg/L, while the potential was scanned from -1.4 to +0.8 V (vs. Ag/AgCl) at an initial scan rate of 40 mV/s.

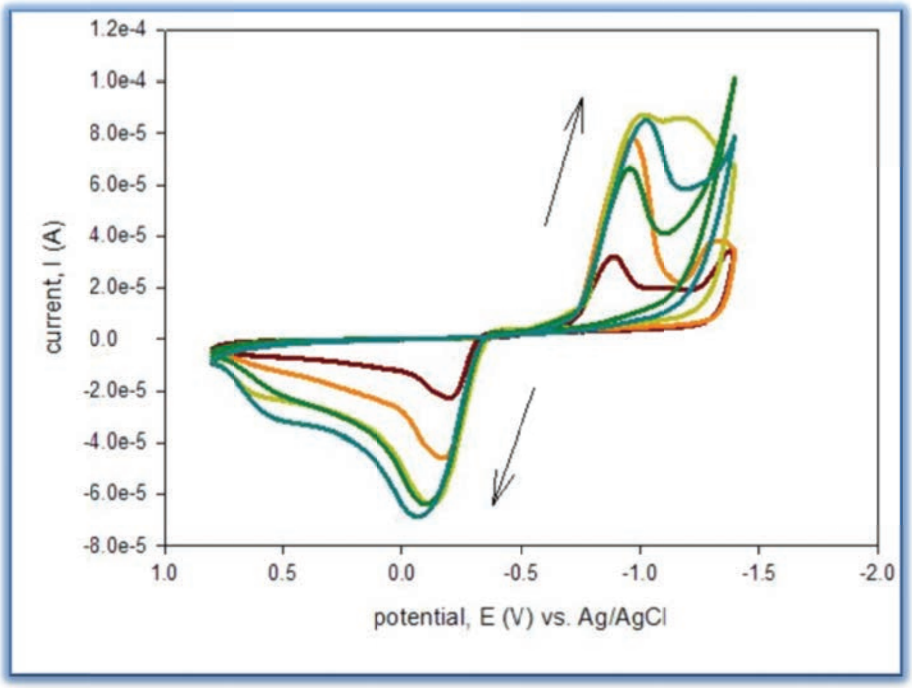

Figure 26. **Cyclic voltammetric (CV) results for the evaluation of the Pd(HDMG)$_2$ complex on a GCE/BiF sensor platform in a 0.1 M ammonia buffer solution at various scan rates. The Pd concentration used was 10 mg/ℓ, while the potential was scanned from -1.4 to +0.8 V (vs. Ag/AgCl) at an initial scan rate of 40 mV/s.**

The results obtained in this buffer solution also showed that the intensity of the peaks was well-resolved and clearly defined, with the peak-to-peak separation (ΔE_p) ranging between 700 to 1200 V (*vs.* Ag/AgCl). This indicates that the adsorbed electroactive material undergoes quasi-reversible electrochemistry.

In comparison of the results for the scan rate studies in the three different buffer solutions, it was observed that the best current responses were obtained when the Pd(HDMG)$_2$ complex was voltammetrically evaluated in the 0.1 M HCl (pH = 2) and 0.1 M ammonia (pH = 9) buffer solutions. Although better resolution of the peaks was observed in the 0.1 M ammonia (pH = 9) buffer solution, a better current response was observed in the 0.1 M HCl (pH = 2) buffer solution.

6.4 Analytical performance of sensor and stripping voltammetric investigation

The results collected for the first differential pulse adsorptive stripping voltammetric (DPAdSV) evaluation of the GCE/BiF/Pd(HDMG)$_2$ sensor towards Pd(II) determination is discussed in this section. During the first stage of the experimental development, all the voltammetric measurements were conducted in a 0.1 M NaOAc buffer solution (pH = 4.5), containing varying Pd(II) concentrations with 5 × 10^{-5} M DMG as complexing agent, in the presence of dissolved oxygen. During the stripping analysis a deposition potential of -0.7 V (*vs.* Ag/AgCl) was applied to the working electrode, for a deposition time (t_d) of 120 s. The solution was stirred during the deposition step, and after an equilibration period of 10 s, the stripping voltammogram was recorded by applying a negative-going potential scan (Hutton *et al*., 2003).

The best conditions of those investigated for the differential pulse adsorptive stripping voltammetric (DPAdSV) evaluation of Pd(II) are summarised in Table 29.

Table 29. Summary of optimal conditions for Pd(II) determination with the GCE/BiF sensor platform and DMG as complexing agent.

Step	Condition
Reduction step	
pH	2
Reduction potential	- 700 mV
Reduction time	120 s
Complexing agent	dimethylglyoxime
Supporting electrolyte	0.2 M NaOAc buffer solution
Measurement step	
Supporting electrolyte	0.2 M NaOAc buffer solution
Measurement technique	Adsorptive differential pulse voltammetry
Potential window	Sweep potential from -1.4 to +0.8 V

Figure 27 shows the results of the first DPAdSV towards Pd(II) determination. Figure 27(a) shows that successive additions of Pd(II) ions to the 0.1 M NaOAc buffer solution (pH = 4.5), resulted in the Pd(II) peak current response at a potential of approximately -0.35 V to -0.37 V (*vs.* Ag/AgCl). The results of the DPAdSV further show that as the concentrations were increased, a linear response was obtained for the calibration plot of increasing Pd(II) concentrations versus peak current response (Figure 27(b)). At this early stage of optimisation of experimental conditions, it was decided not to quantify the limit of detection for the first results obtained (Bobrowski *et al*., 2009; Somerset *et al*., 2010).

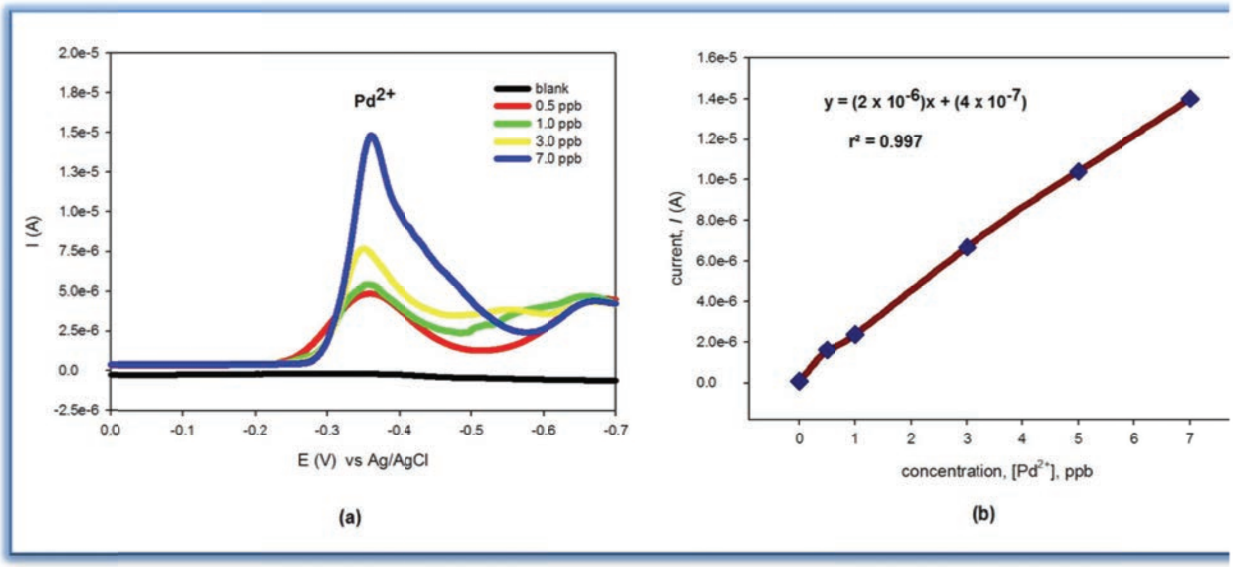

Figure 27. **The results obtained for the differential pulse adsorptive stripping voltammetric (DPAdSV) evaluation of the GCE/BiF/Pd(HDMG)$_2$ sensor towards increasing Pd(II) concentrations in a 0.1 M NaOAc buffer solution (pH = 4.5), are shown in (a). During differential pulse voltammetric analysis, the potential was scanned in the cathodic direction with parameters: ampl. = 50 mV; pulse width = 50 ms; pulse period = 200 ms; t_d = 120 s. In (b) the calibration plot for the increasing Pd(II) concentrations are shown (n = 2).**

6.5 Conclusions

Modifying the surface of a glassy carbon electrode with a bismuth film (BiF) aids in the stripping analysis of the Pd(HDMG)$_2$ complex, while varying results were obtained for evaluation of the GCE/BiF/Pd(HDMG)$_2$

sensor in 0.1 M HCl buffer (pH ≈ 2), 0.2 M NaOAc buffer (pH = 4.5) and 0.1 M ammonia (pH = 9) buffer solutions. For analytical purposes and an electro-analytical application, it is important that the optimum pH, DMG concentration, deposition potential, deposition time and Pd(II) concentration are obtained. Some of these parameters will be further investigated in order to optimise the sensor operating conditions.

Preliminary results have shown that modifying the surface of a glassy carbon electrode with a bismuth film (BiF) aids in the stripping analysis of the $Pd(HDMG)_2$ complex, while varying results were obtained for evaluation of the $GCE/BiF/Pd(HDMG)_2$ sensor in 0.1 M HCl buffer (pH ≈ 2), 0.2 M NaOAc buffer (pH = 4.5) and 0.1 M ammonia (pH = 9) buffer solutions. For analytical purposes and an electro-analytical application, it is important that the optimum pH, DMG concentration, deposition potential, deposition time and Pd(II) concentration are applied in the analysis of samples.

CHAPTER 7: LABORATORY EVALUATION OF SENSORS FOR METAL DETERMINATION AND APPLICATION OF ION-EXCHANGE MATERIALS IN ELECTROCHEMICAL SENSORS

7.1 Introduction

The main purpose of this chapter was to determine the experimental conditions and optimisation of stripping voltammetry parameters for the stripping analysis of Pd(II), Pt(II) and Rh(II) in the presence of dimethylglyoxime (DMG) as chelating agent. To achieve this objective, the surface of a glassy carbon electrode was modified with a bismuth film (BiF) and then applied in the stripping analysis of the $M(HDMG)_2$ complexes (M = Pd, Pt and Rh). All experimental results were determine in a 0.01 M ammonia buffer (pH = 9) solution. Other experimental conditions and parameters, i.e. deposition potential, deposition time and pH was also investigated to understand the stripping analysis conditions for palladium (Pd), platinum (Pt) and rhodium (Rh) as examples of precious group metals (PGMs).

7.2. Methods

7.2.1 Reagents and materials

All the chemicals and acids were of analytical grade (Merck, Germany and Fluka, Germany). All working solutions of Bi(III), Pd(II), Pt(II) and Rh(III) metal ions were prepared by atomic absorption standards (1000 mg/ℓ). All solutions were prepared by Milli-Q (Millipore 18 M Ohm.cm) water. Solutions of 100 mg/ℓ bismuth used to prepare the bismuth film in 0.2 M sodium acetate buffer. A 0.01 M ammonia buffer solution (pH = 9.0) was prepared by mixing ammonium chloride with concentrated ammonia and served as the electrolyte. The 0.01 M DMG solution was prepared in 95% ethanol and served as the chelating agent.

7.2.2 Apparatus

Electrochemical protocols were performed with an Epsilon electrochemical analyzer (BASi Instruments, West Lafayette, IN, USA), using CV or DPV amperometric modes (Figure 28). A conventional three electrode system (Figure 20) was employed, consisting of a BASi 3.0 mm diameter glassy carbon disc working electrode (GCE), a BASi 3 M NaCl-type Ag/AgCl reference electrode, and a platinum wire auxiliary electrode (Somerset *et al.*, 2006; Somerset *et al.*, 2010).

7.2.3 Quality control

Adherence to Quality Assurance (QA) and Quality Control (QC) procedures was of high standard throughout the collection and analysis of samples in this study. All glassware, polypropylene (PP) and other experimental containers were subjected to an adapted USEPA (2000) cleaning procedure, which entails an 8 hour cleaning in a 25% nitric acid solution, followed by rinsing in deionised water and cleaning in a 10% hydrochloric acid solution for another 8 hours. This was followed by rinsing with deionised water and drying in a laminar flowhood before containers were used in laboratory experiments.

7.2.4 Preparation of a metal film electrode

The glassy carbon disk electrode that was used as working electrode was thoroughly polished on a polish pad with 1.0, 0.3 and 0.05 µm alumina powder. The polished electrode was then rinsed with copious amounts of Milli-Q water and then immersed in a 0.2 M acetate buffer solution with a pH of 4.8 containing 100 mg/ℓ Bi(III) ions. In the next steps the deposition of a bismuth film was done by applying a potential of -1.0 V for 5 minutes and stirring the solution with a magnetic stirrer at 300 rpm. After the plating procedure the bismuth-coated glassy carbon electrode was carefully washed with Milli-Q water and was ready for use in sensor analysis (Hutton *et al.,* 2003).

Figure 28. **Epsilon electrochemical workstation and analyser, with the batch cell conventional three electrode set-up for the electrochemical determination of metal ions in aqueous solution (Van der Horst, 2011).**

7.2.5 Analytical procedure optimisation

Previous data were recorded in a 0.2 M sodium acetate (NaOAc) solution (pH = 4.8), while in this report the stripping voltammetric experiments were performed in 0.01 M ammonia buffer (pH = 9.0) solution. The GCE was coated with a bismuth film (BiF) at the surface of the disc electrode using an electrochemical deposition step. The deposition step was performed at -1.0 V (*vs.* Ag/AgCl) using a 0.2 M sodium acetate (NaOAc) solution (pH = 4.8), containing 500 µg/ℓ (III) for a duration of 240 s (Tesarova *et al.*, 2009).

This was followed by differential pulse anodic stripping voltammetry (DPASV) characterisation, with following parameters: (i) differential pulse amplitude (peak to peak), 50 mV; step amplitude, 5 mV; pulse width, 50 ms; pulse period, 200 ms; scan rate, 25 mV/s (Somerset *et al.*, 2010; Somerset *et al.*, 2011).

Cyclic voltammetric characterisation of the metal-dimethylglyoxime ($M(HDMG)_2$) complexes was performed by scanning the potential from -1.4 to +0.8 V (*vs.* Ag/AgCl) at an initial scan rate of 40 mV/s.

Standard solutions of the PGMs (Pt, Pd and Rh) in the 0.01 M ammonia buffer solution were prepared. It consisted of 10 mℓ of 0.01 M ammonia buffer (pH = 9.0) solution, containing 5×10^{-5} M DMG as complexing agent in the stripping electrolyte solution. The prepared GCE/BiF electrode was immersed into the solution and an accumulation potential of -0.7 V (*vs.* Ag/AgCl) was applied while the solution was stirred. A 10 s quiet time was used and the voltammogram was scanned from +0.8 to -1.4 V (*vs.* Ag/AgCl) at a scan rate of 40 mV/s. The PGMs were introduced into the solution after the background voltammogram was recorded. The analysis was performed at least twice for each of Pt, Pd and Rh in the presence of oxygen and at room temperature.

7.3 Results

7.3.1 Optimisation of complexing agent concentration

These results were collected during the second stage of the sensor development, which involved the use of a 0.01 M ammonia buffer (pH = 9) solution. A standard solution containing a 10 ppb Pd(II) concentration with

5×10^{-5} M DMG as complexing agent, was subjected to stripping analysis in the presence of dissolved oxygen.

Adsorptive differential pulse stripping voltammetry (AdDPSV) were used with a deposition potential of -0.3 V (*vs.* Ag/AgCl). The effect of the concentration of complexing agent on the AdDPSV peak current was studied by varying the concentration of DMG at (a) 1×10^{-5} M; (b) 2×10^{-5} M and (c) 5×10^{-5} M. All the results obtained were collected at different deposition times as shown in Figure 29. The peak current values were at a maximum at different times. In further comparison of the results it was it was observed that a DMG concentration of 5×10^{-5} M would be ideal to deliver a peak current within a short deposition time for Pd determination.

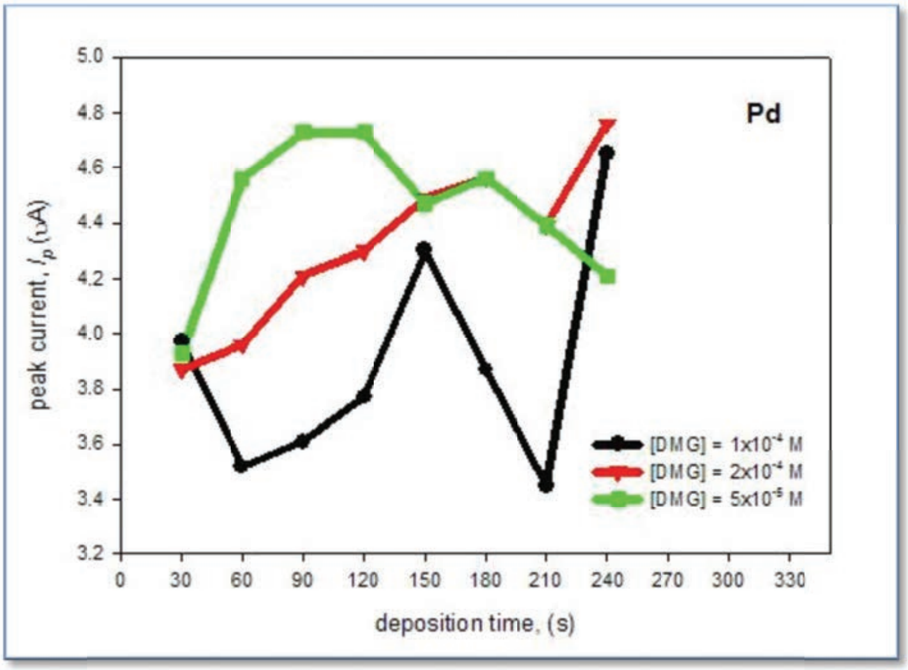

Figure 29. **Results obtained for peak current versus varying dimethylglyoxime (DMG) concentrations in a solution of 10 ppb Pd(II) in the presence of a 0.01 M ammonia buffer (pH = 9) solution. The DMG concentrations of (a) 1 x 10^{-5} M; (b) 2 x 10^{-5} M and (c) 5 x 10^{-5} M were evaluated (*n* = *2*).**

The adsorptive differential pulse stripping voltammetry (AdDPSV) results obtained for the evaluation of the GCE/BiF/Pt(HDMG)$_2$ sensor is shown in Figure 30. In the case of Pt peak currents were obtained at different deposition times for the three concentrations evaluated. At a deposition time of 90 s, a DMG concentration of 5×10^{-5} M resulted in a maximum peak current. At a longer deposition time of 120 s, both the DMG concentrations of 1×10^{-5} M and 2×10^{-5} M delivered maximum peak currents. Although the peak currents obtained at 120 s were a bit higher than the one obtained at 90 s, it was decided that a DMG concentration of 5×10^{-5} M would be ideal to deliver a peak current within a short deposition time for Pt determination.

The adsorptive differential pulse stripping voltammetry (AdDPSV) results obtained for the evaluation of the GCE/BiF/Rh(HDMG)$_3$ sensor is shown in Figure 31. Evaluation of the results for Rh showed that at a short deposition time of 90 s, all three concentrations of DMG delivered a maximum peak current. The results further showed a gradual decrease in the peak current for this specific PGM.

In summary it was determined that a DMG concentration of 5 x 10^{-5} M would be ideal to deliver a peak current for the analysis of Pd, Pt and Rh using the GCE/BiF sensor electrode.

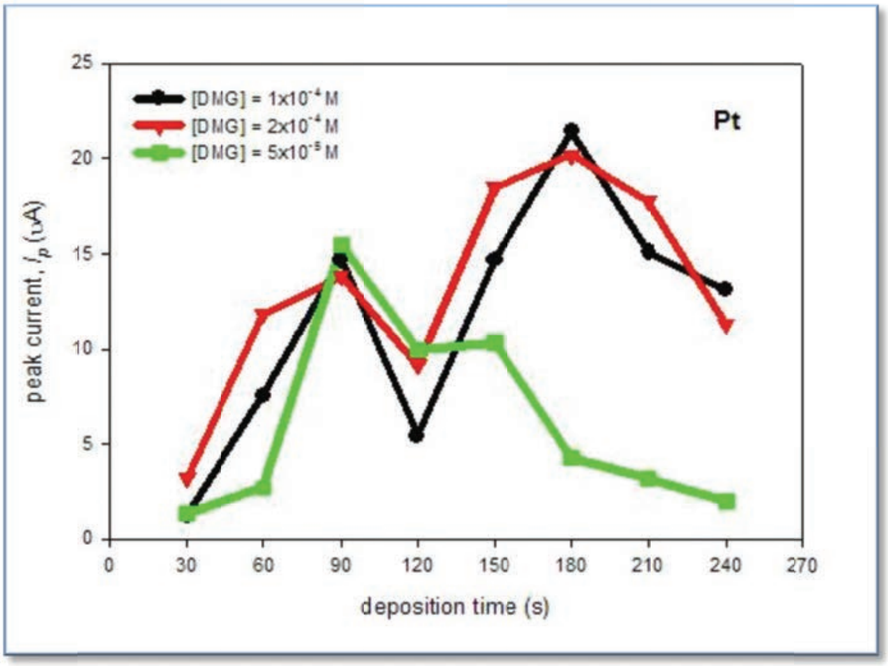

Figure 30. Results obtained for peak current versus varying dimethylglyoxime (DMG) concentrations in a solution of 10 ppb Pt(II) in the presence of a 0.01 M ammonia buffer (pH = 9) solution. The DMG concentrations of (a) 1 x 10^{-5} M; (a) 2 x 10^{-5} M and (c) 1 x 10^{-5} M were evaluated (*n* = *2*).

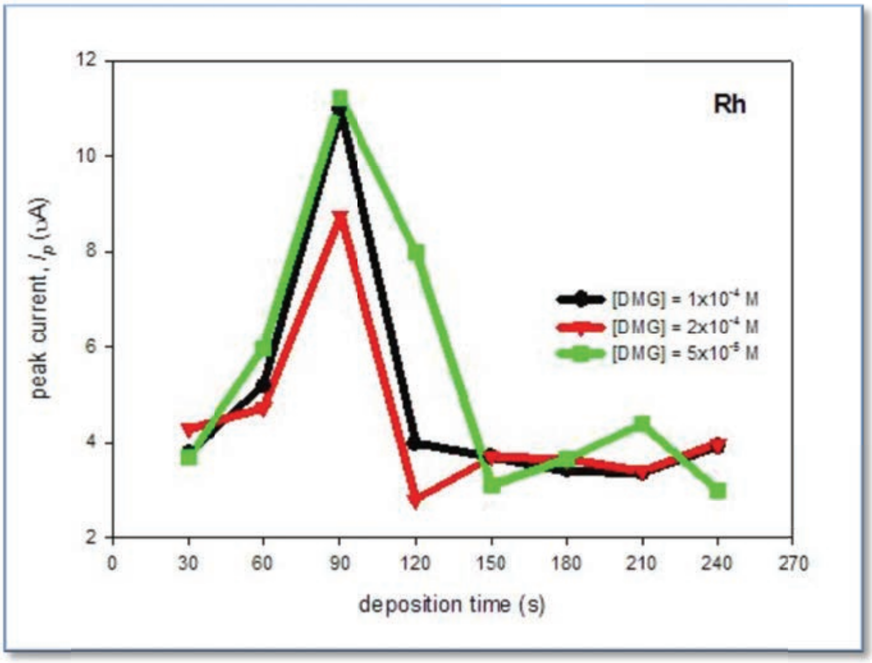

Figure 31. Results obtained for peak current versus varying dimethylglyoxime (DMG) concentrations in a solution of 10 ppb Pt(II) in the presence of a 0.01 M ammonia buffer (pH = 9) solution. The DMG concentrations of (a) 1 x 10^{-5} M; (b) 2 x 10^{-5} M and (c) 5 x 10^{-5} M were evaluated (*n* = *2*).

7.3.2 Deposition potential optimisation

The next parameter optimised in the stripping voltammetric determination of Pd(II) as one of the PGMs was the deposition potential. Stripping analysis is a two-step technique with step 1 dealing with the deposition of the metal ions of interest onto the electrode surface, with the use of a complex ion as in our case. In step 2, which is called the stripping (measurement) step, the metal in the adsorbed complex is reduced and the signal recorded. The current response of the surface-confined species is directly related to its concentration (Wang, 2006).

The deposition potential deals with the appropriate potential at which the reduced metal ion of interest needs to be determined and has to be optimised for analytical procedure (Wang, 2006; Tesarova *et al*., 2009; Somerset s*et al*., 2010; Kokkinos *et al*., 2009).

The effect of the deposition potential on the peak current obtained for the M(HDMG)$_2$ complexes (M = Pd, Pt and Rh) evaluated in a 0.01 M ammonia buffer (pH = 9) solutions, with M(II) concentrations of 10 µg/ℓ is shown in Figure 32. Varying results were obtained for each of the PGMs. In the case of Pd, a maximum peak current was obtained at a potential of -700 mV (*vs.* Ag/AgCl), while the peak current remained relatively constant as the potential was increased to less negative values, with a slight increase at -400 mV (*vs.* Ag/AgCl). In the case of Pt it was observed that lower peak current results were obtained, compared to that of Pd and Rh. A maximum peak current was also observed at -700 mV (*vs.* Ag/AgCl), similar to the results for Pd, while the peak currents decreased at the less negative potentials investigated.

The Rh results in Figure 32 show a gradual increase in peak current, with the peak currents taking a dip at potentials of -700 and -400 mV (*vs.* Ag/AgCl). A peak current of -500 mV (*vs.* Ag/AgCl) delivered a maximum peak current response for the determination of Rh with the current sensor constructed.

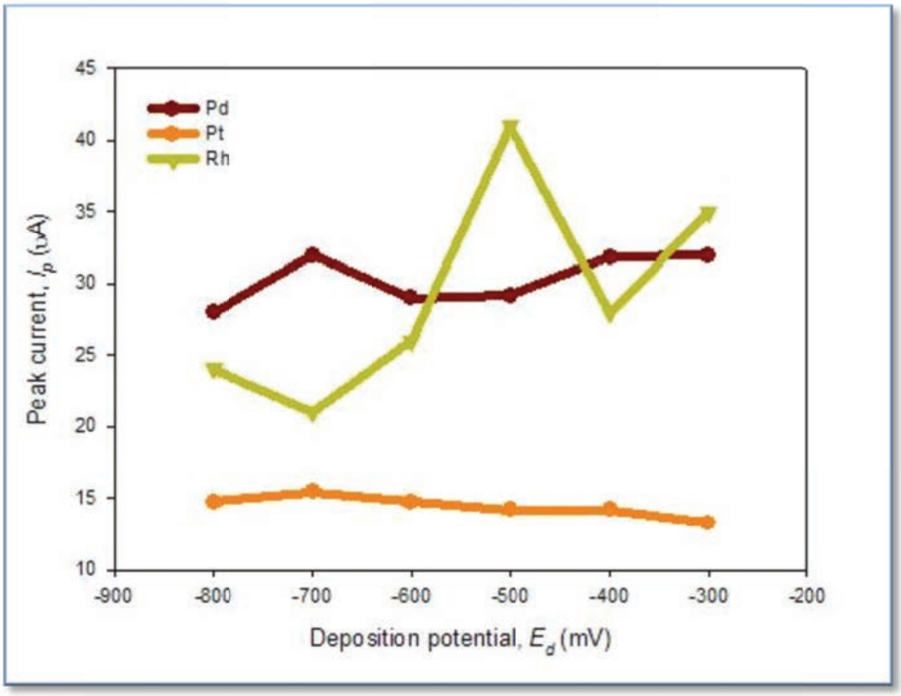

Figure 32. Results obtained for the optimisation of the stripping (deposition) potential at various potential values for the M(HDMG)$_2$ (M = Pd, Pt, Rh) complexes evaluated. Adsorptive stripping differential pulse analysis was performed with a GCE/BiF sensor electrode in a 0.01 M ammonia buffer (pH = 9) solution and parameters; pulse amplitude of 50 mV; step amplitude of 5 mV; pulse width of 50 ms; pulse period of 200 ms; and a scan rate of 25 mV/s (*n* = *2*).

In summary, a deposition potential of -700 mV (*vs.* Ag/AgCl) was the best of those investigated for the determination of Pd and Pt, while a potential of -500 mV (*vs.* Ag/AgCl) was best for the determination of Rh using a 0.01 M ammonia buffer (pH = 9) solution.

7.3.3 Deposition time optimisation

Optimisation of the deposition time is also very important in the analysis of PGMs, since the amount of $M(HDMG)_2$ complex (M = Pd, Pt and Rh) adsorbed onto the bismuth film depends on the time for which the adsorption is performed (Tesarova *et al*., 2009; Somerset s*et al*., 2010).

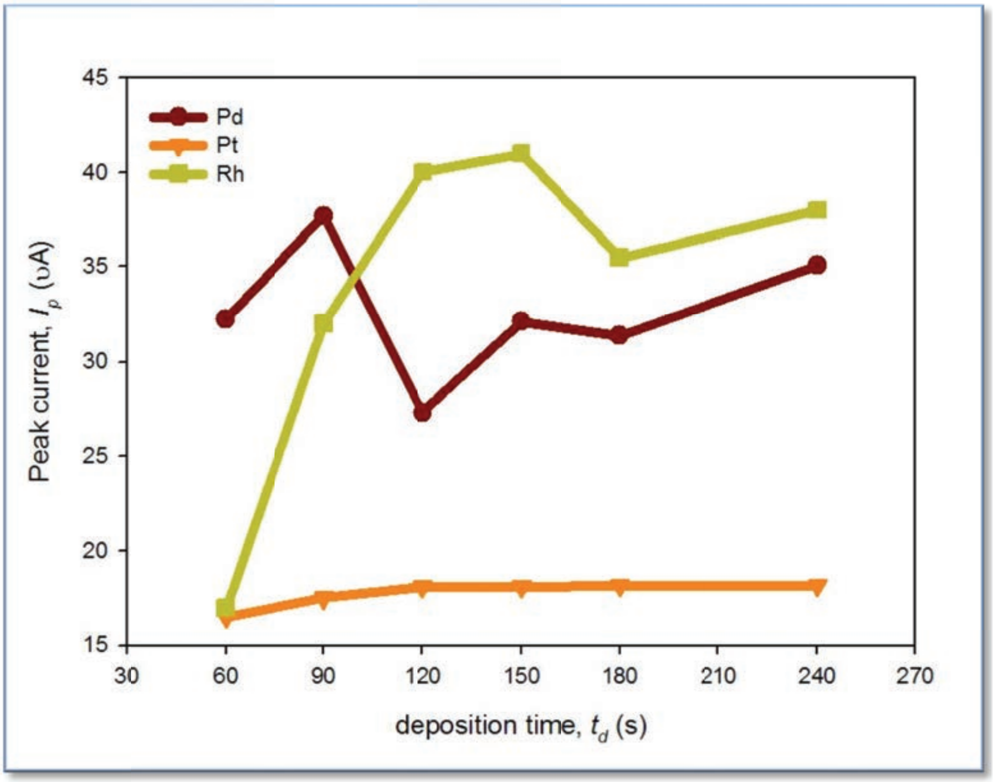

Figure 33. **Effect of deposition time on adsorptive stripping voltammetric responses at a GCE/BiF electrode. The solution of 0.01 M ammonia buffer (pH = 9.0) containing 1 ppb of Pd, Pt and Rh in respective solutions with 5 x 10^{-5} M DMG. The adsorptive stripping voltammetric analysis conditions are defined in Figure 5 (*n* = *1*).**

Figure 33 indicates that maximum peak currents for Pd, Pt and Rh were obtained at three different times. In the case of Pd, a short deposition time of 90 s delivered a maximum peak current, while in the case of Pt it was 120 s and for Rh, 150 s.

Table 30 summarises the optimal conditions for the adsorptive differential pulse stripping voltammetric (AdDPSV) evaluation of Pd(II), Pt(II) and Rh(III). These parameters were applied in the next stage of the investigation for the detection and quantification of PGMs.

Table 30. Summary of the optimal conditions for PGM determination with the GCE/BiF sensor platform and DMG as complexing agent.

Step	PGM		
	Pd	**Pt**	**Rh**
Reduction step			
pH	9	9	9
Reduction potential	- 700 mV	- 700 mV	- 500 mV
Reduction time	90 s	120 s	150 s
Complexing agent	Dimethylglyoxime (DMG)		
Supporting electrolyte	0.01 M ammonia buffer solution		
Measurement step			
Supporting electrolyte	0.01 M ammonia buffer solution		
Measurement technique	Adsorptive differential pulse voltammetry		
Potential window	Sweep potential from -1.4 to +0.8 V		

7.3.4 Analytical performance of sensor and stripping voltammetric investigation

The results collected for the adsorptive differential pulse stripping voltammetric (AdDPSV) evaluation of the GCE/BiF sensor towards the analysis of the Pd(HDMG)$_2$ complexes (M = Pd, Pt and Rh) is discussed in this section. All the stripping voltammetric measurements were conducted in a 0.01 M ammonia buffer solution (pH = 9), containing varying PGM concentrations with 5×10^{-5} M DMG as complexing agent, in the presence of dissolved oxygen. During the stripping analysis a specific deposition potential (E_d) was applied to the working electrode, for a specific deposition time (t_d) characteristic to each of Pd, Pt and Rh. The solution was stirred during the deposition step, and after an equilibration period of 10 s, the stripping voltammogram was recorded by applying a negative-going potential scan (Hutton *et al*., 2003).

Figure 33 shows the AdDPSV curves for Pd in (a), Pt in (b) and Rh in (c). In Figure 34(a) the results for the evaluation of the Pd(HMDG)$_2$ complex are shown, which indicate that definitive peaks were obtained at a peak potential of -0.92 V (*vs.* Ag/AgCl) as the Pd concentrations were increased from 0 to 0.5 µg/ℓ. This peak was not observed in the blank solution, while in the case of 0.2 µg/ℓ the peak potential was obtained at -0.85 V (*vs.* Ag/AgCl). A calibration curve of peak current *vs.* Pd concentration was plotted and a linear graph was obtained with equation, $y = 16.37x + 10.52$ and $R^2 = 0.997$.

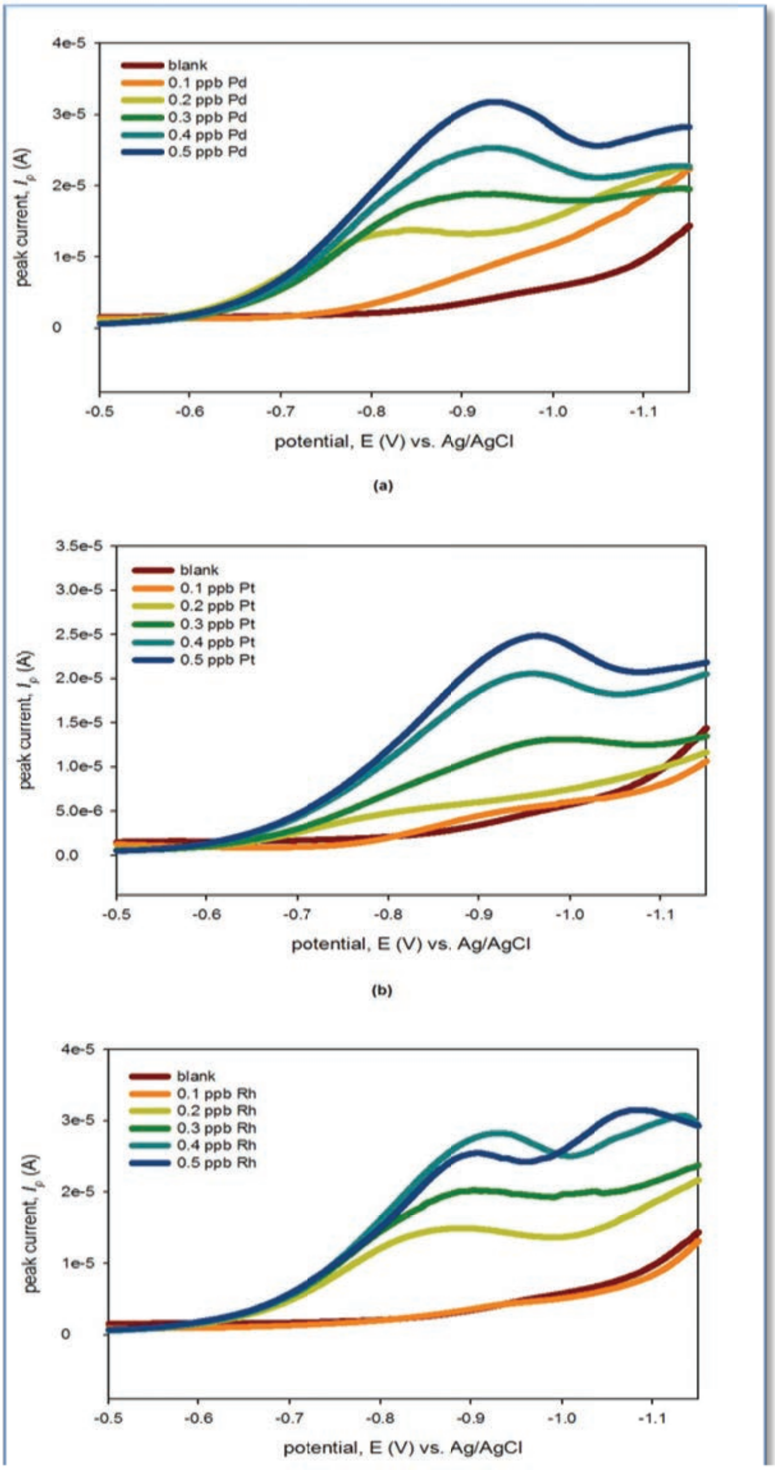

Figure 34. **The results obtained for the differential pulse adsorptive stripping voltammetric (DPAdSV) evaluation of the GCE/BiF sensor towards the determination of the PGMs in a 0.01 ammonia buffer solution (pH = 9), are shown. The potential was scanned in the cathodic direction with parameters: ampl. = 50 mV; pulse width = 50 ms; pulse period = 200 ms (*n* = *2*).**

The evolution of hydrogen gas (H_2 (g)) was observed during each of the PGMs investigated. This is in accordance with recent studies that have shown that the use of ammonia buffer solution (pH = 9) can be attributed to the gas formation (Cordon *et al*., 2002; Hutton *et al*., 2003). When ammonia buffer solution is used, a catalytic hydrogen wave is also absorbed, which can be explained by the following reactions taking place:

$Pd(HDMG)_2+NH_4^+ \leftrightarrows Pd(HDMG)_2H^+ + NH_3(g)$ **Eqn. 8**

$Pd(HDMG)_2H^+ + e^- \leftrightarrows Pd(HDMG)_2H$ **Eqn. 9**

$2Pd(HDMG)_2H \longrightarrow 2Pd(HDMG)_2+H_2(g)$ **Eqn. 10**

The gas formation delivered a characteristic peak at approximately -1.4 V (*vs.* Ag/AgCl), which are not shown in the DPAdSVs in Figure 34. The results obtained for the determination of Pt are shown in Figure 32 (b). The AdDPSV results again showed a definitive peak at -0.95 V (*vs.* Ag/AgCl) as the Pt concentrations were increased from 0 to 0.5 µg/ℓ. A calibration curve of peak current *vs.* Pt concentration was plotted and a linear graph was obtained with equation, $y = 9.440x + 6.646$ and $R^2 = 0.994$.

Similarly, the results obtained for the Rh determination are shown in Figure 32 (c). The AdDPSV results showed peak potentials ranging between -0.85 and -0.92 V (*vs.* Ag/AgCl) for Rh concentrations ranging between 0 and 0.5 µg/ℓ. For the 0.4 and 0.5 ppb Rh concentrations evaluated, a second peak potential at approximately -1.1 V (*vs.* Ag/AgCl) was observed that is attributed to interfering ions present in the standard solution. The presence of the interfering ions will be discussed in the next report. Furthermore, a calibration curve of peak current *vs.* Pt concentration was plotted and a linear graph was obtained with equation, $y = 16.64x + 10.34$ and $R^2 = 0.995$.

7.4 Conclusions

Modifying the surface of a glassy carbon electrode with a bismuth film (BiF) aids in the stripping analysis of the $M(HDMG)_2$ complexes (M = Pd, Pt and Rh). The other parameters optimised included the DMG concentration, deposition potential and deposition time. A DMG concentration of 5×10^{-5} M would be ideal to deliver a peak current for the analysis of Pd, Pt and Rh using the GCE/BiF sensor electrode. A deposition potential of -700 mV (*vs.* Ag/AgCl) would be ideal for the determination of Pd and Pt, while a potential of -500 mV (*vs.* Ag/AgCl) will work best for the determination of Rh using a 0.01 M ammonia buffer (pH = 9) solution. In the case of Pd, a short deposition time of 90 s delivered a maximum peak current, while in the case of Pt it was 120 s. For Rh a deposition time of 150 s delivered a maximum peak current.

Preliminary results have shown that a DMG concentration of 5×10^{-5} M would be ideal to deliver a peak current for the analysis of Pd, Pt and Rh using the GCE/BiF sensor electrode. It was further determined that a deposition potential of -700 mV (*vs.* Ag/AgCl) would be ideal for the determination of Pd and Pt, while a potential of -500 mV (*vs.* Ag/AgCl) will work best for the determination of Rh using a 0.01 M ammonia buffer (pH = 9) solution. In the case of Pd, a short deposition time of 90 s delivered a maximum peak current, while in the case of Pt it was 120 s. For Rh a deposition time of 150 s delivered a maximum peak current.

CHAPTER 8: ADSORPTIVE VOLTAMMETRIC STRIPPING ANALYSIS OF PGMs AND INTERFERENCE STUDIES

8.1 Introduction

The objective of this chapter was to optimise the conditions for the differential pulse cathodic stripping voltammetric analysis of PGMs. Different variables were investigated and included the deposition potential, pre-concentration time, bismuth concentrations, ionic strength of supporting electrolyte, transport rate to the electrode surface and accumulation potential. All the aforementioned variables are very important in the stripping analysis procedure. Using the results obtained in the previous chapter, the investigation focussed on the simultaneous determination of the PGMs to establish which combinations of Pd, Pt and Rh can be examined under which experimental conditions.

8.2 Methods

8.2.1 Reagents

All heavy and precious metal standards (1000 mg/ℓ AAS), dimethylglyoxime (DMG) were purchased from Fluka (Germany). Sodium acetate, ammonia (25%), ammonium chloride, hydrochloric acid and nitric acid were supplied by Merck (South Africa). Glacial acetic acid (95%), ethanol (95%), hexamethylene tetramine (HMTA), hydrazine sulphate, formaldehyde solution were supplied by Kimix (South Africa), All solutions were prepared by Milli-Q (Millipore 18 M Ohm cm) water. Solutions of 100 mg/ℓ bismuth were used to prepare the bismuth film in 0.2 M sodium acetate buffer. Next, 0.5 to 20 µg/L solutions of platinum group elements were prepared by diluting the corresponding standard stock solutions. A 0.01 M ammonia buffer solution (pH 9.0) was prepared by mixing ammonium chloride with concentration ammonia and served as the electrolyte. The 0.01 M DMG solution was prepared in 95% ethanol and served as the chelating agent. A 0.2 M sodium acetate buffer (pH 4.8) was prepared by mixing sodium acetate with acetic acid and deionised water.

8.2.2 Apparatus

Electrochemical measurements were conducted with an Epsilon electrochemical analyzer (BASi Instruments, 2701 Kent Ave., West Lafayette, IN 47906, USA) using cyclic voltammetry (CV), or differential pulse adsorptive stripping voltammetry amperometric (DPAdSV) modes (Figure 28). A conventional three electrode system was employed, consisting of bismuth film prepared on a BASi 1.6 mm diameter glassy carbon disc working electrode. A BASi 3 M NaCl-type Ag/AgCl reference electrode was used, and a platinum wire as auxiliary electrode. All experiments were performed in a 20 mℓ electrochemical cell at conditioned room temperature (Somerset *et al.*, 2010).

8.2.3 Quality control

Adherence to Quality Assurance (QA) and Quality Control (QC) procedures was of high standard throughout the collection and analysis of samples in this study. All glassware, polypropylene (PP) and other experimental containers were subjected to an adapted USEPA (2000) cleaning procedure, which entails an 8 hour cleaning in a 25% nitric acid solution, followed by rinsing in deionised water and cleaning in a 10% hydrochloric acid solution for another 8 hours. This was followed by rinsing with deionised water and drying in a laminar flowhood before containers were used in laboratory experiments.

8.2.4 Preparation of bismuth film (BiFE)

The glassy carbon disk electrode that was used as working electrode was thoroughly cleaned and polished on a polish pad with 1.0, 0.3 and 0.05 µm alumina powders. The polished electrode was first rinsed with deionised water and then immersed in 0.2 M acetate buffer with a pH of 4.8 containing 100 mg/ℓ Bi(III) ions. The deposition of the bismuth film proceeds by applying a potential of -1.0 V (*vs.* Ag/AgCl) for 5 minutes and stirring the solution with a magnetic stirrer at 300 rpm. After the plating procedure, the bismuth-coated glassy carbon electrode was carefully washed with deionised water and was ready for use (Hutton *et al*., 2003).

8.2.5 Procedure for the determination of PGMs

A 10 mℓ of 0.01 M ammonia buffer with pH 9.0 containing 5 x 10^{-5} M DMG were used in the stripping operations as the electrolyte. The film electrode was immersed into the solution and an accumulation potential of -0.7 V (vs. Ag/AgCl) was applied while the solution was stirred. A 10 s quiet time was used and the voltammogram was scanned from 0.8 to -1.4 V (vs. Ag/AgCl) with a scan rate of 40 mV/s. The PGMs were introduced into the solution after the background voltammogram. All the experiments were performed in duplicate in the presence of oxygen and at room temperature.

8.3 Adsorptive stripping analysis of PGMs

8.3.1 Stripping analysis of single precious metal ions

The adsorptive stripping analysis of PGMs with DMG resulted in well-shaped stripping peaks at specific and defined potentials. Ammonia buffer (pH = 9.0) was used as the supporting electrolyte and the evolution of hydrogen peaks appeared consistently in the supporting electrolyte and a peak was observed at approximately -1.4 V (*vs.* Ag/AgCl). Figure 35 shows the set of adsorptive stripping voltammograms obtained upon increasing the Pd(II) concentration from 0.5 to 2.5 µg/ℓ. The electrochemical scan in the cathodic direction shown reduction peaks at ~ -0.91 V (*vs.* Ag/AgCl) for $Pd(HDMG)_2$ chelate. The potential was scanned between -0.4 V and -1.2 V (*vs.* Ag/AgCl) with accumulation time of 90 s and accumulation potential of -0.7 V (*vs.* Ag/AgCl) with a quiet time of 10 s respectively. Well defined peaks were observed with a flat baseline for the blank solution. The calibration curve obtained shown linear response for this voltammogram.

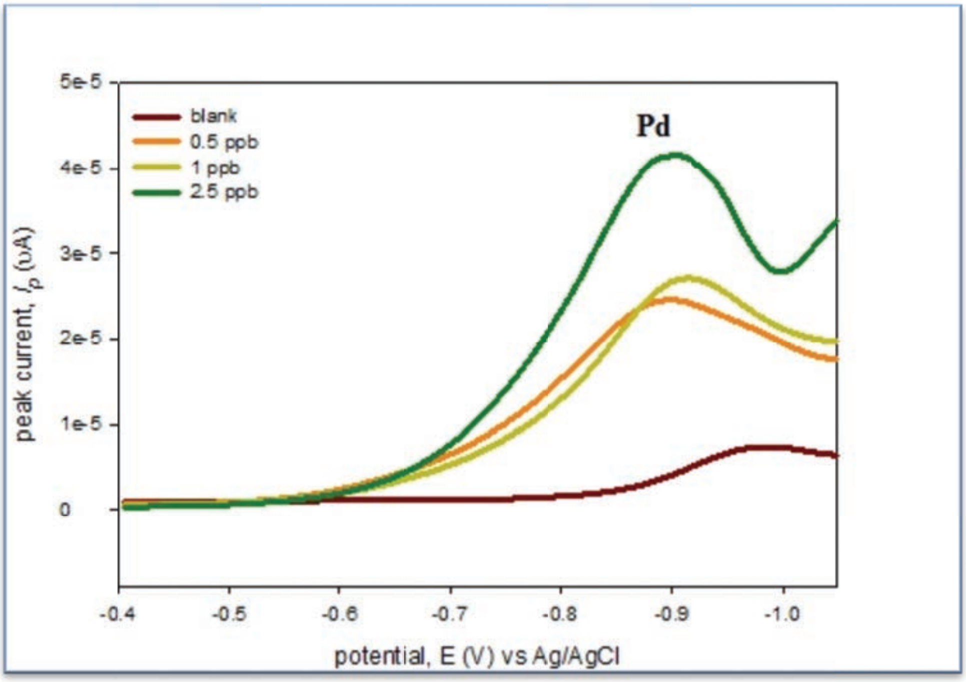

Figure 35. **Differential pulse adsorptive stripping voltammetry for increasing concentrations of Pd at a bismuth film electrode. The solution consisted of 0.01 M ammonia buffer (pH = 9.0) containing 0.5 to 2.5 µg/ℓ Pd with 5 x 10^{-5} M DMG; deposition potential was -0.7 V (vs. Ag/AgCl) and deposition time 90 s (*n* = *2*).**

The calibration plot for stripping peak current upon the increasing concentration for Pd(HDMG)$_2$ complex is revealed in Figure 34. The six concentrations used yielded a highly linear calibration plot. The equation for the linear plot is $y = 16.14x + 10.61$ ($R^2 = 0.992$).

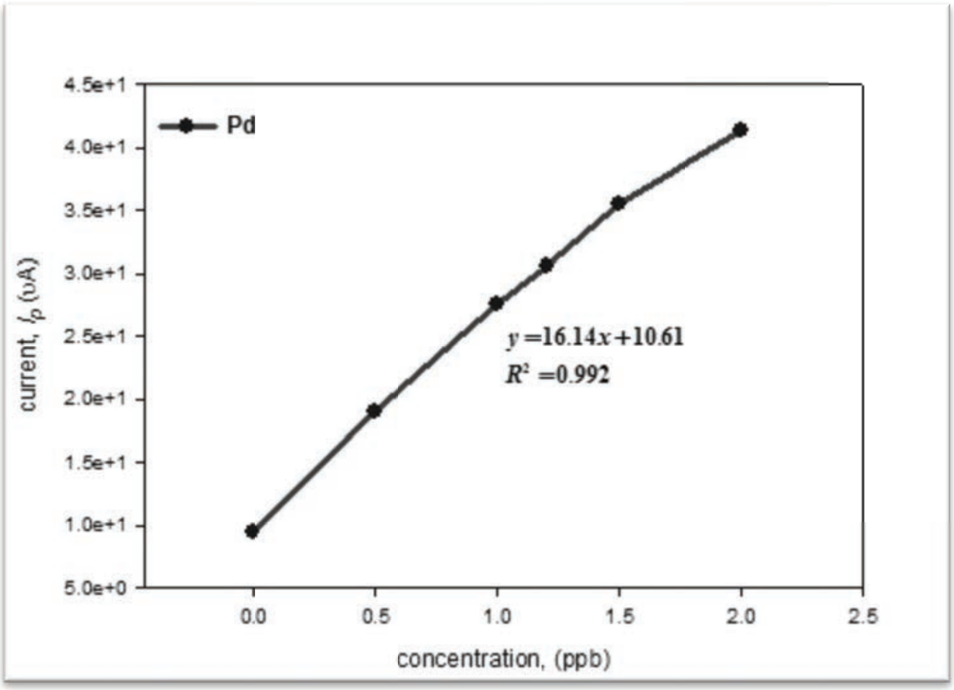

Figure 36. **Corresponding calibration curve obtained for the Pd(II) at deposition potential -0.7 V (vs. Ag/AgCl) and deposition time 90 s (*n* = *2*).**

Figure 37 depicts the stripping voltammogram obtained upon increasing the Pt(HDMG)$_2$ chelate concentrations from 1.0 to 3.5 µg/ℓ. Well-defined peaks were observed for Pt with 150 s accumulation time. The stripping voltammograms have shown the adsorption of the Pt chelate on a GC/BiFE at a stripping potential of -0.7 V (*vs.* Ag/AgCl) in a 0.01 M ammonia buffer (pH = 9.0) solution. The corresponding calibration curve obtained at the bismuth film showed a linear response. Figure 37 also shows the deposition potential at ~ -0.97 V (*vs.* Ag/AgCl) and the potential was scanned in the cathodic direction with amplitude of 50 ms, pulse period of 200 ms, while the potential was scanned from -0.4 V to -1.2 V (*vs.* Ag/AgCl).

Figure 38 presents the calibration plot obtained upon the increasing concentration for Pt(HDMG)$_2$ complex. The six concentrations used yielded a linear calibration plot and the equation of the linear calibration is $y = 9.53x + 5.58$ ($R^2 = 0.989$).

Adsorptive stripping voltammograms of Rh(III) in 0.01 M ammonia buffer (pH = 9.0) and with a 100 mg/ ℓ BiFE are also demonstrated in Figure 39, in which a set of Rh(II) standards were studied, including that of a sample blank. These voltammetric results obtained showed a good increase in peak currents for small increases in the Rh(III) concentrations. Analysis of adsorptive stripping voltammograms also showed peaks at approximately -0.98 V (*vs.* Ag/AgCl), which can be attributed to Rh(III) ions. The small reduction peak at approximately -0.8 V (*vs.* Ag/AgCl) with the use of 2 µg/ℓ solution is due to impurities in the solution.

Figure 40 illustrates the calibration plot obtained for peak current upon the increasing concentrations for Rh(HDMG)$_3$ complex. The six concentrations used yielded a linear response and the equation of the linear calibration curve is $y = 16.65x + 10.34$ ($R^2 = 0.996$).

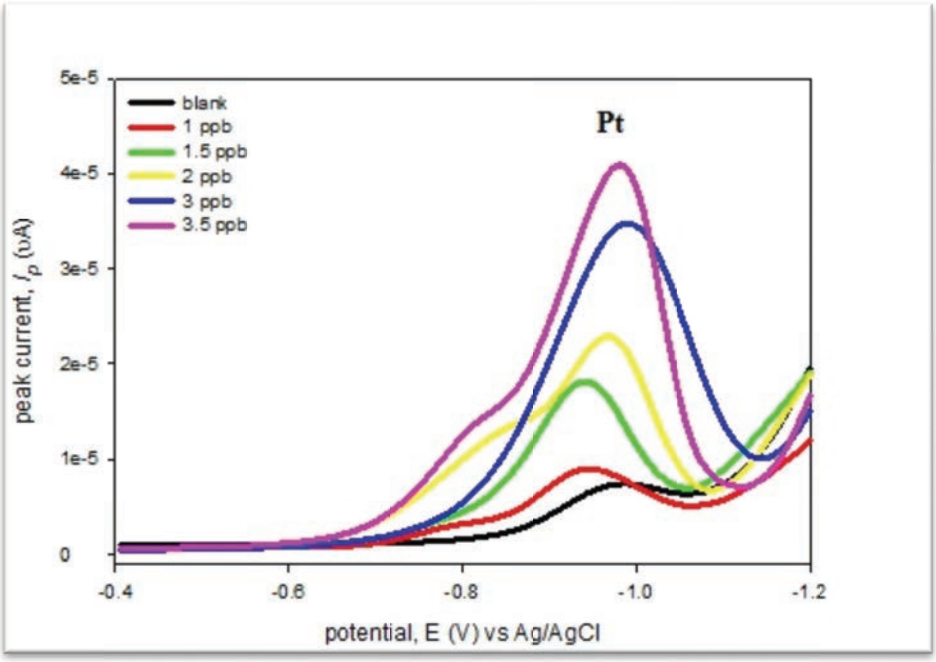

Figure 37. Differential pulse adsorptive stripping voltammetry for increasing concentrations of Pt at a bismuth film electrode. The solution consisted of 0.01 M ammonia buffer (pH = 9.0) containing 1 to 3.5 µg/ℓ Pt with 5 x 10^{-5} M DMG; deposition potential was -0.7 V (vs. Ag/AgCl) and deposition time 150 s (*n* = *2*).

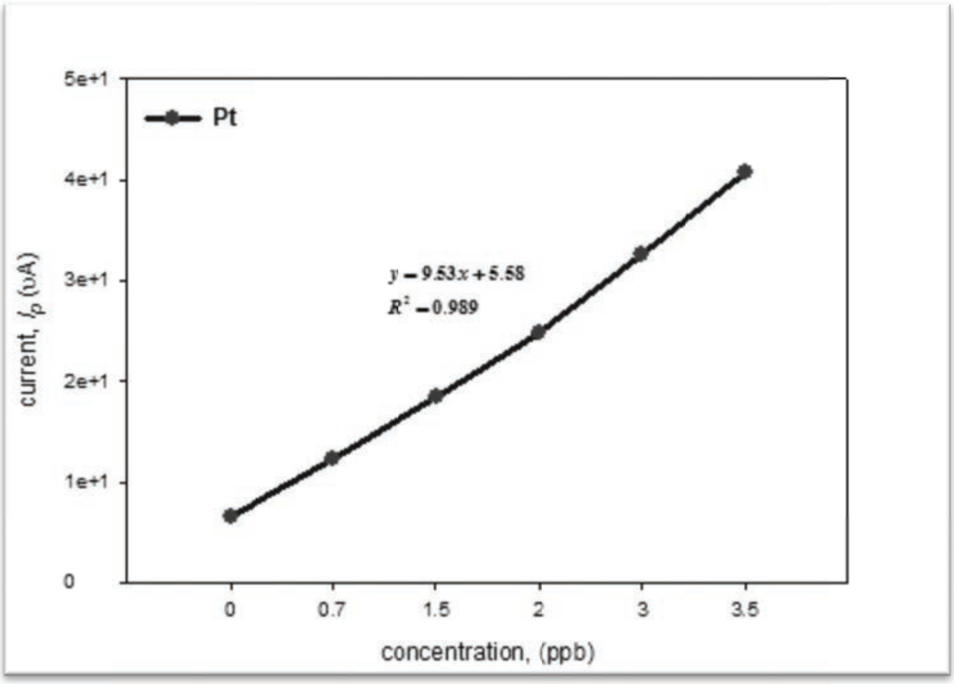

Figure 38. Corresponding calibration curve obtained for the Pt(II) at deposition potential -0.7 V (vs. Ag/AgCl) and deposition time 150 s (*n* = *2*).

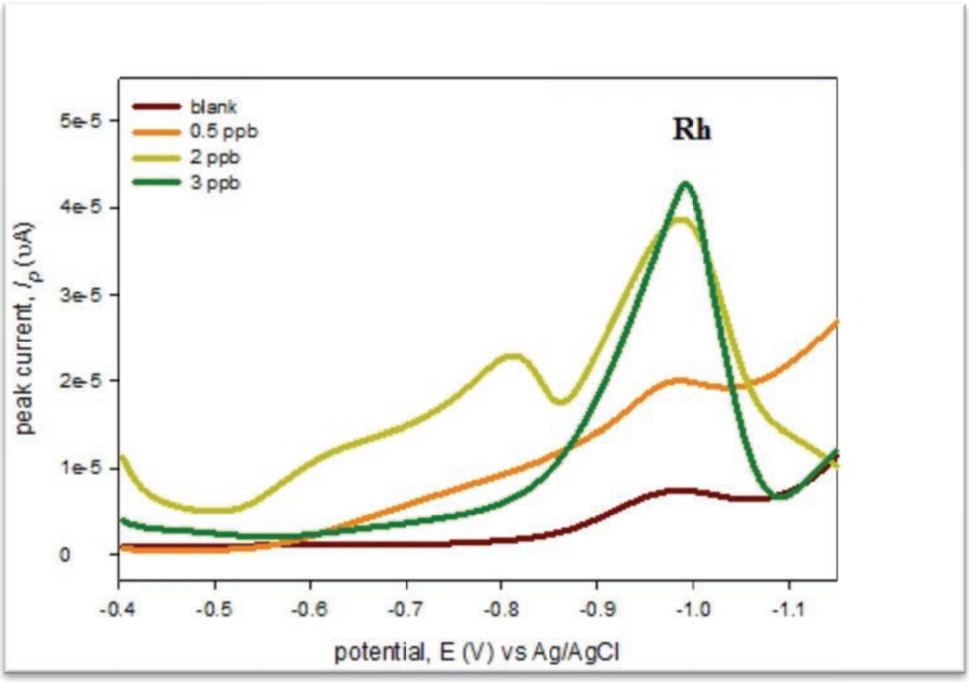

Figure 39 **Differential pulse adsorptive stripping voltammetry for increasing concentration of Rh at a bismuth film electrode. The solution consisted of 0.01 M ammonia buffer (pH = 9.0) containing 0.5 to 3 µg/ℓ Rh with 5 x 10^{-5} M DMG; deposition potential was -0.5 V (vs. Ag/AgCl) and deposition time 150 s (*n* = *2*).**

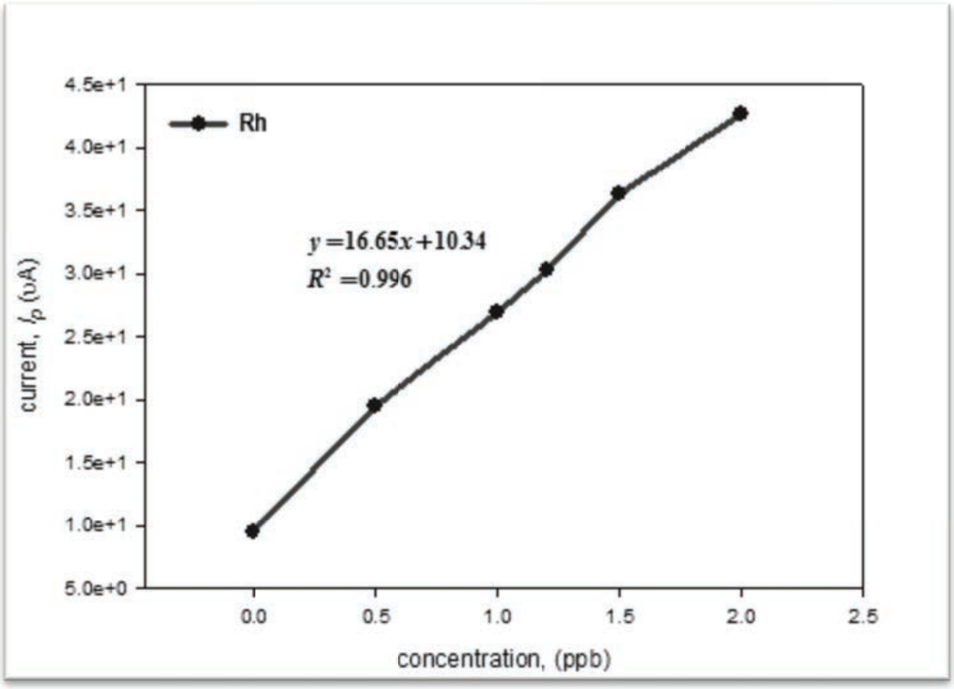

Figure 40. **Corresponding calibration curve obtained for the Rh(III) at deposition potential -0.5 V (vs. Ag/AgCl) and deposition time 150 s (*n* = *2*).**

In conclusion, good results were obtained for the single determination of Pd, Pt and Rh. These three PGMs showed distinctive stripping potentials that may be used for the stripping analysis of PGMs.

8.3.2 Simultaneous stripping analysis of precious metal ions

8.3.2.1. Analytical features for the determination of Pd and Rh

In Figure 41 the results for the determination of Pd in (a), Rh in (b) and simultaneous determination of Pd and Rh in (c) in a 0.01 M ammonia buffer (pH = 9.0) containing 5×10^{-5} M DMG concentration are shown. The adsorptive differential pulse stripping analysis of Pd(II) and Rh(III) with DMG resulted in well-shaped stripping peaks at specific potentials. Ammonia buffer was used as the supporting electrolyte and the evolution of hydrogen peaks appeared consistently in the supporting electrolyte. For Pd(II) the stripping potential was found to be -0.9 V (*vs.* Ag/AgCl) (Figure 41(a)), while for Rh(III) it was -0.98 V (*vs.* Ag/AgCl) (Figure 41(b)). In Figure 41(c) it was observed that the stripping potentials have slightly shifted towards less negative potentials in the simultaneous determination of Pd(II) and Rh(III), with the Pd(II) peaks obtained at a potential of -0.82 V (*vs.* Ag/AgCl) and the Rh(III) peaks at -0.94 V (*vs.* Ag/AgCl).

As the concentration of Pd(II) was increased in Figure 41(a), corresponding increases in the peak current was observed. In the case of Pd(II) the stripping potential was observed at -0.9 V (*vs.* Ag/AgCl). Not all AdDPSV curves are shown but the calibration plot yielded a highly linear calibration plot. The equation for the linear plot is $y = 16.37x + 10.52$ and $R^2 = 0.9970$.

Comparisons of the results obtained for Pd(II) to those obtained by other researchers have shown that the peak potential of Pd(II) is less negative than the peak potential of Rh(III). Also the peak current of Pd(II) is lower than the peak current of Rh(III) in both basic and acidic supporting electrolytes (Locatelli, 2006).

Figure 41(b) shows the AdDPSV curves for the Rh-$(HDMG)_3$ chelate on a GC/BiFE sensor at a stripping potential of -0.7 V (*vs.* Ag/AgCl) in a 0.01 M ammonia buffer (pH = 9.0) solution. As the concentration of Rh(II) increased, corresponding increases in the peak current were observed. In the case of Rh(II) the stripping potential was observed at -0.98 V (*vs.* Ag/AgCl). The small reduction peak at approximately -0.8 V (*vs.* Ag/AgCl) with the use of 2 ppb is due to impurities in the solution. Not all AdDPSV curves are shown but the six concentrations used yielded a linear response and the equation of the linear calibration plot is $y = 16.65x + 10.34$ ($R^2 = 0.996$).

Figure 41(c) displays the results for the AdDPSV curves of the simultaneous determination of Pd and Rh (chelated with DMG) on a GC/BiFE sensor at a stripping potential of -0.7 V (*vs.* Ag/AgCl) in a 0.01 M ammonia buffer (pH = 9.0) solution. The simultaneous determination of Pd(II) and Pt(II) is very problematic due to the interfering of the two metals ions with one another. Locatelli (2006) observed that Pt(II) and Pd(II) interfere in alkaline media and only the simultaneous study for Pd(II) and Rh(II) were done. The results have shown that only the simultaneous determination of Pd(II) and Rh(III), Pt(II) and Rh(III) are possible. It is observed that Pd(II) and Rh(III) overlap at higher concentrations but on a flat baseline which slightly reduce the problem. The voltammogram at the bismuth thin layer shown linear response with the linear calibration equation $y = 8.423x + 11.89$ (R^2= 0.975) for Pd-$(HDMG)_2$ chelate. The calibration plot for the Rh-$(HDMG)_3$ chelate was also constructed and yielded a calibration equation $y = 9.401x + 4.587$ ($R^2 = 0.970$).

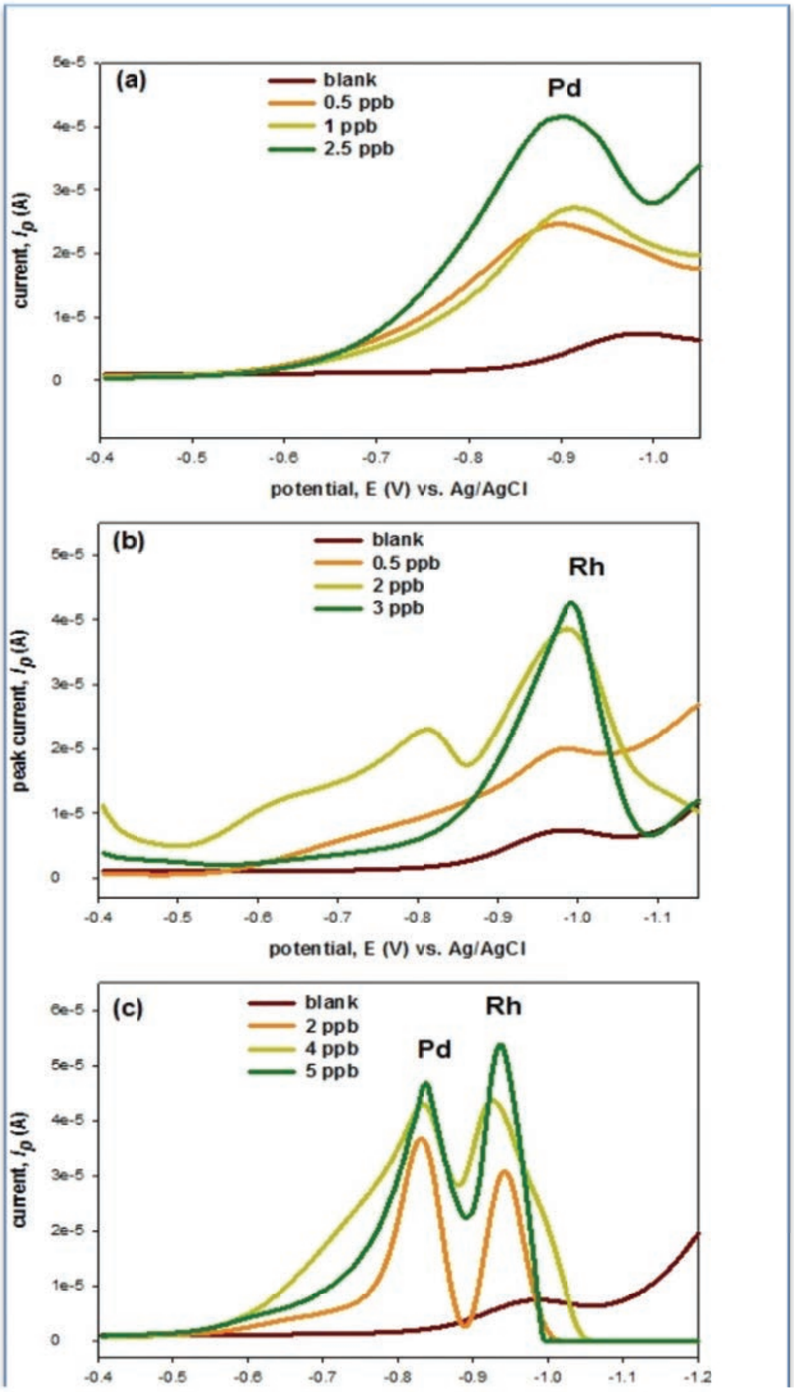

Figure 41. Results for the adsorptive differential pulse stripping voltammetric analysis for increasing concentration of (a) 0.5-2.5 µg/ℓ Pd with E_d = -0.7 V (vs. Ag/AgCl) and t_d = 90 s, (b) 0.5-3.0 µg/ℓ Rh with E_d = -0.5 V (vs. Ag/AgCl) and t_d = 150 s and (c) 2.0-5.0 µg/ℓ Pd-Rh with E_d = -0.6 V (vs. Ag/AgCl) and t_d = 150 s at the GC/BiFE sensor. The solutions used consisted of 0.01 M ammonia buffer (pH = 9.0) containing 5 x 10^{-5} M DMG concentration (*n* = *2*).

8.3.2.2. Analytical features for the determination of Pt and Rh

Figure 42 reports the results for the determination of Pt(II) in (a), Rh(III) in (b) and simultaneous determination of Pt(II) and Rh(III) in (c) in a 0.01 M ammonia buffer (pH = 9.0) containing 5 × 10^{-5} M DMG concentration. The adsorptive differential pulse stripping analysis of Pt(II) and Rh(III) with DMG resulted in well-shaped stripping peaks at specific stripping potentials. Ammonia buffer was used as the supporting electrolyte and the evolution of hydrogen peaks appears consistently in the supporting electrolyte. For Pt(II) the stripping potential was found to be -0.97 V (*vs.* Ag/AgCl) (Figure 40 (a)), while for Rh(III) it was -0.98 V (*vs.* Ag/AgCl) (Figure 42(b)). In Figure 42(c) it was also observed that the stripping potentials have slightly shifted towards less negative potentials in the simultaneous determination of Pt(II) and Rh(III), with the Pt(II) peaks obtained at a potential of -0.75 V (*vs.* Ag/AgCl) and the Rh(II) peaks at -0.93 V (*vs.* Ag/AgCl).

Figure 42(a) depicts stripping voltammogram obtained upon increasing Pt-$(HDMG)_2$ chelate concentrations from 1.0 to 3.5 ppb. Well-defined peaks are observed for the Pt-$(HDMG)_2$ chelate with 150 s accumulation time. The stripping voltammogram has shown the adsorption of the Pt chelate on a GC/BiFE at stripping potential of -0.7 V (*vs.* Ag/AgCl) in a 0.01 M ammonia buffer (pH 9.0) solution. According to the calibration curve the bismuth film showed a linear response. Figure 40 (a) shown the deposition potential at -0.97 V and the potential was scanned in the cathodic direction with amplitude is 50 ms, pulse period is 200 ms. The potential was scanned from -0.4 V to -1.4 V. The six concentrations used yielded a linear calibration plot and the equation of the linear calibration is $y = 9.440x + 6.646$ ($R^2 = 0.9940$).

The results of the simultaneous determination of Pt(II) and Rh(III) are shown in Figure 42(c). Pt(II) and Rh(III) overlapped at the higher concentration but not at the two lower concentrations and on a flat baseline, which slightly mitigated the problem. The voltammogram at the bismuth thin layer shown slightly linear response with the linear calibration equation is $y = 11.29x + 6.39$ ($R^2= 0.954$) for Pt-$(HDMG)_2$ chelate.

Comparison of the results obtained for Pt(II) and Rh(III) in this studies to that obtained by other researchers have shown similarities in peak potentials. According to the work done by Dalvi *et al*. (2008) and Locatelli (2006) similar results were obtained with a hanging mercury drop electrode for Pt(II) and Rh(III) in solutions of acidic mediums as the supporting electrolyte.

In this last section we have seen that very interesting results were obtained for the simultaneous determination of Pd and Rh, compared to the results obtained for Pt and Rh. Most important was the results obtained for the stripping potentials for the individual PGMs, compared to the shift in potentials obtained for the simultaneous analysis.

Table 31 provides a summary of the results for the single and simultaneous voltammetric determination of the PGMs and shows the deposition potential (E_d) and deposition time (t_d) for the single and simultaneous voltammetric determination of the PGMs. In the case of the single PGM voltammetric analysis, it was observed that the same deposition potential of -0.7 V (*vs.* Ag/AgCl) can be used, while for Rh the result was -0.5 V (*vs.* Ag/AgCl). Furthermore, Pd-Rh can be simultaneously determined at a deposition potential of -0.6 V (*vs.* Ag/AgCl) and Pt-Rh, while for the Pt-Rh couple the same deposition potential can be applied. Except for Pd at 90 s, all the other combinations of PGMs can be analysed using a deposition time of 150 s making the stripping analysis a short voltammetric procedure.

Table 31. Results obtained for the determination of Pd(II), Pt(II), Rh(II), Pd(II)-Rh(III) and Pt(II)-Rh(III) by differential pulse adsorptive stripping voltammetry (DPAdSV).

	Pd(II) (DPAdSV)	Pt(II) (DPAdSV)	Rh(III) (DPAdSV)	Pd(II)-Rh(III) (DPAdSV)	Pt(II)-Rh(III) (DPAdSV)
E_d (V)	-0.7	-0.7	-0.5	-0.6	-0.6
t_d (s)	90	150	150	150	150

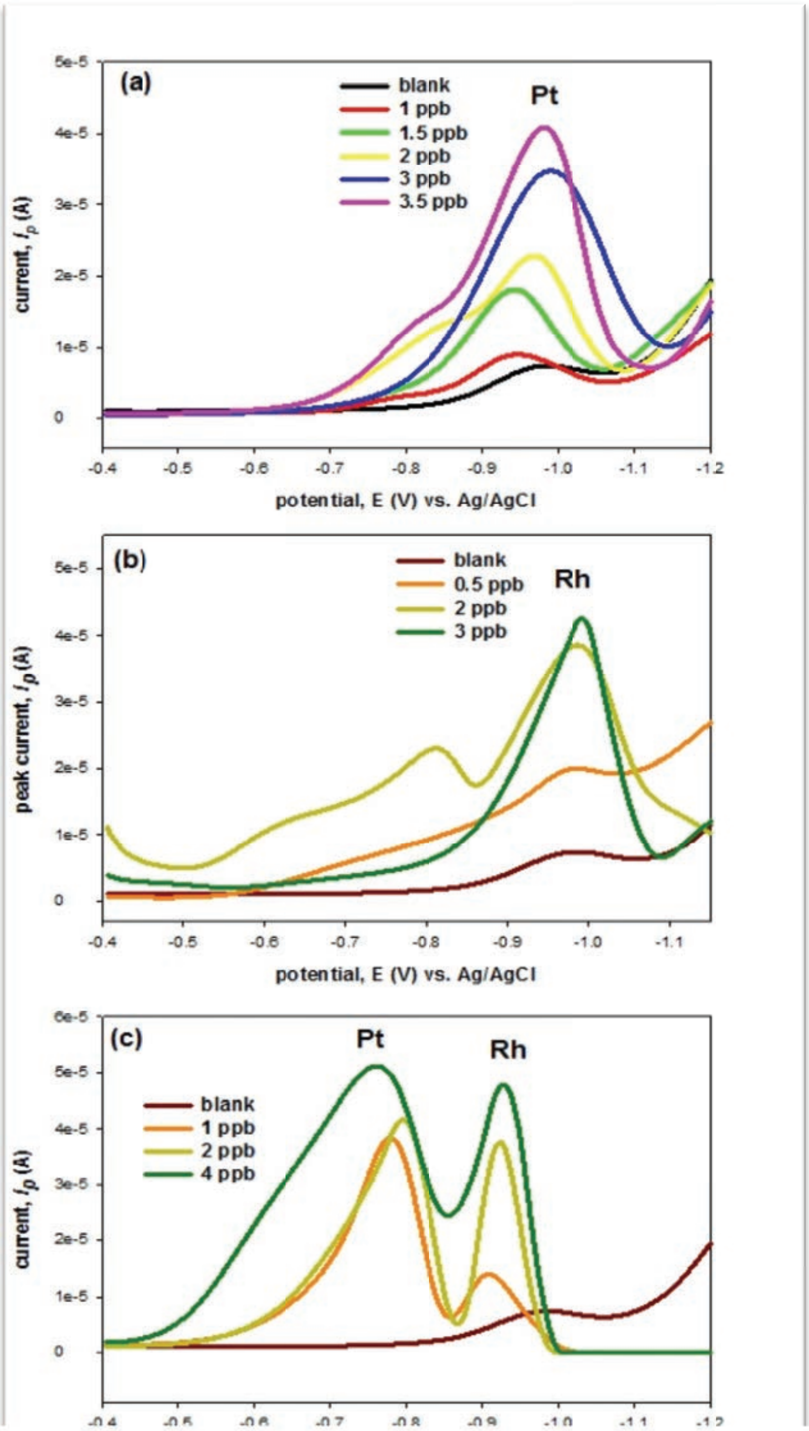

Figure 42. Adsorptive differential pulse stripping voltammetric analysis for increasing concentration of (a) 1.0-3.5 µg/ℓ Pt with E_d = of -0.7 V (vs. Ag/AgCl) and t_d = 150 s, (b) 0.5-3.0 µg/ℓ Rh with E_d = -0.5 V (vs. Ag/AgCl) and t_d = 150 s and (c) 1.0-4.0 µg/ℓ Pd-Rh with E_d = -0.6 V (vs. Ag/AgCl) and t_d = 150 s at a Bismuth film electrode. The solutions also consisted of 0.01 M ammonia buffer (pH = 9.0) containing 5 x 10^{-5} M DMG concentration (*n* = *2*).

8.4 Interference studies

Platinum group metals were studied in the presence of interfering ions such as nickel, cobalt, sodium, iron, at low concentrations. Other studies on the determination of Ni(II) and Co(II) in the presence of DMG in alkaline electrolytes are widely published (Locatelli, 2006). Nickel (Ni) and cobalt (Co) showed voltammetric peaks about -1.05 V (*vs.* Ag/AgCl) saturated [Ni(II)] and -1.15 V (*vs.* Ag/AgCl) saturated [Co(II)]. According to the literature, Ni(II) and Co(II) may also interfere with Rh(II) (Zhang *et al*., 1996).

Figure 43 reveals the effect of Ni(II) and Co(II) interfering with Pd(II) ions in the same solution. It appeared that Ni(II) did not interfere extensively with Pd(II) in all three concentrations investigated in this study. At the two low concentrations investigated, Co(II) interfered with Pd(II) but did not interfere at the higher concentration.

Figure 44 demonstrates the effect of Ni(II) and Co(II) interfering with Pt(II). For the results obtained it was observed that Co(II) does not interfere with Pt(II) in all three concentrations. Ni(II) does not interfere with Pt(II) at the two low concentrations investigated, but interferes with Pt(II) at the higher concentration investigated. It was also observed that a high concentration of Pt(II) delivered no distinct peak for it, but it was rather "swallowed" by the Ni(II) peak obtained.

According to Locatelli (2006), Ni(II) and Co(II) interfere with Rh(III) in basic electrolytes because they presents voltammetric signals in the same potential range. In Figure 45 the interfering effect of Ni(II) and Co(II) upon Rh(III) is illustrated, as no well separated peaks were obtained for the three metal ions. At a Rh(III) concentration of 0.5 µg/ℓ, it was observed that three peaks were obtained while the first peak at ~ -0.65 V (*vs.* Ag/AgCl) is broad and not sharp and destruct. Better peak results for all three metal ions were obtained at a Rh(III) concentration of 1 µg/ℓ. A high Rh(III) concentration of 2 µg/ℓ delivered no destruct peaks and peak potentials for Rh(III) and Ni(II), respectively.

It has been observed in Figures 43 and 45 that sodium and iron interfere with Pd(II) and Rh(III) in the alkaline ammonia buffer. It seems that the DMG complexing agent could not be used in the presence of these two metal ions. From Figure 47 good peaks are observed for Pt(II) with sodium and iron.

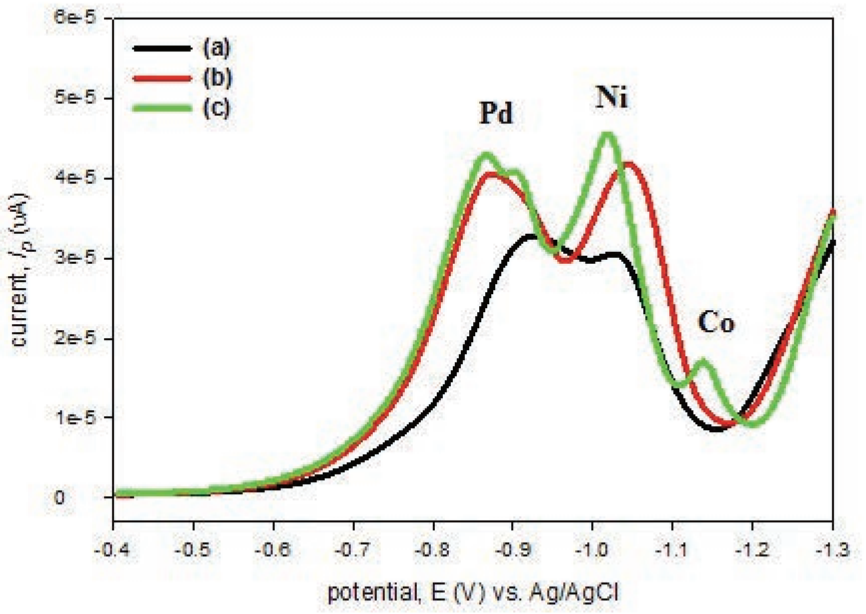

Figure 43. **Effect of interfering ions on the peak current responses for three solutions containing (a) Pd (0.5 µg/ℓ), Ni (1.0 µg/ℓ)), Co (1.0 µg/ℓ)); (b) Pd (1.0 µg/ℓ)), Ni (1.0 µg/ℓ)), Co (1.0 µg/ℓ)) and (c) Pd (1.5 µg/ℓ)), Ni(1.0 µg/ℓ)), Co(1.0 µg/ℓ)) respectively.**

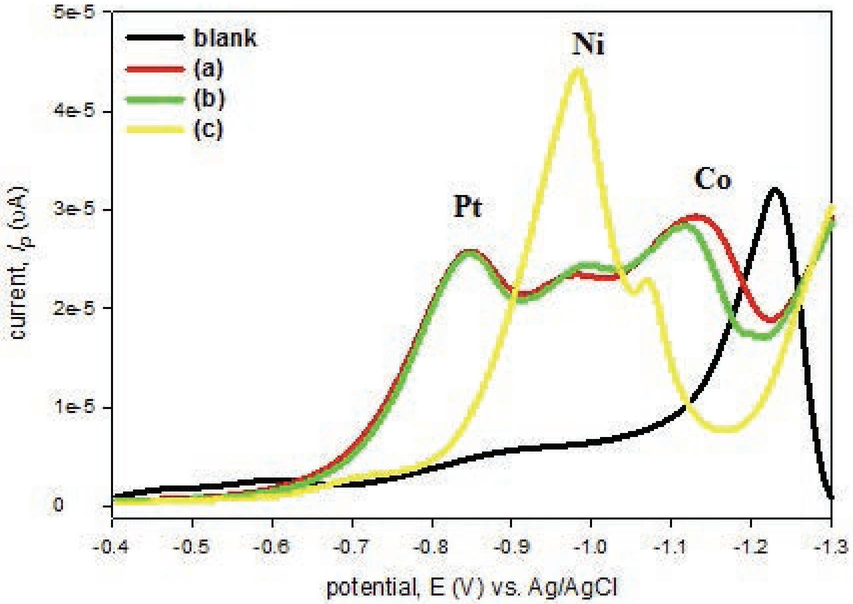

Figure 44. Effect of interfering ions on the peak current responses for three solutions containing (a) Pt (0.5 µg/ℓ), Ni (1.0 µg/ℓ), Co (1.0 µg/ℓ); (b) Pt (1.0 µg/ℓ), Ni (1.0 µg/ℓ), Co (1.0 µg/ℓ) and (c) Pt (2.0 µg/ℓ), Ni(1.0 µg/ℓ), Co(1.0 µg/ℓ) respectively.

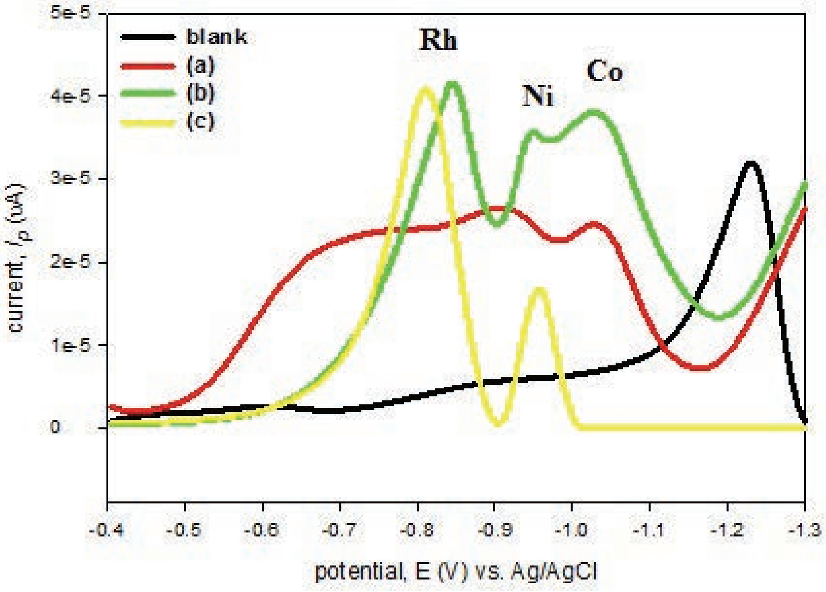

Figure 45. Effect of interfering ions on the peak current responses for three solutions containing (a) Rh (0.5 µg/ℓ), Ni (1.0 µg/ℓ), Co (1.0 µg/ℓ); (b) Rh (1.0 µg/ℓ), Ni (1.0 µg/ℓ), Co (1.0 µg/ℓ) and (c) Rh (2.0 µg/ℓ), Ni(1.µg/ℓ), Co(1.0 µg/ℓ) respectively.

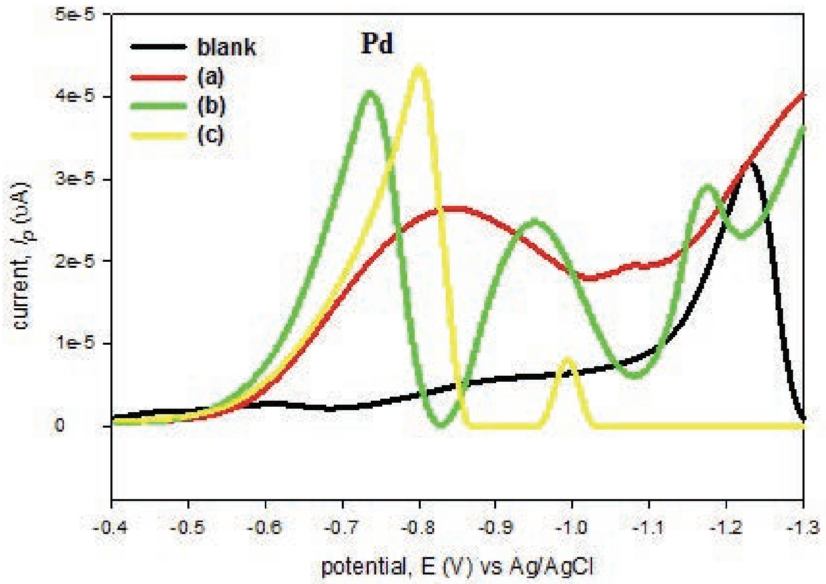

Figure 46. Effect of interfering ions on the peak current responses for a solutions containing (a) Pd (0.5 µg/ℓ), Na (1.0 µg/ℓ), Fe (1.0 µg/ℓ); (b) Pd (1.0 µg/ℓ), Na (1.0 µg/ℓ), Fe (1.0 µg/ℓ) and (c) Pd (2.0 µg/ℓ), Na (1.0 µg/ℓ), Fe (1.0 µg/ℓ) respectively.

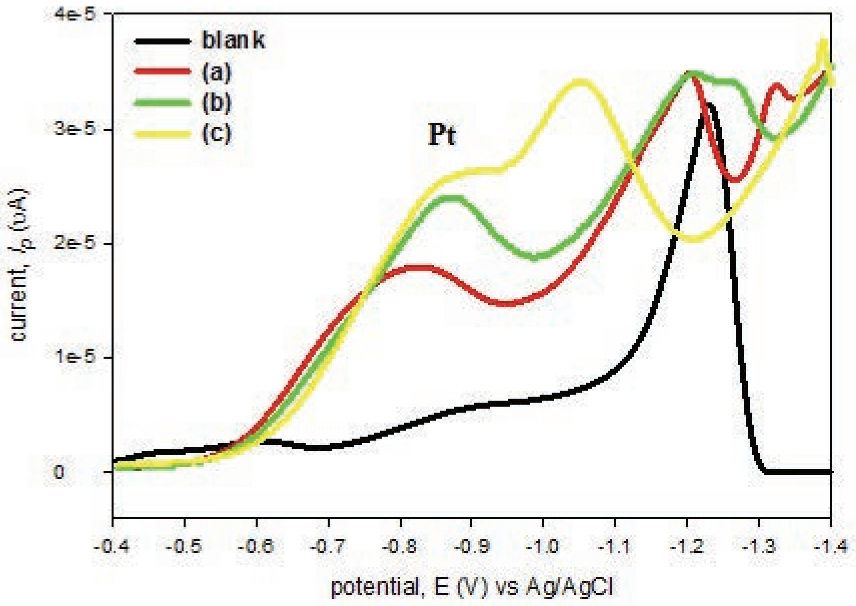

Figure 47. Effect of interfering ions on the peak current responses for a solutions containing (a) Pt (0.5 µg/ℓ), Na (1.0 µg/ℓ), Fe (1.0 µg/ℓ); (b) Pt (1.0 µg/ℓ), Na (1.0 µg/ℓ), Fe (1.0 µg/ℓ); (c) Pt (2.0 µg/ℓ), Na (1.0 µg/ℓ), Fe (1.0 µg/ℓ) respectively.

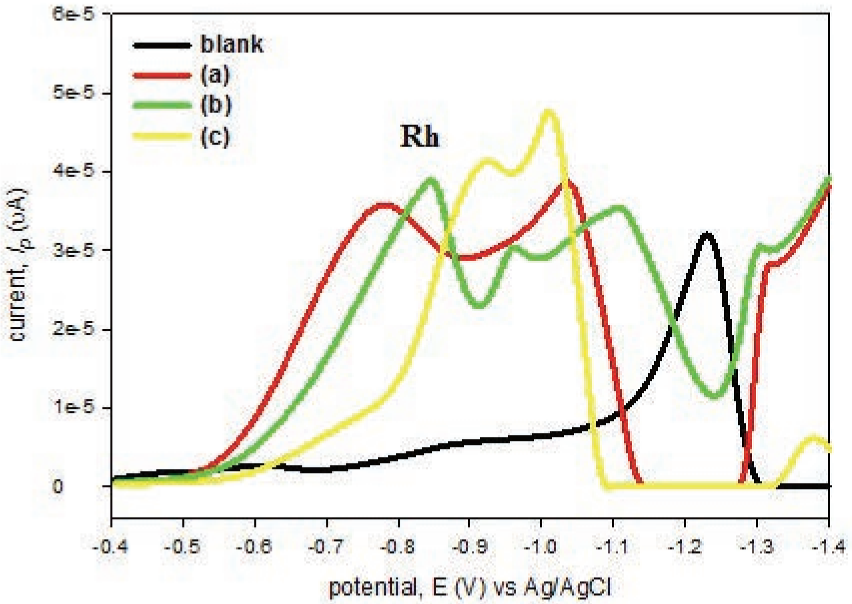

Figure 48. **Effect of interfering ions on the peak current responses for a solutions containing (a) Rh (0.5 µg/ℓ), Na (1.0 µg/ℓ), Fe (1.0 µg/ℓ); (b) Rh (1.0 µg/ℓ), Na (1.0 µg/ℓ), Fe (1.0 µg/ℓ); (c) Rh (2.0 µg/ℓ), Na (1.0 µg/ℓ), Fe (1.0 µg/ℓ) respectively.**

The effect of sulphates (SO_4^{2-}) and phosphates (PO_4^{3-}) upon Pd(II), Pt(II) and Rh(III) are shown in Figures 49 to 51 (using sodium sulphate Na_2SO_4 and sodium phosphate H_2NaPO_4); $SO4^{2-}$ and PO_4^{3-} did not interfere with the PGMs. From the observed results DMG could be used in the presence of these two ions and with ammonia as the supporting electrolyte.

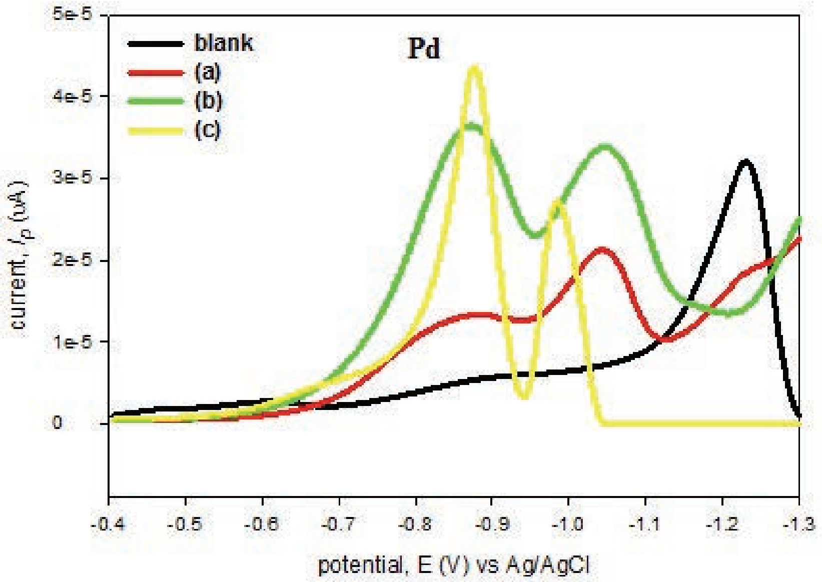

Figure 49. **Effect of interfering ions on the peak current responses for a solutions containing (a) Pd (0.5 µg/ℓ), SO_4^{2-} (1.0 µg/ℓ), PO_4^{2-} (1.0 µg/ℓ); (b) Pd (1.0 µg/ℓ), SO_4^{2-} (1.0 µg/ℓ), PO_4^{2-} (1.0 µg/ℓ); (c) Pd (2.0 µg/ℓ), SO_4^{2-} (1.0 µg/ℓ), PO_4^{2-} (1.0 µg/ℓ) respectively.**

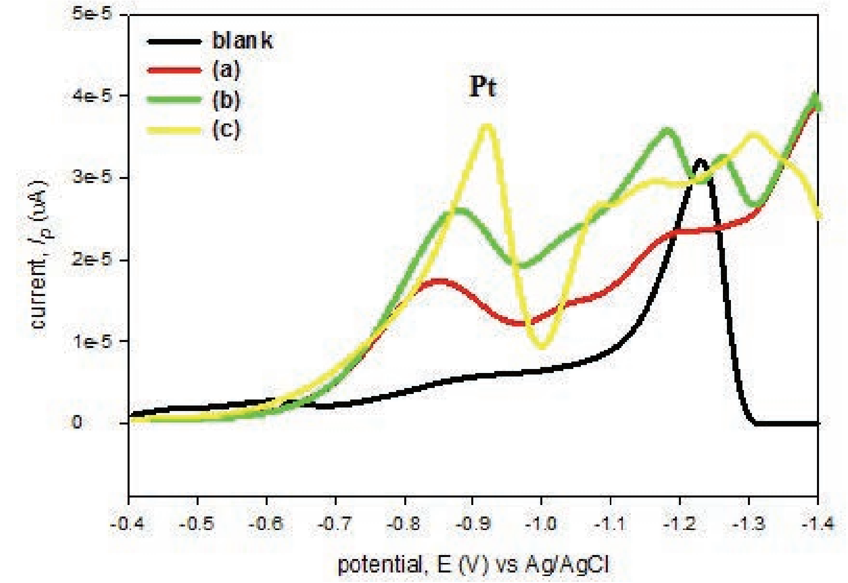

Figure 50. Effect of interfering ions on the peak current responses for a solutions containing (a) Pt (0.5 µg/ℓ), SO_4^{2-} (1.0 µg/ℓ), PO_4^{3-} (1.0 µg/ℓ); (b) Pt (1.0 µg/ℓ), SO_4^{2-} (1.0 µg/ℓ), PO_4^{3-} (1.0 µg/ℓ); (c) Pt (2.0 µg/ℓ), SO_4^{2-} (1.0 µg/ℓ), PO_4^{3-} (1.0 µg/ℓ) respectively.

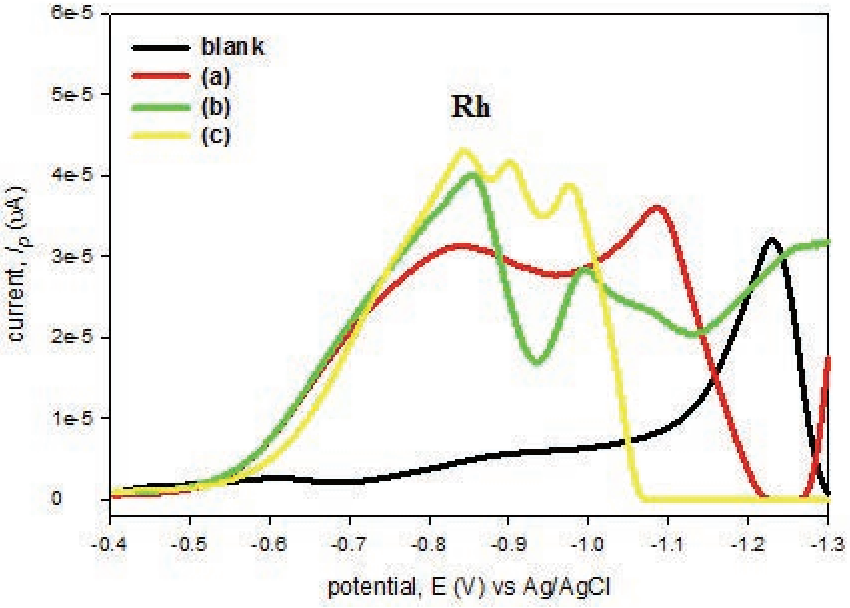

Figure 51. Effect of interfering ions on the peak current responses for a solutions containing (a) Rh (0.5 µg/ℓ), SO_4^{2-} (1.0 µg/ℓ), PO_4^{3-} (1.0 µg/ℓ); (b) Rh (1.0 µg/ℓ), SO_4^{2-} (1.0 µg/ℓ), PO_4^{3-} (1.0 µg/ℓ); (c) Rh (2.0 µg/ℓ), SO_4^{2-} (1.0 µg/ℓ), PO_4^{3-} (1.0 µg/ℓ) respectively.

Mixed results were obtained for the interference studies as some voltammograms showed no clear peak potentials for individual PGMs and the interfering metal ions. However, the results do show that Ni(II) and Co(II) are the main metal ion interferences that affect the stripping analysis of Pt, Pd and Rh when the GC/BiFE/$(HDMG)_2$ sensor are applied to the stripping analysis of PGMs. Several unaccounted peaks were also observed, which could not be easily resolved and warrant further investigation, especially for the sulphate and phosphate ion interference studies. What was clearly evident from the interference studies is the fact that concentration of the individual metal ions is a key factor in peak attenuation. This means that if some of the interfering metal ions have a higher or equal concentration than the PGMs, the peak resolution is a problem and the analysed PGM does not show a clear voltammogram and peak potential. This aspect of the study needs further investigation.

8.5 Conclusions

The parameters of the deposition potential (E_d) and deposition time (t_d) for the single and simultaneous voltammetric determination of the PGMs were established. In the case of the single PGM voltammetric analysis, it was observed that the same deposition potential of -0.7 V (*vs.* Ag/AgCl) can be used, while for Rh the result was -0.5 V (*vs.* Ag/AgCl). The limit of detection (LOD) was also determined for the developed sensor and the LOD values for individual metal ion determination were found to be 0.12 ± 0.06 µg/ℓ for Pd, 0.04 ± 0.007 µg/ℓ for Pt and 0.23 ± 0.04 µg/ℓ for Rh respectively. The linear ranges to which the sensor can be applied were determined as 0.1-3.5 µg/ℓ for Pd, 0.5-4.0 µg/ℓ for Pt and 0.1-4.0 µg/ℓ for Rh. Furthermore, Pd-Rh can be simultaneously determined at a deposition potential of -0.6 V (*vs.* Ag/AgCl) and Pt-Rh, while for the Pt-Rh couple the same deposition potential can be applied. Except for Pd at 90 s, all the other combinations of PGMs can be analysed using a deposition time of 150 s making the stripping analysis a short voltammetric procedure. Mixed results were obtained for the interference studies as some voltammograms showed no clear peak potentials for individual PGMs and the interfering metal ions. However, the results do show that Ni(II) and Co(II) are the main metal ion interferences that affect the stripping analysis of Pt, Pd and Rh when the GC/BiFE/$(HDMG)_2$ sensor are applied to the stripping analysis of PGMs. Several unaccounted peaks were also observed, which could not be easily resolved and warrants further investigation. What was clearly evident from the interference studies is the fact that concentration of the individual metal ions is a key factor in peak attenuation.

CHAPTER 9: LABORATORY ASSESSMENT OF PGM POLLUTION IN ENVIRONMENTAL SAMPLES

9.1 Introduction

The purpose of this chapter was to apply the analytical sensor developed in this project to the voltammetric analysis of freshwater and sediment samples from sampling sites closely located to mining activities. The laboratory testing of the glassy carbon-bismuth film electrode (GC/BiFE) sensor involved the construction of the electrochemical sensor and followed by application to specific samples using the optimised voltammetric conditions for stripping voltammetric determination. This provided information on how successfully the GC/BiFE sensor can be applied to stripping analysis of environmental samples. It also shows other parameters that need to be optimised in the next step of the sensor development.

In summary, the results so far have shown that the GC/BiFE sensor with DMG as chelating agent (abbreviated as GC/BiFE/$(HDMG)_2^{2+}$) successfully analysed concentrations of Pd, Pt and Rh in freshwater samples. In this chapter work was performed in which freshwater samples were spiked with a known concentration of PGM (4 ppb), and then they were voltammetrically analysed to determine the accuracy and sensitivity of the constructed sensor. The results obtained indicated that the technique is very sensitive towards the determination of Pd in freshwater samples, while further optimisation of deposition time and / or deposition potential may still be required for the successful analysis of Pt and Rh.

Applying the GC/BiFE/$(HDMG)_2$ sensor to the analysis of the sediment sample fractions showed that good recoveries were obtained for Pd in the carbonate-bound fraction. Pt showed weaker recoveries in the Fe-Mn bound fractions, while poor results for Rh in the organic-bound fraction of the sample matrix were obtained. This indicates that further optimisation of experimental conditions and sample matrix preparation is required.

9.2 Methods

9.2.1 Sampling sites

In this study specific attention was given to four water management areas (WMAs) that include locations of mining activities: the Limpopo, Luvuvhu-Letaba, Crocodile (West) and Marico and Olifants WMAs. Several rivers were identified in the overall project and the details were given in Chapter 4. Six sampling sites (Table 32) were then identified for the laboratory testing of the glassy carbon-bismuth film electrode (GC/BiFE) sensor.

9.2.2 Surface water sampling procedure

Clean handling techniques were followed during sample collection, storage and analyses to minimise the occurrence of cross-contamination and erroneous results. Polyethylene sampling bottles were rinsed at the site three times with river water before duplicate samples were collected. The bottle was filled to the top to displace any air, acidified with HCl solution and placed inside double ziplock bags. The samples were transported on ice to the laboratory.

Surface water samples for standard chemical analysis were collected in pre-rinsed, 500 mL polyethylene bottles that were firmly sealed following acidification with 0.5% v/v HCl solution. The samples were then labelled, double-bagged and transported on ice to the laboratory for analysis within 72 hours of collection in the field (Somerset *et al*., 2010; Williams *et al*., 2010).

Table 32. **Location and brief description of sampling sites identified for the collection of freshwater and sediment samples, analysed using the GC/BiFE sensor. The selected sites were in close proximity to PGM mining activities in the three WMAs identified.**

Site Code	River	Site Description	WMA	Geographical Coordinates	
				Latitude	Longitude
Hex River 1	Hex River	Downstream of Pt mines, close to Boitekong Township off R510	Crocodile (West) and Marico	S 25º 43.620'	E 27º 18.272'
Hex River 2	Hex River	Upstream of Pt mines, at bridge over N4	Crocodile (West) and Marico	S 25º 36.498'	E 27º 17.338'
Crocodile River 1	Crocodile River	South of Brits CBD on R512 to Rustenburg	Crocodile (West) and Marico	S 25º 38.844'	E 27º 46.767'
Olifants River 1	Olifants River	Outside Zeekoeigat close to Bokoni Pt Mine	Olifants	S 24º 16.052'	E 29º 47.964'
Motse River	Motse River	At bridge over dried-up Motse river close to Twickenham Pt mine after turn-off on R37	Olifants	S 24º 25.814'	E 30º 04.173'
Elands River	Elands River	Elands River downstream of Swartruggens Dam	Crocodile (West) and Marico	S 25º 28.970'	E 26º 41.406'

9.2.3 Sediment sampling procedure

Surface sediment samples (up to 6 cm in depth) were extruded using a 5 cm diameter polypropylene sediment corer and sectioned at 2 cm intervals. Each sediment layer was collected in a 50 mL centrifuge tube, labelled and double-bagged. All sediment samples were collected in duplicate and transported on ice to the laboratory, where they were stored at -20ºC, until further analysis (Balcom *et al*., 2004; Somerset *et al*., 2010).

Sediment samples were subjected to a multi-step sequential extraction procedure to determine the fractionation of metals in the sediment samples, namely the exchangeable, carbonates-bound, Fe–Mn oxides bound, and organic matter-bound fractions that were collected using different chemicals during each of the extraction process steps (Li *et al*., 2010).

9.2.4 Reagents and materials

All reagents were of analytical grade and obtained from Merck Chemicals Pty (Ltd), South Africa and Sigma-Aldrich, Germany. All standard solutions of Bi(III), Pd(II), Pt(II) and Rh(II) metal ions were prepared using atomic absorption standards (1000 mg/ℓ) as purchased. All solutions were prepared using Milli-Q (Millipore 18 M Ohm.cm) water. A solution of 100 mg/ℓ bismuth in 0.2 M sodium acetate buffer solution was used to prepare the bismuth film. A 0.01 M ammonia buffer solution (pH 9.0) was prepared by mixing ammonium chloride with concentrated ammonia to serve as the electrolyte during stripping analysis. A 5×10^{-5} M DMG solution was prepared in 95% ethanol and served as the chelating agent. The 0.2 M sodium acetate buffer (pH 4.8) solution was prepared by mixing appropriate concentrations of sodium acetate with acetic acid and deionised water.

9.2.5 Instrumentation

An Epsilon electrochemical analyzer (BASi Instruments, 2701 Kent Ave., West Lafayette, IN 47906, USA) was used for all electrochemical protocols performed. A conventional three electrode system was employed, consisting of bismuth film preplated on a BASi 1.6 mm diameter glassy carbon disc working electrode, a BASi 3M NaCl-type Ag/AgCl reference electrode, and a platinum wire auxiliary electrode. The determination of Pd(II), Pt(II) and Rh(III) was performed by cyclic voltammetry (CV) and adsorptive differential pulse stripping voltammetry (AdDPSV) modes. All experiments were performed in a 20 ml electrochemical cell at room temperature of 20 ± 1ºC (Somerset *et al*., 2010; 2011).

Water and sediment samples were collected in rivers in close proximity to Pt mining activities around Rustenburg, North-West Province, South Africa. An inductively coupled plasma mass spectrometer (ICP-MS; Agilent Technologies, 7500 CX, Chemetrix, Midrand, RSA) was used for PGM measurement in the environmental samples. These results were compared with those obtained by AdDPSV.

9.2.6 Analytical procedure and voltammetric measurements

Water and sediment samples collected were prepared prior to the analysis of their PGMs content. The sediment samples were prepared by four-step sequential extraction during which four factions were extracted: (i) exchangeable weakly-adsorbed; (ii) carbonated bound; (iii) iron-manganese oxides bound; (iv) organic bound. These samples were analysed using ICP-MS, to determine in which fraction the highest concentrations of the PGMs were present (Li *et al*., 2010; Morera *et al*., 2001).

Following the above procedure the bismuth film electrode (BiFE) was prepared. The glassy carbon disk working electrode was thoroughly polished on a pad with 1.0, 0.3 and 0.05 µm alumina powders. The polished electrode was first rinsed with Milli-Q water and then immersed into a 0.2 M acetate buffer solution (pH = 4.8) containing 100 mg/ℓ Bi(III) ions. The glassy carbon electrode (GCE) was then coated with a bismuth film (BiF) at the surface of the disk electrode using an electrochemical deposition step. The deposition of the bismuth film proceeded by applying a potential of -1.0 V (*vs.* Ag/AgCl) for 5 minutes and stirring the solution with a magnetic stirrer at 300 rpm. After the plating procedure the bismuth-coated GCE was carefully rinsed with Milli-Q water and was ready for use (Hutton *et al*., 2003; Tesarova *et al*., 2009).

This was followed by the preparation of the environmental water and sediment samples for voltammetric analysis. A 1 mℓ aliquot of the sediment extracted solution or freshwater sample was added to 9 mℓ of 0.01 M ammonia (pH = 9.0) solution, containing 5×10^{-5} M DMG and 0.4 mg/ℓ PGM standard to give a final volume of 10 mℓ. The determination of Pd, Pt, Rh was performed using DPAdSV.

The last step consisted of the voltammetric determination and analysis. A 10 mℓ 0.01 M ammonia buffer (pH = 9.0) solution containing 5×10^{-5} M DMG was used as electrolyte in the cyclic and stripping voltammetric procedures. The film electrode was immersed in the solution and an accumulation potential of -0.7 V (*vs.* Ag/AgCl) for Pd(II) and Pt(II), and -0.5 V (*vs.* Ag/AgCl) for Rh(III) was applied while the solution was stirred. A 10 s quiet time was used and the voltammogram was scanned from -0.4 to -1.4 V (*vs.* Ag/AgCl) for AdDPSV measurements. The PGMs were introduced into the solution after the background voltammogram was recorded. All the experiments were performed in triplicate (*n = 3*) in the presence of oxygen and at a room temperature of 20±1°C.

9.3 Results

9.3.1 Voltammetric analysis using constructed metal film electrode sensor

The voltammetric analysis of the environmental samples (listed in Table 32) was conducted with the optimised conditions determined for PGM determination in real samples. The optimised working conditions for the adsorptive differential pulse stripping voltammetric (AdDPSV) determination of a series of standard (or model) solutions of Pd(II), Pt(II) and Rh(III) are shown in Table 33.

Similarities and differences in the optimum working conditions for the voltammetric determination of PGMs were observed (Table 33). It was found that both Pd and Pt could be reduced at -0.7 V (*vs.* Ag/AgCl), while in the case of Rh, reduction should proceed at -0.5 V (*vs.* Ag/AgCl). In the case of the deposition time, an optimum result for Pd could be obtained within 90 s, while for both Pt and Rh a time of 150 s was required. It was further established that a chelating agent concentration of 5×10^{-5} M dimethylglyoxime (DMG) should be used. These conditions were applied to the determination of PGMs in environmental samples with the results discussed in the next section.

Table 33. Summary of optimum stripping voltammetry conditions for the determination of Pd(II), Pt(II) and Rh(II) with the constructed GC/BiFE sensor.

Step	Condition		
	Pd	**Pt**	**Rh**
Reduction step			
pH	9.0		
Reduction potential	-0.7 (vs. Ag/AgCl)	-0.7 (vs. Ag/AgCl)	-0.5 (vs. Ag/AgCl)
Reduction time	90 s	150 s	150 s
Supporting electrolyte	0.01 M ammonia buffer solution		
Chelating agent	5×10^{-5} M dimethylglyoxime (DMG)		
Measurement step			
Supporting electrolyte	0.01 M ammonia buffer solution		
Measurement technique	Adsorptive differential pulse stripping voltammetry		
Potential window	-400 to -1400 mV (*vs.* Ag/AgCl)		

9.3.2 Analysis of environmental samples

9.3.2.1 Freshwater samples

Three sets of current-potential curves obtained with adsorptive DPAdSV determination of a series of standard solutions of Pd(II), Pt(II) and Rh(III) were constructed for the analysis of the samples. Experimental details are shown in Table 33. Using the AdPDSV data the corresponding current-concentration calibration curves were constructed with the details given in Table 34. Table 34 shows the information of the calibration curves obtained where I_p is the current in microamperes and C is the concentration in parts per billion (ppb). These data were in turn used to determine the concentrations of Pd, Pt and Rh in the recovery tests that were performed by adding a known quantity of the PGMs to each sample (Dalvi *et al*., 2008; Bobrowski *et al*., 2009). Individual samples were spiked with a known amount of PGM concentration (4 µg/ℓ), followed by voltammetric analysis to determine the accuracy and sensitivity of the constructed sensor. In all analyses, single PGM analysis was performed and no simultaneous determination of Pd and Rh or Pt and Rh was investigated.

Table 34. Results obtained for the construction of standard addition calibration plots from the current-concentration curves of the respective Pd, Pt and Rh-DMG complexes and the experimental details outlined in Table 33. These calibration plots were constructed for the analysis of the freshwater samples.

Complex	Regression line equation	R²	SD
$Pd(HDMG)_2$	$I_p = 20.07 + 21.868C$	0.961	4.82
$Pt(HDMG)_2$	$I_p = 17.99 + 43.288C$	0.983	8.39
$Rh(HDMG)_3$	$I_p = 14.44 + 45.085C$	0.979	10.55

The recovery efficiency results obtained for freshwater samples from Elands River were mixed, with individual recoveries of 25% (Pt), 28% (Rh) and 103% (Pd). These values indicate a good recovery was obtained for the detection of Pd, while weak recoveries were obtained for Pt and Rh (Table 35). The results for freshwater sample Hex River 1 showed recoveries of 200% (Pd), 63% (Pt) and 45% (Rh) respectively. These results are very mixed; the recovery of Pd was too high. For freshwater sample Hex River 2, the individual recoveries were 125% (Pd), 15% (Pt) and 33% (Rh), which indicates weak recovery of Pt and Rh, and average results for Pd. In the two cases where higher than 100% recoveries were obtained, the results indicated that the interference of co-existing ions amplified the analytical signal and further optimisation of future analysis will be required.

Table 35. **Results for the detection of PGM concentrations using the GC/BiFE sensor on freshwater samples from rivers in the Limpopo and North-West Provinces, closely located to platinum mining activities.**

Site ID	Quantity of PGM added (µg/ℓ)	Quantity of PGM recovered (µg/ℓ)	Recovery (%)
Elands River	0.4 [Pd^{2+}]	0.41 ± 0.02	103
	0.4 [Pt^{2+}]	0.10 ± 0.03	25
	0.4 [Rh^{3+}]	0.11 ± 0.03	28
Hex River 1	0.4 [Pd^{2+}]	0.80 ± 0.04	200
	0.4 [Pt^{2+}]	0.25 ± 0.02	63
	0.4 [Rh^{3+}]	0.18 ± 0.08	45
Hex River 2	0.4 [Pd^{2+}]	0.50 ± 0.03	125
	0.4 [Pt^{2+}]	0.06 ± 0.05	15
	0.4 [Rh^{3+}]	0.13 ± 0.01	33

Further analysis of the results indicated that the technique is very sensitive towards the determination of Pd in environmental samples, while further optimisation of deposition time and / or deposition potential may be required for the accurate determination of Pt and Rh in environmental samples.

9.3.2.2 Sediment samples

Table 36 shows the information of the calibration curves obtained where I_p is the current in microamperes and C is the concentration in parts per billion (ppb or µg/ℓ). It should be noted that the results obtained from ICP-MS analysis of the sediment fractions indicated that Pd was the highest in the carbonate-bound fraction, Rh in the organic-bound fraction and Pt in the Fe-Mn bound fraction. With this information, the respective Pd, Pt and Rh concentrations were determined in the three different fractions. All of the above data were in turn used to determine the concentrations of Pd, Pt and Rh in the recovery tests that were performed by adding a known quantity of the PGMs to each sediment fraction.

Table 36. **Results obtained for the construction of standard addition calibration plots from the current-concentration curves of the respective Pd, Pt and Rh-DMG complexes and the experimental details outlined in Table 33. These calibration plots were constructed for the analysis of the sediment samples.**

Complex	Fraction	PGM	Regression line equation	R²	SD
$Pd(HDMG)_2$	Carbonate-bound	Pd	$I_p = 19.78 + 21.868C$	0.993	4.74
	Organic-bound	Rh	$I_p = 13.01 + 46.203C$	0.999	10.71
	Fe-Mn bound	Pt	$I_p = 17.19 + 44.396C$	0.997	8.55
$Pt(HDMG)_2$	Carbonate-bound	Pd	$I_p = 19.78 + 21.868C$	0.993	4.74
	Organic-bound	Rh	$I_p = 13.01 + 46.203C$	0.999	10.71
	Fe-Mn bound	Pt	$I_p = 17.19 + 44.396C$	0.997	8.55
$Rh(HDMG)_3$	Carbonate-bound	Pd	$I_p = 19.78 + 21.868C$	0.993	4.74
	Organic-bound	Rh	$I_p = 13.01 + 46.203C$	0.999	10.71
	Fe-Mn bound	Pt	$I_p = 17.19 + 44.396C$	0.997	8.55

The voltammetric results obtained using the GC/BiFE sensor in the PGM analysis of the sediment fractions are displayed in Table 37. Individual samples were spiked with 4 ppb PGM, followed by voltammetric analysis of these samples to determine the accuracy and sensitivity of the sensor (Dalvi *et al.*, 2008; Bobrowski *et al.*, 2009).

Table 37. Results for the detection of PGM concentrations using the GC/BiFE sensor on digested and extracted sediment samples from rivers in the Limpopo and North-West Provinces, closely located to platinum mining activities.

Site ID	Sample extracted fraction	Reference added (µg/ℓ)	Detected (µg/ℓ)	Recovery (%)
Olifants River	Carbonate-bound	0.4 [Pd^{2+}]	0.44 ± 0.01	110
	Organic-bound	0.4 [Rh^{3+}]	UR	0
	Fe-Mn bound	0.4 [Pt^{2+}]	0.19 ± 0.01	48
Motse River	Carbonate-bound	0.4; [Pd^{2+}]	0.41 ± 0.01	103
	Organic-bound	0.4 [Rh^{3+}]	UR	0
	Fe-Mn bound	0.4 [Pt^{2+}]	0.08 ± 0.01	20
Crocodile River 1	Carbonate-bound	0.4 [Pd^{2+}]	0.43 ± 0.04	108
	Organic-bound	0.4 [Rh^{3+}]	UR	0
	Fe-Mn bound	0.4 [Pt^{2+}]	0.14 ± 0.01	35

UR = Unresolved due to sample matrix complications.

Table 37 shows that good recoveries were obtained for Pd in the carbonate-bound fraction of the sediment samples. The individual results for the Pd recoveries were 110% (Olifants River), 108% (Crocodile River 1) and 103% (Motse River). In the case of Pt, weak recoveries were obtained in the Fe-Mn bound fractions with the results of 48% (Olifants River), 35% (Crocodile River 1) and 20% (Motse River). A reduction in the recoveries for Pt was obtained and none of the results showed a recovery $\geq$ 50%. Table 37 further indicates that a decrease in the sensitivity from Pd to Pt was obtained. In the case of Rh, the recovery of the spiked amount was unresolved (UR), with the sensor being unable to detect the amount of Rh added to the organic-bound fraction of the sample matrix. Similarly as for the water samples, the results were higher than 100% recoveries were obtained, indicated that the interference of co-existing ions amplified the analytical signal and further optimisation of future analysis will be required.

It can therefore be concluded that the sample matrices of the Fe-Mn bound fractions (containing hydroxylamine hydrochloride, acetic and nitric acid solutions) and the organic-bound fractions (containing hydrogen peroxide and nitric acid solutions) posed other interferences that need to be resolved in PGM detection in the sediment fractions. Furthermore, in the case of the carbonate-bound fraction that was prepared with sodium acetate solution, more favourable results were obtained indicating that this matrix was compatible with the voltammetric analysis procedure.

9.4 Conclusions

Modifying the surface of a glassy carbon electrode with a bismuth film (BiF) aids in the stripping analysis of the $M(HDMG)_2$ complexes (M = Pd, Pt and Rh).

The optimisation of the key parameters for the stripping voltammetric procedure has demonstrated that the constructed GC/BiFE sensor can be successfully applied for the determination of Pd(II), Pt(II) and Rh(III) by means of AdDPSV preceded by adsorptive pre-concentration of the $M(HDMG)_2$ complexes (M = Pd, Pt and Rh) on the electrode surface.

In the next step the GC/BiFE sensor with DMG as chelating agent (abbreviated as $GC/BiFE/(HDMG)_2^{2+}$) was successfully applied in the analysis of freshwater samples for its Pd, Pt and Rh concentrations. This step involved spiking the freshwater samples with a known amount of PGM concentration (4 µg/ℓ), followed by voltammetric analysis of these samples to determine the accuracy and sensitivity of the constructed sensor. Analysis of the results obtained indicated that the technique is very sensitive towards the determination of Pd in freshwater samples, while further optimisation of deposition time and / or deposition potential may still be required for the determination of Pt and Rh in these samples.

Applying the GC/BiFE/$(HDMG)_2^{2+}$ sensor to the analysis of the sediment sample fractions showed that good recoveries were obtained for Pd in the carbonate-bound fraction, with weaker recoveries for Pt in the Fe-Mn bound fractions, while poor results for Rh in the organic-bound fraction of the sample matrix were obtained. It further indicated that more optimisation of experimental conditions and sample matrix preparation are needed.

CHAPTER 10: SUMMARY AND RECOMMENDATIONS

In this project the emphasis was on: (i) assessing the aquatic environment around PGM mining activities to determine which national water resources are in close proximity to these mines, and determining to what extent the aquatic environment has been polluted by these mining activities; and (ii) to the determine whether the current analytical tools and techniques used to analyse heavy and precious metal containing effluent is adequate for the task at hand. The project was therefore designed with a main aim and several minor objectives were identified. The main aim of this project was the design, synthesis and characterisation of an electrochemical sensor with controlled surface structure and chemical activity towards metal ions such as lead, zinc, cadmium, nickel, arsenic, platinum, palladium and rhodium. Different objectives were identified as listed in Chapter 1, section 1.2 and through this project work has been conducted to meet several of these objectives. Throughout the project, different aspects of the electrochemical sensor development were addressed and reported, with the purpose of meeting all of the identified objectives or sections thereof as identified in the following paragraphs.

The first objective focussed on the design, development and synthesis of new electrochemical sensor materials and chemical compounds with nanoscopic and controlled surface structure and chemical activity towards metal ions such as lead, zinc, cadmium, nickel, arsenic, aluminium, platinum and palladium. Mixed results were obtained for the experiments performed to address this objective. The initial experiments did not deliver a successful nanoscopic compound for electrochemical sensor development. It was then decided to utilise a thin metal film for the sensor development and voltammetric studies and a bismuth metal film was used. The results obtained have shown that modifying the surface of a glassy carbon electrode with a bismuth film (BiF) assists in the stripping analysis of the M(HDMG)$_2$ complexes, with M as the PGM (Pd, Pt and Rh) and dimethylglyoxime (DMG) as the chelating agent. The results obtained for the evaluation of the GCE/BiF/M(HDMG)$_2$ sensor in 0.1 M HCl buffer (pH $\approx$ 2), 0.2 M NaOAc buffer (pH = 4.5) and 0.1 M ammonia (pH = 9) buffer solutions have showed varying results. For analytical purposes and the successful application of the electrochemical sensor, several parameters were optimised that included the pH, DMG concentration, deposition potential, deposition time and PGM concentration. The effect of interfering ions was also investigated.

The second objective focussed on the analysis of environmental samples collected from sampling sites in close proximity to PGM mining activities, in order to characterise and identify the metals typically found in these samples. This partly involved identifying the national WMAs in which platinum mining activities are currently taking place, which include the Limpopo, Luvuvhu-Letaba, Crocodile (West) and Marico, and Olifants WMAs. Little or no information was available in the scientific literature on any pollution that could be associated with mining in the four selected WMAs. Limited information was however available in publications of the River Health Programme. Environmental samples were collected and the results revealed the following. The metal concentrations were low in the surface water samples analysed. For some sampling sites elevated nutrient concentrations were obtained during both the August and November 2010 sampling trips. Seasonal influences affected the diversity of taxa for the biota samples collected and the metal concentrations within these samples. Higher Ni, Pb and Zn concentrations were recorded than the other metals and it is therefore possible that these metals are released from the sediment-water interface into solution in the overlying waters. Once in solution these metals may then be absorbed in the overlying algae that were collected, since the algae also contained elevated Ni, Pb and Zn concentrations. The concentrations measured in the biota and algae were low, indicating that mining activities had a low impact on the aquatic environment at the sampling sites. Nevertheless, in the case of the metal concentrations in biota samples, results for the August 2010 samples showed higher concentrations of Al, Fe, Ni, Zn and Pt for all biota sampled compared to that in samples from November 2010. This may be due to higher water flow during November 2010, since sampling was done during the rainy season.

The third objective dealt with the integration of synthesised nanoscopic chemical compounds into electrochemical sensor and screen-printed electrode formats, and optimisation of screen-printing parameters. This section of the study was not fully investigated in this project due to time constraints. It is recommended that the coating of a screen-printed electrode with a bismuth film and its application in the voltammetric determination of PGMs forms part of an ancillary study that is reported in a publication in an appropriate journal.

The fourth objective focussed on the development, integration and application of ion-exchange materials in electrochemical sensor construction for the identification of metal ions. The experiments conducted investigated the applicability of ion exchange resins in the removal or adsorption of Pt(II), Pd(II) and Rh(III) from acidic (pH ≤ 2) and alkaline (pH ≥ 8) aqueous solutions. Two synthetic sidestream solutions (designated A and B) were prepared and used in the adsorption experiments. Four resins were investigated: (i) strongly acidic cation exchange resin (Amberlite IRP-69); (ii) cation exchange resin (Dowex 50WX8-100); (iii) strongly basic anion exchange resin (Amberlite IRA-400); and (iv) universal pH ranged (Chitosan). The results obtained have shown that at pH 2, the highest removal efficiency of 64% was obtained when Chitosan was used on solution A. In the case of Amberlite® IRP-69, the highest removal efficiency was 57% when solution B was subjected to the adsorption studies. For both solutions A and B, Amberlite® IRA-400 was able to absorb Pt more effectively, followed closely by Pd and least effective results were obtained for Rh. The highest removal efficiency was 99% for Pt from solution A. Dowex® 50WX8-100 resin showed limited removal of Pt, Pd and Rh from the synthetic sidestream solutions, especially when the results are compared to the three other resins efficiencies. The removal efficiencies of the PGMs ranged between 40-99% and the sorbents interacted well with solution A, removing Pd from both solutions at acidic pH. Under alkaline conditions the highest removal efficiency of 99% was obtained with Amberlite® IRA-400 and Dowex® 50WX8-100 and Rh. The highest removal efficiency of Pd was 65% using Amberlite® IRA-400, while the weakest results (0.6%) were obtained using Dowex® 50WX8-100. Amberlite® IRA-400 removed 90% Pt – the highest Pt removal at pH 8 – and Amberlite® IRP-69 the lowest (5%). It is recommended that further studies and analysis are conducted to address some of the shortcomings presented in this section of the work.

The purpose of the fifth objective was the development, integration, testing and optimisation (screen-printed) chemical sensor formats into a portable potentiostat tool-kit for laboratory testing of samples. Only the results for the investigation of the chemical sensor formats are reported in this project. In order to address this objective, the chemical sensor consisting of a glassy carbon electrode coated with a bismuth film (BiF) was used for the stripping analysis of the PGMs in the presence of DMG as chelating agent. The sensor is abbreviated as GCE/BiF/M(HDMG)$_2$ and was evaluated to optimise the conditions for the differential pulse cathodic stripping voltammetric analysis of PGMs. Different variables were investigated and included the deposition potential, pre-concentration time, bismuth concentrations, ionic strength of supporting electrolyte, transport rate to the electrode surface and accumulation potential. The parameters of the deposition potential (E_d) and deposition time (t_d) for the single and simultaneous voltammetric determination of the PGMs were established. In the case of the single PGM voltammetric analysis, it was observed that the same deposition potential of -0.7 V (*vs.* Ag/AgCl) can be used for Pt and Pd, while for Rh the result was -0.5 V (*vs.* Ag/AgCl). Furthermore, Pd-Rh can be simultaneously determined at a deposition potential of -0.6 V (*vs.* Ag/AgCl), while for the Pt-Rh couple the same deposition potential can be applied. Except for Pd at 90 s, all the other combinations of PGMs can be analysed using a deposition time of 150 s making the stripping analysis a short voltammetric procedure. The limit of detection (LOD) was also determined for the developed sensor and the LOD values for individual metal ion determination were found to be 0.12 ± 0.06 µg/ℓ for Pd, 0.04 ± 0.007 µg/ℓ for Pt and 0.23 ± 0.04 µg/ℓ for Rh respectively. The linear ranges to which the sensor can be applied were determined as 0.1-3.5 µg/ℓ for Pd, 0.5-4.0 µg/ℓ for Pt and 0.1-4.0 µg/ℓ for Rh. Mixed results were obtained for the interference studies as some voltammograms showed no clear peak potentials for individual PGMs and the interfering metal ions. However, the results did show that Ni(II) and Co(II) are the main metal ion interferences that affect the stripping analysis of Pt, Pd and Rh when the GC/BiFE/(HDMG)$_2$ sensor are applied to the stripping analysis of PGMs. Several unaccounted peaks were also observed, which could not be easily resolved and warrants further investigation. What was clearly evident from the interference studies is the fact that the concentration of the individual metal ions is a key factor in peak attenuation. It is recommended that the investigation of the screen-printed sensor formats and portable potentiostat evaluation of the sensor for PGM evaluation, forms part of an ancillary study for which additional funding will be required.

The sixth objective dealt with the testing and optimisation of the (screen-printed) chemical sensor formats and portable tool-kit for on-site analysis of identified heavy and precious metals. In the absence of the screen-printed sensor formats integrated into a portable tool-kit for on-site analysis, the constructed chemical sensor formats were employed in the laboratory analysis of environmental samples. Thus, results were collected for the GC/BiFE sensor with DMG as chelating agent (abbreviated as GC/BiFE/$(HDMG)_2^{2+}$) and was successfully applied for the determination of Pd, Pt and Rh in freshwater samples and sediment sample fractions. The results obtained for the analysis of the freshwater samples for its Pd, Pt and Rh concentrations, involved spiking the freshwater samples with a known amount of PGM concentration (4 µg/ℓ), and followed by voltammetric analysis of these samples to determine the accuracy and sensitivity of the constructed sensor. Analysis of the results obtained indicated that the technique is very sensitive towards the determination of Pd in freshwater samples, while further optimisation of deposition time and / or deposition potential may still be required for the determination of Pt and Rh in these samples. Applying the GC/BiFE/$(HDMG)_2^{2+}$ sensor to the analysis of the sediment sample fractions showed that good recoveries were obtained for Pd in the carbonate-bound fraction, with weaker recoveries for Pt in the Fe-Mn bound fractions, while poor results for Rh in the organic-bound fraction of the sample matrix were obtained. It further indicated that more optimisation of experimental conditions and sample matrix preparation are needed.

The seventh objective focussed on the development, identification and application of chemical precipitation techniques for specific metal ions, focussing on solution equilibria, speciation, pH-dependence and related chemical parameters. For this objective very little of the identified experimental work has been completed, partly due to the absence of real PGM sidestream samples. It is recommended that future experimental work focus on comparing synthetic and real PGM sidestream samples for the collection of identified experimental data.

Overall, the results presented in this study have demonstrated that modifying the surface of a glassy carbon electrode with a bismuth film (BiF) aids in the stripping analysis of Pt, Pd and Rh with the use of dimethylglyoxime (DMG) as chelating agent, utilising adsorptive stripping voltammetry as technique. The results further encourages the advances and efforts towards on-site environmental and industrial monitoring, enabling decentralised testing and complete replacement of common toxic mercury electrodes for stripping analysis of metal ions.

REFERENCES

AL-ANBER ZA and AL-ANBER MAS (2008) Thermodynamics and Kinetic Studies of Iron(III) Adsorption by Olive Cake in a Batch System. Journal of the Mexican Chemical Society **52(2)** 108-115.

ABDULLAH MA, CHIANG L and NADEEM M (2009) Comparative evaluation of adsorption kinetics and isotherms of a natural product removal by Amberlite polymeric adsorbents. Chemical Engineering Journal **146** 370-376.

ALCORLO P, OTERO M, CREHUET M, BALTANÁS A and MONTES C (2006) The use of the red swamp crayfish (*Procambarus clarkii*, Girard) as indicator of the bioavailability of heavy metals in environmental monitoring in the River Guadiamar (SW, Spain). The Science of the Total Environment **366** 380-390.

APHA (AMERICAN PUBLIC HEALTH ASSOCIATION) AWWA and WEF (1992) *Standard Methods for the Examination of Water and Wastewater. (19th edition)*. APHA, AWWA, and WEF, Washington, D.C., USA.

AMUNDSENAT P, STALDVIK FJ, LUKIN AA, KASHULIN NA, POPOVA OA and RESHETNIKOV YS (1997) Heavy metal contamination in freshwater fish from the border region between Norway and Russia. The Science of the Total Environment **201** 211-224.

ANDRES S, RIBEYRE F, TOURENCQ J-N. and BOUDOU A (2000) Interspecific comparison of cadmium and zinc contamination in the organs of four fish species along a polymetallic pollution gradient – Lot River, France. The Science of the Total Environment **248** 11-25.

ARRIBERE M, GUEVARA SR, SANCHEZ RS, GIL MI, ROSS GR, DAURADE LE, FAJON V, HORVAT M, ALCALDE R and KESTELMAN AJ (2003) Heavy metals in the vicinity of a chlor-alkali factory in the upper Negro River ecosystem, Northern Patagonia, Argentina. The Science of the Total Environment **301** 187-203.

BALCOM PH, FITZGERALD WF, VANDAL GM, LAMBORG CH, ROLFHUS KR, LANGER CS and HAMMERSCHMIDT, CR (2004) Mercury sources and cycling in the Connecticut River and Long Island Sound. Marine Chemistry **90** 53-74.

BANK MS, BURGESS JR, EVERS DC and LOFTIN CS (2007) Mercury Contamination of Biota from Acadia National Park, Maine: A Review. Environmental Monitoring and Assessment **126** 105-115.

BARWICK M and MAHER W (2003) Biotransference and biomagnification of selenium copper, cadmium, zinc, arsenic and lead in a temperate seagrass ecosystem from Lake Macquarie Estuary, NSW, Australia. Marine Environmental Research **56** 471-502.

BELTMAN DJ, CLEMENTS WH, LIPTON J and CACELA D (1999) Benthic invertebrate metals exposure, accumulation, and community- level effects downstream from a hard-rock mine site. Environmental Toxicology and Chemistry 1999 **18 (2)** 299-307.

BERNARDIS FL, GRANT RA and SHERRINGTON DC (2005) A review of methods of separation of the platinum-group metals through their chloro-complexes. Reactive & Functional Polymers **65** 205-217.

BLOOM NS (1989) Determination of picogram levels of methyl mercury by aqueous phase ethylation, followed by cryogenic gas chromatography with cold vapor atomic fluorescence detection. Canadian Journal Fisheries and Aquatic Science **46** 1131-1140.

BOBROWSKI A, GAWLICKI M, KAPTURSKI P, MIRCESKI V, SPASOVSKI F and ZAREBSKI J (2009) The Silver Amalgam Film Electrode in Adsorptive Stripping Voltammetric Determination of Palladium(II) as Its Dimethyldioxime Complex. Electroanalysis **21(1)** 36-40.

CANADIAN COUNCIL OF MINISTERS OF THE ENVIRONMENT (CCME) (2001) Canadian sediment quality guidelines for the protection of aquatic life: Introduction. Updated. In: Canadian environmental quality guidelines, 1999, Canadian Council of Ministers of the Environment, Winnipeg, MB, Canada.

CHABANI M, AMRANE A and BENSMAILI A (2009) Equilibrium sorption isotherms for nitrate on resin Amberlite IRA 400. Journal of Hazardous Materials **165** 27-33.

CHASSARY P, VINCENT T, MARCANO JS, MACASKIE LE and GUIBAL E (2005) Palladium and platinum recovery from bicomponent mixtures using chitosan derivatives. Hydrometallurgy **76** 131-147.

CHATAIN V, HANNA K, DE BRAUER C, BAYARD R and GERMAIN P (2004) Enhanced solubilization of arsenic and 2,3,4,6 tetrachlorophenol from soils by a cyclodextrin derivative. Chemosphere **57** 197-206.

CHOUDHARI SK and KARIDURAGANAVAR MY (2009) Development of novel composite membranes using quaternized chitosan and Na+-MMT clay for the pervaporation dehydration of isopropanol. Journal of Colloid and Interface Science **338** 111-120.

COLE PM, SOLE KC and FEATHER AM (2006) Solvent extraction developments in Southern Africa. Tsinghua Science and Technology **11 (2)** 153-159.

CORDON F, RAMIREZ SA and GORDILLO GJ (2002) Adsorption and electrochemical reduction of Co(II)-dimethylglyoxime on mercury. Journal of Electroanalytical Chemistry **534** 131-141.

CORVALAN SM, ORTIZ I and ELICECHE AM (2004) Optimal design for membrane processes for wastewater treatment and metal recovery. Computers and Chemical Engineering **28**, 103-109.

DALVI AA, SATPATI AK and PALRECHA MM (2008)Simultaneous determination of Pt and Rh by catalytic adsorptive stripping voltammetry, using hexamethylene tetramine (HMTA) as complexing agent. Talanta **75** 1382-1387.

DAS BK, ROY A, KOSCHORRECK M, MANDAL SM, WENDT-POTTHOFF K and BHATTACHARYA J (2009) Review. Occurrence and role of algae and fungi in acid mine drainage environment with special reference to metals and sulphate immobilization. Water Research **43** 883-894.

DAS N (2010) Recovery of precious metals through biosorption — A review. Hydrometallurgy **103** 180-189.

DAVIES TC (2010) Environmental health impacts of dispersed mineralisation in South Africa, African Earth Sciences doi: 10.1016/j.jafrearsci.2010.08.009

DAVIS CA, AUSTIN JE and BUHL DA (2006) Factors Influencing Soil Invertebrate Communities In Riparian Grasslands Of The Central Platte River Floodplain. Wetlands **26(2)** 438-454.

DWAF (1996a) South African Water Quality Guidelines, Volume 7: Aquatic Ecosystems. Department of Water Affairs and Forestry, Pretoria, South Africa.

DWAF (1996b) South African Water Quality Guidelines, Volume 4: Agricultural Use: Irrigation. Department of Water Affairs and Forestry, Pretoria, South Africa.

DWAF (1996c) South African Water Quality Guidelines, Volume 3: Domestic Use. Department of Water Affairs and Forestry, Pretoria, South Africa.

DWAF (2003a) Limpopo Water Management Area. Overview of Water Resources Availability and Utilization. Report No. P WMA01000/00/0203.

DWAF (2003b) Luvuvhu and Letaba Water Management Area. Overview of Water Resources Availability and Utilization. Report No. P WMA02000/00/0203.

DWAF (2003c) Olifants Water Management Area. Overview of Water Resources Availability and Utilization. Report No. P WMA04000/00/0203.

DESY JC, AMYOT M, PINEL-ALLOUL B and CAMPBELL PGC (2002). Relating cadmium concentrations in three macrophyte-associated freshwater invertebrates to those in macrophytes, water and sediments. Environmental Pollution **120** 759-769.

DOBSON RS and BURGESS JE (2007) Biological treatment of precious metal refinery wastewater: A review. Minerals Engineering **20** 519-532.

ELBERLING B, KNUDSEN KL, KRISTENSEN PH and ASMUND, G (2003) Applying fora miniferal stratigraphy as a biomarker for heavy metal contamination and mining impact in a fiord in West Greenland. Marine Environmental Research **55** 235-256.

ELS ER, LORENZEN L and ALDRICH C (2000) The adsorption of precious metals and base metals on a quaternary ammonium group ion exchange resin. Minerals Engineering **13** 401-414.

EL-SAID AG, BADAWY NA and GARAMON SE (2010) Adsorption of Cadmium (II) and Mercury (II) onto Natural Adsorbent Rice Husk Ash (RHA) from Aqueous Solutions: Study in Single and Binary System. Journal of American Science **6(12)** 400-409.

FATIN-ROUGE N, DUPONT A, VIDONNE A, DEJEU J, FIEVET P and FOISSY A (2006) Removal of some divalent cations from water by membrane-filtration assisted with alginate. Water Research **40** 1303-1309.

FERGUSON PL and CHANDLE GT (1998) A Laboratory and Field Comparison of Sediment Polycyclic Aromatic Hydrocarbon Bioaccumulation by the Cosmopolitan. Estuarine Polychaete *Strebhpio benedicti* (Webster). Marine Environmental Research **45 (415)** 387-401.

FU J, ZHOU Q, LIU J, LIU W, WANG T, ZHANG Q and JIANG G (2008) High levels of heavy metals in rice (Oryza *sativa* L.) from a typical E-waste recycling area in southeast China and its potential risk to human health. Chemosphere **71** 1269-1275.

FUJIWARA K, RAMESH A, MAKI T, HASEGAWA H and UEDA K (2007) Adsorption of platinum (IV), palladium (II) and gold (III) from aqueous solutions onto L-lysine modified crosslinked chitosan resin. Journal of Hazardous Materials **146** 39-50.

GEORGIEVA M and PIHLUR B (1996) Study of the Reduction of Palladium (r1) on a Mercury Electrode in the Presence of Dimethylglyoxime. Electroanalysis **8(12)** 1155-1159.

GHOLIVAND MB and NOZARI N (2000) Extraction and spectrophotometric determination of trace amounts of Pd(II) with 2,2’-dithiodianiline. Talanta **52(6)** 1055-1060.

GIRGIN S, KAZANCI N and DÜGEL M (2010) Relationship between aquatic insects and heavy metals in an urban stream using multivariate techniques. International Journal of Environmental Science and Technology **7(4)** 653-664.

GLAISTER BJ and MUDD GM (2010) The environmental costs of platinum -- PGM mining and sustainability: Is the glass half-full or half-empty? Minerals Engineering **23** 438-450.

GOMEZ B, PALACIOS MA, GOMEZ M, SANCHEZ JL, MORRISON G, RAUCH S, MCLEOD C, MA R, CAROLI S, ALIMONTI A, PETRUCCI F, BOCCA B, SCHRAMEL P, ZISCHKA M, PETTERSON C and WASS, U (2002) Levels and risk assessment for humans and ecosystems of platinum-group elements in the airborne particles and road dust of some European cities. The Science of the Total Environment **299** 1-19.

GRAY JS (2002) Biomagnification in marine systems: the perspective of an ecologist. Marine Pollution Bulletin **45** 46-52.

GREIG HS, NIYOGI DK, HOGSDEN KL, JELLYMAN PG and HARDING JS (2010) Heavy metals: confounding factors in the response of New Zealand freshwater fish assemblages to natural and anthropogenic acidity. The Science of the Total Environment **408** 3240-3250.

HAASE P, LOHSE S, PAULS S, SCHINDEHUTTE K, SUNDERMAN A, ROLAUFFS P and HERING D (2004) Assessing streams in Germany with benthic invertebrates: development of a practical standardised protocol for macroinvertebrate sampling and sorting. Limnology **34** 349-365.

HUBICKI Z and WOŁOWICZ A (2009) A comparative study of chelating and cationic ion exchange resins for the removal of palladium(II) complexes from acidic chloride media. Journal of Hazardous Materials **164** 1414-1419.

HUTTON EA, HOČEVAR SM, OGOREVC B and SMYTH MR (2003) Bismuth film electrode for simultaneous adsorptive stripping analysis of trace cobalt and nickel using constant current chronopotentiometric and voltammetric protocol. Electrochemistry Communications **5** 765-769.

IP CCM, LI X-D, ZHANG G, WAI OWH and LI Y-S (2007) Trace metal distribution in sediments of the Pearl River Estuary and the surrounding coastal area, South China. Environmental Pollution **147** 311-323.

JACKSON S (2006) The Policy Gap. Review of the corporate social responsibility programs of the platinum mining industry in the platinum producing region of the North West Province. Bench Marks Foundation Report, pp 78, Pretoria, South Africa.

JOHNSON BE, ESSER BK, WHYTE DC, GANGULI PM, AUSTIN CM and HUNT JR (2009) Mercury accumulation and attenuation at a rapidly forming delta with a point source of mining waste. The Science of the Total Environment **407** 5056-5070.

JOHNSON-MATTHEY (2002) Platinum Interim Review. www.platinum.matthey.com (accessed 03/02/2003).

JOHNSON-MATTHEY (2003). Platinum Today. www.platinum.matthey.com (accessed 03/02/2003).

KISHE MA and MACHIWA JF (2003) Distribution of heavy metals in sediments of Mwanza Gulf of Lake Victoria, Tanzania. Environment International **28** 619-625.

KOKKINOS C, ECONOMOU A, RAPTIS I and SPELIOTIS T (2008) Disposable mercury-free cell-on-a-chip devices with integrated microfabricated electrodes for the determination of trace nickel(II) by adsorptive stripping voltammetry. Analytica Chimica Acta **622** 111-118.

KRAMER J, DRIESSEN WL, KOCH KR and REEDIJK J (2004) Highly Selective and Efficient Recovery of Pd, Pt, and Rh from Precious Metal-Containing Industrial Effluents with Silica-Based (Poly)Amine Ion Exchangers. Separation Science and Technology **39(1)** 63-75.

KRAMER J, DRIESSEN WL, KOCH KR and REEDIJK J (2004) Highly selective and efficient recovery of Pd, Pt and Rh from precious metal-containing industrial effluents with silica-based (poly)amine ion exchangers. Separation Science and Technology **39(1),** 63-75.

KURNIAWAN TA, CHAN GYS, LO W-H and BABEL S (2006) Physico-chemical treatment techniques for wastewater laden with heavy metals. Chemical Engineering Journal **118** 83-98.

LABUDA J and BUCKOVA M (2000) Selectivity of voltammetric determination at an ion-exchanger modified electrode. Electrochemistry Communications **2** 322-324.

LAI Y-L, THIRUMAVALAVAN M and LEE J-F (2010) Effective adsorption of heavy metal ions (Cu^{2+}, Pb^{2+}, Zn^{2+}) from aqueous solution by immobilization of adsorbents on Ca-alginate beads. Toxicological & Environmental Chemistry **92(4)** 697-705.

LALONDE BA, ERNST W, and COMEAU F (2010) Trace Metal Concentrations in Sediments and Fish in the Vicinity of Ash Lagoon Discharges from Coal-Combustion Plants in New Brunswick and Nova Scotia, Canada. Archives of Environmental Contamination and Toxicology 1-10.

LAWRENCE JR, CHENIES MR, ROY R, BEAMER D, FORTIN N, SWEHONE GDW, NEU TR and GREER CW (2004) Microscale and molecular assessment of impacts of Nickel, nutrients and oxygen level on structure and function of river biofilm communities. Applied and Environmental Microbiology **70(7)** 4326-4339.

LEDIN M and PEDERSEN K (1996) The environmental impact of mine wastes – Roles of microorganisms and their significance in treatment of mine wastes. Earth-Science Reviews **41** 67-108.

LENZ K, HANN S, KOELLENSPERGER G, STEFANKA Z, STINGEDER G, WEISSENBACHER N, MAHNIK SN and FUERHACKER M (2005) Presence of cancerostatic platinum compounds in hospital wastewater and possible elimination by adsorption to activated sludge. Science of the Total Environment 345 141-152.

LEWIS MA (1995) Use Of Freshwater Plants For Phytotoxicity Testing: A Review? Environmental Pollution **87** 319-336.

LI JT, LIAO B, LAN CY, QIU JW and SHU WS (2007) Zinc, nickel and cadmium in carambolas marketed in Guangzhou and Hong Kong, China: Implication for human health. The Science of the Total Environment **388** 405-412.

LIM H-S, LEE J-S, CHON H-T and SAGER M (2008) Heavy metal contamination and health risk assessment in the vicinity of the abandoned Songcheon Au–Ag mine in Korea. Journal of Geochemical Exploration **96** 223-230.

LOCATELLI C (2006) Simultaneous square wave stripping voltammetric determination of platinum group metals (PGMs) and lead at trace and ultratrace concentration level. Application to surface water. Analytica Chimica Acta **557** 70-77.

LU Z, JIN Y, LU J and ZHANG C (2009) Concentration, distribution and bioaccumulation of mercury in the Xunyang mercury mining area, Shaanxi Province, China. Applied Geochemistry **24** 950-956.

MABOETA MS, CLAASSENS S, VAN RENSBURG L and JANSEN VAN RENSBURG, PJ (2006) The effects of platinum mining on the environment from a soil microbial perspective. Water, Air, and Soil Pollution **175** 149-161.

MACKAY D and FRASER A (2000) Bioaccumulation of persistent organic chemicals: mechanisms and models. Environmental Pollution **110** 375-391.

MADEJON P, MARANONA T, MURILLO JM and ROBINSON B (2004) White poplar (*Populus alba*) as a biomonitor of trace elements in contaminated riparian forests. Environmental Pollution **132** 145-155.

MALMQVIST B and HOFFSTEN PO (1999) Influence of drainage from old mine deposits on benthic macroinvertebrate communities in central Swedish streams. Water Research **33** 2415-2423.

MANDIL A, IDRISSI L and AMINE A (2010) Stripping voltammetric determination of mercury(II) and lead(II) using screen-printed electrodes modified with gold films, and metal ion preconcentration with thiol-modified magnetic particles. Microchimica Acta **170** 299-305.

MARTINS RJE, PARDO R and BOAVENTURA RAR (2004) Cadmium(II) and zinc(II) adsorption by the aquatic moss *Fontinalis antipyretica*: effect of temperature, pH and water hardness. Water Research **38** 693-699.

MECK M, LOVE D and MAPANI B (2006) Zimbabwean mine dumps and their impacts on river water quality -- a reconnaissance study. Physics and Chemistry of the Earth **31** 797-803.

MOLDOVAN M, RAUCH S, GOMEZ M, PALACIOS MA and MORRISON GM (2001) Bioaccumulation of palladium, platinum and rhodium from urban particulates and sediments by the freshwater isopod *Asellus aquaticus*. Water Resources **35 (17)** 4175-4183.

MOORE BA, DUNCAN, JR and BURGESS JE (2008) Fungal bioaccumulation of copper, nickel, gold and platinum. Minerals Engineering **21** 55-60.

MORAN R (2006) Mining Environmental Impact -- Integrating an Economic Perspective. CIPMA Consultancy Report, pp 27, Toronto, Canada.

NAICKER K, CUKROWSKA E and MCCARTHY, TS (2003) Acid mine drainage arising from gold mining activity in Johannesburg, South Africa and environs. Environmental Pollution **122** 29-40.

NAITO W, KAMO M, TSUSHIMA K and IWASAKI Y (2010) Review. Exposure and risk assessment of zinc in Japanese surface waters. Science of the Total Environment **408** 4271-4284.

OBERHOLSTER PJ, ASHTON PJ, DABROWSKI JM, KLEYNHANS CJ, HARDWICK D, WOODBOURNE S, HALL G and MACMILLAN P (2009) *Waterberg Project: Full Report on Progress in Year 1*. CSIR-NRE Internal Report, 27 February 2009. CSIR-NRE Report No. CSIR/NRE/WR/IR/20090047/A. iii + 65 pages.

ORECCHIO S and AMORELLO D (2010) Platinum and rhodium associated with the leaves of *Nerium oleander* L.; analytical method using voltammetry; assessment of air quality in the Palermo (Italy) area. Journal of Hazardous Materials **174** 720-727.

PAGNANELLI F, MOSCARDINI E, GIULIANO V and TORO L (2004) Sequential extraction of heavy metals in river sediments of an abandoned pyrite mining area: pollution detection and affinity series. Environmental Pollution **132** 189-201.

PERAMAKI LA and DECKER JF (2000) Lead in soil and sediment in Iqaluit, Nunavut, Canada, and links with human health. Environmental Monitoring and Assessment 63 329-339.

PEREIRA MJ, RESENDE P, AZEITEIRO UM, OLIVEIRA J and DE FIGUEIREDO DR (2005) Differences in the Effects of Metals on Growth of Two Freshwater Green Algae (*Pseudokirchneriella subcapitat* (Korshikov) Hindak and *Gonium pectoral* (Müller). Bulletin of Environmental Contamination and Toxicology **75** 515-522.

PHILLIPS DJH (1995) The Chemistries and Environmental Fates of Trace Metals and Organochlorines in Aquatic Ecosystems. Marine Pollution Bulletin **31**(4-12) 193-200.

RAMADAN H, GHANEM A and EL-RASSY H (2010) Mercury removal from aqueous solutions using silica, polyacrylamide and hybrid silica-polyacrylamide aerogels. Chemical Engineering Journal 159 107-115.

RAMESH A, HASEGAWA H, SUGIMOTO W, MAKI T and UEDA K (2008) Adsorption of gold(III), platinum(IV) and palladium(II) onto glycine modified crosslinked chitosan resin. Bioresource Technology **99** 3801-3809.

RAMÍREZ SA and GORDILLO GJ (2009) Adsorption and reduction of palladium-dimethylglyoxime complex. Journal of Electroanalytical Chemistry **629** 147-151.

RAO CRK and TRIVEDI DC (2005) Chemical and electrochemical depositions of platinum group metals and their applications. Review. Coordination Chemistry Reviews **249** 613-631.

RAVINDRA K, BENCS L and VAN GRIEKEN R (2004) Review. Platinum group elements in the environment and their health risk. The Science of the Total Environment **318** 1-43.

REIS MF, SAMPAIO C, BRANTES A, ANICETOA P, MELIM M, CARDOSO L, GABRIEL C, SIMAO F and MIGUEL JP (2010) Human exposure to heavy metals in the vicinity of Portuguese solid waste incinerators – Part 1: Biomonitoring of Pb, Cd and Hg in blood of the general population. International Journal of Hygiene and Environmental Health 210 439-446.

RESANO M, GARCIA-RUIZ E, BELARRA MA, VANHAECKE F and MCINTOSH KS (2007) Solid sampling in the determination of precious metals at ultratrace levels. Trends in Analytical Chemistry 26(5) 385-395. 2007

RESANO M, GARCIA-RUIZ E, BELARRA MA, VANHAECKE F and MCINTOSH KS (2007) Solid sampling in the determination of precious metals at ultratrace levels. Trends in Analytical Chemistry 26(5) 385-395. 2007

RIVER HEALTH PROGRAMME (RHP) (2001) State-of-Rivers Report: Letaba and Luvuvhu River Systems -- 2001. Department of Water Affairs and Forestry, Pretoria. ISBN No. 1-86845-825-3.

RIVER HEALTH PROGRAMME (RHP) (2005) State-of-Rivers Report: Monitoring and Managing the Ecological States of Rivers in the Crocodile (West) Marico Water Management Area. Department of Water Affairs and Forestry, Pretoria. ISBN No. 0-620-34054-1.

RIVER HEALTH PROGRAMME (RHP) (2006) Achievements of the River Health Programme 1994-2004: A national perspective on the ecological health of selected South African rivers. Department of Water Affairs and Forestry, Pretoria. ISBN No. 0-620-36168-9.

ROBINSON D (2002) Personal communication.

RUUS A, SCHAANNING M, ØXNEVAD S and HYLLAND K (2005) Experimental results on bioaccumulation of metals and organic contaminants from marine sediments. Aquatic Toxicology **72** 273-292.

SOMERSET V, LEANER J, MASON R, IWUOHA E and MORRIN A (2010) Development and application of a poly(2,2'-dithiodianiline) (PDTDA)-coated screen-printed carbon electrode in inorganic mercury determination. Electrochimica Acta **55** 4240-4246.

SOMERSET V, LEANER JJ, WILLIAMS CR, PETERSEN CR, MASON RP, MASEKOAMENG E, DABROWSKI J, MACMILLAN P, ASHTON PJ, MURRAY K, BUGAN R and CROUCH, A (2010) A National Survey of Mercury Levels in South African Water Resources. CSIR, Stellenbosch. Report No. CSIR/NRE/WR/IR/2010/0021/B.

SOMERSET V, LEANER JJ, WILLIAMS CR, PETERSEN CR, MASON RP, MASEKOAMENG E, DABROWSKI J, MACMILLAN P, ASHTON PJ, MURRAY K, BUGAN R and CROUCH, A (2010) A National Survey of Mercury Levels in South African Water Resources. CSIR, Stellenbosch. Report No. CSIR/NRE/WR/IR/2010/0021/B.

SOMERSET VS, HERNANDEZ LH and IWUOHA EI (2011) Stripping voltammetric measurement of trace metal ions using screen-printed carbon and modified carbon paste electrodes on river water from the Eerste-Kuils River System. Journal of Environmental Science and Health A **46** 17-32.

SONUNE A and GHATE R (2004) Developments in wastewater treatment methods. Desalination **167** 55-63.

SOUCEK DJ, CHERRY DS, CURRIE RJ, LATIMER HA, TRENT GC (2000) Laboratory to field validation in an integrative assessment of an acid mine drainage-impacted watershed. Environmental Toxicology and Chemistry **19(4)**1036-1043.

STERNER RW, SMUTKA TM, MCKAY RML, XIAOMING Q, BROWN ET and SHERRELL RM (2004) Phosphorus and Trace Metal Limitation of Algae and Bacteria in Lake Superior. Limnology and Oceanography **49(2)** 495-507.

STIMIE C, RICHTERS E, THOMPSON H, PERRET S, MATETE M, ABDALLAH K, KAU K AND MULIBANA E (2001) *Hydro-institutional mapping in the Steelpoort River basin, South Africa.* Working Paper 17 (South Africa Working Paper No. 6). Colombo, Sri Lanka: International Water Management Institute.

TAKAMURA N, KASAI F and WATANABE MW (1989) Effects of Cu, Cd and Zn on photosynthesis of freshwater benthic algae. Journal of Applied Phycology **1** 39-52.

TARRAS-WAHLBERG NH, FLACHIER A, LANE SN, SANGFORS O (2001) Environmental impacts and metal exposure of aquatic ecosystems in rivers contaminated by small scale gold mining: the Puyango River basin, southern Ecuador. The Science of the Total Environment **278** 239-261

TESAROVA E, BALDRIANOVA L, HOCEVAR SB, SVANCARA I, VYTRAS K and OGOREVC B (2009) Anodic stripping voltammetric measurement of trace heavy metals at antimony film carbon paste electrode. Electrochimica Acta **54** 1506-1510.

TØNNING E, SAPELNIKOVA S, CHRISTENSEN J, CARLSSON C, WINTHER-NIELSEN M, DOCK E, SOLNA R, SKLADAL P, NØRGAARD L, RUZGAS T and EMNEUS J (2005) Chemometric exploration of an amperometric biosensor array for fast determination of wastewater quality. Biosensors and Bioelectronics **21** 608-617.

UNITED STATES ENVIRONMENTAL PROTECTION AGENCY (US EPA) (1992) Water quality standards; establishment of numeric criteria for priority toxic pollutants; states' compliance; final rule. Federal Register 40 CFR Part 131 5;. 246 (60) 847-860, 916.

UNITED STATES ENVIRONMENTAL PROTECTION AGENCY (USEPA) (2000) Guidance for assessing chemical contamination data for use in fish advisories. Vol 1: field sampling and analysis, Third Ed. Washington DC, US EPA, Office of Water. EPA publication no. EPA-823-B-00-007.

UNITED STATES ENVIRONMENTAL PROTECTION AGENCY (USEPA) (2002) Method 1631. Revision E. Mercury in Water by Oxidation, Purge and Trap, and Cold Vapor Atomic Fluorescence Spectrometry. EPA-821/R-02-019.

VAN DAMME PA, HAMEL C, AYALA A and BERVOETS L (2008) Macroinvertebrate community response to acid mine drainage in rivers of the High Andes (Bolivia). Environmental Pollution **156** 1061-1068.

WALCARIUS A and DELACOTE C (2005) Mercury(II) binding to thiol-functionalized mesoporous silicas: critical effect of pH and sorbent properties on capacity and selectivity. Analytica Chimica Acta **547** 3-13.

WANG J and LU J (2000) Bismuth film electrodes for adsorptive stripping voltammetry of trace nickel. Electrochemistry Communications **2** 390-393.

WANG Z-Y, LEE JHW, CHENG D and DUAN (2008) Benthic invertebrates investigation in the East River and habitat restoration strategies. Journal of Hydro-environment Research **2** 19-27.

WANG J (2006) Analytical Electrochemistry. 3rd Edition. John Wiley & Sons, Inc., New Jersey, USA.

WILLIAMS CR (2010) A national survey of mercury levels in South Africa's Water Management Area. MSc Thesis: University of the Western Cape, Bellville, South Africa.

WOŁOWICZ A and HUBICKI Z (2010) Effect of matrix and structure types of ion exchangers on palladium(II) sorption from acidic medium. Chemical Engineering Journal **160** 660-670.

WOŁOWICZ A and HUBICKI Z (2011) Comparison of strongly basic anion exchange resins applicability for the removal of palladium(II) ions from acidic solutions. Chemical Engineering Journal **171** 206-215.

WONG KK, LEE CK, LOW KS and HARON MJ (2003) Removal of Cu and Pb from electroplating wastewater using tartaric acid modified rice husk. Process Biochemistry **39(4)** 437-445

WOODFINE DG, HAVAS M and ACREMAN J (2002) Nickel and copper tolerance of phytoplankton isolated from a recovering lake near Sudbury, Canada. Geochemistry: Exploration, Environment, Analysis **2** 203-207.

ZALACK JT, SMUCKER NJ and VIS ML (2010) Development of a diatom index of biotic integrity for acid mine drainage impacted streams. Ecological Indicators **10** 287-295.

ZHANG Z-Q, LIU H, ZHANG H and LI Y-F (1996) Simultaneous cathodic stripping voltammetric determination of mercury, cobalt, nickel and palladium by mixed binder carbon paste electrode containing dimethylglyoxime. Analytica Chimica Acta **333** 191-124.

ZHENG N, WANG Q, ZHANG X, ZHENG D, ZHANG Z and ZHANG S (2007) Population health risk due to dietary intake of heavy metals in the industrial area of Huludao city, China. The Science of the Total Environment **387** 96-104.

ZHOU L, XU J, LIANG X and LIU Z (2010) Adsorption of platinum(IV) and palladium(II) from aqueous solutions by magnetic cross-linking chitosan nanoparticles modified with ethylenediamine. Journal of Hazardous Materials **182** 518-524.

ZHU WW, LI NB and LUO HQ (2006) Anodic Stripping Voltammetry Determination of Pb(II) and Cd(II) at a Bismuth/Poly(aniline) Film Electrode. Analytical Letters **39** 2273-2284.

APPENDIX: PHOTOGRAPHIC DESCRIPTION OF SAMPLING SITES

Figure 52. Hex River 2

Figure 53. Maretlwane River

Figure 54. Crocodile River

Figure 55. Rooikoppies Dam

Figure 56. Crocodile River (Thabazimbi) 1

Figure 57. Crocodile River (Thabazimbi) 2

Figure 58. Elands River

Figure 59. Hex River 1

Figure 60. Sterkstroom River 1

Figure 61. Sterkstroom River 2

Figure 62. Mogalakwena River 1

Figure 63. Mogalakwena River 2

Figure 64. Olifants River

Figure 65. Motse River

Figure 66. Steelpoort River

Figure 67. Mohlapitsi River